VOL. 508 NO. 1 MAY 25, 1990

JOURNAL OF CHROMATOGRAPHY

INTERNATIONAL JOURNAL ON CHROMATOGRAPHY, ELECTROPHORESIS AND RELATED METHODS

ELSEVIER

JOURNAL OF CHROMATOGRAPHY

Scope. The *Journal of Chromatography* publishes papers on all aspects of chromatography, electrophoresis and related methods. Contributions consist mainly of research papers dealing with chromatographic theory, instrumental development and their applications. The section *Biomedical Applications*, which is under separate editorship, deals with the following aspects: developments in and applications of chromatographic and electrophoretic techniques related to clinical diagnosis or alterations during medical treatment; screening and profiling of body fluids or tissues with special reference to metabolic disorders; results from basic medical research with direct consequences in clinical practice; drug level monitoring and pharmacokinetic studies; clinical toxicology; analytical studies in occupational medicine.

Submission of Papers. Papers in English, French and German may be submitted, in three copies. Manuscripts should be submitted to: The Editor of *Journal of Chromatography*, P.O. Box 681, 1000 AR Amsterdam, The Netherlands, or to: The Editor of *Journal of Chromatography, Biomedical Applications*, P.O. Box 681, 1000 AR Amsterdam, The Netherlands. Review articles are invited or proposed by letter to the Editors. An outline of the proposed review should first be forwarded to the Editors for preliminary discussion prior to preparation. Submission of an article is understood to imply that the article is original and unpublished and is not being considered for publication elsewhere. For copyright regulations, see below.

Subscription Orders. Subscription orders should be sent to: Elsevier Science Publishers B.V., P.O. Box 211, 1000 AE Amsterdam, The Netherlands, Tel. 5803 911, Telex 18582 ESPA NL. The *Journal of Chromatography* and the *Biomedical Applications* section can be subscribed to separately.

Publication. The *Journal of Chromatography* (incl. *Biomedical Applications*) has 37 volumes in 1990. The subscription prices for 1990 are:

J. Chromatogr. (incl. *Cum. Indexes, Vols. 451–500*) + *Biomed. Appl.* (Vols. 498–534):
Dfl. 6734.00 plus Dfl. 1036.00 (p.p.h.) (total *ca.* US$ 3885.00)

J. Chromatogr. (incl. *Cum. Indexes, Vols. 451–500*) only (Vols. 498–524):
Dfl. 5616.00 plus Dfl. 756.00 (p.p.h.) (total *ca.* US$ 3186.00)

Biomed. Appl. only (Vols. 525–534):
Dfl. 2080.00 plus Dfl. 280.00 (p.p.h.) (total *ca.* US$ 1180.00).

Our p.p.h. (postage, package and handling) charge includes surface delivery of all issues, except to subscribers in Argentina, Australia, Brasil, Canada, China, Hong Kong, India, Israel, Malaysia, Mexico, New Zealand, Pakistan, Singapore, South Africa, South Korea, Taiwan, Thailand and the U.S.A. who receive all issues by air delivery (S.A.L. — Surface Air Lifted) at no extra cost. For Japan, air delivery requires 50% additional charge; for all other countries airmail and S.A.L. charges are available upon request. Back volumes of the *Journal of Chromatography* (Vols. 1–497) are available at Dfl. 195.00 (plus postage). Claims for missing issues will be honoured, free of charge, within three months after publication of the issue. Customers in the U.S.A. and Canada wishing information on this and other Elsevier journals, please contact Journal Information Center, Elsevier Science Publishing Co. Inc., 655 Avenue of the Americas, New York, NY 10010. Tel. (212) 633-3750.

Abstracts/Contents Lists published in Analytical Abstracts, ASCA, Biochemical Abstracts, Biological Abstracts, Chemical Abstracts, Chemical Titles, Chromatography Abstracts, Clinical Chemistry Lookout, Current Contents/Life Sciences, Current Contents/Physical, Chemical & Earth Sciences, Deep-Sea Research/Part B: Oceanographic Literature Review, Excerpta Medica, Index Medicus, Mass Spectrometry Bulletin, PASCAL-CNRS, Pharmaceutical Abstracts, Referativnyi Zhurnal, Science Citation Index and Trends in Biotechnology.

See inside back cover for Publication Schedule, Information for Authors and information on Advertisements.

0021-9673/90/$03.50

Printed in The Netherlands

CONTENTS

(Abstracts/Contents Lists published in Analytical Abstracts, ASCA, Biochemical Abstracts, Biological Abstracts, Chemical Abstracts, Chemical Titles, Chromatography Abstracts, Current Contents/Life Sciences, Current Contents/Physical, Chemical & Earth Sciences, Deep-Sea Research/Part B: Oceanographic Literature Review, Excerpta Medica, Index Medicus, Mass Spectrometry Bulletin, PASCAL-CNRS, Referativnyi Zhurnal and Science Citation Index)

(Continued overleaf)

In articles with more than one author, the name of the author to whom correspondence should be addressed is indicated in the article heading by a 6-pointed asterisk (*)

JOURNAL OF ANALYTICAL AND APPLIED PYROLYSIS

The international *Journal of Analytical and Applied Pyrolysis* is devoted to the publication of qualitative and quantitative results relating to:

- Controlled thermal degradation and pyrolysis of technical and biological macromolecules;
- Environmental, geochemical, biological and medical applications of analytical pyrolysis;
- Basic studies in high temperature chemistry, reaction kinetics and pyrolysis mechanisms;
- Pyrolysis investigations of energy related problems, fingerprinting of fossil and synthetic fuels, coal extraction and liquefaction products.

The scope of the journal includes:

- Fundamental investigations of pyrolysis processes by chemical, physical and physicochemical methods.
- Structural analysis and fingerprinting of synthetic and natural polymers or products of high molecular weight.
- Technical developments and new instrumentation for pyrolysis techniques in combination with various chromatographic or spectrometric methods with special attention given to automation, optimization and standardization.
- Computer handling and processing of pyrolysis data, including library filing and retrieval techniques, as well as computer matching and advanced pattern recognition techniques.

Abstracted/Indexed in:
Analytical Abstracts, Biological Abstracts, Chemical Abstracts, Current Contents/Physical, Chemical & Earth Sciences, Mass Spectrometry Bulletin, Science Citation Index

Subscription Information:
1989: Vols. 15 & 16 (8 issues)
US$ 357.00 / Dfl. 714.00 including postage
ISSN 0165-2370

For a free sample copy write to:

ELSEVIER SCIENCE PUBLISHERS
P.O. Box 211, 1000 AE Amsterdam, The Netherlands
P.O. Box 882, Madison Square Station, New York, NY 10159, USA

Experimental Design

A Chemometric Approach

S.N. Deming, *University of Houston, Houston, TX, USA, and* **S.L. Morgan,** *University of South Carolina, Columbia, SC, USA*

Now also available in a paperback edition!

"Deming and Morgan should be given high praise for bringing the principles of experimental design to the level of the practicing analytical chemist... an exceptionally lucid, easy-to-read presentation... an excellent addition to the collection of every analytical chemist. I recommend it with great enthusiasm." *(Analytical Chemistry)*

Unlike most current textbooks, this book approaches experimental design from the viewpoint of the experimenter rather than that of the statistician. It adopts a practical approach to experimental design and allows the reader to obtain the required information in the minimum number of experiments. It introduces the fundamentals of experimental design. Systems theory, response surface concepts, and basic statistics serve as a basis for the further development of matrix least squares and hypothesis testing. The effects of different experimental designs and models on the variance-covariance matrix and on the analysis of variance (ANOVA) are extensively discussed. Applications and advanced topics complete the text. Numerous worked examples are given.

The clear, practical approach adopted by the authors makes the book applicable to a wide audience. It will appeal particularly to those with a practical need (scientists, engineers, managers, research workers) who have completed their formal education but who still need to know efficient ways of carrying out experiments. It will also be an ideal text for advanced undergraduate and graduate students following courses in chemometrics, data acquisition and treatment, and design of experiments.

Contents: 1. System Theory. 2. Response Surfaces. 3. Basic Statistics. 4. One Experiment. 5. Two Experiments. 6. Hypothesis Testing. 7. The Variance-Covariance Matrix. 8. Three Experiments. 9. Analysis of Variance (ANOVA) for Linear Models. 10. A Ten-Experiment Example. 11. Approximating a Region of a Multi-factor Response Surface. 12. Additional Multifactor Concepts and Experimental Designs. Appendices: Matrix Algebra. Critical Values of t. Critical Values of F, (a) = 0.05. Index.

Data Handling in Science and Technology, 3
1987 1st repr. 1988 xiv + 286 pages
US$ 118.50 / Dfl. 225.00; 0-444-42734-1
Paperback: US$ 65.75 / Dfl. 125.00
Paperback ISBN: 0-444-43032-6

ELSEVIER

P.O. Box 211, 1000 AE Amsterdam, The Netherlands.

P.O. Box 882, Madison Square Station, New York, NY 10159, USA.

JOURNAL OF CHROMATOGRAPHY

VOL. 508 (1990)

JOURNAL *of* CHROMATOGRAPHY

INTERNATIONAL JOURNAL ON CHROMATOGRAPHY,
ELECTROPHORESIS AND RELATED METHODS

ELSEVIER
AMSTERDAM — OXFORD — NEW YORK — TOKYO

J. Chromatogr., Vol. 508 (1990)

0021-9673/90/$03.50

Printed in The Netherlands

Journal of Chromatography, 508 (1990) 1–2
Elsevier Science Publishers B.V., Amsterdam — Printed in The Netherlands

CHROM. 22 359

Editorial

Authors often inquire as to the policy and practice of the *Journal of Chromatography* concerning the review process for submitted articles. The primary aim of the editors and staff is to ensure that the articles published in the journal satisfy the journal's standards for quality of content and presentation. With regard to the quality of the content of an article, this implies that it should significantly contribute to the development of the field. With regard to the quality of presentation, this means that the published work should be as clear, complete and accurate as possible. At the same time, efforts should be made to minimize excessive verbiage and to avoid repeating facts which are well known or contained in the prior literature. Authors should use the recommended chromatographic terminology, and preferably SI units and the generic names of drugs, avoiding commercial names. Also sorbents should be described chemically –at least to some degree. The journal also encourages authors to strive for a writing style that is interesting and 'readable'. To the degree that authors attain these goals, the final paper should be of maximum value to our readers, in turn reflecting credit on the authors.

When an article is first received for publication, it is normally sent to two outside reviewers. The accompanying review forms request both a summary opinion of the paper ("acceptable as is", "after minor revision", etc.) as well as detailed comments where these are applicable. Reviewers are selected on the basis of both general and specific expertise, with "difficult" papers being sent to reviewers who have specialized in the subject of the paper. Articles that pass the review process without serious questions or problems are usually accepted at this point for publication. *However, authors are nevertheless expected to respond in detail to each issue raised by the reviewers.*

Some articles will be returned by the reviewers with the recommendation that the paper be accepted only after major revision –or not at all. In these cases, when the author feels that the work still meets the standards of the journal, it is necessary to consider all points raised by the reviewers, and to both (1) modify the article as appropriate and (2) provide a detailed response to the reviewers' comments. In the absence of a satisfactory response to major questions raised by the reviewers, it will be necessary to reject a manuscript. Authors who believe that their work has not received a competent or fair appraisal from the initial reviewers can request additional reviews by other reviewers. The editors and staff of the journal also attempt to maintain an evenhanded review process.

Rapid publication of results is in the interest of the authors and the journal. Authors are therefore requested to return the revised version of a manuscript as soon as possible. If a revised version is submitted more than six months after the request for revision was communicated to the author, it will generally be regarded as a new submission and be refereed again, because a similar work may have been published in the meantime. If a revised version is not submitted within a year, it is assumed that the

author is no longer interested in publication in the journal, and the file will be closed.

The field of chromatography continues to expand at a rapid rate, with a corresponding increase in the amount and quality of related research activities. With every passing year, the standards by which we judge research articles will be more demanding. Unhappily, this also means an increasing rejection rate for articles submitted to this and other research journals. However, this is the inevitable price of progress. We ask for understanding on the part of both our authors and readers in these changing times.

Journal of Chromatography, 508 (1990) 3–17
Elsevier Science Publishers B.V., Amsterdam — Printed in The Netherlands

CHROM. 22 300

Isotachophoresis with two leading ions and migration behaviour in capillary zone electrophoresis

I. Isotachophoresis with two leading ions

J. L. BECKERS* and F. M. EVERAERTS
Laboratory of Instrumental Analysis, Eindhoven University of Technology, P.O. Box 513, 5600 MB Eindhoven (The Netherlands)
(First received December 1st, 1989; revised manuscript received January 22nd, 1990)

SUMMARY

A mathematical model for isotachophoresis with two leading ions is presented and, based on this model, computer programs are set up for the calculation of the parameters of the different zones. With this model it is possible to calculate at what level a second leading ion may be present, *e.g.*, carbonate ions in the separation of anions at a high pH, without disturbing the isotachophoretic separation.

Calculated values of the specific zone resistance and response values are compared with values experimentally obtained showing good agreement. Calculations with this model show that with the presence of a second leading ion the zone lengths elongate (higher values of the response factor) and at a certain concentration ratio of the two leading ions, also dependent on the effective mobilities of the ions, the isotachophoretic condition is lost and isotachophoresis changes into zone electrophoresis.

INTRODUCTION

Sometimes disturbances in isotachophoretic (ITP) separations can occur as a result of the presence of an (unwanted) second leading ion in the leading electrolyte (*e.g.*, carbonate ions in the separation of anions at high pH). Mikkers and Everaerts[1] mentioned earlier that ITP with two leading ions can be applied. In this paper, a previously described mathematical model for the steady state in ITP[2,3] is extended for the use of leading electrolytes with two leading ions in order to establish the level at which a second leading ion can be present without disturbing the ITP separation. Calculations with this model show that at a certain concentration ratio of the two leading ions, also dependent on the effective mobilities of these ions, the ITP condition is lost. At that point, ITP changes into zone electrophoresis (ZE).

With this model, it can be understood why sometimes extremely high plate numbers can be obtained in capillary zone electrophoresis (CZE), as will be explained in Part II.

0021-9673/90/$03.50

THEORY

Using a mathematical model for the description of the steady state in ITP, the reduced number of parameters is always four in all zones, *viz.*, $[L]_t$ or $[A]_t$, $[B]_t$, E and pH. For all zones always four known parameters and/or equations are necessary, by means of which all parameters can be calculated. For the leading zone the known parameters are generally $[L]_t$ and $[B]_t$ and the equations are Ohm's law and the electroneutrality (EN). For all other zones the four available equations are the EN, Ohm's law, the buffer equation and the isotachophoretic condition (IC).

Considering a leading electrolyte with two leading ions (a so-called 2L system), the reduced number of parameters will be five for all zones. For the leading electrolyte the parameters are $[L1]_t$, $[L2]_t$, $[B]_t$, E and pH, where L1 is the leading ion with the highest and L2 that with the lowest effective mobility. For the sample zones the parameters will be $[A]_t$, $[L2]_t$, $[B]_t$, E and pH, under the assumption that L2 will remain behind and will form a mixed zone with the sample ions. Consequently, five known parameters and/or equations are needed for the calculations, *viz.*, for the leading zone $[L1]_t$, $[L2]_t$, $[B]_t$, Ohm's law and the EN and for the sample zones the EN, Ohm's law, the buffer balance, the L2 balance and the IC.

For the use of the last equation, the crucial question is whether a component migrates in the ITP mode, because in principle it is not essential that a sample zone must follow the L1 zone owing to the presence of a second leading ion partially remaining behind in the proceeding zone.

If the amount of L2 remaining behind L1 is sufficient to form a terminating L2 zone without any sample ionic species and if this terminating L2 zone has an E gradient smaller than that of a sample zone, the IC is no longer valid. In fact, the ITP mode changes into a ZE mode, whereby that sample zone migrates in a ZE way in the terminating L2 zone.

In our treatment, we assume that a sample ion migrates in the ITP mode if the calculated value of the specific zone resistance[4] at 25°C (SZR_{25}) or the E are smaller than those of the terminating L2 zone. For the terminating L2 zone the reduced number of parameters is only four, *viz.*, $[L2]_t$, $[B]_t$, E and pH. Only four equations are needed for the calculations, *viz.*, the EN, Ohm's law, the buffer equation and the L2 balance.

The mathematical model is therefore extended in two ways, *viz.*, for the calculation of parameters for a terminating L2 zone and for sample zones in a 2L system.

Mathematical model for the terminating L2 zone in a 2L system

At known pH, the concentrations of all ionic forms of a substance A with a charge of $z-i$ can be expressed as the total concentration of A by[3]

$$[A^{z-1}] = [A^z]\frac{\prod_{j=1}^{i} K_j}{[H_3O^+]^i} = [A]_t \frac{\dfrac{\prod_{j=1}^{i} K_j}{[H_3O^+]^i}}{1 + \sum_{i=1}^{n} \dfrac{\prod_{j=1}^{i} K_j}{[H_3O^+]^i}} \qquad (1)$$

where K_j are the concentration equilibrium constants for the n protolysis reactions.

Tiselius[5] pointed out that a substance that consists of several forms with different mobilities in equilibrium with each other will generally migrate as a uniform substance with an effective mobility given by

$$\bar{m} = \sum_{i=0}^{n} \alpha_i m_i = \sum_{i=0}^{n} [A^{z-i}] m_{z-i} / [A]_t \tag{2}$$

For simplicity, the effect of the ionic strength is not considered in this equation. In the computer programs, however, a correction is made for this effect using the Debye–Hückel–Onsager relation.

Substituting eqn. 1 into eqn. 2, we can write for the effective mobility of an ionic species A

$$\bar{m} = \frac{\sum_{i=1}^{n} m_{z-i} \frac{\prod_{j=1}^{i} K_j}{[H_3O^+]^i} + m_z}{1 + \sum_{i=1}^{n} \frac{\prod_{j=1}^{i} K_j}{[H_3O^+]^i}} \tag{3}$$

Although in these general descriptions of the equilibria and effective mobility of a substance, no differences exist between the leading, sample, terminating and buffer ionic species, we shall distinguish between them using the symbols L, A, T and B.

In addition to the general descriptions of the equilibria and effective mobilities of ionic species, we further need the principle of electroneutrality, the modified Ohm's law, the mass balance of the buffer and the mass balance of the leading ion L2 with the lowest effective mobility to describe the "steady-state" for the terminating L2 zone in ITP for two leading ions.

The principle of electroneutrality. In accordance with the principle of electroneutrality (EN), the arithmetic sum of all products of the concentration of all forms for all ionic species and the corresponding valences, present in each zone, must be zero. For the electroneutrality of a zone we can write

$$[H_3O^+] - [OH^-] + \sum_{i=0}^{n_A} (z - i)[A^{z-i}] + \sum_{i=0}^{n_B} (z - i)[B^{z-i}] = 0 \tag{4}^a$$

Modified Ohm's law. Working at a constant current density:

$$E_L \sigma_L = E_T \sigma_T \tag{5}$$

---

[a] Arbitrarily the contribution of a sample ion A and a buffer ion B are given. Of course, for the leading zone in an L2 system the contribution of L1, L2 and B and for the terminating L2 zone the contribution of L2 and B have to be taken into account.

or the function

$$RFQ = E_L\sigma_L/E_T\sigma_T - 1 \tag{6}$$

must be zero.

The overall electric conductivity σ of a zone is the sum of the values $c|\bar{m}z|F$ and consequently

$$E\{[H_3O^+]|\bar{m}_H| + [OH^-]|\bar{m}_{OH}| + \sum_{i=0}^{n_A}[A^{z-i}]|\bar{m}_{z-i}(z-i)| + \sum_{i=0}^{n_B}[B^{z-i}]|\bar{m}_{z-i}(z-i)|\} \tag{7}^a$$

in all zones is constant.

Mass balance of the buffer. With the mass balance of the buffer (Ohm's law and the principle of electroneutrality must also be obeyed), the leading zone determines the conditions of the proceeding zones. For the mass balance of the buffer, the following equation (8A) can be derived (see Fig. 1).

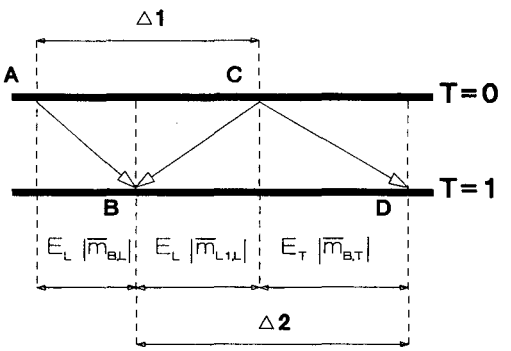

Fig. 1. Migration paths of the buffering counter ionic species over a zone boundary between a leading zone with two leading ions L1 and L2 and the terminating L2 zone.

The zone boundary between the leading electrolyte consisting of L1 and L2 and the terminating zone with L2, present at $t = 0$ at point C, moves in unit time to point B at $t = 1$ over a distance BC of $E_L|\bar{m}_{L1,L}|$. The buffer ionic species at time $t = 0$ present at the zone boundary C will reach point D at $t = 1$. The distance from C to D will then be $E_T|\bar{m}_{B,T}|$. The buffer ionic species at $t = 0$ present at point A will just reach the boundary in B at $t = 1$. The distance from A to B is then $E_L|\bar{m}_{B,L}|$.

This means that all buffer ionic particles present in the leading zone between A and C with a concentration $[B]_{t,L}$ at time $t = 0$ ($\Delta 1$) will be present in the terminating zone with a concentration $[B]_{t,T}$ between B and D at $t = 1$ ($\Delta 2$). Therefore, the buffer mass balance will be

$$[B]_{t,T}(E_T|\bar{m}_{B,T}| + E_L|\bar{m}_{L1,L}|) = [B]_{t,L}(E_L|\bar{m}_{B,L}| + E_L|\bar{m}_{L1,L}|) \tag{8A}$$

[a] See footnote on p. 5.

or

$$[B]_{t,T}(E_T|\bar{m}_{B,T}|/E_L + |\bar{m}_{L1,L}|) = [B]_{t,L}(|\bar{m}_{B,L}| + |\bar{m}_{L1,L}|) \tag{8B}$$

Mass balance of L2. The zone boundary between the leading electrolyte consisting of L1 and L2 and the terminating zone with L2 present at $t = 0$ at point E (see Fig. 2) moves in unit time to point B at $t = 1$ over a distance EB of $E_L|\bar{m}_{L1,L}|$. The leading ionic species L2 (and terminating ionic species at the same time!) at time $t = 0$ present at point F will just reach C at $t = 1$. The distance from F to C will then be $E_T|\bar{m}_{L2,T}|$. The leading ionic species L2 at $t = 0$ present at point D will reach point A at $t = 1$. The distance from D to A is then $E_L|\bar{m}_{L2,L}|$.

This means that all ionic particles L2 present between D and F (partially in the leading and partially in the terminating zone) at time $t = 0$ ($\Delta 1$) will be present between C and A at $t = 1$ ($\Delta 2$). The mass balance for ionic species L2 will therefore be

$$E_L|\bar{m}_{L1,L}|[L2]_{t,L} + E_T|\bar{m}_{L2,T}|[L2]_{t,T} = E_L|\bar{m}_{L2,L}|[L2]_{t,L} + E_L|\bar{m}_{L1,L}|[L2]_{t,T} \tag{9A}$$

or

$$|\bar{m}_{L1,L}|[L2]_{t,L} + E_T/E_L|\bar{m}_{L2,T}|[L2]_{t,T} = |\bar{m}_{L2,L}|[L2]_{t,L} + |\bar{m}_{L1,L}|[L2]_{t,T} \tag{9B}$$

It can be seen that if $[L2]_{t,L}$ is zero, this balance changes into the isotachophoretic condition

$$E_T/E_L|\bar{m}_{L2,T}|[L2]_{t,T} = |\bar{m}_{L1,L}|[L2]_{t,T} \tag{10A}$$

or

$$E_T|\bar{m}_{L2,T}| = E_L|\bar{m}_{L1,L}| \tag{10B}$$

Calculation procedure. If a pH_L is assumed, then $[H_3O^+]$ and $[OH^-]$ can be calculated. If $[L1]_{t,L}$, $[L2]_{t,L}$ and $[B]_{t,L}$ are known, all ionic concentrations of the ionic

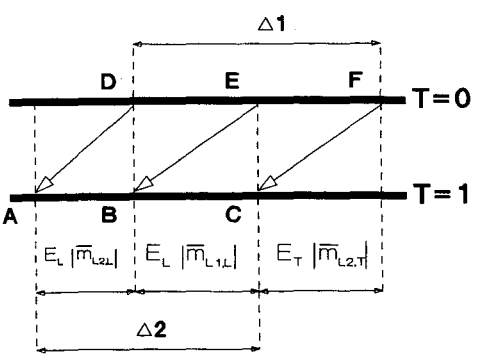

Fig. 2. Migration paths for the ionic species L2 over a zone boundary between a leading zone with two leading ions L1 and L2 and the terminating L2 zone.

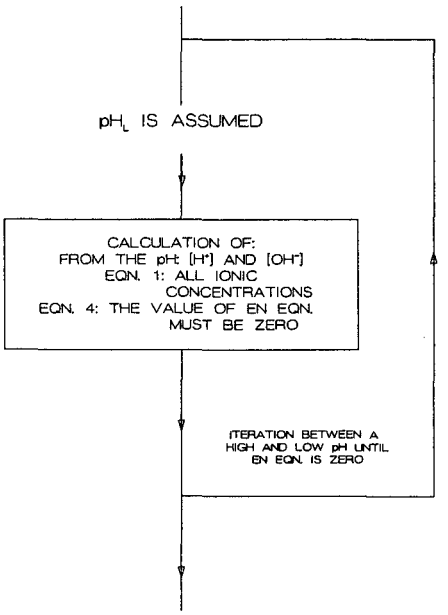

Fig. 3. Calculation procedure for the leading zone in ITP with two leading ions if the total concentrations of both the leading and buffering counter ionic species are known.

species can be calculated and by iterating between a low and high pH_L until the EN equation is met, the right pH_L can be obtained (see Fig. 3). For the calculation of the terminating L2 zone, first a pH_T is assumed (see Fig. 4), then the ratio E_T/E_L is assumed. From the buffer equation the buffer concentration and from the L2 balance the L2 concentration can be obtained. Using eqn. 1, all ionic concentrations can be obtained. Iterating, at the chosen pH_T, between a low and high E_T/E_L value the correct E_T/E_L value can be obtained using the EN. The correct pH_T can be found iterating between a low and high pH_T value using Ohm's law (see Fig. 4).

Mathematical model for the consecutive zones in a 2L system

The calculation of the parameters for the leading zone for a leading electrolyte with a known composition is similar to that for the foregoing model (see Fig. 3).

For the calculation of the sample zones in a 2L system, five equations are needed. The EN equation and Ohm's law are identical with those in the foregoing model, substituting the contribution of the ionic species L2 and A in these equations. The other three equations are the isotachophoretic condition and the mass balances of the buffer and L2 ions.

The isotachophoretic condition. In the steady state, all zones move with a velocity equal to that of the leading zone. This velocity is determined by the velocity of the L1 ion in the leading zone, and therefore

$$E_L \bar{m}_{L1,L} = E_A \bar{m}_{A,A} \tag{11}$$

Mass balance of the buffer. The mass balance of the buffer can be obtained by

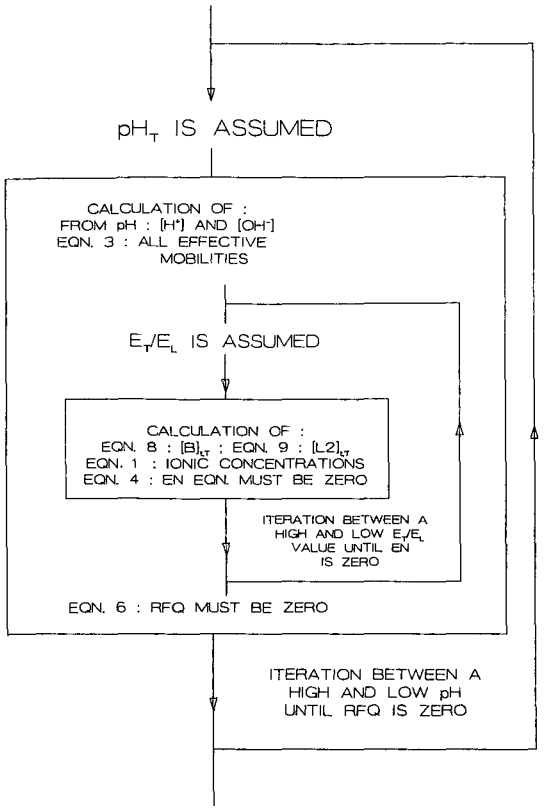

Fig. 4. Calculation procedure for the terminating L2 zone in ITP with two leading ions.

exchanging all parameters of the terminating zone by those of the A zone in eqn. 8. The mass balance will be

$$[B]_{t,A}(E_A|\bar{m}_{B,A}| + E_L|\bar{m}_{L1,L}|) = [B]_{t,L}(E_L|\bar{m}_{B,L}| + E_L|\bar{m}_{L1,L}|) \quad (12)$$

L2 balance. In a similar way to that described for the buffer balance, the L2 balance can be obtained by exchanging the T indices with A indices in eqns. 9. The L2 balance will be

$$E_L|\bar{m}_{L1,L}|[L2]_{t,L} + E_A|\bar{m}_{L2,A}|[L2]_{t,A} = E_L|\bar{m}_{L2,L}|[L2]_{t,L} + E_L|\bar{m}_{L1,L}|[L2]_{t,A} \quad (13A)$$

or

$$|\bar{m}_{L1,L}|[L2]_{t,L} + E_A/E_L|\bar{m}_{L2,A}|[L2]_{t,A} = |\bar{m}_{L2,L}|[L2]_{t,L} + |\bar{m}_{L1,L}|[L2]_{t,A} \quad (13B)$$

Calculation procedure. If a pH_A is assumed (see Fig. 5), then $[H^+]$ and $[OH^-]$ can be calculated and with eqn. 3 the effective mobilities can be calculated. With the IC (eqn. 11) the ratio E_A/E_L can be obtained. With the buffer balance the $[B]_{t,A}$ and with

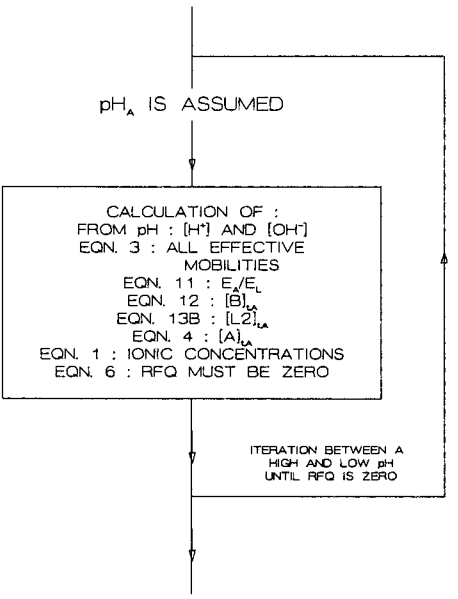

Fig. 5. Calculation procedure for the sample zones in ITP with two leading ions.

the L2 balance the $[L2]_{t,A}$ can be calculated. With the EN $[A]_{t,A}$ can be obtained. The correct pH_A can be found iterating between a low and high pH using Ohm's law.

EXPERIMENTAL

In the first instance, computer programs are set up for the calculation of parameters of the sample and terminating L2 zones with leading electrolytes consisting of two leading ions.

In Table I all ionic mobilities and pK values used in the calculations are given. In Table II some characteristic calculated parameters for the leading, sample and terminating L2 zone are given using these computer programs, *viz.*, the concentrations

TABLE I

pK VALUES AND IONIC MOBILITIES (m) FOR THE IONIC SPECIES USED IN THE CALCULATIONS

Ionic species	$m \times 10^5$ $(cm^2/V \cdot s)$	pK_A
Acetic acid	−42.4	4.76
Formic acid	−56.6	3.75
Histidine	+29.7	6.03
Hydrochloric acid	−79.1	−3.00
MES	−28.0	6.10
Propionic acid	−37.1	4.87

TABLE II

CALCULATED VALUES OF THE TOTAL CONCENTRATIONS OF THE SAMPLE IONS ($[A]_t$) AND L2 ($[L2]_t$), pH, SPECIFIC ZONE RESISTANCE AT 25°C (SZR_{25}), R_E AND RF FOR THE LEADING ZONE, SAMPLE ZONES AND TERMINATING L2 ZONE FOR SEVERAL COMPOSITIONS OF THE LEADING ELECTROLYTE AT A pH OF 6

Zone	$[A]_t$ *(mol/l)*	$[L2]_t$ *(mol/l)*	*pH*	SZR_{25} *(Ω m)*	R_E	RF *(10^5 C/mol)*
Leading: 0.01 M Cl^- + 0 M MES at pH 6:						
Leading L1/L2	–	0	6.0	10.33	1.00	1.30
70/3	0.0097	0	6.02	11.73	1.14	1.35
60/3	0.0092	0	6.04	13.76	1.33	1.42
50/3	0.0086	0	6.06	16.63	1.61	1.52
40/3	0.0078	0	6.10	21.01	2.03	1.67
30/3	0.0068	0	6.16	28.48	2.76	1.92
20/3	0.0053	0	6.27	43.93	4.26	2.46
Terminating L2	–	0.0065	6.42	43.21	4.18	–
Leading: 0.01 M Cl^- + 0.005 M MES at pH 6:						
Leading L1/L2	–	0.0050	6.0	9.33	1.00	1.45
70/3	0.0094	0.0052	6.02	10.60	1.14	1.54
60/3	0.0086	0.0054	6.04	12.43	1.33	1.69
50/3	0.0075	0.0058	6.08	15.04	1.61	1.94
40/3	0.0058	0.0067	6.13	19.02	2.04	2.51
30/3	0.0020	0.0096	6.24	25.74	2.76	7.43
20/3	No real values					
Terminating L2	–	0.0115	6.29	27.76	2.98	–
Leading: 0.01 M Cl^- + 0.01 M MES at pH 6:						
Leading L1/L2	–	0.0100	6.00	8.51	1.00	1.60
70/3	0.0092	0.0103	6.02	9.68	1.14	1.74
60/3	0.0080	0.0108	6.04	11.36	1.33	1.99
50/3	0.0064	0.0117	6.08	13.75	1.62	2.52
40/3	0.0036	0.0135	6.14	17.39	2.04	4.50
30/3	No real values					
20/3	No real values					
Terminating L2	–	0.017	6.22	20.90	2.45	–
Leading: 0.01 M Cl^- + 0.015 M MES at pH 6:						
Leading L1/L2	–	0.0150	6.00	7.84	1.00	1.75
70/3	0.0090	0.0155	6.02	8.92	1.14	1.95
60/3	0.0074	0.0162	6.05	10.48	1.34	2.35
50/3	0.0052	0.0176	6.09	12.69	1.62	3.37
40/3	0.0013	0.0205	6.16	16.06	2.05	14.02
30/3	No real values					
Terminating L2	–	0.0215	6.18	16.93	2.16	–
Leading: 0.01 M Cl^- + 0.02 M MES at pH 6:						
Leading L1/L2	–	0.0200	6.00	7.28	1.00	1.90
70/3	0.0087	0.0206	6.02	8.27	1.14	2.17
60/3	0.0069	0.0216	6.05	9.72	1.34	2.77
50/3	0.0040	0.0234	6.09	11.78	1.62	4.72
40/3	No real values					
30/3	No real values					
Terminating L2	–	0.0265	6.15	14.30	1.96	–

of the sample ions A and L2, the pH of the zones, the specific zone resistances at 25°C (SZR_{25}), the R_E values and the RF values[4]. The leading electrolytes consisted of 0.01 M Cl^- (L1) and different concentrations of MES (L2), at a pH_L of 6 by adding the buffer histidine. For the sample ionic species a pK of 3 was assumed and ionic mobilities varying from -70 to $-20 \cdot 10^{-5}$ cm^2/V · s. A sample ionic species denoted by 30/3 has a pK value of 3 and an anionic mobility of $30 \cdot 10^{-5}$ cm^2/V · s.

It can be concluded from Table II that with increasing concentration of L2 in the leading zone for all sample zones the SZR_{25} values decrease (increasing conductivity), the R_E values are nearly constant (according to the IC) but the R_E value of the terminating L2 zone decreases rapidly to low values, implying that a growing number of sample ions with low effective mobility will be passed by the terminator and consequently will not migrate in the ITP mode. In Fig. 6 the relationship between the calculated R_E values and the anionic mobility is shown. The arrows indicate the R_E value of the terminating L2 zone for a specific concentration of L2 in the leading electrolyte.

Ionic species with R_E values smaller than those of the terminating L2 zone will migrate in a proper ITP mode and ionic species with higher R_E values will migrate in a ZE mode. Further, the RF values of the sample ions increase at the same time because the sample ion concentrations are decreasing.

As a check on these mathematical models, we measured the RF values for formate, acetate and propionate in leading 2L systems, consisting of 0.01 M Cl^- and different concentrations of MES at a pH_L of 6 by adding the counter ionic species histidine. In Table III all calculated and experimentally determined RF and SZR_{25}

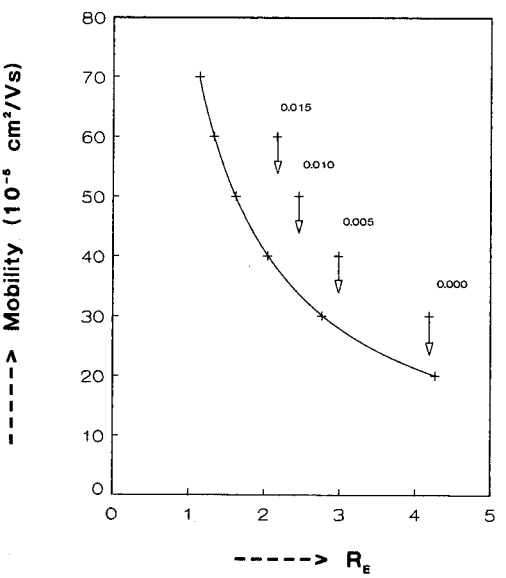

Fig. 6. Relationship between calculated R_E values and anionic mobility of ionic species for ITP systems with 0.01 M Cl^- and various concentrations of MES as leading ions at a pH_L of 6. The arrows indicate the calculated R_E values of the terminating MES zone. The numbers represent the concentration of MES (in M) in the leading electrolyte.

TABLE III

CALCULATED AND EXPERIMENTALLY DETERMINED SZR_{25} VALUES (Ω m) AND RF VALUES (10^5 C/mol) FOR THE ZONES IN A 2L SYSTEM WITH 0.01 M Cl^- AND DIFFERENT MES CONCENTRATIONS AS LEADING IONS AT A pH_L OF 6

Value	*Leading [MES] (M)*	*Calc.*	*Exptl.*	*Formate*		*Acetate*		*Propionate*		*Terminating*	
				Calc.	*Exptl.*	*Calc.*	*Exptl.*	*Calc.*	*Exptl.*	*Calc.*	*Exptl.*
SZR_{25}	0.000	10.33	10.33	14.67	14.61	20.50	20.49	23.78	23.76	43.21	39.55
	0.005	9.33	9.51	13.27	13.34	18.52	18.70	21.45	21.39	27.76	26.29
	0.010	8.51	8.45	12.12	11.91	16.94	16.61	19.60	19.02	20.90	19.76
		Formate		*Acetate*		*Propionate*					
		Calc.	*Exptl.*	*Calc.*	*Exptl.*	*Calc.*	*Exptl.*				
RF	0.000	1.45	1.41	1.62	1.61	1.72	1.71				
	0.005	1.76	1.80	2.41	2.71	3.15	3.68				
	0.010	2.13	2.25	4.07	5.00	10.81	12.20				

values are given. It can be concluded that the experimentally determined SZR_{25} and RF values fit the calculated values, although for high concentrations of MES in the leading electrolyte the experimentally determined RF values are too high. Possibly the steady state was not reached because very long zones with small differences in SZR_{25} values were the result.

In addition to the strong shift in RF values, another interesting point was the decreasing effect of the R_E values of the terminating L2 zone. For systems with 0.01 M Cl^- and MES concentrations varying from 0 to 0.02 M in the leading electrolyte, the R_E values of the terminating L2 zone changed from 4.18 to 1.96. It can be assumed, however, that at relative higher concentrations of L2 in the leading zones this effect will be even greater.

In Table IV the results of the calculations are given for leading electrolytes with 0.01 M MES and Cl^- concentrations varying from 0 to 0.01 M for the sample ionic species formate, acetate and propionate. The column mode indicates whether the ionic species really migrate in the ITP or CZE mode during experiments.

In Fig. 7 all electropherograms with the sample ionic species formate (F), acetate (A) and propionate (P) are shown, obtained using different leading electrolytes at pH_L 6 by adding the buffer histidine. The terminating zones are indicated with L2, the starting point of the analyses with an arrow and the leading electrolyte with two numbers indicating the concentrations of Cl^- and MES of the two leading ions. The experiments were carried out in a laboratory-made ITP apparatus with a conductivity detector (I.D. 0.4 mm)[2]. The electric current was 70 μA and the paper speed was 10 mm/min for all experiments. In order to see the ITP zones, large amounts of the sample have to be introduced. The sample consists of a mixture of 0.01 M formate, 0.01 M acetate and 0.01 M propionate. In this instance the zone electrophoretic zones are very broad and small because the amplification of the signals was the same as in the ITP experiments. Further, the rear sides of the zone electrophoretic peaks are sharp because the effective mobilities of the sample anions are higher than that of the anion

TABLE IV

CALCULATED VALUES OF THE CONCENTRATIONS OF SAMPLE IONS ($[A]_t$) AND L2 ($[L2]_t$), THE MIGRATION MODE, THE SPECIFIC ZONE RESISTANCE AT 25°C (SZR_{25}), R_E AND RF FOR THE LEADING ZONE, SAMPLE ZONE AND TERMINATING L2 ZONE FOR SEVERAL COMPOSITIONS OF THE LEADING ZONE AT A pH_L OF 6

Zone	$[A]_t$ *(mol/l)*	$[L2]_t$ *(mol/l)*	*Mode*	SZR_{25} *(Ω m)*	R_E	RF *(10^5 C/mol)*
Leading: 0 M Cl^- + 0.01 M MES:						
Leading L1/L2	–	0.01	–	42.35	1.00	–
Formate	No real values		Zone			
Acetate	No real values		Zone			
Propionate	No real values		Zone			
Leading: 0.002 M Cl^- + 0.01 M MES:						
Leading L1/L2	–	0.01	–	23.26	1.00	–
Formate	0.00029	0.011	ITP?	32.94	1.42	19.7
Acetate	No real values		Zone			
Propionate	No real values		Zone			
Terminating L2	No real values					
Leading: 0.004 M Cl^- + 0.01 M MES:						
Leading L1/L2	–	0.01	–	16.12	1.00	–
Formate	0.0021	0.0111	ITP	22.87	1.42	3.95
Acetate	No real values		Zone			
Propionate	No real values		Zone			
Terminating L2	–	0.0126	ITP	29.34	1.82	–
Leading: 0.007 M Cl^- + 0.01 M MES:						
Leading L1/L2	–	0.01	–	11.11	1.00	–
Formate	0.00481	0.0111	ITP	15.79	1.42	2.53
Acetate	0.00152	0.0133	ITP	22.01	1.98	8.00
Propionate	No real values		Zone			
Terminating L2	–	0.0146	ITP	24.34	2.19	–
Leading: 0.01 M Cl^- + 0.01 M MES:						
Leading L1/L2	–	0.01	–	8.51	1.00	–
Formate	0.00752	0.0111	ITP	12.11	1.42	2.13
Acetate	0.00394	0.0133	ITP	16.94	1.99	4.07
Propionate	0.00148	0.0152	ITP	19.6	2.30	10.81
Terminating L2	–	0.0165	ITP	20.90	2.45	–

of the background electrolyte (self-correcting boundary) where the fronts are diffuse.

However, some interesting conclusions can be drawn (see also Table IV). In the ITP experiment with the leading ion Cl^- at a concentration of 0.01 *M* (0.01/0, injected sample volume 4 μl), all sample ions migrate in the ITP mode. Using the leading ions 0.01 *M* Cl^- and 0.01 *M* MES (injected sample volume 3 μl), the sample ions also migrate in the ITP mode, although a relatively strong elongation of the propionate can be observed. In the system 0.007/0.01, formate and acetate migrate in the ITP mode (injected sample volume 2 μl; note the elongation of the acetate zone), whereas propionate migrates in the ZE mode. In the system 0.004/0.01 (injected sample volume 2 μl) only formate migrates in a proper ITP mode. In the system 0.002/0.01 (injected sample volume 2 μl), formate migrates just (or just not?) in the ITP mode and in the

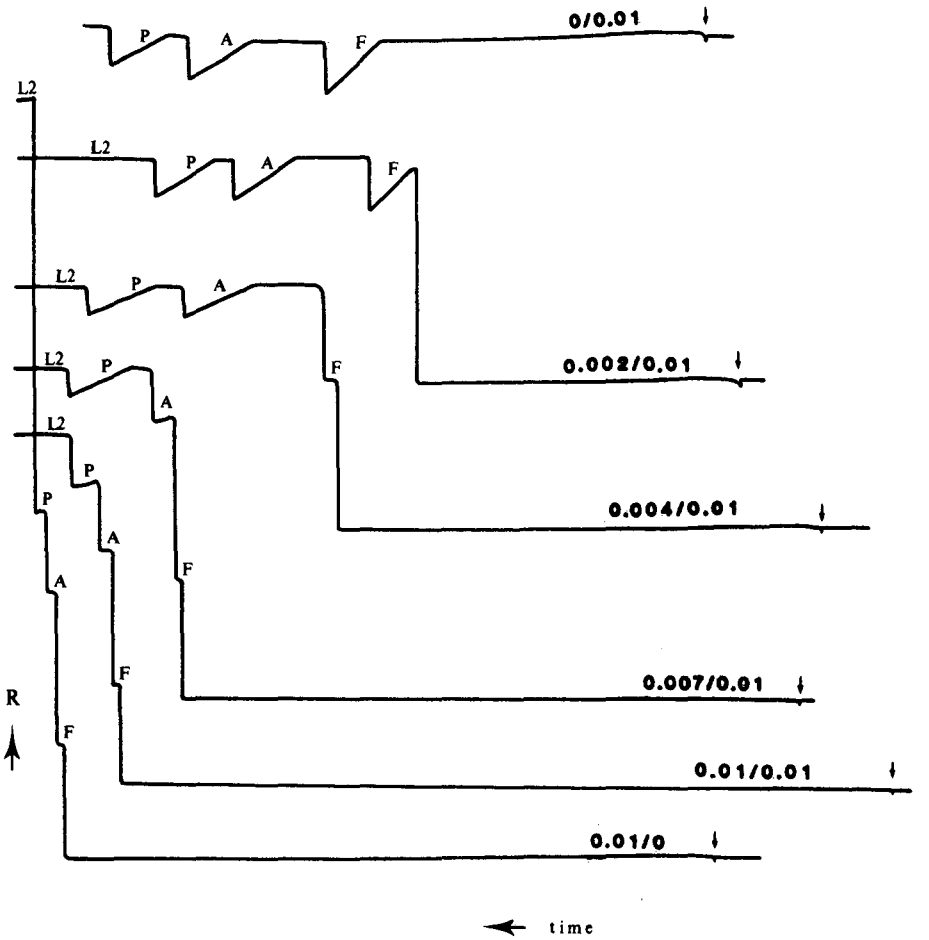

Fig. 7. Electropherograms for the separation of formate (F), acetate (A) and propionate (P) in different electrolyte systems. The leading electrolytes contain two leading ions, Cl^- (L1) and MES (L2), at a pH_L of 6 adjusted by adding the buffer histidine. The numbers refer to the leading ion concentrations L1 and L2, *e.g.*, 0.002/0.01 means that the concentrations of Cl^- and MES are 0.002 and 0.01 *M*, respectively. The terminator was 0.01 *M* MES. It can clearly be seen that ITP changes into ZE at lower Cl^- concentrations. All experiments were carried out at an electric current of 70 μA and a paper speed of 10 mm/min with an ITP apparatus with a capillary tube of 0.4 mm I.D. and a conductivity detector.

system 0/0.01 (injected sample volume 2 μl) all sample ions migrate clearly in the ZE mode.

It is clear that it is possible to obtain in one electropherogram several different modes[1], *e.g.*, first sample ions migrating in the ZE mode (if their effective mobilities are larger than that of the leading ion), followed by ionic species migrating in the ITP mode, followed by sample ions again migrating in the ZE mode (if their mobilities are smaller than that of the terminating ion).

CONCLUSION

The mathematical model for the steady state in ITP has been extended for the use of leading electrolytes with two leading ionic species. Experimentally obtained values for R_E and RF confirm the validity of this model. The interesting point in the use of 2L systems is that RF values increase in the presence of a second leading ion L2, with a low effective mobility, through which the detection limit can be lowered. This may be the reason for too high RF values in anionic systems at higher pH_L values, owing to the presence of unwanted (hydrogen)carbonate in the leading electrolyte. Further, this model shows that using a second leading ion L2, the R_E value of the terminating L2 zone decreases strongly and the ITP mode changes into a ZE mode for many sample ions.

SYMBOLS

A	sample ionic species A
B	buffering counter ionic species B
E	electric field strength (V/m)
F	Faraday constant (C/equiv.)
K	concentration equilibrium constant
L	leading ionic species L
L1	leading ionic species with the highest mobility in a 2L system
L2	leading ionic species with the lowest mobility in a 2L system
m	mobility at infinite dilution ($m^2/V \cdot s$)
$\bar{m}$	effective mobility ($m^2/V \cdot s$)
n	number of protolysis steps
T	terminating ionic species
z	charge of an ionic species (equiv./mol)
α	degree of dissociation
σ	zone conductivity ($\Omega^{-1}m^{-1}$)

First subscripts

A, B, T and L	according to substance A, B, T and L
t	total

Second subscripts

A, B, T and L	in the zone of substance A, B, T and L

Superscripts

z	maximum charge of an ionic species
i	to the ith degree

Examples

$[B]_{t,A}$	total concentration of substance B in zone A
$\lvert\bar{m}_{B,A}\rvert$	absolute value of the effective mobility of substance B in the zone of substance A

ABBREVIATIONS

2L	system with two leading ions
CZE	capillary zone electrophoresis
EN	electroneutrality condition
IC	isotachophoretic condition
ITP	isotachophoresis
MES	2-(N-morpholino)ethanesulphonic acid
R_E	electric field strength in a zone divided by the electric field strength of the leading zone
RF	response factor (C/mol)
SZR_{25}	specific zone resistance at 25°C (Ω m)

REFERENCES

1 F. E. P. Mikkers and F. M. Everaerts, in F. M. Everaerts, F. E. P. Mikkers and Th. P. E. M. Verheggen (Editors), *Analytical Isotachophoresis*, Elsevier, Amsterdam, 1981, pp. 1–17.
2 F. M. Everaerts, J. L. Beckers and Th. P. E. M. Verheggen, *Isotachophoresis—Theory, Instrumentation and Applications*, Elsevier, Amsterdam, 1976.
3 J. L. Beckers and F. M. Everaerts, *J. Chromatogr.*, 480 (1989) 69.
4 J. L. Beckers and F. M. Everaerts, *J. Chromatogr.*, 470 (1989) 277.
5 A. Tiselius, *Nova Acta Reg. Soc. Sci. Ups., Ser. 4*, (1930) 4.

Journal of Chromatography, 508 (1990) 19–26
Elsevier Science Publishers B.V., Amsterdam — Printed in The Netherlands

CHROM. 22 301

Isotachophoresis with two leading ions and migration behaviour in capillary zone electrophoresis

II. Migration behaviour in capillary zone electrophoresis

J. L. BECKERS* and F. M. EVERAERTS
Laboratory of Instrumental Analysis, Eindhoven University of Technology, P.O. Box 513, 5600 MB Eindhoven (The Netherlands)
(First received December 1st, 1989; revised manuscript received January 22nd, 1990)

SUMMARY

During a zone electrophoretic analysis, components can migrate in the isotachophoretic mode. If, for example in anionic separation in capillary zone electrophoresis an anion with a high effective mobility is present in the sample at a very high concentration, it migrates forwards into the background electrolyte, separates from the other components and forms an isotachophoretic system with two leading ions together with the anion of the background electrolyte. Some of the sample components will therefore migrate in the isotachophoretic mode for the greater part of the analysis time. Because in the isotachophoretic mode the zone lengths are constant, very small sample zone lengths will give extremely high plate numbers. Of course, migration times will vary strongly depending on the composition of the sample.

INTRODUCTION[a]

Electrophoretic techniques can be divided in four main types, *viz.*, isotachophoresis (ITP), zone electrophoresis (ZE), moving-boundary electrophoresis (MB) and isoelectric focusing (IEF). The apparatus needed for all these techniques is identical in essence and consists of modules, *viz.*, separation, injection, detection and electrode modules. The only difference in order to carry out an experiment in a specific mode is the choice of the electrolytes in the different parts of the apparatus. If, for example an ITP analysis has to be performed, the separation module has to be filled with a leading electrolyte the anion (cation) of which has an effective mobility higher than any of the sample anions (cations), whereas the effective mobility of the anion (cation) of the terminating electrolyte must be lower. In ZE the whole apparatus generally will be filled with one background electrolyte.

[a] Symbols and abbreviations follow those defined in Part I.

0021-9673/90/$03.50

If these requirements are not met, disturbances in the separation can be expected. If in an ITP mode a sample ion is present with an effective mobility higher than that of the leading ion, this ion will migrate into the leading zone and will migrate there in a ZE mode. Analogously, a sample ion with a lower effective mobility than that of the terminator will migrate in a ZE mode in the terminator zone. It will be clear that often one can hardly distinguish between the four main types of electrophoresis as several electrophoretic modes can exist in a single experiment.

Recently, Verheggen *et al.*[1] reported on the phenomenon that extremely high plate numbers could be obtained in the anionic ZE analysis of, *e.g.*, uric and hippuric acid in serum. Schoots *et al.*[2] recognized the fact that these high plate numbers are due to the presence of the large amount of chloride in the samples and noted the analogy with the solvent effect in chromatography. Plate numbers of over 10^6 could easily be obtained by adding large amounts of chloride to a sample.

Using the concept of plate numbers[3,4], generally maximum numbers of 10^6 can be obtained theoretically. Extremely high plate numbers can only be explained if sample ions were to migrate in the ITP mode during a ZE analysis. Because in ITP the zone lengths are constant and the zones are sharp owing to the self-correcting effect of the ITP zones, very small sample zone lengths will give very high plate numbers. The question is, however, why an ITP procedure can exist in a CZE procedure and whether it leads to a steady state. Mikkers and Everaerts[5] mentioned earlier that ITP with two leading ions can be applied.

In Part I[6], we gave a mathematical model for isotachophoresis with a leading electrolyte with two leading ions. Calculations showed that at a certain concentration ratio of the two leading ions, also dependent on the effective mobilities of these ions, the terminating zone, consisting of the leading ion with the lowest effective mobility, has a smaller E gradient than that of a specific sample ion, *i.e.*, that this ionic species will migrate in a CZE mode. Isotachophoresis changes into CZE. A close relationship exists in this way between ITP and CZE, as often the first stage in the CZE separation is a moving-boundary procedure followed by a non-steady-state ITP separation. Later in the separation procedure a CZE procedure is the result.

The idea was now that in the first instance the large amount of chloride separates from the other components, migrates forwards into the background electrolyte and hence will create an ITP separation mode with a leading electrolyte with two leading ions, *viz.*, the chloride ions and the anions of the background (MES). By this means, some other sample ions will migrate in an ITP mode behind the two leading ions (see Part I), showing extremely high plate numbers.

Because it is not possible with our apparatus to follow the migration procedure with detectors at the injection point, simulations are used to show these migration phenomena in the first stage of CZE separations.

THEORY

A typical difference between electrophoretic and chromatographic techniques is that in electrophoresis at any point the situation is determined by the initial conditions. Kohlrausch formulated this in 1897 by his "regulation function". This means that in electrophoresis the concentration of the injected sample adapts to the initial concentration of the background electrolyte migrating in the separation capillary tube.

Very dilute samples will be concentrated. Using electromigration injection, this concentration effect occurs directly during the injection by a moving-boundary migration. In that event, no representative aliquot will be introduced. The quality of the CZE separation depends for the greater part on this concentration effect. Parameters such as mobilities and concentrations of all ions present in the system play an important role.

In order to illustrate the effect of these parameters, simulations of the CZE process are carried out by means of a numerical solution of the basic transport equation:

$$\frac{\delta c}{\delta t} = -\frac{\delta(mEc)}{\delta x} + \mathrm{D} \cdot \frac{\delta^2 c}{\delta x^2} \tag{1}$$

where c is the concentration of the ionic species and x is the position in the separation tube. The electric field strength E was calculated from the electric current density i by

$$i = E \sum_j c_j m_j F z \tag{2}$$

whereby F is the Faraday constant and j represents the summation over all ionic particles.

The diffusion constant D was calculated using the equation

$$D = mkT/ze \tag{3}$$

where k is the Boltzmann constant, T is the absolute temperature and ze is the charge of the ionic species.

Concentration effect of the sample

During the first stage of CZE, the sample ionic species in diluted samples will be concentrated. In Fig. 1 this effect is shown by a simulation for the introduction of a dilute sample consisting of two anions. The conditions for the simulation of the zone electrophoretic separation are given in Table I. The sample is introduced into the separation chamber between the positions 1 and 2 mm. After 0.01 s the sample anion 1 is partially concentrated at the original boundary between leading ion and sample ions (see Fig. 1A 2 mm) to about 0.0016 M and shows a diffuse front. At the same time sample anion 2 shows a similar behaviour but shows also an increase in concentration at the rear side (see Fig. 1B). There it is partially separated from sample anion 1 and its concentration is adapted to the orginal total concentration of both sample anions. If sample anion 1 were to be present at a higher concentration, this effect would also be much stronger. The background anions do not pass the sample ions (not shown in the figures) because their mobility is lower than those of the sample anions. In fact, at the rear side the anions migrate in the ITP mode. Further, it can be noted that at the injection point the E gradient is very high because of the low concentration of the sample ions. Owing to this very high E gradient between positions 1 and 2 mm, the concentration effect occurs very quickly.

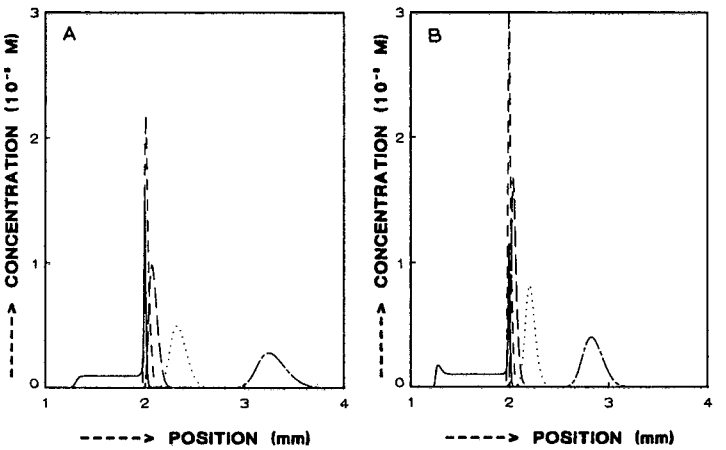

Fig. 1. Concentration profiles for the simulation of a zone electrophoretic separation of two anions. (A) Concentration profiles of anion 1 and (B) those of anion 2 after a separation time of (———) 0.01 s, (– – –) 0.04 s, (— —) 0.1 s, (· · · · · ·) 0.3 s and (— · — ·) 1 s. On the horizontal axis the position in the separation tube is given in mm. The sample introduction was between 1 and 2 mm.

After 0.04 s the concentration effect is completed and the concentration of sample anion 1 is about 0.0022 *M* and that of sample anion 2 is 0.0033 *M*. The peaks are very sharp. The simulation at 0.1, 0.3 and 1 s show that in the first stage of the ZE separation the effect of the zone broadening is very strong.

Effect of two leading ions in ITP

In Fig. 2 the simulation is given for an anionic ITP separation using two leading ions after 15 s. In Table II the conditions for this simulation are given. In the simulation it is clearly shown that sample anion 1 migrates in the ITP mode and follows the leading zone L1/L2 whereas sample anions 2 and 3 migrate in the ZE mode with peaks broadening in time.

The original injection point was between 1 and 2 mm and at $t = 15$ s the terminating L2 zone is still adapted to the original concentrations of the sample anions.

TABLE I

CONDITIONS FOR THE SIMULATION OF AN ANIONIC ZONE ELECTROPHORETIC SEPARATION

Electric current, 20 μA; capillary I.D., 0.2 mm.

Species	*Concentration (M)*	*Ionic mobility* × 10^5 *(cm²/V · s)*
Background anion	0.01	−20
Counter ion	0.01	+15
Sample anion 1	0.0001	−75
Sample anion 2	0.0001	−50

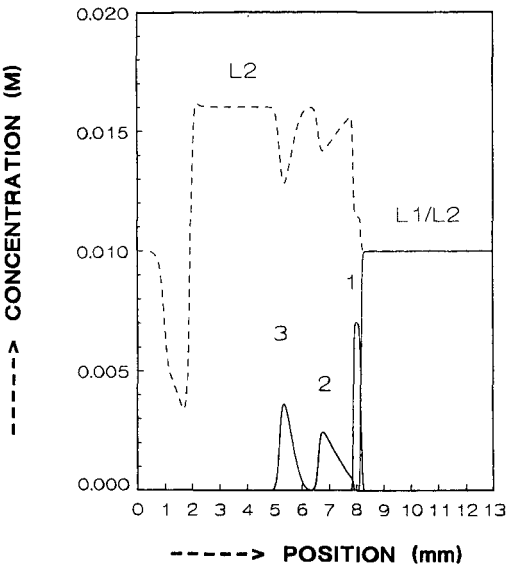

Fig. 2. Concentration profiles for the simulation of a separation of three anions in ITP with two leading ions. Sample anion 1 migrates in the ITP mode behind the leading ions L1 and L2. The sample anion 2 and 3 migrate in the ZE mode.

Effect of an excess of one of the sample ions in ZE

In Figs. 3 and 4 the simulations are given for an anionic ZE separation of a sample containing one of the components in a large excess. The conditions for the simulation are given in Table III. The original injection point was between 1 and 2 mm.

In Fig. 3 the concentration profiles of the four components after 4, 7, 10, 13, 16

TABLE II

CONDITIONS FOR THE SIMULATION OF AN ANIONIC ITP SEPARATION USING TWO LEADING IONS

Electric current, 20 μA; capillary I.D., 0.2 mm.

Species	*Concentration (M)*	*Ionic mobility* $\times 10^5$ *($cm^2/V \cdot s$)*
Leading electrolyte:		
Leading L1	0.01	−75
Leading L2	0.01	−15
Counter	0.02	+15
Terminating electrolyte:		
Terminating L2	0.01	−15
Counter	0.01	+15
Sample anions:		
Sample anion 1	0.002	−50
Sample anion 2	0.002	−30
Sample anion 3	0.002	−20

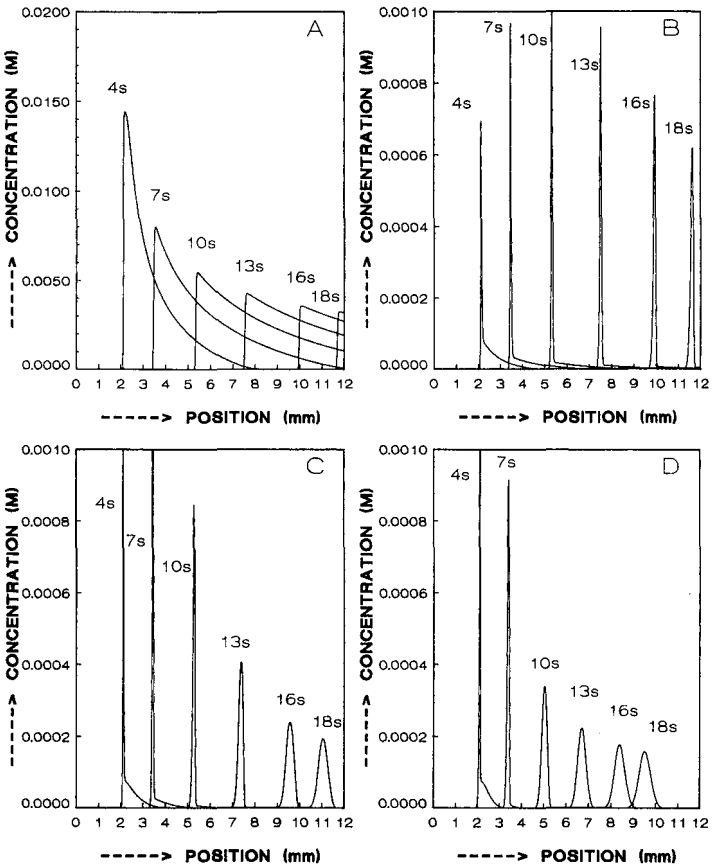

Fig. 3. Concentration profiles for the simulation of a ZE separation of four anions. The anion 1 with the highest mobility is present in excess in the sample. In A, B, C and D the concentration profiles are given for the sample anions 1, 2, 3 and 4, respectively, at separation times of 4, 7, 10, 13, 16 and 18 s.

and 18 s are shown. In Fig. 3A it can clearly be seen that the rearside of the component present in a large excess in the sample is sharp and that the component diffuses into the background electrolyte. This component forms together with the anion of the background an ITP leading electrolyte with two leading ions. The concentration of this component in this leading electrolyte decreases with time, as a result of which only the most mobile of other components will ultimately migrate in the ITP mode. This can be seen in Fig. 3B, where the most mobile of the sample ions migrates ultimately in the ITP mode and shows nearly no peak broadening with time. From Fig. 3C and D it can be concluded that these anions migrate from 13 and 10 s, respectively, in the CZE mode (zone broadening).

In Fig. 4 the concentration profiles of all sample components are given after 18 s. In Fig. 4 the concentration of the component in excess is ten times higher as indiated. The similarity with the ITP separation with two leading ions in Fig. 2 can clearly be seen. In Fig. 2, sample anion 1 migrates in the ITP mode behind the leading zone with

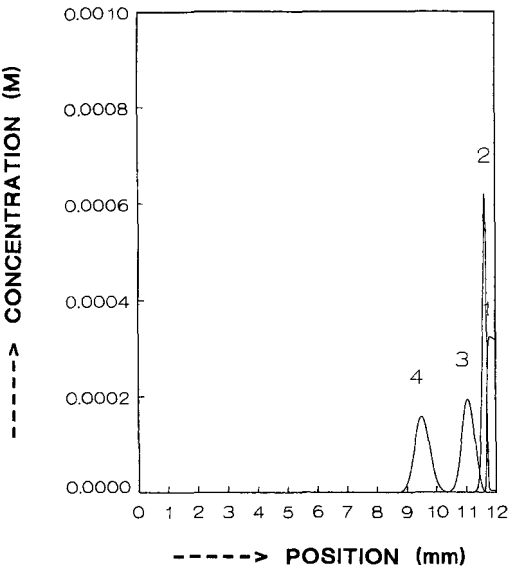

Fig. 4. Concentration profiles for the simulation of a ZE separation of four anions after 18 s. The anion 1 with the highest mobility is present in excess in the sample.

two leading ions (L1 and L2) where as in Fig. 4 the anion 2 migrates in the ITP mode behind the leading zone consisting of the anion of the background electrolyte and anion 1, the sample anion present in the sample in excess. The other two sample anions migrate in the ZE mode and show lower concentrations and zone broadening.

TABLE III

CONDITIONS FOR THE SIMULATION OF AN ANIONIC ZONE ELECTROPHORETICAL SEPARATION OF A SAMPLE CONTAINING A LARGE EXCESS OF ONE SAMPLE COMPONENT

Electric current, 20 μA, capillary I.D., 0.2 mm.

Species	*Concentration (M)*	*Ionic mobility* $\times 10^5$ *($cm^2/V \cdot s$)*
Background electrolyte:		
Anion	0.01	−20
Counter ion	0.01	+15
Sample anions:		
Sample anion 1	0.02	−75
Sample anion 2	0.0001	−50
Sample anion 3	0.0001	−40
Sample anion 4	0.0001	−30

CONCLUSIONS

If in ITP the leading electrolyte contains two leading ions, some sample components will migrate in the ITP mode and others in the CZE mode (see Part I). If in CZE a sample is analysed with a large amount of, *e.g.*, chloride, in first instance the ions separate and if the separation is (partially) completed the chloride ions migrate in front of the other sample ions. The chloride ions migrate from the injection position into the background electrolyte and will form in first instance an ITP system with two leading ions. Depending on the concentrations and the effective mobilities, some sample ions will migrate in the ITP and others in the CZE mode. The composition of the two leading ion system changes continuously because chloride migrates through the background electrolyte. This means that the concentration ratio L1/L2 of the 2L system decreases with time and more components will finally migrate in the CZE mode. If the capillary tube is long enough, all components will ultimately migrate in the CZE mode.

The number of plates strongly depends on this procedure. A component migrating all the time in the CZE mode will show plate numbers determined by the CZE migration behaviour. A component migrating (nearly) all the time in the ITP mode will show extremly high plate numbers, because the zone lengths are constant. This means that the use of the traditional concept of plate numbers often will be not useful. The separation capacity is often determined by the ITP behaviour. The use of migration times can also be troublesome, especially when working in the electro-osmostic flow (EOF) mode. Further investigations are needed to decide what the effects are of sampling, sample composition and the use of EOF on separation capacity, plate numbers and migration times. It is extremely important to report sufficient experimental conditions in papers concerning CZE experiments.

REFERENCES

1 Th. P. E. M. Verheggen, A. C. Schoots and F. M. Everaerts, *J. Chromatogr.*, 503 (1990) 245.
2 A. C. Schoots, Th. P. E. M. Verheggen, P. M. J. M. de Vries and F. M. Everaerts, *Clin. Chem. (Winston-Salem, N.C.)*, 36 (1990) 435.
3 J. W. Jorgenson and K. DeArman Lukacs, *Anal. Chem.*, 53 (1981) 1298.
4 J. H. Knox, *Chromatographia*, 26 (1988) 329.
5 F. E. P. Mikkers and F. M. Everaerts, in F. M. Everaerts, F. E. P. Mikkers and Th. P. E. M. Verheggen (Editors), *Analytical Isotachophoresis*, Elsevier, Amsterdam, 1981, pp. 1–17.
6 J. L. Beckers and F. M. Everaerts, *J. Chromatogr.*, 508 (1990) 3.

Journal of Chromatography, 508 (1990) 27–36
Elsevier Science Publishers B.V., Amsterdam — Printed in The Netherlands

CHROM. 22 280

Perturbation analysis of the influence of the isotherm coupling factor on the resolution between two compounds in chromatography

BINGCHANG LIN, SADRODDIN GOLSHAN-SHIRAZI and GEORGES GUIOCHON*
**Department of Chemistry, University of Tennessee, Knoxville, TN 37996-1600, and Division of Analytical Chemistry, Oak Ridge National Laboratory, Oak Ridge, TN 37831-6120 (U.S.A.)*
(First received February 21st, 1989; revised manuscript received January 1st, 1990)

SUMMARY

The influence of the coupling factor between the adsorption isotherms of the two components of a binary mixture on the elution profiles of their bands in liquid chromatography, on their retention times and on the resolution between these bands is discussed using a perturbation approach.

INTRODUCTION

The elution of the components of a complex mixture through a chromatographic column is easily described in linear chromatography. The migration of each band and its progressive broadening are independent of the migration and broadening of the other component bands. The chromatogram of the mixture is the superimposition of the chromatograms obtained with each of the individual components injected pure, successively, in the same amount as is in the sample mixture. A series of Gaussian bands is obtained, provided that there is a single retention mechanism involved and the kinetics of mass transfer between and across phases are fast enough. Obviously, some of these bands may interfere, but these interferences result merely in the addition of the detector signals corresponding to each band profile. The local concentrations of the two or more component whose bands interfere remain independent.

A different situation arises when the sample size is not negligible. Then, the chromatogram of the mixture is not the sum of the chromatograms of all the components of the mixture, and the chromatographic phenomenon becomes non-linear. This happens because the equilibrium isotherms of at least some of the components (the main ones) are not linear and because the equilibrium isotherms of most of these components depend on the concentrations of all or almost all the other components.

Several recent studies have been published on the behavior of the bands of a binary mixture at high concentrations involving the use of numerical solutions calculated with a computer[1–6]. When samples of large or very large sizes are injected,

0021-9673/90/$03.50

the non-linear behavior of the equilibrium isotherm is the main source of band broadening and is, in fact, the factor which controls the band profile. The shock and shock layer theories[7] and the semi-ideal model[8] account very well for the band profiles obtained in elution and displacement chromatography, for the progressive separation of these bands and for their interference when separation is incomplete.

More fundamental approaches have been tried. The characteristic method has been extremely useful in providing an accurate description of the phenomena involved in the migration of the high-concentration bands and in explaining their profiles[7,9,10]. The shock theory is based on the results of this method[11]. The hodograph transform has been applied to the study of the elution band of a binary mixture and the results have been explained by the characteristic theory[12].

A complementary approach, focusing on the phenomena that take place at the onset of non-linear behavior, would be interesting. Of special importance is an understanding of the various effects arising in analytical applications of chromatography when columns are overloaded, such as in trace analysis. The approach of Houghton[13], who assumed a parabolic equilibrium isotherm and integrated a simplified mass balance equation, permits the investigation of the band profile at the beginning of column overload. Lin *et al.*[14] have successfully applied the perturbation theory to the same mass balance equation and predicted the progressive transition of the band profile from a symmetrical Gaussian curve to a tailing profile.

The aim of this work was to extend this type of investigation to the case of a binary mixture and to study how the bands of two closely eluted compounds begin to interfere when the sample size is increased. The work was carried out within the framework of the ideal model[10–12].

MATHEMATICAL MODEL

We used the ideal model of chromatography, which assumes constant equilibrium between the two phases of the chromatographic system during the migration of a concentration signal. More specifically, we assume that the kinetics of mass transfers between phases are infinitely fast and that the axial dispersion proceeds at a negligible rate. Under these conditions the mass balances of the two components of a binary mixture can be written as

$$\frac{\partial C_1}{\partial t} + F\frac{\partial q_1}{\partial t} + u\frac{\partial C_1}{\partial x} = 0 \tag{1}$$

$$\frac{\partial C_2}{\partial t} + F\frac{\partial q_2}{\partial t} + u\frac{\partial C_2}{\partial x} = 0 \tag{2}$$

We assume that the injection profile is a rectangular pulse of maximum concentrations C_1^0 and C_2^0 and width t_p, and consequently that the initial condition is described by

$$C_1(x,0) = C_2(x,0) = q_1(x,0) = q_2(x,0) = 0 \qquad x>0 \tag{3}$$

and that the boundary condition is given by

$$C_1(0,t) = C_1^0 \qquad C_2(0,t) = C_2^0 \qquad 0<t\leqslant t_p$$

and

$$C_1(0,t) = C_2(0,t) = 0 \qquad t > t_p \tag{4}$$

C_1, C_2, q_1 and q_2 are the concentrations of components 1 and 2 in the mobile and the stationary phases at time t and abscissa x, respectively; u is the mobile phase velocity and F the phase ratio, *i.e.*, V_s/V_m.

We have also assumed that the equilibrium isotherms of the two compounds studied are given by the classical binary Langmuir isotherm equations:

$$q_1 = \frac{a_1 C_1}{1 + b_1 C_1 + b_2 C_2} \tag{5}$$

$$q_2 = \frac{a_2 C_2}{1 + b_1 C_1 + b_2 C_2} \tag{6}$$

In eqns. 5 and 6, a_1, a_2, b_1 and b_2 are constants. They are the parameters of the Langmuir isotherm. The considerable advantage of this equation is that the coupling terms which are $b_2 C_2$ for the first component and $b_1 C_1$ for the second component, can be determined directly from experimental results regarding the single compound equilibrium isotherms of the pure components 1 and 2. No experiment involving mixtures of the two compounds is required, which is a great simplification.

PERTURBATION ANALYSIS

Since q_1 and q_2 are both functions of the two concentrations, C_1 and C_2, we have the following relationships between their partial differentials:

$$\frac{\partial q_1}{\partial t} = \frac{\partial q_1}{\partial C_1} \cdot \frac{\partial C_1}{\partial t} + \frac{\partial q_1}{\partial C_2} \cdot \frac{\partial C_2}{\partial t} \tag{7}$$

and

$$\frac{\partial q_2}{\partial t} = \frac{\partial q_2}{\partial C_2} \cdot \frac{\partial C_2}{\partial t} + \frac{\partial q_2}{\partial C_1} \cdot \frac{\partial C_1}{\partial t} \tag{8}$$

The partial differentials of the concentrations in the stationary phase, q_1 and q_2 can be derived from eqns. 5 and 6:

$$\frac{\partial q_1}{\partial C_1} = \frac{a_1(1+b_2C_2)}{(1+b_1C_1+b_2C_2)^2} \tag{9}$$

$$\frac{\partial q_2}{\partial C_2} = \frac{a_2(1+b_1C_1)}{(1+b_1C_1+b_2C_2)^2} \tag{10}$$

$$\frac{\partial q_1}{\partial C_2} = \frac{-a_1 b_2 C_1}{(1+b_1 C_1+b_2 C_2)^2} \tag{11}$$

$$\frac{\partial q_2}{\partial C_1} = \frac{-a_2 b_1 C_2}{(1+b_1 C_1+b_2 C_2)^2} \tag{12}$$

As we are studying the changes in band profiles, retention times and resolution which take place at the onset of column overloading with a binary mixture, we may assume that the concentrations C_1 and C_2 are small and that the terms $b_1 C_1$ and $b_2 C_2$ are much smaller than unity. Then we may simplify eqns. 9–12 using the classical approximation $1/(1+x) \approx 1-x$:

$$\frac{\partial q_1}{\partial C_1} = a_1 - 2a_1 b_1 C_1 - a_1 b_2 C_2 \tag{13}$$

$$\frac{\partial q_2}{\partial C_2} = a_2 - 2a_2 b_2 C_2 - a_2 b_1 C_1 \tag{14}$$

$$\frac{\partial q_1}{\partial C_2} = -a_1 b_2 C_1 \tag{15}$$

$$\frac{\partial q_2}{\partial C_1} = -a_2 b_1 C_2 \tag{16}$$

Combination of eqns. 7, 8 and 13–16 with eqns. 1 and 2 gives the following equations, which are first-order approximations of the mass balance equations:

$$(1 + Fa_1 - 2Fa_1 b_1 C_1 - Fa_1 b_2 C_2) \frac{\partial C_1}{\partial t} - Fa_1 b_2 C_1 \frac{\partial C_2}{\partial t} + u \frac{\partial C_1}{\partial x} = 0 \tag{17}$$

and:

$$(1 + Fa_2 - 2Fa_2 b_2 C_2 - Fa_2 b_1 C_1) \frac{\partial C_2}{\partial t} - Fa_2 b_1 C_2 \frac{\partial C_1}{\partial t} + u \frac{\partial C_2}{\partial x} = 0 \tag{18}$$

The principle of the perturbation method consists in assuming that the solutions of the system of non-linear partial differential eqns. 1 and 2 are close to the solutions of the corresponding system of linear equations, *i.e.*, of the system of eqns. 1 and 2 in which the isotherms q_1 and q_2 are merely proportional to C_1 and C_2, respectively. Then we can write

$$C_1 = C_1^{\mathrm{d}} + C_1' \tag{19}$$

$$C_2 = C_2^{\mathrm{d}} + C_2' \tag{20}$$

where C_1^d and C_2^d are the solutions of the system of eqns. 1 and 2, where the two isotherms are $q_1 = a_1C_1$ and $q_2 = a_2C_2$ instead and where C_1' and C_2', which are both functions of C_1 and C_2, are small.

C_1^d and C_2^d are given by the following equations:

$$(1 + Fa_1)\frac{\partial C_1^d}{\partial t} + u\frac{\partial C_1^d}{\partial x} = 0 \tag{21}$$

$$(1 + Fa_2)\frac{\partial C_2^d}{\partial t} + u\frac{\partial C_2^d}{\partial x} = 0 \tag{22}$$

Replacing C_1 and C_2 in the left-hand side of eqns. 17 and 18 by their new expressions (eqns. 19 and 20), subtracting eqns. 21 and 22 from eqns. 17 and 18, respectively, and considering only the first-order terms, we obtain

$$(1 + Fa_1)\frac{\partial C_1'}{\partial t} + u\frac{\partial C_1'}{\partial x} = (2Fa_1b_1C_1^d + Fa_1b_2C_2^d)\frac{\partial C_1^d}{\partial t} + Fa_1b_2C_2^d\frac{\partial C_2^d}{\partial t} \tag{23}$$

$$(1 + Fa_2)\frac{\partial C_2'}{\partial t} + u\frac{\partial C_2'}{\partial x} = (2Fa_2b_2C_2^d + Fa_2b_1C_1^d)\frac{\partial C_2^d}{\partial t} + Fa_2b_1C_2^d\frac{\partial C_1^d}{\partial t} \tag{24}$$

Eqns. 23 and 24 are linear partial differential equations for the perturbation terms C_1' and C_2'. They are still coupled, however, through the terms in their right-hand sides.

LAPLACE TRANSFORMS AND MOMENT ANALYSIS

In spite of the simplification made, it is still impossible to solve eqns. 23 and 24. As they are linear, it is possible, however, to take their Laplace transform and to derive the first moment of the band of each compound of the binary mixture. This permits the calculation of the variation of the retention time with increasing sample size.

The Laplace transforms are

$$(1 + Fa_1)\overline{PC_1'} + u\frac{d\overline{C_1'}}{dx} = Fa_1p(b_1\overline{C_1^{d^2}} + b_2\overline{C_1^dC_2^d}) \tag{25}$$

$$(1 + Fa_2)\overline{PC_2'} + u\frac{d\overline{C_2'}}{dx} = Fa_2p(b_2\overline{C_2^{d^2}} + b_1\overline{C_1^dC_2^d}) \tag{26}$$

where

$$\bar{w} = \int_0^\infty e^{-pt}w(x,t)dt \tag{27}$$

Eqns. 25 and 26 are first-order non-homogeneous differential equations. Their solutions are

$$\overline{C_1'} = \exp\left[\frac{-p(1 + Fa_1)x}{u}\right]\left\{\int_0^x \frac{Fa_1}{u}\left(b_1 p\overline{C_1^{d^2}} + b_2 p\overline{C_1^d C_2^d}\right)\exp\left[\frac{p(1 + Fa_1)x'}{u}\right]dx'\right\} \quad (28)$$

and

$$\overline{C_2'} = \exp\left[\frac{-p(1 + Fa_2)x}{u}\right]\left\{\int_0^x \frac{Fa_2}{u}\left(b_2 p\overline{C_2^{d^2}} + b_1 p\overline{C_1^d C_2^d}\right)\exp\left[\frac{p(1 + Fa_2)x'}{u}\right]dx'\right\} \quad (29)$$

The two integration constants are 0, because $C_1'(x=0) = C_2'(x=0) = 0$. The first-order moments, $\mu_{1,i}$, of the two compounds, $i = 1, 2$, are related to the Laplace transform, $\overline{C_i}$, by the following equation:

$$\mu_{1,i} = -\lim_{p\to 0}\frac{1}{\overline{C_i}}\cdot\frac{d\overline{C_i}}{dp} \qquad (i = 1, 2) \quad (30)$$

Let

$$\mu_{1,i} = \mu_{1,i}^0 + \mu_{1,i}' \quad (31)$$

where $\mu_{1,i}^0$ is the first moment, *i.e.*, the retention time, of compound i under linear conditions:

$$\mu_{1,i}^0 = -\lim_{p\to 0}\frac{1}{\overline{C_i^d}}\cdot\frac{d\overline{C_i^d}}{dp} \quad (32)$$

In the ideal model, we have no band broadening. Thus the retention time under linear conditions is

$$\begin{aligned}\mu_{1,i}^0 &= t_p + \frac{L}{u_{zi}} \\ &= t_p + t_0(1 + k_i'^0) = t_p + t_{R,i}^0\end{aligned} \quad (33)$$

since the limiting velocity associated with an infinitely small concentration is $u/(1 + Fa_i) = u/(1 + k_i'^0)$. The second term of the right-hand side of eqn. 31, $\mu_{1,i}'$, is the first-order perturbation term, which we shall now calculate.

The two perturbation terms corresponding to the first-order moments at the end of the column ($x = L$) are given by

$$\begin{aligned}\mu_{1,1}' &= -\lim_{p\to 0}\frac{1}{\overline{C_1}}\cdot\frac{d\overline{C_1'}}{dp} \\ &= -\frac{1}{\int_0^\infty C_1 dt}\cdot\frac{Fa_1}{u}\left(b_1\int_0^L\int_0^\infty C_1^{d^2}dtdx' + b_2\int_0^L\int_0^\infty C_1^d C_2^d dtdx'\right)\end{aligned} \quad (34)$$

and

$$\mu'_{1,2} = -\lim_{p\to 0}\frac{1}{\overline{C_2}}\cdot\frac{\mathrm{d}\overline{C'_2}}{\mathrm{d}p}$$

$$= -\frac{1}{\int_0^\infty C_2\mathrm{d}t}\cdot\frac{Fa_2}{u}\left(b_2\int_0^L\int_0^\infty C_2^{\mathrm{d}^2}\mathrm{d}t\mathrm{d}x' + b_1\int_0^L\int_0^\infty C_1^{\mathrm{d}}C_2^{\mathrm{d}}dt\mathrm{d}x'\right) \tag{35}$$

As we assume the column to have an infinite efficiency (ideal model), the elution profile in linear chromatography is identical with the injection profile and we have

$$\int_0^\infty C_i\mathrm{d}t = C_i^0 t_p \tag{36}$$

and:

$$\int_0^L\int_0^\infty C_i^{\mathrm{d}^2}\,\mathrm{d}t\mathrm{d}x' = C_i^{0^2}t_pL \tag{37}$$

The elution profiles of both components are rectangles (see Fig. 1). The difference between the elution times of the rear of the first component profile and the front of the second component profile (*i.e.*, $t_B - t_C$, see Fig. 1) is

$$\Delta t = t_p + \frac{x'}{u_{z1}} - \frac{x'}{u_{z2}} = t_p - \frac{x'}{u}(k_2'^0 - k_1'^0) \tag{38}$$

Complete separation is achieved when Δt becomes zero and the migration distance in the column is

$$x' = x_s = \frac{Lt_p}{(k_2'^0 - k_1'^0)t_0} \tag{39}$$

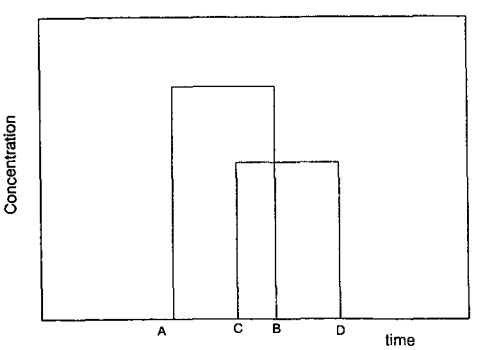

Fig. 1. Partially resolved band profiles in the case of a rectangular injection in ideal chromatography. Elution profiles at the position x' in the column. Retention times: A, $t_A = x'/u_{z1}$; B, $t_B = t_A + t_p$; C, $t_C = x'/u_{z2}$; D, $t_D = t_C + t_p$. $\Delta t = t_B - t_C$.

The overlap integral gives

$$\int_0^\infty C_1^d C_2^d dt = C_1^0 C_2^0 \Delta t \tag{40}$$

when $\Delta t > 0$ and $x < x_s$ and

$$\int_0^\infty C_1^d C_2^d dt = 0 \tag{41}$$

when $\Delta t \leqslant 0$. Therefore, when the separation is incomplete, *i.e.*, for

$$L < x_s \quad or \quad t_p > (k_2'^0 - k_1'^0)t_0$$

we have

$$\int_0^L \int_0^\infty C_1^d C_2^d dx' dt = C_1^0 C_2^0 \int_0^L \left[t_p - \frac{x'}{u}(k_2'^0 - k_1'^0) \right] dx' = C_1^0 C_2^0 L \left[t_p - \frac{t_0(k_2'^0 - k_1'^0)}{2} \right] \tag{42}$$

Inserting eqns. 36–42 into eqns. 34 and 35 gives

$$\mu'_{1,i} = -(t_{R0,i} - t_0) \left\{ b_i C_i + b_j C_j \left[1 - \frac{t_0(k_2'^0 - k_1'^0)}{2t_p} \right] \right\} \tag{43}$$

On the other hand, when the column length exceeds the critical value x_s, we have

$$\int_0^L \int_0^\infty C_1^d C_2^d dx' dt = C_1^0 C_2^0 \int_0^{x_s} \left[t_p - \frac{x'}{u}(k_2'^0 - k_1'^0) \right] dx' = \frac{C_1^0 C_2^0 t_p^2}{2t_0(k_2'^0 - k_1'^0)} \tag{44}$$

Inserting eqns. 36, 37 and 44 in eqns. 34 and 35 gives

$$\mu'_{1,i} = -(t_{R0,i} - t_0) \left[b_i C_i + \frac{b_j C_j t_p}{2t_0(k_2'^0 - k_1'^0)} \right] \tag{45}$$

RESOLUTION

If the sample size is very small, we have $\mu_{1,i} = t_{Ri}$, where t_{Ri} is the retention time observed for the band of a finite amount of component i, and we can write, as a first approximation,

$$t_{R2} - t_{R1} \approx \mu_{1,2} - \mu_{1,1} \approx (\mu^0_{1,2} - \mu^0_{1,1}) + (\mu'_{1,2} - \mu'_{1,1}) \tag{46}$$

If, as a first approximation, we assume that the band width does not increase with increasing sample size at very low values[15], the resolution between the two bands becomes

$$R = 2\left(\frac{t_{R2} - t_{R1}}{\sigma_1 + \sigma_2}\right) = \frac{2}{\sigma_1 + \sigma_2}[(\mu^0_{1,2} - \mu^0_{1,1}) + (\mu'_{1,2} - \mu'_{1,1})] = R^0 + \Delta R \qquad (47)$$

where R^0 is the resolution between these two bands under linear conditions. When the column length is smaller than x_s, the decrease in resolution, ΔR is given by

$$\Delta R = 2\left[\frac{(\alpha - 1)\cdot(t_{R0,1} - t_0)}{\sigma_1 + \sigma_2}\right]\left[b_1 C_1^0\left(\frac{k'^0_2 t_0}{2t_p} - 1\right) - b_2 C_2^0\left(\frac{k'^0_1 t_0}{2t_p} + 1\right)\right] \qquad (48)$$

When the column length is larger than x_s, the two band profiles are resolved in linear ideal chromatography. This is not necessarily so in non-linear, ideal chromatography. The change in the resolution is now given by

$$\Delta R = 2\left[\frac{(t_{R0,1} - t_0)}{\sigma_1 + \sigma_2}\right]\left\{b_1 C_1^0\left[1 - \frac{\alpha t_p}{2t_0(k'^0_2 - k'^0_1)}\right] - b_2 C_2^0\left[\alpha - \frac{t_p}{2t_0(k'^0_2 - k'^0_1)}\right]\right\} \qquad (49)$$

From eqns. 48 and 49, it is clear that ΔR is related to the parameters b_1 and b_2 which are at the origin of the non-linear behavior of the equilibrium isotherms and of the coupling between these isotherms. Obviously, if $b_1 = b_2 = 0$, then the chromatographic behavior is linear and $\Delta R = 0$.

RESULTS AND DISCUSSION

The essential results derived above are eqns. 43, 45, 48 and 49. They illustrate qualitatively the phenomena that take place when the sample size increases and non-linear behavior begins to affect the band profiles and their retention times. The most important effects are the following.

From eqns. 43 and 45, the variation of the first-order moment, *i.e.*, of the retention time of the band of each component of a binary mixture with increasing sample size, depends on the value of both coefficients b_1 and b_2 of the equilibrium isotherms of these two compounds. If b_1 and b_2 are both positive (such as with competitive Langmuir isotherms, as in eqns. 5 and 6), $\mu'_{1,1}$ and $\mu'_{1,2}$ are both negative. Both retention times decrease with increasing sample size. The sign and the magnitude of the variation of the resolution between the bands depend on the relative value of the coefficients b_i of the isotherms and on the relative concentration of the feed.

If the isotherms are accurately approximated by equation similar to eqns. 5 and 6, with negative values for both coeffients b_1 and b_2 (anti-Langmuir isotherms), the retention times of both components increase with increasing retention times and the resolution may increase or decrease, depending mainly on the relative composition of the feed.

When eqns. 5 and 6 are still valid, but with values of the two coefficients b_1 and b_2 which have opposite signs, the retention times of the components of a binary mixture can initially vary in either the same or the opposite direction, depending on the relative magnitude of the terms in eqns. 43 and 45. Situations where the retention time of one compound could remain constant are conceivable. Then the two terms in the right-hand side of either eqn. 43 or 45 are equal and opposite in sign.

The variation of the resolution between the two bands, ΔR, is given by eqns. 48 and 49. The magnitude of the effect is determined by the importance of the two terms. If these two terms are close, the change in the resolution can be small. It would be better if the resolution could increase with increasing sample size. This takes place if b_1 is positive and b_2 is negative, as seen in eqns. 48 and 49. This can be only an exceptional case.

ACKNOWLEDGEMENTS

This work was supported in part by grant CHE-8715211 from the National Science Foundation and by the cooperative agreement between the University of Tennessee and the Oak Ridge National Laboratory. We acknowledge support of our computational efforts by the University of Tennessee Computing Center.

REFERENCES

1 G. Guiochon and S. Ghodbane, *J. Phys. Chem.*, 92 (1988) 3682.
2 S. Ghodbane and G. Guiochon, *J. Chromatogr.*, 452 (1988) 209.
3 A. Katti and G. Guiochon, *J. Chromatogr.*, 449 (1988) 25.
4 A. Katti and G. Guiochon, *Anal. Chem.*, 61 (1989) 982.
5 S. Golshan-Shirazi and G. Guiochon, *J. Chromatogr.*, 461 (1989) 1.
6 S. Golshan-Shirazi, B. Lin and G. Guiochon, *J. Phys. Chem.*, 93 (1989) 3363.
7 B. Lin, S. Golshan-Shirazi, Z. Ma and G. Guiochon, *Anal. Chem.*, 60 (1988) 2647.
8 G. Guiochon, S. Golshan-Shirazi and A. Jaulmes, *Anal. Chem.*, 60 (1988) 1856.
9 H.-K. Rhee, *NATO Adv. Study Inst. Ser., Ser. E,* 33 (1981) 285.
10 G. Guiochon and L. Jacob, *J. Chromatogr.*, 14 (1971) 77.
11 S. Golshan-Shirazi and G. Guiochon, *J. Chromatogr.*, 506 (1990) 495.
12 R. Aris and N. R. Amundson, *Mathematical Methods in Chemical Engineering,* Prentice Hall, Englewood Cliffs, NJ, 1973, p. 438.
13 G. Houghton, *J. Phys. Chem.*, 67 (1963) 84.
14 B. Lin, J. Wang and B. Lin, *J. Chromatogr.*, 438 (1988) 171.
15 S. Golshan-Shirazi and G. Guiochon, *Anal. Chem.*, 60 (1988) 2364.

Journal of Chromatography, 508 (1990) 37–49
Elsevier Science Publishers B.V., Amsterdam — Printed in The Netherlands

CHROM. 22 358

Solid-surface room-temperature phosphorescence detection for high-performance liquid chromatography

A. D. CAMPIGLIA, A. BERTHOD[a] and J. D. WINEFORDNER*
Department of Chemistry, University of Florida, Gainesville, FL 32611 (U.S.A.)
(First received December 15th, 1989; revised manuscript received February 16th, 1990)

SUMMARY

In the present study, we have optimized the use of a two nebulizer system for solid-surface room-temperature phosphorescence (SSRTP) as a selective, permanent record detector for high-performance liquid chromatography (HPLC). The chromatographic parameters and the analytical figures of merit of five well known phosphorescent compounds were compared to those obtained by ultraviolet detection. Calibration curves with satisfactory linear dynamic ranges and limits of detection in the nanogram and subnanogram level showed the feasibility of the SSRTP detector for HPLC. In addition, overlapped compounds were individually identified demonstrating that the selectivity of the proposed detector can be a useful feature in case of incomplete chromatographic separations of complex mixtures.

INTRODUCTION

Solid-surface room-temperature phosphorescence (SSRTP) has been developed into a sensitive, selective and simple analytical tool for the determination of compounds of diversified interest[1–5]. Among the solid supports investigated for SSRTP[6–9], cellulose, and particularly filter paper, appears to be the most suitable substrate for the technique. The sensitivity of SSRTP can be improved by using appropriate concentrations of heavy-atom salts. Thallium(I), silver(I), and lead(II) cations and iodide are among the most common heavy-atom perturbers succesfully used to perform qualitative analysis at the nanogram and subnanogram level[3,9,10]. The reproducibility of the technique ranges from 5 to 15% and depends on the kind of substrate, analyte, experimental conditions and experimentator's expertise[10,11]. Since cellulose is susceptible to moisture, special attention must be taken to avoid humidity on the substrate[12]. Quenching of the analyte signal by water will certainly affect the precision and the sensitivity of the method. As a consequence, a drying step prior to detection is usually performed by either placing the sample under an infrared lamp or

[a] Permanent address: Laboratoire des Sciences Analytiques, Université de Lyon 1, 69622 Villeurbanne Cedex, France

0021-9673/90/$03.50

in an oven at high temperature. Quenching effects can also be caused by oxygen. Its presence is usually avoided by performing the RTP measurements under a flow of dry nitrogen.

The selectivity of the technique allows the qualitative and quantitative analysis of multicomponent mixtures without previous separation[12]. When the desired compound is the predominant phosphor of the mixture, the excitation and/or the emission spectrum of the sample can be easily used for detection purposes[13,14]. When the sample contains several compounds with comparable phosphorescent intensity signal, the similarity and/or overlapping of phosphorescence bands usually interfere in the characterization process. Many alternatives have been proposed to overcome this problem including synchronous scanning[15], selective external heavy-atom perturbation[10,16], and the combination of substrate and heavy-atom effects to preferentially enhance the phosphorescent signal of the target compound[16].

When dealing with complex matrices in various applications, previous separation is usually necessary to eliminate possible interferences and therefore facilitate the detection procedure. Several workers have proposed paper and thin-layer chromatography as separation techniques for SSRTP detection[5,17,18]. The unique possibility of complete analysis of complex mixtures using the same substrate turns this combination into a relatively simple and useful tool for analytical purposes.

SSRTP has also been associated with high-performance liquid chromatography (HPLC). Ford and Hurtubise[19] used silica chromatoplates as solid substrates to identify benzo[*f*]quinoline and phenanthridine in shale oil samples. The RTP spectra of the HPLC fractions corresponding to the retention times of those two compounds were compared to those obtained with the pure analytes. Filter paper discs were utilized by Vo-Dinh[12] to quantitatively determine benzo[*a*]pyrene and benzo[*e*]pyrene in coal liquid sales. In both cases[12,19], the HPLC fractions were manually collected and spotted onto the substrates for SSRTP detection.

In two previous studies[20,21], we reported the development of a two nebulizer automatic system which eliminated the manual steps usually involved in SSRTP analysis. In this report, the system is optimized as a selective detector for HPLC. To our knowledge, this is the first time that SSRTP is employed as a detection technique for HPLC analysis in a continuous automated mode. The chromatographic parameters and the analytical figures of merit (AFOMs) of five well known phosphorescent compounds of environmental interest were compared to the ones obtained by UV detection. The versatility and selectivity of the SSRTP detector is demonstrated by showing that overlapped compounds can be identified either from the SSRTP chromatogram or from their RTP spectral characteristics. Quantitative determination can be done by selecting the appropriate excitation and emission wavelengths of measurement. A permanent record of the analyzed sample can then be obtained by storing the substrate under proper conditions.

EXPERIMENTAL

Instrumentation

The HPLC system consisted on an Altex pump Model 110A used with a Rheodyne valve and a 20-μl sample loop. The Altex column was 15 cm $\times$ 4.6 mm I.D., and filled with ultrasphere ODS (5 μm particle diameter). The UV detector was

an Altex Model 153 with a cell volume of 8 μl, response time constant of 1 s and fixed wavelength at 254 nm. The two nebulizer system for SSRTP detection has been described in detail elsewere[20,21]. The eluent from the chromatographic column was sprayed onto the moving filter paper strip by connecting, with a PTFE tube (0.25 mm I.D.), the exit of the UV detector cell to the analyte nebulizer of the automatic system. The PTFE tube was kept as short as possible (< 15 cm) to minimize band broadening. Prior to detection, the paper strip was irradiated by two infrared lamps to evaporate continuously the solvent of the heavy-atom solution and the mobile phase. The dry substrate was then pulled into the detection unit by means of a Technicon AutoAnalyzer continuous filter (Technicon, Tarrytown, NY, U.S.A.). The detector consisted of a Perkin-Elmer LS-5 luminescence spectrofluorimeter driven by a Perkin-Elmer 3600 data station with a laboratory-constructed filter paper guide. All the SSRTP measurements were performed under a flow of dry nitrogen with a delay time of 0.03 ms and a gate time for collection of data of 9.0 ms. The excitation and the emission slits were set to 10 nm and 5 nm, respectively.

Reagents and procedure

All chemicals were analytical-reagent grade and used as received. Carbazole was purchased from Eastman Kodak; pyrene, benzo[*e*]pyrene, fluoranthene, phenanthrene and thallium(I) acetate (TlOAc) were obtained from Aldrich. HPLC-grade methanol (Fischer Scientific) and "nanopure" demineralized water (Barnsted Sybron) were used throughout. S&S 2043-A filter paper (Schleicher and Schuell) was obtained as a 2.5 cm wide $\times$ 24 m long filter paper roll and utilized as a substrate. Methanol–water solution of different volume ratios were employed a solvents to prepare 200-μg/ml stock solutions of carbazole and phenanthrene (80:20, v/v), and pyrene and fluoranthene (70:30, v/v). The same mass of benzo[*e*]pyrene was dissolved in pure methanol. A 0.1 *M* solution of TlOAc in methanol–water (50:50, v/v) was employed as a heavy-atom enhancer and continuously sprayed onto the moving filter paper at a flow-rate adjusted to deliver approximately 10 μl of solution per cm^2 of substrate. All the RTP measurements were performed in a continuous mode with the use of a kinetic program which permitted plotting the phosphorescent intensity as a function of time. While the desired section of filter paper was passing through the sample compartment of the spectrofluorimeter, the excitation slit was opened and the RTP emission at the selected excitation and emission wavelengths was registered. The total sampling time was chosen according to the separation time in the chromatographic column and a data interval of 0.2 s was kept constant through all the experiments. For all the AFOMs, a sampling time of 800 s was employed to obtain 4000 points per chromatogram. The mobile phase drying process introduced a delay time of 330 s. This delay time in the SSRTP chromatogram corresponded to the time spent by the analyte on the substrate to "travel" from the nebulizer to the excitation slit of the spectrofluorimeter. Since the time spent for the effluent to go from the UV detector to the analyte nebulizer was negligible for all the flow-rates tested, the same delay time was observed through all the experiments. The retention times in the SSRTP chromatograms were then corrected with respect to the observed values (330 s).

RESULTS AND DISCUSSION

Five well known phosphorescent compounds, carbazole, phenanthrene, pyrene, benzo[*e*]pyrene (B*e*P) and fluoranthene, were selected to compare the UV and the SSRTP system for HPLC detection. All of them strongly absorbed at 254 nm, at which the UV measurements were performed. The 0.1 *M* TlOAc solution, chosen as a heavy-atom perturber, was shown to be particularly efficient in the enhancement signal of most of the probe analytes[9].

Fig. 1 shows a SSRTP chromatogram along with the corresponding classical UV chromatogram of a mixture containing carbazole, phenanthrene, pyrene and B*e*P. In order to simplify the measurement procedure, only two sets of detection wavelengths were employed. The measurement wavelengths selected took into consideration the relative phosphorescent intensity of the studied compounds. When necessary, the chosen wavelength pair was set closer to the wavelengths for maximum RTP signal of the weaker phosphor. The wavelength and chromatographic parameters are listed in Table I.

Chromatographic band broadening

The peak efficiencies were obtained assuming Gaussian peaks and are listed in Table I. The low efficiency obtained for carbazole (N_{UV} = 400, N_{RTP} = 370) was not

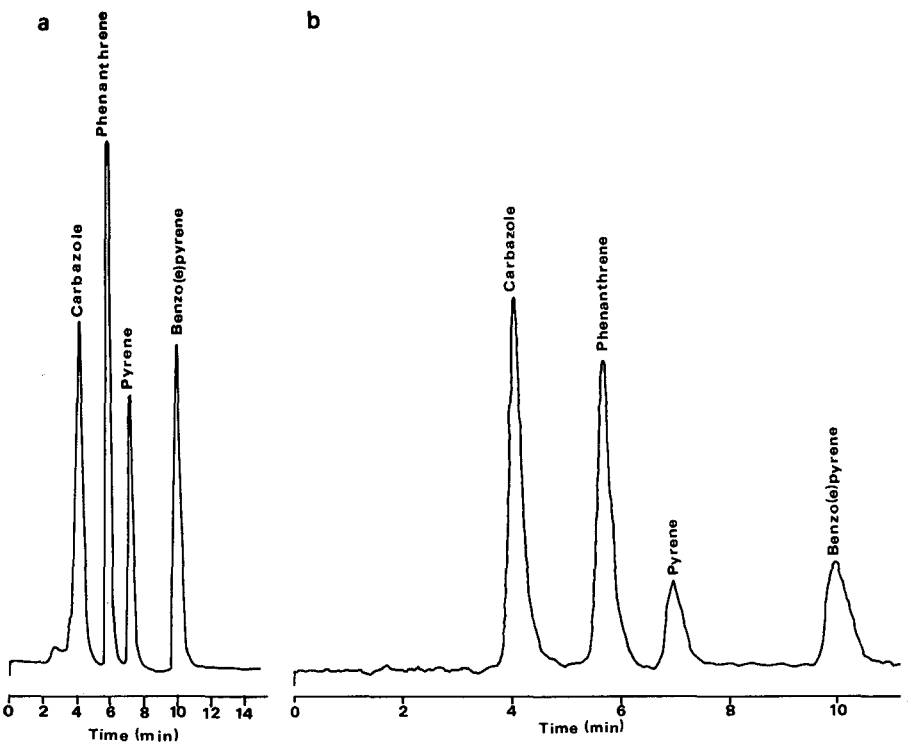

Fig. 1. UV (a) and SSRTP (b) chromatogram showing the separation of a mixture containing 200 pg of phenanthrene and 500 pg of carbazole, pyrene and benzo[*e*]pyrene. Mobile phase: methanol; flow-rate: 0.443 ml/min; sample volume: 20 μl.

TABLE I

WAVELENGTH SETTINGS AND CHROMATOGRAPHIC PARAMETERS

Retention volumes (V_R) obtained with a flow-rate of 0.443 ml/min. Capacity factors (k') calculated for a dead volume (V_0) of 0.97 ml. Efficiencies calculated using $N=4(V_R/W_{0.6H})^2$ where $W_{0.6H}$ is the peak width at 60% of the peak height expressed in volume units and N is the plate number; accuracy 20%.

Solute	*Excitation wavelength (nm)*[a]	*Emission wavelength (nm)*[a]	V_R *(ml)*	k'	*Efficiency*	
					UV plates	*RTP plates*
Carbazole	290 (296)	470 (440)	1.95	1.00	400	370
Phenanthrene	290 (285)	470 (505)	2.66	1.73	1400	1300
Pyrene	343 (343)	585 (595)	3.10	2.18	3000	2400
Benzo[*e*]pyrene	343 (335)	585 (543)	4.34	3.45	3200	2800
Fluoranthene	343 (365)	585 (545)	2.92	2.00	3000	2400

[a] The values in parenthesis correspond to the wavelengths for maximum emission. The others are the selected wavelengths for the SSRTP chromatogram.

surprising. Carbazole, or dibenzopyrrole, is an amino-containing basic compound. The –NH amino group of the pyrrole ring has a high affinity for surface silanols of the silica stationary phase. This affinity induces a peak tailing and low efficiency. The relatively low efficiency measured for phenanthrene (N_{UV} = 1400, N_{RTP} = 1300) may be due to extra column band broadening effects apart from the detectors. We point out that the chromatographic system was not optimized for maximum efficiency. However, it is interesting to estimate the band broadening induced by the SSRTP detector. A 15% efficiency loss was observed comparing the UV absorption to the SSRTP values (Table I). The band broadening produced by the connecting tubing, nebulizer and moving paper strip can be roughly quantified through variance estimation using the equation $\sigma^2 = V_R^2/N$. Defining σ_{SSRTP} and σ_{UV} from the SSRTP and the UV absorption chromatograms, the difference $\sigma^2_{SSRTP} - \sigma^2_{UV}$ corresponds to the band broadening due to the SSRTP detector because variances are additive. The estimated value was found to be approximately 900 $\pm$ 300 μl^2 which corresponded to a dead volume of 30 $\pm$ 15 μl for the SSRTP detector. It is important to note that, although the moving filter paper strip induced a 330-s response delay for drying and reaching the observation window, it did not produce excessive band broadening. Since the mobile phase and the solvent of the heavy atom solution were evaporated by infrared lamps, the solutes were trapped into the cellulose fibers of the paper which restrained their mobilities. By reducing the UV–SSRTP connecting tubing (16 μl) and using a micronebulizer, it should be possible to minimize the band broadening even more.

Flow-rate effect

When a constant ratio between the HPLC flow-rate and the strip chart recorder speed was maintained, we observed little variations of UV peak areas with the flow-rate for fixed sample weight. Important variations of SSRTP peak areas were observed with flow-rate changes. The phosphorescent intensity was very dependent on the flow-rate of the mobile phase. Fig. 2 shows the chromatographic SSRTP response

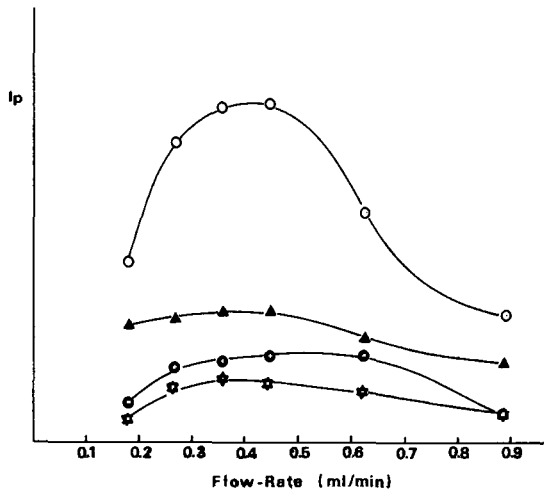

Fig. 2. SSRTP peak area (I_p) *versus* mobile phase flow-rate variations of carbazole's (▲), phenanthrene's (○), pyrene's (●) and benzo[*e*]pyrene's (★) signal with flow-rate variation of mobile phase (methanol). Sample size: 200 pg of phenanthrene, 500 pg of others, injected volume 20 μl.

(SSRTP peak area) *versus* flow-rate. It can be noticed that there is an optimum flow-rate for maximum RTP signal and therefore for highest sensitivity. Several parameters related to the flow-rate variation could be responsible for the observed phenomenon. By keeping constant the filter paper speed, the amount of analyte deposited per surface area of substrate increased with the flow-rate. If a peak has a base width of 1 min, the corresponding paper length on which the analyte would be sprayed was 21 cm; if the peak has a base width of 10 s, the same amount of analyte would be sprayed on 3.5 cm and so on. Since the analyte was deposited on a shorter length of substrate, it would be reasonable to expect higher phosphorescent signals at higher flow-rates. However, by increasing the flow-rate of the mobile phase, a larger volume of solvent per substrate length was also delivered. Since the filter paper speed was kept constant, the drying time remained the same and was insufficient for complete drying of the solvent. If this was the case, moisture could be responsible to some extent, for quenching the phosphorescent signal. In addition, the increase in the flow-rate was followed by an increase in the width of the sprayed area. Since the excitation slit of the spectrofluorimeter was kept constant, a possible diffusion of the analyte to the edges of the filter paper could also be responsible for the decrease observed in the phosphorescence intensities. With the exception of pyrene, all the other compounds showed the strongest phosphorescent signals between 0.354 and 0.443 ml/min. Considering the advantage of short analysis time, 0.443 ml/min was chosen as the optimum mobile phase flow-rate resulting in a total analysis time of approximately 17 min per SSRTP chromatogram.

AFOMs

Table II compares the AFOMs obtained with the UV absorption and the SSRTP system for HPLC detection. It is important to mention that both detectors were compared under experimental conditions for maximum SSRTP sensitivity and

TABLE II

ANALYTICAL FIGURES OF MERIT OBTAINED FOR HPLC USING SSRTP AND UV ABSORPTION DETECTION

All AFOMs were obtained under experimental conditions for maximum SSRTP sensitivity and reproducibility. The values listed in parenthesis correspond to the AFOMs obtained with the UV detector. Linear dynamic range (LDR) was estimated by dividing the upper linear concentration by the limit of detection. The slope was calculated from the curve log phosphorescence intensity (absorbance) *versus* log concentration. Signal-to-noise ratio = 3 and volumes of 20 μl (RTP) and 8 μl (UV) were used to estimate the limits of detection (LOD).

Solute	*LDR*	*Slope*	*Correlation coefficient*	*LOD (ng)*
Carbazole	$3.0 \cdot 10^3$ ($6.5 \cdot 10^2$)	1.06 (0.93)	0.983 (0.926)	0.77 (1.26)
Phenanthrene	$3.3 \cdot 10^3$ ($2.5 \cdot 10^2$)	1.04 (0.86)	0.999 (0.999)	0.96 (0.98)
Pyrene	$2.2 \cdot 10^2$ ($2.6 \cdot 10^3$)	0.95 (0.99)	0.985 (0.998)	5.24 (0.46)
Benzo[*e*]pyrene	$3.6 \cdot 10^2$ ($3.4 \cdot 10^2$)	1.00 (0.98)	0.983 (0.998)	3.16 (4.62)

reproducibility. The HPLC system was not optimized for UV-absorption detection. The limits of detection and the reproducibilities of measurements obtained with the UV detector, however, were comparable with those commonly observed when these kinds of devices are used for HPLC analysis. When measured by SSRTP, carbazole and phenanthrene showed calibration curves with larger linear dynamic ranges. Pyrene absorbed strongly in the UV and so had a low limit of detection with the UV detector; the SSRTP calibration curves for pyrene had a shorter linear dynamic range. In all cases, slopes close to unity and satisfactory correlation coefficients were obtained with both systems. The limits of detection with the UV detector were calculated from the equation $\mathrm{LOD} = 3/5(I_{p-p}/m)$ where I_{p-p} is the peak-to-peak background noise and m is the slope of the calibration curve[22]. The SSRTP values were estimated by multiplying the equation above by the factor A_i/A_t, where A_i is the irradiated area in the sample compartment and A_t is the total area of substrate on which the analyte has been sprayed. With both detection systems, carbazole, phenanthrene and B*e*P showed comparable limits of detection (LOD) in the nanogram range. The higher LOD value obtained for pyrene with the SSRTP detector can be attributed to the weak phosphorescence signal presented for this phoshor under the experimental conditions employed in the study. The relative standard deviations obtained with the SSRTP detector were within the reproducibility range of the technique (4–15%), and as expected, were poorer than those obtained by UV-absorption detection (2–7.6%).

Special features

Although conventional UV-absorption detectors operated at fixed wavelengths are able to discriminate between absorbing and non-absorbing species, they lack versatility and selectivity for the determination of absorbing compounds. The separation process in the chromatographic column has to be either complete or performed in such a way that compounds with minimum overlapping reach the detector. Most times this is a tedious procedure which usually involves either the optimization of a volume ratio between two solvents or the search for a convenient mobile phase. In addition, the detector wavelength does not usually coincide with the

maximum absorbance peak of the desired compound, which restricts the sensitivity of HPLC.

Commercially available UV–visible absorption detectors that consist of a scanning spectrometer or a photodetector array with grating optics offer the possibility to

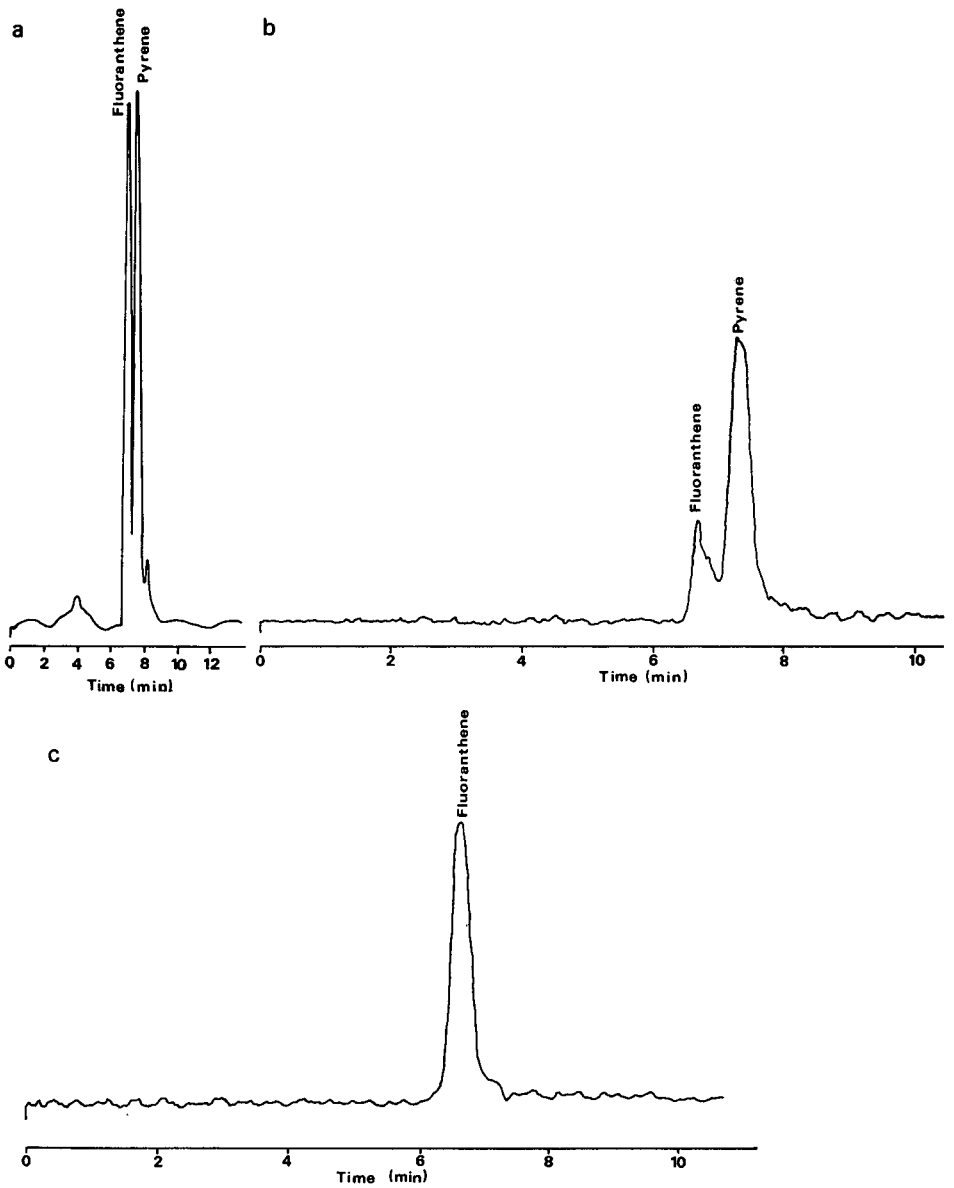

Fig. 3. Chromatograms showing the incomplete separation of fluoranthene and pyrene with methanol as a mobile phase. (a) UV absorption detection. (b) SSRTP detection using 343/585 nm as measurement wavelengths. (c) Selective SSRTP detection of fluoranthene employing 365/545 nm as measurement wavelengths. Sample size: 200 ng of each compound, injected volume 20 μl. Flow-rate: 0.443 ml/min.

select the best wavelength for each analyte. If overlapped compounds reach the detector, the selection of an appropriate detection wavelength for a single compound is often difficult due to the normally broad absorbance bands.

Even though broad molecular phosphorescence bands commonly overlap, it is unusual for different compounds to have coincident spectra in such a way that neither excitation nor emission wavelengths can be selected to measure a single component of the mixture. This unique feature of SSRTP is responsible for the high selectivity of the technique[10,12,15,16]. Fig. 3 shows the UV chromatogram of a mixture containing fluoranthene and pyrene along with the respective SSRTP chromatograms. The chromatographic parameters of fluoranthene are listed in Table I. From the UV chromatogram (Fig. 3a), it can be seen that complete resolution was not achieved by

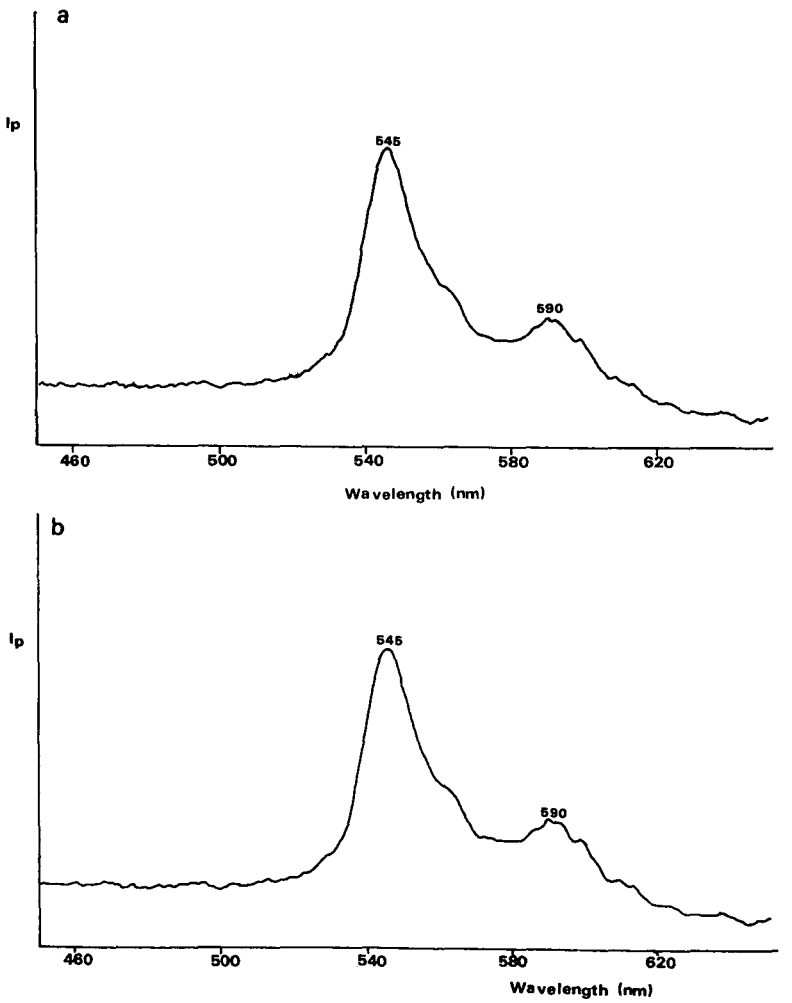

Fig. 4. (a) RTP emission (I_p) spectrum of the first eluted compound using the maximum excitation wavelength of fluoranthene (365 nm). (b) RTP emission spectrum of fluoranthene obtained under the same experimental conditions as (a).

using pure methanol as a mobile phase. Although the UV-absorption detection of either component is possible at these experimental condition, the example is useful to illustrate the selectivity of the SSRTP detector. By exciting at 343 nm and registering the phosporescent emission at 585 nm, the SSRTP chromatogram showed the presence of both solutes (Fig. 3b). When the detection wavelengths were shifted to the maximum excitation and emission of fluoranthene, the phosphorescence of pyrene was no longer registered (Fig. 3c) and the single detection of fluoranthene was possible without the presence of pyrene in the chromatogram. Further identification of fluoranthene was then performed by stopping the filter paper strip at the maximum phosphorescent intensity of the first eluted compound and comparing its emission spectrum with the corresponding spectrum of fluoranthene (see Fig. 4). The spectral identification of pyrene was done in a similar way. The substrate was stopped at the maximum phosphorescent intensity of the second eluted compound, and the emission spectrum was registered at the maximum excitation wavelength of pyrene. A spectrum with the same characteristics of the emission spectrum of pure pyrene was obtained (Fig. 5). Spectral identification was also possible when both compounds were present at the same level of concentration on the substrate. By stopping the filter paper strip at the maximum phosphorescence intensity detected between the elution of the compounds, and irradiating the substrate at the maximum excitation wavelength of pyrene, the presence of both analytes was confirmed by registering two phosphorescence bands with emission maxima at 545 nm (fluoranthene) and 592 nm (pyrene) (see Fig. 6a). When the substrate was irradiated at the maximum excitation wavelength of fluoranthene, the phosphorescence emission of pyrene was no longer detected (Fig. 6b). By comparing Figs. 5 and 6a, it can be noticed that even a weak phosphor like pyrene could be spectrally identified in the presence of similar concentrations of a strong phosphor like fluoranthene.

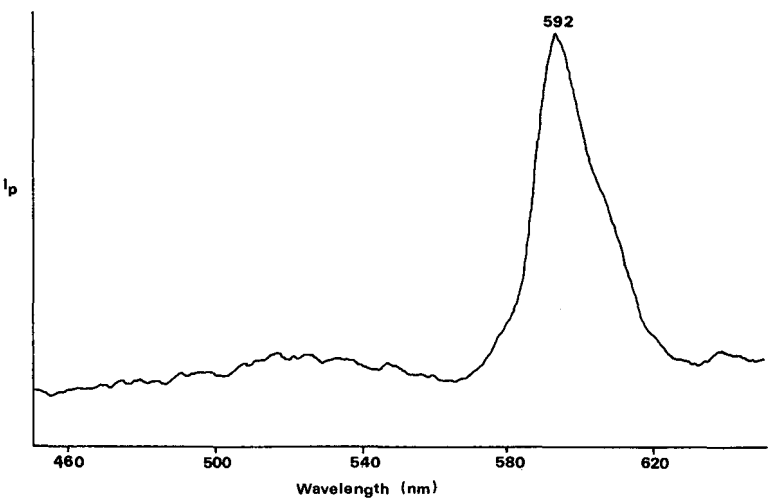

Fig. 5. RTP emission (I_p) of the second eluted compound registered at the maximum excitation wavelength of pyrene (343 nm).

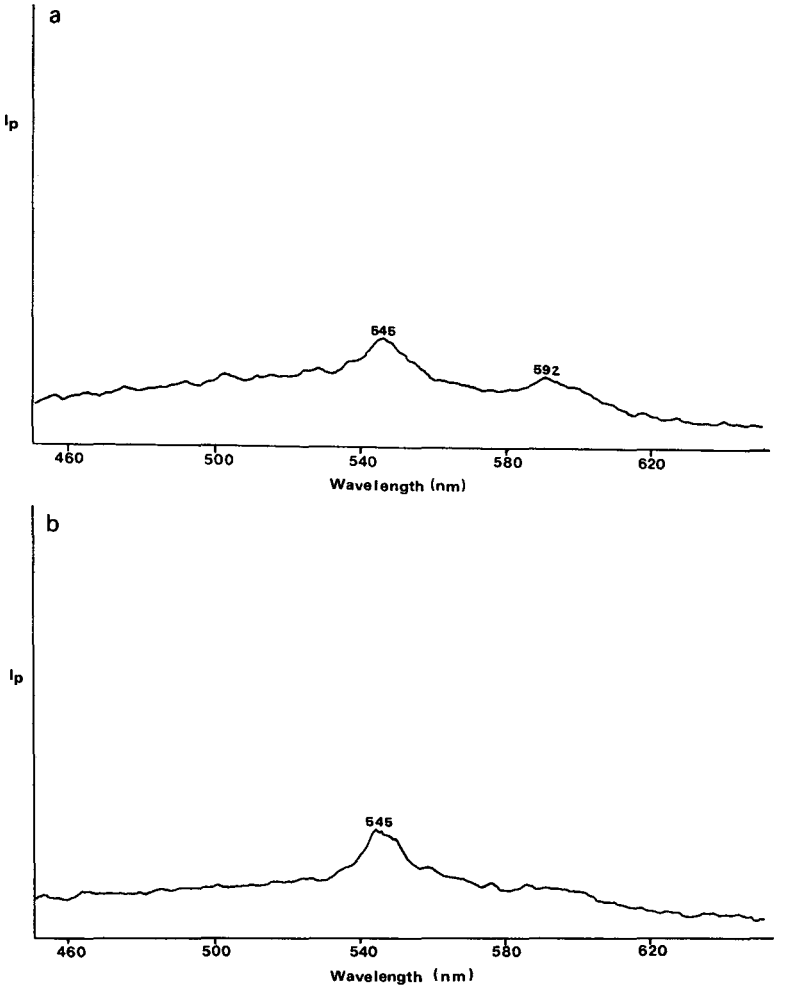

Fig. 6. RTP emission (I_p) spectra of the substrate registered at the minimum phosphorescence intensity observed between the elution of the two compounds. (a) When excited at 343 nm, two emission bands showed the presence of both compounds, fluoranthene (545 nm) and pyrene (592 nm). (b) When exited at 365 nm, only the phosphorescence emission of fluoranthene was observed.

CONCLUSIONS

In this report, we have shown the feasibility of using SSRTP as a detection technique for HPLC. By using the two nebulizer automatic system, it was possible to perform HPLC analysis in a continuous mode. The proposed detector has been evaluated by comparing its performance to the classical UV-absorption detector under the same experimental conditions. A 15% efficiency loss was observed in the SSRTP chromatograms mainly due to the UV-absorption–SSRTP detector connecting tubing (16 μl), nebulizer and moving filter paper strip. By reducing the length of the connecting tubing and using a micronebulizer, it should be possible to minimize the

observed band broadening. Comparable analytical figures of merit were obtained for both detection modes. By selecting the appropriate excitation and emission wavelengths of measurement, it was possible to characterize a single component of a mixture partially resolved by HPLC. This special feature makes the SSRTP detector a useful tool for liquid chromatographic operations. Complex systems can be separated into simpler ones, and the individual components of a mixture can be selectivily determined by choosing the appropriate set of measurement wavelengths. The versatility of the new detector permitted identification of compounds either from the retention times or from their RTP spectral characteristics, showing its potentiality for qualitative purposes. The greatest versatility, however, would result with the use of an intensified photodiode array detector. This instrument would allow phosphorescence spectra to be recorded as the peaks elute permitting "impure" probes to be resolved into individual components. We also believe that the SSRTP detector could be very useful in areas such as forensic science, where a permanent record of the analyzed samples would be extremely helpful. Compounds adsorbed on solid substrates and stored under a nitrogen atmosphere for several weeks have presented constant phosphorescence intensity[23,24]. This offers the possibility of identifying the constituents of a stored sample at any required time. By knowing the position of every compound on the filter paper strip, a new chromatogram (phosphorescence *versus* distance) can be obtained. If further identification is necessary, the substrate can then be stopped at the maximum phosphorescence intensity of every compound to run its excitation and emission spectra. Additional work, however, is necessary in the future to optimize the storing conditions for compounds of forensic interest.

ACKNOWLEDGEMENTS

A. D. C. would like to thank the "Coordenacao de Aperfeicoamento de Nivel Superior–Capes" for the grant which is making possible his stay in Gainesville and the University of Brasilia (Brazil) for permission to leave.

This work was supported by NIH ROI-GM 11 373-26.

REFERENCES

1 S. L. Wellon, R. A. Paynter and J. D. Winefordner, *Spectrochim. Acta*, 30A (1974) 2133.
2 R. A. Paynter, S. L. Wellon and J. D. Winefordner, *Anal. Chem.*, 46 (1974) 736.
3 T. Vo-Dinh, E. Lue-Yen and J. D. Winefordner, *Anal. Chem.*, 48 (1976) 1186.
4 T. Vo-Dinh, E. Lue-Yen and J. D. Winefordner, *Talanta*, 24 (1977) 146.
5 T. Vo-Dinh, G. Walden and J. D. Winefordner, *Anal. Chem.*, 49 (1979) 1126.
6 R. A. Dalterio and R. J. Hurtubise, *Anal. Chem.*, 54 (1982) 224.
7 R. A. Burell and R. J. Hurtubise, *Anal. Chem.*, 60 (1988) 564.
8 R. M. A. von Wandruszka and R. J. Hurtubise, *Anal. Chem.*, 49 (1977) 2164.
9 E. Lue-Yen Bower and J. D. Winefordner, *Anal. Chim. Acta*, 102 (1978) 1.
10 T. Vo-Dinh and J. R. Hooyman, *Anal. Chem.*, 51 (1979) 1915.
11 T. Vo-Dinh and J. D. Winefordner, *Appl. Spectrosc. Rev.*, 13 (2) (1977) 261.
12 T. Vo-Dinh, *Room Temperature Phoshorimetry for Chemical Analysis*, Wiley, New York, 1984.
13 R. M. A. von Wandruszka and R. J. Hurtubise, *Anal. Chem.*, 48 (1976) 1784.
14 R. P. Bateh and J. D. Winefordner, *Anal. Lett.*, 15B (1982) 373.
15 T. Vo-Dinh and R. B. Gammage, *Anal. Chem.*, 50 (1978) 2054.
16 E. B. Asafu-Adjaye, J. I. Yun and S. Y. Su, *Anal. Chem.*, 57 (1985) 904.
17 C. G. De Lima and E. M. de M. Nicola, *Anal. Chem.*, 50 (1978) 1658.

18 C. D. Ford and R. J. Hurtubise, *Anal. Chem.*, 50 (1978) 610.
19 C. D. Ford and R. J. Hurtubise, *Anal. Lett.*, 13 (1980) 485.
20 A. D. Campiglia, L. M. Perry and J. D. Winefordner, *Appl. Spectrosc.*, 43 (1989) 1341.
21 A. D. Campiglia, L. M. Perry and J. D. Winefordner, *Appl. Spectrosc.*, (1990) in press.
22 G. L. Long and J. D. Winefordner, *Anal. Chem.*, 55 (1983) 712A.
23 E. M. Schulman and C. Walling, *Science (Washington, D.C.)*, 178 (1972) 53.
24 E. M. Schulman and C. Walling, *J. Phys. Chem.*, 77 (1973) 902.

Journal of Chromatography, 508 (1990) 51–60
Elsevier Science Publishers B.V., Amsterdam — Printed in The Netherlands

CHROM. 22 305

Influence of dissociation equilibria on the elution behaviour of the sample anion in anion chromatography

NAOKI HIRAYAMA and TOORU KUWAMOTO*
Department of Chemistry, Faculty of Science, Kyoto University, Kitashirakawa-Oiwake-Cho, Sakyo-ku, Kyoto 606 (Japan)
(First received July 4th, 1989; revised manuscript received January 22nd, 1990)

SUMMARY

In anion chromatography, the influence of the dissociation equilibria on the measured capacity factor of a sample is controlled by the capacity factors of species in the sample, the dissociation constants and the pH of eluent. A method has been developed for interpreting the elution behaviour by using the ratio of the capacity factor of the sample to that of a standard anion with a fixed charge. The dissociation constants and the ratios of the capacity factors of various species to that of the standard were calculated. As a result, the elution behaviour of the sample at any eluent concentration was numerically estimated and the estimated values agreed with the measured values.

INTRODUCTION

Ion chromatography[1] is an effective method for the separation and determination of many sample cations and anions. Although the eluent is limited in suppressed (dual-column) ion chromatography[1], many eluents have been used in developing of non-suppressed (single-column) ion chromatography[2]. We have studied the effect of the eluent on the elution mechanism of samples.

The elution behaviour of a sample ion is controlled by four factors: (1) concentration of the eluent ion; (2) charge on the eluent ion; (3) charge on the sample ion; and (4) pH of the eluent. Whereas factors 1–3 have already been investigated[3], factor 4 has not yet been completely studied.

Owing to changes in the eluent pH, the sample ion or eluent ion may be present in several states having different charges, which complicates the analysis of elution behaviour. Jenke and Pagenkopf[4–8] studied the elution mechanism accompanying changes in eluent charge, and Hoover[9] studied variations in both eluent and sample charges.

The eluent pH also changes the physical state of an ion-exchange resin and changes the retention behaviour of the sample even if the charges of the sample and eluent ions are fixed.

0021-9673/90/$03.50

In this work, we studied the influence of dissociation equilibria on the elution behaviour of samples in anion chromatography by investigating the effect of the state of the resin. It was found that this effect could be eliminated by using the ratio of the capacity factor of the sample anion to that of a standard anion having a fixed charge. As a result, we succeeded in interpreting the elution behaviour. Moreover, the behaviour at any eluent concentration could be numerically estimated by using the data obtained at a fixed eluent concentration.

THEORY

Elution behaviour of the sample anion

In anion chromatography, the measured capacity factor (k') of a sample A is expressed by

$$\begin{aligned} k' &= D_A w/V_0 \\ &= ([A]_R/[A])w/V_0 \end{aligned} \tag{1}$$

where D_A is the distribution coefficient of A, w is the weight of the resin, V_0 is the dead volume of the column, $[A]_R$ is the concentration of A on the resin surface (ion-exchange phase) and [A] is the concentration of A in the liquid phase. The k' value is experimentally determined as follows:

$$k' = (V_R - V_0)/V_0 \tag{2}$$

where V_R is the retention volume of A.

Influence of dissociation equilibria on the elution behaviour of the sample anion

In general, a sample anion is involved in the following dissociation equilibria:

$$A^{(i-1)-} \overset{K_{ai}}{\rightleftharpoons} A^{i-} + H^+ \tag{3}$$

$$K_{ai} = [H^+][A^{i-}]/[A^{(i-1)-}] \tag{4}$$

where K_{ai} denotes dissociation constant of $A^{(i-1)-}$. $[A]_R$ and [A] in eqn. 1 can be represented as follows:

$$[A]_R = \sum_i [A^{i-}]_R \tag{5}$$

$$[A] = \sum_i [A^{i-}] \tag{6}$$

The ratios $[A^{i-}]/[A]$ and $[A^{i-}]_R/[A]_R$ are constant at a fixed eluent pH and the k' value is obtained by substituting eqns. 5 and 6 for eqn. 1 as follows[9]:

$$k' = \left(\sum_i [A^{i-}]_R / \sum_i [A^{i-}]\right) w/V_0$$

$$= \sum_i (P_i[A^{i-}]_R/[A^{i-}])w/V_0$$

$$= \sum_i (P_i D_{Ai})w/V_0$$

$$= \sum_i (P_i k'_i) \tag{7}$$

where

$$k'_i = D_{Ai}w/V_0 = ([A^{i-}]_R/[A^{i-}])w/V_0 \tag{8}$$

and

$$P_i = [A^{i-}]/[A] \tag{9}$$

$$\left(\sum_i P_i = 1\right)$$

When the states $i = 0$ to $i = q$ are equilibrated, the P_i are determined by using eqns. 4, 6 and 9 as follows:

$$P_i = \left\{\left(\prod_{y=0}^{i} K_{ay}\right)\Big/[H^+]^i\right\}\Big/\sum_{z=0}^{q}\left\{\left(\prod_{y=0}^{z} K_{ay}\right)\Big/[H^+]^z\right\} \tag{10}$$

provided $K_{a0} = 1$, where the P_i are functions of $K_{a1}, K_{a2}, \ldots, K_{aq}$ and $[H^+]$. Therefore, k' is determined only by k'_i, K_{ai} and $[H^+]$, by substituting eqn. 10 for eqn. 7 as follows:

$$k' = \sum_i \left(\left\{\left(\prod_{y=0}^{i} K_{ay}\right)\Big/[H^+]^i\right\}\Big/\sum_{z=0}^{q}\left\{\left(\prod_{y=0}^{z} K_{ay}\right)\Big/[H^+]^z\right\}k'_i\right) \tag{11}$$

As a result, k' at any eluent pH can be calculated if the k'_i values are known.

Elimination of effect of eluent pH on resin

However, even if a fixed-charge eluent anion (E^{n-}, *e.g.*, Cl^-, Br^-) is used, the k'_i value changes depending on the eluent pH because the physical state of resin is changed, accompanied by swelling.

The factor most influenced by pH is the column dead volume (V_0), as follows[10,11]:

$$V_0 = V_{all} - V_{resin,w} = V_{all} - (V_{resin,d} + a + b\pi) \tag{12}$$

where V_{all}, $V_{resin,w}$ and $V_{resin,d}$ are the whole volume of the column, the wet resin volume and the dry resin volume, respectively, and a and b are constants determined by

the resin system; π is thermodynamic osmotic (swelling) pressure, which is determined by the equivalent fractions and partial equivalent volumes of species in the eluent[10]. When the eluent pH changes, the π value is also changed by an amount that is too large to neglect.

To eliminate the effect of V_0 on k'_i, the ratio of k'_i to k'_B (capacity factor of a fixed-charge anion, B^{m-}, *e.g.*, NO_3^-) is introduced as follows:

$$\begin{aligned} k'_i/k'_B &= (D_{Ai}w/V_0)/(D_Bw/V_0) \\ &= D_{Ai}/D_B \end{aligned} \tag{13}$$

In other words, k'_i/k'_B is constant at a fixed eluent anion concentration, regardless of the eluent pH. Therefore, k'/k'_B is a function only of P_i, as follows:

$$\begin{aligned} k'/k'_B &= \sum_i (P_i k'_i)/k'_B \\ &= \sum_i (P_i k'_i/k'_B) \end{aligned} \tag{14}$$

Determination of k'_i/k'_B values using k'/k'_B values at fixed eluent concentration

From eqns. 9 and 10, P_i is a function of pH and pK_{ai}. Therefore, the k'_i/k'_B and pK_{ai} values of sample A are determined by mathematical regression of eqn. 14 as follows:

(1) Measure k'/k'_B (equal to the ratios of retention times) at several eluent pH values and a fixed eluent concentration.

(2) Assume tentative pK_{ai} values successively at intervals of 0.01 within the range of measured pH.

(3) Calculate tentative P_i values at measured pH by using tentative pK_{ai} values obtained by process 2.

(4) Determine the tentative k'_i/k'_B values by the linear regression of k'/k'_B *vs.* tentative P_i with using the least-squares method corresponding to tentative pK_{ai} values.

Finally, only one set of pK_{ai} values, in which the correlation coefficient (r) of the regression is the nearest to unity, is selected, and the values of k'_i/k'_B are determined by these pK_{ai} values.

Prediction of k'/k'_B values at different eluent concentrations

There is the following correlation between k'_i or k'_B and the concentration of an eluent anion E^{n-} (ref. 3):

$$k'_i = [E^{n-}]^{-i/n} \cdot C_i \tag{15}$$

$$k'_B = [E^{n-}]^{-m/n} \cdot C_B \tag{16}$$

where C_i and C_B are constants. k'_0 (k'_i with $i = 0$) is regarded as independent of $[E^{n-}]$.

By dividing eqn. 15 by eqn. 16, the relationship between k'_i/k'_B and $[E^{n-}]$ is as follows:

$$k'_i/k'_B = [E^{n-}]^{(m-i)/n} \cdot C_i/C_B \tag{17}$$

In order to eliminate C_i/C_B, by dividing eqn. 17 by $(k'_i/k'_B)_0$ at a fixed concentration ($[E^{n-}]_0$), the following equation is obtained:

$$k'_i/k'_B = (k'_i/k'_B)_0([E^{n-}]/[E^{n-}]_0)^{(m-i)/n} \quad (18)$$

From eqns. 7 and 18,

$$k'/k'_B = \sum_i \{P_i(k'_i/k'_B)_0([E^{n-}]/[E^{n-}]_0)^{(m-i)/n}\} \quad (19)$$

EXPERIMENTAL

Analytical-reagent grade chemicals were used throughout.

Standard sample solutions

Stock standard solutions of 1000 μg/ml (as anion) of sodium chloride, bromide, iodate, sulphate, nitrate, nitrite, benzoate, acetate, propionate and hydrogenphosphate, potassium arsenate, succinic acid and fumaric acid were prepared by dissolving the chemicals in distilled water. Working standards solutions were obtained by diluting the stock solutions to 20 μg/ml (as anion) with distilled water.

Eluents

Chloride, bromide, sulphate ($pK_{a2} = 1.99$)[12] and salicylate ($pK_{a1} = 2.98$, $pK_{a2} = 12.38$)[12] anions were used as the eluent anion. Stock solutions (1 *M*) of chloride, bromide and sulphate were prepared by diluting concentrated hydrochloric acid, hydrobromic acid and sulphuric acid, respectively. A stock solution (100 m*M*) of salicylate was prepared by dissolving salicylic acid in dilute ammonia solution.

The reagents used for controlling the eluent pH were sodium hydroxide solution (1 *M*) and ammonia solution (100 m*M*). These solutions were prepared by dissolving sodium hydroxide in water or diluting concentrated ammonia solution.

The eluents were prepared by mixing and diluting the acidic solutions and the basic solutions, and then these eluents were deaerated.

Apparatus

A Tosoh Model HLC-601 non-suppressed ion chromatograph equipped with an anion-exchange column (50 mm × 4.6 mm I.D.) packed with TSKgel IC-Anion-PW (particle size 10 ± 0.005 μm, capacity 0.03 ± 0.003 mequiv./g) or TSKgel IC-Anion-SW (particle size 5 ± 0.005 μm, capacity 0.4 ± 0.1 mequiv./g) and a Tosoh Model UV-8 II ultraviolet detector were used. HLC-601 instrument consisted of a computer-controlled pump, conductivity detector, sample injector (100 μl) and oven. The flow-rate was maintained at 1.0 ml/min under a pressure of 20–40 kg/cm^2. The separation column and a conductivity detector were placed in an oven regulated at 30°C. The data were recorded by a Shimadzu Chromatopac C-R1A recorder. An NEC Model PC-9801VM personal computer was used to calculate the above-mentioned values.

RESULTS AND DISCUSSION

k'_i/k'_B values

In order to prove the constancy of k'_i/k'_B, the relationship between k'/k'_{NO_3} ($B^{m-} = NO_3^-$, equal to k'_i/k'_{NO_3} or k'_2/k'_{NO_3}) and eluent pH was investigated by using k' values for several anions with a fixed charge under various conditions. As shown in Fig. 1, the deviation of these k'/k'_{NO_3} values was less than 5% and it was concluded that this theoretical approach is suitable.

Determination of pK_{ai} and k'_i/k'_B values

In anion chromatography, a low concentration of the sample anion exists with relatively high concentrations of eluent anion and counter cation and flows continuously. Hence the pK_{ai} values in the literature, which were obtained statically, are not suitable. Therefore, it is necessary to determine the pK_{ai} values by using the method outlined under Theory. Moreover, this method is very useful for determining k'_i/k'_B values, particularly when the difference between the pK_{ai} and $pK_{a(i+1)}$ values is small.

Fig. 2 shows the k'/k'_{NO_3} values for phosphate and arsenate anions obtained by using 3 m*M* salicylate anion (charge -1) as the eluent. In Fig. 2a, the abscissa is the eluent pH and in Fig. 2b it is P_2 under the condition of maximum (nearest to 1) r value, where the pK_{a2} values are 7.36 for phosphate and 7.27 for arsenate. The lines in Fig. 2b show the results of regression under the conditions mentioned above and expressed by the following equations:

phospate:

$$k'/k'_{NO_3} = 0.348 + 2.480\ P_2 = 0.348\ P_1 + 2.828\ P_2 \quad (20)$$

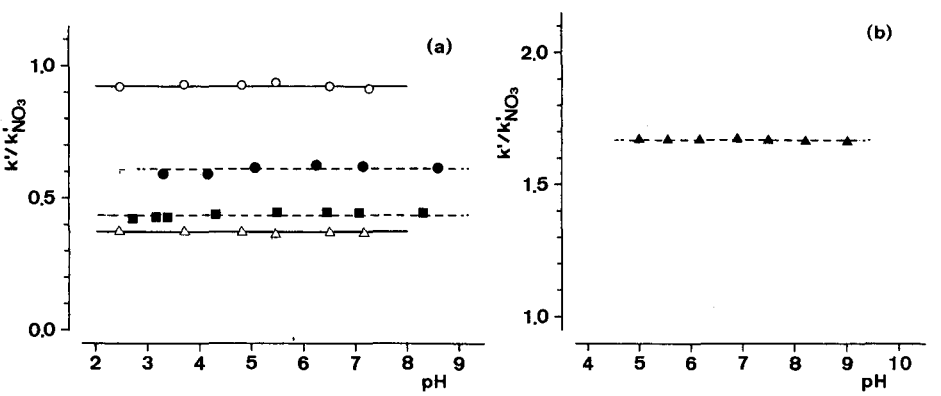

Fig. 1. Relationship between k'/k'_{NO_3} for solutes with a constant charge of (a) -1 or (b) -2 and eluent pH. Column: TSKgel IC-Anion-SW (solid line); TSKgel IC-Anion-PW (broken line). ○ = Sample bromide, eluent 20 m*M* chloride; ● = bromide, 10 m*M* sulphate; ■ = chloride, 10 m*M* bromide; △ = iodate, 20 m*M* chloride; ▲ = sulphate, 6 m*M* salicylate.

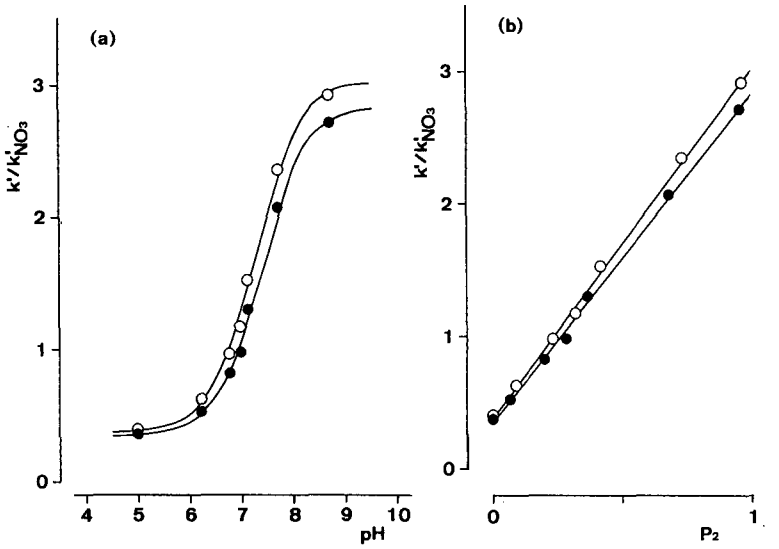

Fig. 2. Relationship between k'/k'_{NO_3} for solutes with change in charge from -1 to -2 and (a) eluent pH or (b) P_2 value obtained by using calculated pK_{a2} value. Sample: ● = phosphate; ○ = arsenate. Eluent: 3 m*M* salicylate. Column: TSKgel IC-Anion-PW.

arsenate:

$$k'/k'_{NO_3} = 0.375 + 2.659\ P_2 = 0.375\ P_1 + 3.034\ P_2 \quad (21)$$

In both instances, $P_1 + P_2 = 1$. The correlation coefficients were >0.999. The values of k'_1/k'_{NO_3} and k'_2/k'_{NO_3} for phosphate were 0.348 and 2.828 and those of arsenate were 0.375 and 3.034. The curves in Fig. 2a were obtained by converting the abscissa in Fig. 2b to eluent pH.

Table I gives the pK_{ai} and k'_i/k'_B values for several anions calculated by using this method. All the calculated correlation coefficients were >0.999.

Comparison between numerically calculated and observed k'/k'_B values at different eluent concentrations

By using eqn. 19, it is possible to establish the elution behaviour of sample anions, provided that the following two assumptions are satisfied: (1) the pK_{ai} values of the sample anion do not change with variation in the concentration of the eluent anion, and (2) the k'_0 value of the sample (k'_i with $i = 0$) does not depend on the concentration of the eluent anion.

Fig. 3 shows the results of numerically calculated and observed k'/k'_{NO_3} values. In Fig. 3a the sample is benzoate and the eluent is bromide. In 20 m*M* bromide eluent, pK_{a1} was 4.21 and the k'/k'_{NO_3} value was expressed as follows:

$$k'/k'_{NO_3} = 2.777\ P_0 + 1.383\ P_1 \quad (22)$$

TABLE I

CALCULATED k'_i/k'_B AND pK_{ai} VALUES

Sa^- = Salicylate anion.

Sample	*Eluent*	*Column*[a]	B^{m-}	k'_0/k'_B	k'_1/k'_B	k'_2/k'_B	pK_{a1}[b]	pK_{a2}[b]
Nitrite	10 m*M* Br^-	SW	NO_3^-	0.042	0.797		2.98 (3.14)	
	20 m*M* Cl^-	SW	NO_3^-	0.006	0.829		2.92	
	20 m*M* Br^-	PW	NO_3^-	0.321	0.626		3.22	
Benzoate	20 m*M* Cl^-	SW	NO_3^-	0.149	1.747		3.82 (4.20)	
	20 m*M* Br^-	PW	NO_3^-	2.777	1.383		4.21	
Acetate	4 m*M* Sa^-	SW	Cl^-	0.028	0.782		4.56 (4.76)	
Propionate	4 m*M* Sa^-	SW	Cl^-	0.059	0.796		4.69 (4.87)	
Phosphate	3 m*M* Sa^-	PW	NO_3^-		0.348	2.828		7.36 (7.20)
Arsenate	3 m*M* Sa^-	PW	NO_3^-		0.375	3.034		7.27 (6.98)
Succinate	50 m*M* Cl^-	PW	NO_3^-	0.094	0.249	0.611	3.93 (4.21)	5.43 (5.64)
Fumarate	40 m*M* Cl^-	PW	NO_3^-	0.242	0.417	1.386	2.35 (3.10)	4.20 (4.60)

[a] PW = TSKgel IC-Anion-PW; SW = TSKgel IC-Anion-SW.
[b] Literature values[12] in parentheses.

The k'/k'_{NO_3} value at an arbitrary concentration of bromide was numerically calculated by using eqn. 19 as follows:

$$k'/k'_{NO_3} = 2.777\ P_0\ \{[Br^-]/(20\ mM)\} + 1.383\ P_1 \qquad (23)$$

and the observed k'/k'_{NO_3} value agreed very well with the calculated value.

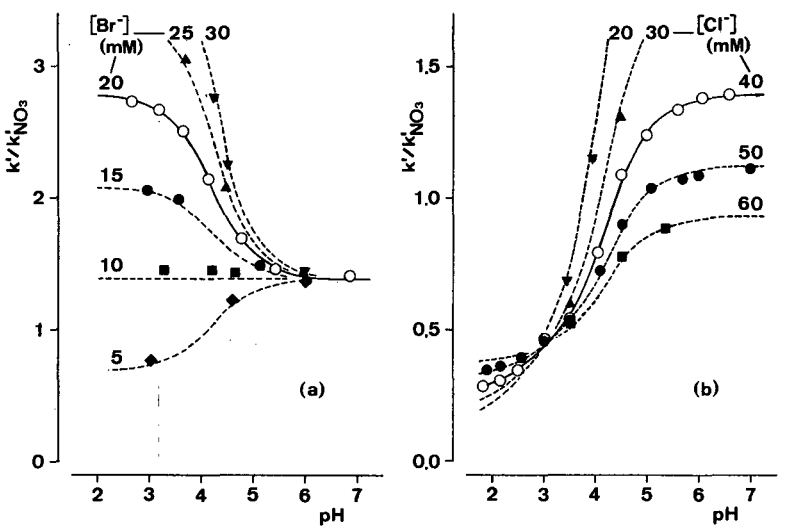

Fig. 3. Comparison between calculated and observed k'/k'_{NO_3} values. Broken curves: calculated from solid curve. (a) Sample, benzoate; eluent, bromide [◆ = 5; ■ = 10; ● = 15; ○ = 20; ▲ = 25; ▼ = 30 m*M*]; column, TSKgel IC-Anion-PW. (b) Sample, fumarate; eluent, chloride [▼ = 20; ▲ = 30; ○ = 40; ● = 50; ■ = 60 m*M*]; column, TSKgel IC-Anion-PW.

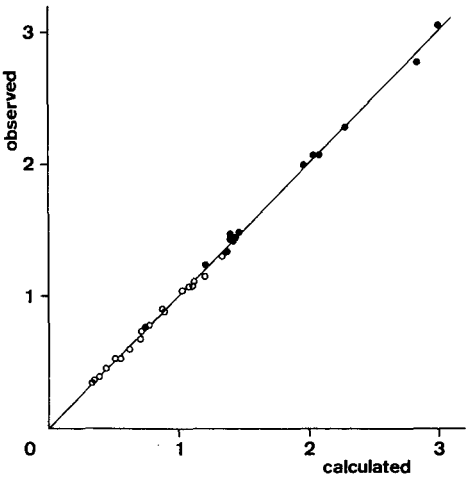

Fig. 4. Correlation between calculated and observed k'/k'_{NO_3} values. Data: ● = solid points shown in Fig. 3a; ○ = solid points shown in Fig. 3b.

In Fig. 3b, the sample is fumarate and the eluent is chloride. In 40 mM chloride eluent, pK_{a_1} and pK_{a_2} were 2.35 and 4.20, respectively, and the k'/k'_{NO_3} value was expressed as follows:

$$k'/k'_{NO_3} = 0.242\ P_0 + 0.417\ P_1 + 1.386\ P_2 \quad (24)$$

The k'/k'_{NO_3} value at an arbitrary concentration of chloride was calculated as follows:

$$k'/k'_{NO_3} = 0.242\ P_0\ \{[Cl^-]/(40\ mM)\} + 0.417\ P_1 + 1.386\ P_2\ \{(40\ mM)/[Cl^-]\} \quad (25)$$

and the observed k'/k'_{NO_3} value agreed very well with the calculated value.

Fig. 4 shows the relationship between the calculated and observed k'/k'_{NO_3} values shown in Fig. 3a and b. The correlation coefficients of the observed to calculated k'/k'_{NO_3} are 0.999 in both instances. As mentioned above, it is concluded that this numerical method is very accurate and precise.

CONCLUSION

A method for analysing the influence of dissociation equilibria on the elution behaviour of sample anions in anion chromatography has been presented. In this method, the ratio of the capacity factor (k') of the sample anion to that (k'_B) of an anion with a fixed charge is introduced in order to eliminate the change in physical state of the resin resulting from the change in eluent pH. The method has been demonstrated to be very useful for the analysis and numerical determination of sample anions involved in dissociation equilibria. Further, the method is useful even when using a mixed solution of water and an organic solvent as the eluent.

SYMBOLS

A	sample anion
A^{i-}	species A with charge $-i$
B^{m-}	fixed-charge anion used for the calculation of the ratio of capacity factors
D_A	distribution coefficient of A
D_{Ai}	distribution coefficient of A^{i-}
D_B	distribution coefficient of B^{m-}
E^{n-}	eluent anion
$[E^{n-}]_0$	fixed concentration of E^{n-}
i	charge number of A^{i-}
K_{ai}	dissociation constant of $A^{(i-1)-}$
k'	(measured) capacity factor of A
k'_i	capacity factor of A^{i-}
k'_B	capacity factor of B^{m-}
$(k'_i/k'_B)_0$	k'_i/k'_B at a fixed concentration of E^{n-}
m	fixed charge of B
n	fixed charge of E
P_i	ratio of $[A^{i-}]$ to total [A]
V_0	dead volume of the column
V_{all}	whole volume of the column
$V_{resin,d}$	dry resin volume
$V_{resin,w}$	wet resin volume
w	weight of the resin
π	osmotic (swelling) pressure

ACKNOWLEDGEMENT

The authors gratefully acknowledge financial support of the Nippon Life Insurance Foundation.

REFERENCES

1 H. Small, T. S. Stevens and W. C. Bauman, *Anal. Chem.*, 47 (1975) 1801.
2 D. T. Gjerde, J. S. Fritz and G. Schmuckler, *J. Chromatogr.*, 186 (1979) 509.
3 D. T. Gjerde, G. Schmuckler and J. S. Fritz, *J. Chromatogr.*, 187 (1980) 35.
4 D. R. Jenke, *Anal. Chem.*, 53 (1981) 1535.
5 D. R. Jenke and G. K. Pagenkopf, *J. Chromatogr.*, 269 (1983) 202.
6 D. R. Jenke and G. K. Pagenkopf, *Anal. Chem.*, 56 (1984) 85.
7 D. R. Jenke and G. K. Pagenkopf, *Anal. Chem.*, 56 (1984) 88.
8 D. R. Jenke, *Anal. Chem.*, 56 (1984) 2674.
9 T. B. Hoover, *Sep. Sci. Technol.*, 17 (1982) 295.
10 H. P. Gregor, *J. Am. Chem. Soc.*, 73 (1951) 642.
11 H. P. Gregor, F. Gutoff and J. I. Bregman, *J. Colloid Sci.*, 6 (1951) 245.
12 A. J. Dean, *Lange's Handbook of Chemistry*, McGraw-Hill, New York, 1985.

Journal of Chromatography, 508 (1990) 61–73
Elsevier Science Publishers B.V., Amsterdam — Printed in The Netherlands

CHROM. 22 344

Rapid high-performance liquid chromatography of nucleic acids with polystyrene-based micropellicular anion exchangers

YIH-FEN MAA, SUNG-CHYR LIN and CSABA HORVÁTH*
Department of Chemical Engineering, P.O. Box 2159, Yale Station, New Haven, CT 06520-2159 (U.S.A.)
and
UENG-CHENG YANG and DONALD M. CROTHERS
Department of Chemistry, Yale University, New Haven, CT 06520 (U.S.A.)
(First received November 6th, 1989; revised manuscript received February 13th, 1990)

SUMMARY

Nucleic acids were separated by ion-exchange chromatography on 30 × 4.6 and 100 × 4.6 mm columns packed with a micropellicular anion exchanger made of 3-μm rigid polystyrene-based non-porous microspheres with a covalently bound hydrophilic layer and DEAE functional groups at the surface. The stationary phase particles showed negligible swelling in methanol according to permeability measurements with water and methanol. Nucleic acids and their fragments including synthetic single-stranded oligonucleotides, linear, nicked and supercoiled DNAs as well as DNA restriction fragments were separated in less than 5 min, a time scale that is much smaller than that of conventional high-performance liquid chromatographic analysis for such samples. When only buffer and sodium chloride were used in the eluent for the separation of double-stranded DNA restriction fragments pGEM-3Z/Taq I, electrophoretic analysis of the effluent revealed the presence of smaller fragments in the bands of the larger ones. Upon addition of ethylenediaminetetraacetic (EDTA) salt to the eluent, however, such contamination by shorter fragments was no longer observed. In the absence of EDTA, magnesium chloride in the eluent at a concentration of 1 m*M* precluded the separation of the restriction fragments under otherwise identical chromatographic conditions.

INTRODUCTION

Rapid developments in recombinant DNA technology have created the need for isolating and purifying nucleic acids. The standard methods to purify plasmid DNA, DNA restriction fragments, and oligonucleotides are time consuming and labor intensive. In the case of plasmid DNA, a cesium chloride gradient containing ethidium bromide is frequently used. Although the supercoiled DNA can be separat-

0021-9673/90/$03.50

ed from other types of DNA, it is often difficult to purify it from RNA[1]. Excluding the time and labor in processing the sample before and after centrifugation, it takes at least 3 h to complete the centrifugation[1]. Restriction fragments are typically separated by gel electrophoresis, which has excellent resolution but low loading capacity. Preparative separation of DNA with high resolution requires extended time and recovery is often problematic. Certain unidentified substances from the gel may accompany the purified nucleic acid fractions and inhibit some enzymatic reactions; therefore, the DNA recovered after gel electrophoresis has often to be further purified.

Much of the importance of synthetic oligonucleotides derives from their increasingly widespread use in different areas, such as the site-specific mutagenesis[2–5], sequence-specific hybridization[6], priming of different enzymatic reactions[7,8] and affinity chromatography[9]. With an automated DNA synthesizer, oligonucleotides containing up to 60 bases can be made easily. The purity of a 60-mer thus obtained, however, is only 54–60% and its purification is carried out by chromatography or gel electrophoresis. Electrophoretic separation methods employing capillary tubes[10,11] are expected to bring about improvements, yet the loading capacity of these techniques are believed to be very low. For those reasons there is a need to develop appropriate high-performance liquid chromatographic (HPLC) methods, to complement both slab and capillary electrophoresis.

Recent advances in HPLC, particularly the introduction of novel microparticulate sorbents, have already extended the scope of its applications in nucleic acids research. However, HPLC of DNA fragments has been hampered by low diffusivities of the biopolymer molecules and their entrapment in the cavernous interior of conventional sorbents with the result of poor separation efficiency and low recovery. Further developments are expected from the introduction of micropellicular sorbents which are made of spherical, fluid-impervious support particles of a few microns in diameter with an appropriate retentive coating at the surface. The lack of internal pore structure offers advantages such as absence of significant intraparticulate diffusion resistances and good recovery[12,13] and these sorbents have been successfully used for rapid separation of proteins and peptides in different modes of chromatography[14–18].

This report examines the potential of a polymer-based micropellicular ion-exchange sorbent in rapid analysis as well as micropreparative purification of nucleic acids. Micropellicular anion-exchanger with DEAE ligates was prepared with a spherical, highly cross-linked polyaromatic support of 3.3 μm particle diameter[18]. Thus the operating pH range of the column could be extended to alkaline eluents to reduce inter- and intra-molecular interactions, which can impede DNA separations[19–21]. Furthermore, the use of the polymeric support also allows cleaning of the column with sodium hydroxide solution.

EXPERIMENTAL

Chemicals

Reagent-grade fuming nitric acid, granulated tin metal, sodium hydroxide and sodium nitrite were purchased from Mallinckrodt (Paris, KY, U.S.A.). Acrylamide and bisacrylamide, both electrophoresis grade, ammonium persulfate and

N,N,N′,N′-tetramethylethylenediamine were from Bio-Rad (Richmond, CA, U.S.A.). Triglycidoxyglycerol was purchased from Polysciences (Warrington, PA, U.S.A.). Trizma base [Tris(hydroxymethyl)aminomethane], ethidium bromide, and β-lactoglobulin B were purchased from Sigma (St. Louis, MO, U.S.A.). Sodium chloride, sulfuric acid, hydrochloric acid, EDTA, boric acid and N,N-dimethylformamide were obtained from Fisher Scientific (Springfield, NJ, U.S.A.). Diethylethanolamine was from Aldrich (Milwaukee, WI, U.S.A.) and the other solvents and salts were purchased from J.T. Baker (Phillipsburg, NJ, U.S.A.).

Nucleic acids and enzymes

pGEM-3Z plasmid DNA was purchased from Promega (Madison, WI, U.S.A.) and pXbs201 plasmid DNA was a gift by Dr. D. D. Brown of Carnegie Institution of Washington (Baltimore, MD, U.S.A.). The plasmids were amplified in bacterial strain DH1 and purified by ultracentrifugation with cesium chloride gradient[22]. Oligonucleotides, except the mixture of p(dT)12–18, which was purchased from P-L Biochemicals (Milwaukee, WI, U.S.A.), were synthesized by the phosphoramidite method on a Model 380B DNA synthesizer (Applied Biosystems, Foster City, CA, U.S.A.) with reagents supplied by the manufacturer. The sequences of the SQ1 and H3H-22 oligonucleotides were 5′-GTACTAGTGTCATCTAGTGTCA-3′ and 5′-GCATCGCGTGTGCTTTCCGCCG-3′, respectively. The single-stranded DNA used in the study, which is a 12-mer, was also synthesized by the same synthesizer and the double stranded DNA was obtained by mixing equal molar amounts of the pairing 12-mers at 37°C for 5 min and then cooled down to room temperature. Restriction endonucleases, BamHI, HindIII, MspI, and TaqI, were purchased from Promega and used according to the manufacturer's instructions. Cleaving of pGEM-3Z with MspI yielded eleven fragments shown in Fig. 8A. Upon cleaving pGEM-3Z with TaqI, five fragments were obtained but only the three major fragments containing 469, 763 and 1447 base-pairs were seen on electropherogram and chromatogram (*cf.* Figs. 6A–D). All enzymes were removed by phenol extraction after cleaving.

Stationary phase

Highly cross-linked polyaromatic microspheres having a mean particle diameter of 3.3 μm, as measured by electronmicroscopy, were prepared by suspension polymerization of styrene and divinylbenzene[18]. The particles were superficially nitrated, reduced and then reacted with diethylethanolamine in the presence of glycidoxyglycerol as described belows.

Nitration. A 10-g amount of dry polystyrene particles was dispersed in 50 ml of N,N-dimethylformamide by sonication. A 60-ml volume of fuming nitric acid and 20 ml of concentrated sulfuric acid were placed into a 300-ml three-neck flask equipped with a stirrer and a thermometer and cooled by an ice bath. The suspension was added slowly to the contents of the flask under stirring at 5–10°C. Thereafter the reaction mixture was stirred at that temperature for 3 h and subsequently heated at 60°C for 3 h. The nitrated product was filtered on a sintered-glass filter, washed with water, 0.1 *M* sodium hydroxide, water and dimethylformamide.

Reduction. Air-dried particles from the above reaction were dispersed in 60 ml of dimethylformamide by using the above reaction flask and cooled in an ice bath,

and 4 g of granulated tin metal were added. From a dripping funnel 100 ml of concentrated hydrochloric acid were added over 1 h. The reaction mixture was stirred at room temperature for another hour, and subsequently heated at 90°C for 9 h. At the end, the product was filtered, and washed with concentrated sodium hydroxide, water and methanol. The particles were dried at 60°C for 2 h.

Diazotization and hydrolysis. A 360-ml volume of 16% (v/v) aqueous sulfuric acid was placed in a 1-l three-neck flask equipped with a stirrer and a thermometer. Then, 100 ml of an aqueous suspension containing 10 g of the product from the previous reaction step were added to the flask under stirring. Subsequently 400 ml of cold water were added to the well-mixed mixture and the reaction flask was immersed in an ice bath. After stirring for an additional 15 min, a cold solution of 70 ml water and 36 g of sodium nitrite was added very slowly in about 1 h. The stirring was continued for another 20 min in the ice bath and followed by stirring at 45°C for 2 h. The product was filtered and washed in a sintered-glass filter with water and dimethylformamide. The particles were dried in the oven at 80°C for 5 h.

Reaction with diethylethanolamine and triglycidoxyglycerol. The product of previous step was dispersed in a mixture of 80 ml dimethylformamide, 50 ml diethylethanolamine and 20 ml triglycidoxyglycerol. The mixture was heated at 90°C for 18 h with stirring. The suspension was filtered and washed with water and acetone. The particles were dried in the oven at 60°C for 3 h.

The reproducibility of the surface treatment was measured by the chromatography of DNA fragments under conditions given in Fig. 8. Three out of five batches of the stationary phase yielded essentially identical chromatograms. The permeability of the columns with 20 m*M* Tris buffer as the mobile phase varied less than 5%.

Columns. In most instances 30 × 4.6 mm I.D. column made of 1/4 in. 316 stainless-steel tubing with 2-μm stainless-steel end frits were used. Some experiments were carried out with a 100 mm long, otherwise identical column. All the columns were slurry-packed at 850 bar by using an air-driven fluid pump Model DSHT-300 from Haskel (Burbank, CA, U.S.A.). Methanol was used for the slurry and also as the packing fluid.

Chromatograph

HPLC was performed on a Hewlett-Packard (Palo Alto, CA, U.S.A.) 1090 liquid chromatography system equipped with an oven, an auto injector and a diode-array detector. The chromatograms were stored and evaluated by Hewlett-Packard Model 9000-300 and 9153B data system.

Electrophoresis

The HPLC fractions, usually between 0.5 and *ca.* 1 ml, were collected manually following the detector signal and adjusted to have 0.5 *M* sodium chloride. After addition of two volumes of 95% aqueous ethanol the DNA precipitated and was recovered by centrifugation. The DNA pellet was dried and resuspended in 10 μl of loading solution containing 5% (v/v) glycerol, 10 m*M* EDTA (pH 8.0), 0.1% (w/v) sodium dodecyl sulfate and 0.01% (w/v) bromophenol blue. The DNA solution was subjected to electrophoresis at 10 V/cm for 5 h by using a 20 cm long and 1.0 mm thick 8% polyacrylamide gel slab made from acrylamide and bisacrylamide at a ratio of 37.5:1, 0.1% (w/v) ammonium persulfate and 0.05% (v/v) N,N,N′,N′-tetramethyl-

ethylenediamine, a TBE buffer containing 89 m*M* Tris-borate, 89 m*M* boric acid and 2 m*M* EDTA. After electrophoresis, the gel was stained with 0.5 mg/ml of aqueous ethidium bromide solution for 10 min and photographed on an UV transilluminator (UVP, San Gabriel, CA, U.S.A.).

RESULTS AND DISCUSSION

Characterization of the column

The permeability of the 30 × 4.6 mm I.D. column was investigated by measuring the pressure drop at various flow-rates of water and methanol as described previously[18]. It is seen from the results depicted in Fig. 1 that the pressure drop is a linear function of the flow-rate at least at inlet pressures up to 300 bar. From the Kozeny–Carman[18] equation with a particle diameter of 3.3 μm, the interstitial porosity[23] of the column was calculated as 0.375 and 0.342 in water and methanol, respectively. The decrease of specific permeability in contact with methanol corresponded to only a 1.7% increase in particle diameter with respect to that in water. Perfusion of the column alternatively with methanol and water did not have any untoward effect on the column efficiency.

In order to estimate the loading capacity of the 30 × 4.6 mm I.D. micropellicular DEAE column for biopolymers, the adsorption isotherm of β-lactoglobulin B was measured by frontal chromatography as described in the literature[24,25]. The experiments were carried out at room temperature with protein solutions in 20 m*M* Tris · HCl buffer, pH 8.0, at a flow-rate of 0.15 ml/min. The saturation value of β-lactoglobulin B was found to be about 9 mg per ml of stationary phase volume and this compares to protein binding capacity of 40 and 20 mg/ml for conventional porous particles having 250 and 550 Å mean pore diameter, respectively[26]. Therefore such micropellicular columns may also be used for preparative purification of proteins and nucleic acids.

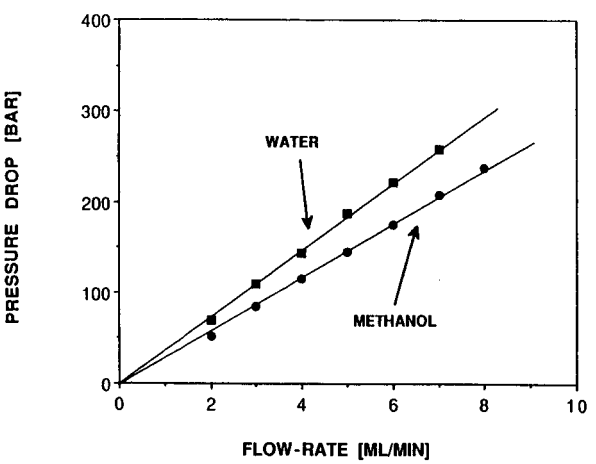

Fig. 1. Plots of pressure drop *versus* flow-rate of water and methanol at 25°C. Column, 30 × 4.6 mm I.D. packed with 3.3-μm micropellicular anion exchanger.

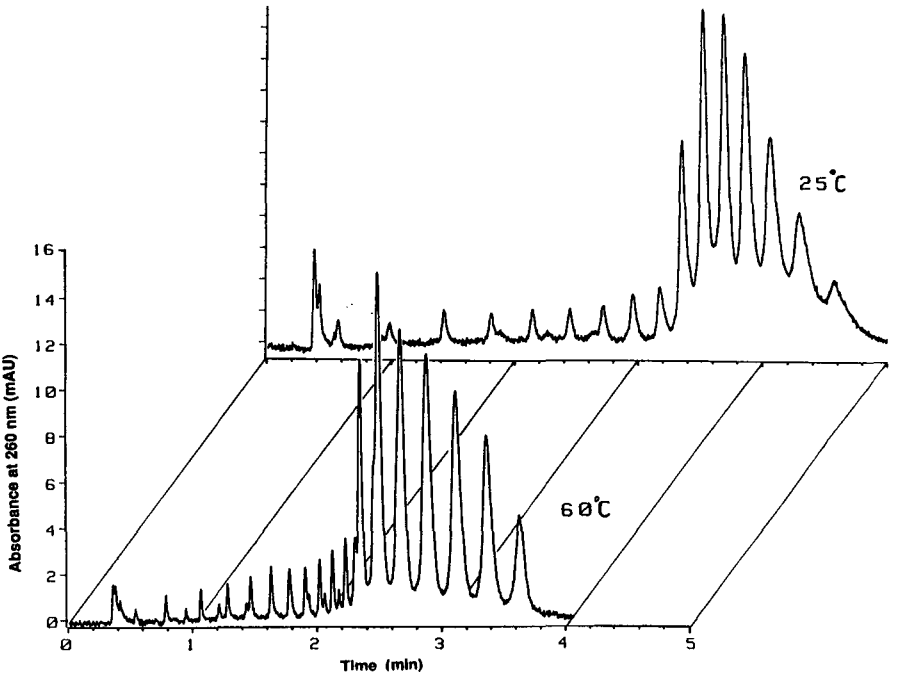

Fig. 2. Chromatograms of the crude products of p(dT)12–18 synthesis at column temperature of 25 and 60°C. Column, 100 × 4.6 mm I.D. packed with 3.3-μm micropellicular DEAE sorbent; flow-rate, 2.0 ml/min; buffer A, 20 m*M* Tris · HCl, pH 9.0; buffer B, 1 *M* NaCl in buffer A; linear gradient from 5 to 30% buffer B in 1.5 min followed by 30 to 45% buffer B in 4.5 min; sample size, 1 μg.

Synthetic oligonucleotides

Fig. 2 shows separations of a mixture of p(dT) oligonucleotides which contains 12 to 18 bases according to the supplier. The short separation time of less than 5 min illustrates that columns packed with micropellicular sorbents offer a means to reduce the time of such analysis to minutes from hours needed when using conventional columns[19,27]. As shown, the speed and efficiency of the separation can be further increased by operating at 60°C. Comparison of the two chromatograms confirms the predictions regarding the benefits of elevated temperatures in analytical HPLC of biopolymers that have recently been discussed in the literature[28].

Solid-phase synthesis of oligonucleotides is widely carried out with automated DNA synthesizers. The product must be purified preferably by HPLC in order to remove various oligonucleotide side products which contaminate the main product. Columns packed with micropellicular sorbents are very promising to bring about such purification rapidly. Fig. 3 shows the chromatogram of an oligonucleotide mixture in which the main product is a 48-mer from an automated DNA synthesizer.

Despite the high resolving power of gel electrophoresis, it is difficult, if not impossible to resolve by this technique DNA fragments that have the same chain length even if they differ in base composition. On the other hand, such separations can be readily performed by the use of the HPLC technique described here as il-

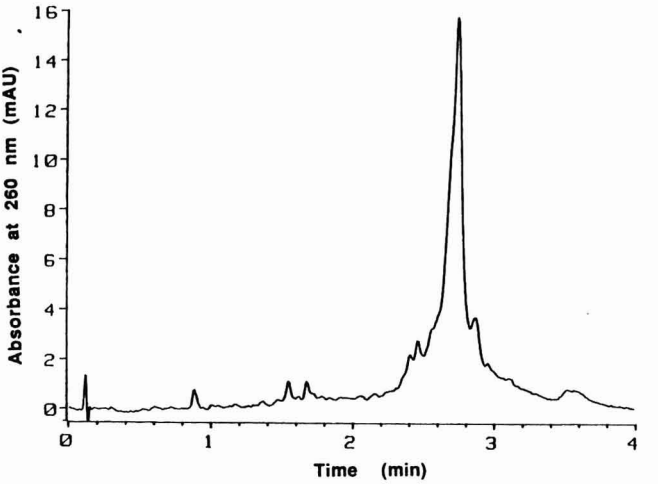

Fig. 3. Chromatogram of a crude 48-mer synthetic oligonucleotide. Column, 30 × 4.6 mm I.D.; flow-rate, 2.0 ml/min; buffer A, 20 m*M* Tris·HCl, pH 8.0; buffer B, 1 *M* NaCl in buffer A; linear gradient from 10 to 90% buffer B in 5 min; temperature, 60°C; sample size, 1 μg.

lustrated in Fig. 4. The two 22-mer oligonucleotides of different base composition, whose molecular weights are different only by 0.68%, are well resolved and the time of separation is less than 2 min.

Single-stranded DNA is usually separated from double-stranded DNA by gel electrophoresis or by liquid chromatography on a hydroxyapatite column. Fig. 5 shows a baseline separation of such a mixture on the micropellicular DEAE stationary phase in less than 4 min.

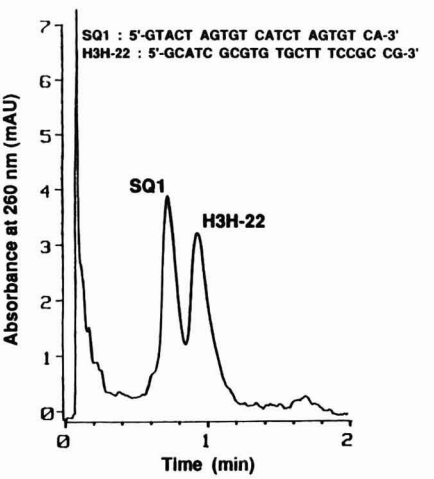

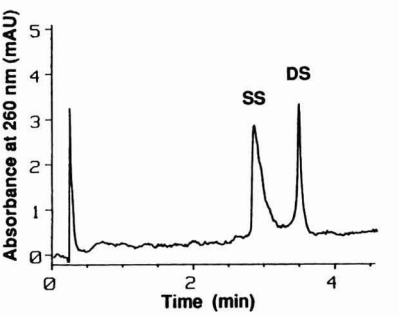

Fig. 4. Separation of two 22-mer oligonucleotides of different base composition. Chromatographic conditions as in Fig. 3, except linear gradient from 3 to 38% buffer B in 3 min; sample size, 0.5 μg.

Fig. 5. Separation of 12-mer single-stranded (SS) and double-stranded (DS) DNA. Column, 30 x 4.6 mm I.D.; flow-rate, 2.0 ml/min; buffer A, 1 m*M* EDTA in 20 m*M* Tris · HCl, pH 8.0; buffer B, 1 *M* NaCl in A; linear gradient from 10 to 15% buffer B in 5 min; temperature, 25°C; sample 0.2 μg of each component.

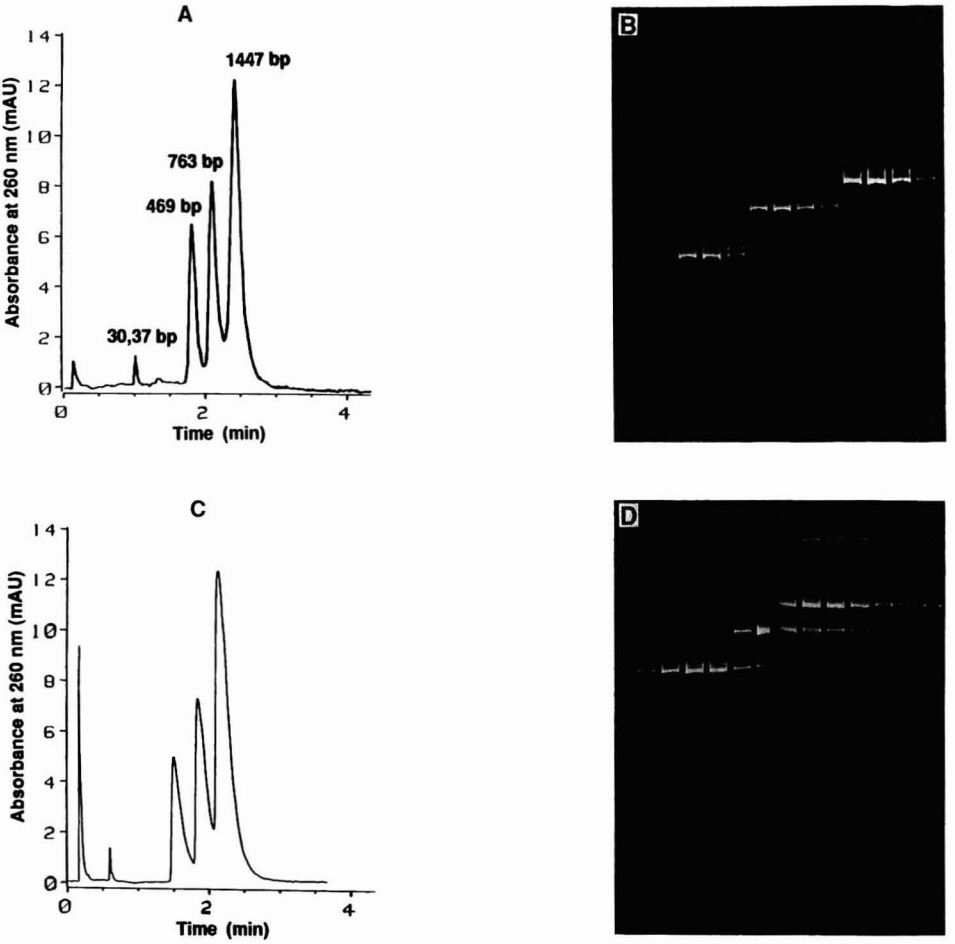

Fig. 6. Separation of DNA fragments from the digest of pGEM-3Z DNA by TaqI endonuclease. (A) Chromatogram was obtained under conditions as in Fig. 5 except linear gradient from 30 to 45% buffer B in 0.5 min followed by 45 to 48% buffer B in 4.5 min was used; sample size, 2 μg; bp = base pairs. (B) Electropherograms of the fractions collected from (A). (C) Chromatogram obtained under conditions as in (A) except no EDTA was added. (D) Electropherograms of the fractions collected from (C).

Restriction fragments

Enzymatic digestion of DNA with a restriction endonuclease yields a mixture of well-defined DNA fragments. The purification of specific restriction fragments is necessary for subcloning, DNA sequencing, and sequence-specific hybridization as well as in many other studies. The separation of such mixture on the micropellicular DEAE column is illustrated in Fig. 6A. It is seen that fragments containing less than 1500 base pairs can be readily separated in less than 5 min. In contradistinction, similar separations may require hours with conventional ion-exchange chromatography on porous DEAE stationary phase[29] or by reversed-phase ion-pair chromatography[30].

The chromatogram of the pGEM-3Z/TaqI restriction fragments in Fig. 6C shows a reasonably good separation of the three major DNA fragments when Tris buffer and NaCl were used in the eluents. However, analysis of the effluent fractions by polyacrylamide gel electrophoresis in Fig. 6D shows that the peaks of the larger fragments are contaminated by the lower-molecular-weight fragments. A similar phenomenon was observed in other chromatographic systems already and referred to as "cross-contamination"[30–32]. We could not eliminate or reduce this "carry-over" of shorter fragments by the larges ones upon varying the flow-rate, column temperature and/or the eluent pH in the range from 6.0 to 9.0. On the other hand, with 1 m*M* of EDTA in the mobile phase we obtained peaks that were electrophoretically pure as shown in Fig. 6B.

Addition of EDTA to the eluent in DNA chromatography is occasionally recommended in the literature to protect the DNA from digestion by non-specific nucleases[33]. It was suggested that "cross-contamination" was also due to the degrading effect of ubiquitous nucleases which need metal for activity. In our case, however, this explanation is highly unlikely. According to electrophoretic analysis shown in Fig. 6B the lower-molecular-weight fragments, present in the bands of the higher-molecular-weight fragments, appeared on the gel only at the same positions as the less retained lower-molecular-weight fragments formed upon the action of the restriction enzyme. Thus, no other fragments were generated in the course of chromatographic procedure.

It has been known that metal ions are released from the wetted steel parts of the HPLC apparatus[34] into the eluent and the adventitious heavy metal ions could facilitate interactions between the various DNA fragments present in the digest. On the other hand EDTA in the eluent may complex the adventitious metal ions and thereby eliminate the observed "carry-over" phenomenon if it is due to binding of the smaller fragments to the larger ones. In order to examine the effect of a divalent metal ion on the chromatographic separation, experiments were carried out with added metal ions

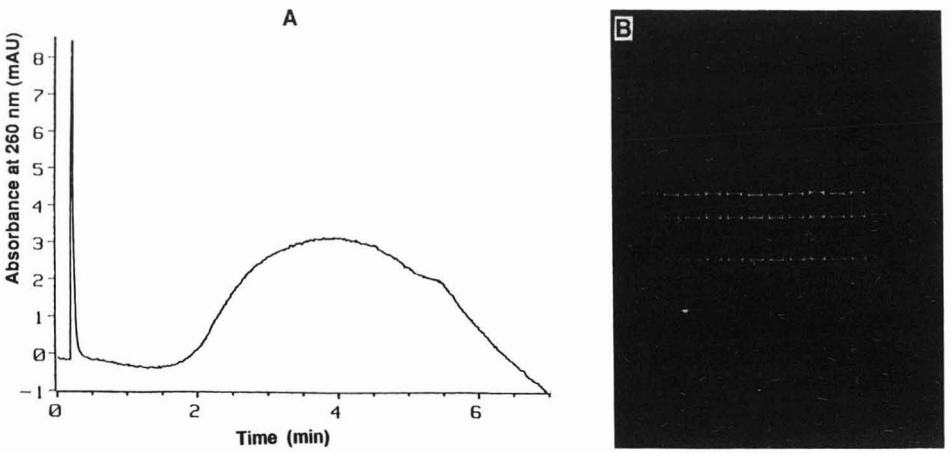

Fig. 7. Chromatogram of pGEM-3Z/TaqI fragments obtained with 1 m*M* $MgCl_2$ in the starting eluent and electropherograms of the fractions. (A) Chromatographic conditions as in Fig. 5 except buffer A, 1 m*M* $MgCl_2$ in 20 m*M* Tris/HCl, pH 8.0; buffer B: 1 *M* NaCl in 20 mM Tris · HCl, pH 8.0; linear gradient from 50 to 100% B in 5 min; sample size, 2 μg. (B) Electrophoretic analysis of the fractions collected from (A).

in the eluent. When 2 m*M* magnesium chloride was present in both the starting eluent and the gradient former the pGEM-3Z/TaqI fragments were not eluted in a gradient from 0 to 1.0 *M* of sodium chloride. When the starting eluent contained 1 m*M* magnesium chloride and no magnesium chloride was added to the gradient former, the DNA fragments eluted in the above gradient as a single broad peak without resolution of the individual fragments as shown in Fig. 7A. Electrophoretic analysis of the fractions collected from the beginning to the end of the peak confirmed, as seen in Fig. 7B, that all three components coeluted. These observations give further support to the hypothesis that the carry-over could be the result of an aggregation of the fragments via metal complexation. In this case the role of the EDTA in the eluent would be to preclude such agglomeration by chelating adventitious metal ions in the chromatographic system. Indeed the chromatographic separation of the restriction fragment mixture pGEM-3Z/MspI obtained by digesting the same plasmid with another restriction enzyme in the presence of 1 m*M* EDTA in the eluent, yielded fractions that did not exhibit carry-over as shown in Fig. 8B. Aggregation of DNA mediated by multivalent ions has been reported previously[35].

"Memory" peaks from the previous injection were reported in the literature[31,32] when some commercial columns were used for the chromatography of DNA fragments. In order to examine the possible occurrence of such phenomenon with the micropellicular column, a blank run was carried out immediately after the analysis of pMEG-3Z/TaqI restriction fragments under conditions given in Fig. 6A. As no "memory" or other ghost peaks appeared on the chromatogram, we conclude that the micropellicular sorbent configuration offers excellent recoveries in such separations in contradistinction to some conventional porous stationary phases. Furthermore, the equilibration time after a gradient run is usually 2 to 5 min on the polystyrene-based micropellicular DEAE column depending on the flow-rate. Thus column regeneration can be performed in a much shorter time than that required for conven-

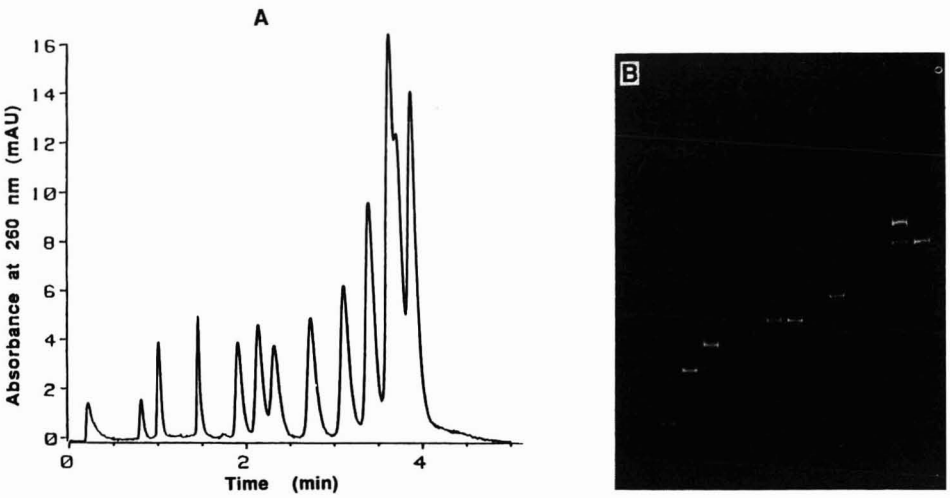

Fig. 8. Separation of DNA fragments from the digest of pGEM-3Z plasmid by MspI endonuclease. (A) Chromatogram obtained under conditions as in Fig. 5 except linear gradient from 33 to 40% buffer B in 1 min followed by 40 to 47% buffer B in 4 min, sample size, 1 μg. (B) Electropherograms of the fractions collected from (A).

tional sorbents according to the literature[31]. This can be readily explained by the rapid mass transfer facilitated by the particular structure of the micropellicular stationary phase in which the thin retentive layer confined to the surface of a fluid impervious support.

About the time when this manuscript was submitted a publication by Kato *et al.*[36] described the use of another kind of micropellicular anion exchanger for the separation of DNA restriction fragments. The authors observed no significant improvement in the resolution upon increasing the temperature from 25 to 65°C. We had similar experience in the chromatography of large double-stranded restriction fragments in contradistinction to the effect of temperature on the separation of the relatively small single-stranded oligonucleotides shown in Fig. 3.

Supercoiled DNA and its conformational isomers

After removal of high-molecular-weight cellular RNA and DNA, plasmid DNA is further purified by separating its supercoiled and nicked forms. In experiments with porous ion-exchange stationary phases, it was noted that size-exclusion effects interfered with the purification of supercoiled plasmid DNAs[37] when the mean pore size of the stationary phase was not larger than 2000 Å. Therefore sorbents having even larger pore dimensions would be needed to eliminate such size-exclusion effects as well as entrapment of some sample components in the cavernous interior of conventional stationary phase particles. Although sorbents having mean pore diameters of 4000 Å are now commercially available, the non-uniformity of the pore size distribution and the relatively poor mechanical stability of the support may limit their use. On the other hand, non-porous sorbents are not plagued with such problems and are, therefore, particularly suitable for the chromatography of megamolecules, *i.e.*, molecules having molecular weights higher than 10^6 daltons. This is illustrated by the

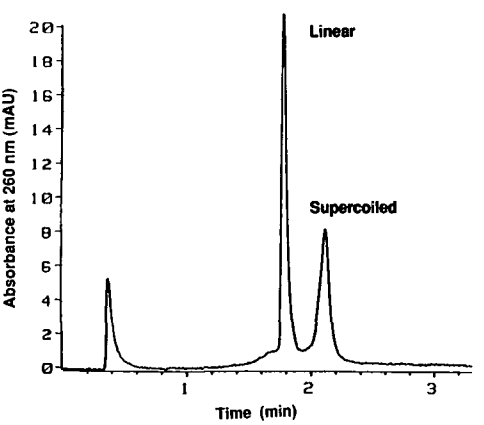

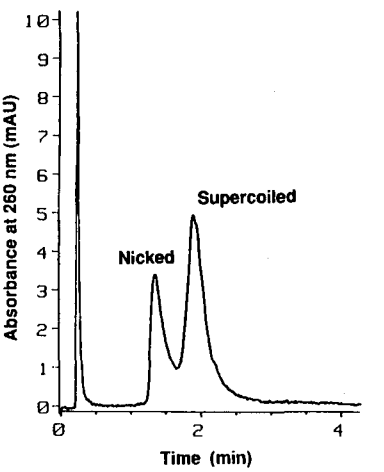

Fig. 9. Separation of linear and supercoiled DNA. Chromatographic conditions as in Fig. 6 except linear gradient from 40 to 55% buffer B was used in 5 min; sample, pGEM-3Z and pGEM-3Z/HINDIII, 0.25 μg each.

Fig. 10. Separation of nicked and supercoiled DNA. Chromatographic conditions as in Fig. 6 except linear gradient from 45 to 50% buffer B in 5 min; sample size, 0.3 μg each.

chromatogram in Fig. 9 which shows a separation of pGEM-3Z from linearized form pGEM-3Z/HINDIII on the micropellicular DEAE column in 3 min. This is a rather rapid separation since such HPLC analysis with conventional columns usually require at least 30 min according to the literature[31,33]. Moreover, by using this approach, the open circular, or nicked form, could also be rapidly separated from the supercoiled form, as depicted by the chromatogram in Fig. 10.

CONCLUSIONS

The results of this study have demonstrated that polystyrene-based micropellicular DEAE ion exchangers are well suited for rapid, high-efficiency separation of nucleic acids and their fragments and require very short postgradient column reequilibration. Their use therefore is associated with a considerable saving in time, eluent consumption and instrument usage, which can be important in routine analysis process monitoring and method development.

The microparticulate sorbent configuration also facilitates high recoveries of the sample components so that "carry-over" and "memory" effects do not interfere with the analysis and the efficiency of micropreparative work is enhanced.

ACKNOWLEDGEMENTS

This work was supported by Grants Nos. CA 21948 and GM 20993 from the National Institute of Health, U.S. Department of Health and Human Resources, and a contract from the National Foundation for Cancer Research.

REFERENCES

1 S. J. Garger, O.M. Griffith and L. K. Grill, *Biochem. Biophys. Res. Commun.*, 117 (1983) 835.
2 W. Kramer and H.-J- Fritz, *Methods Enzymol.*, 154 (1987) 350.
3 T. A. Kunkel, J. D. Roberts and R. A. Zakour, *Methods Enzymol.*, 154 (1987) 367.
4 W. Mandecki, *Proc. Natl. Acad. Sci. U.S.A.*, 83 (1986) 7177.
5 R. M. Myers, L. S. Lerman and T. Maniatis, *Science (Washington, D.C.)*, 229 (1985) 242.
6 A. M. Ginsberg, B. O. King and R. G. Roeder, *Cell*, 39 (1984) 479.
7 K. B. Mullis and F. Faloona, *Methods Enzymol.*, 155 (1987) 335.
8 L. B. Agellon and T. T. Chen, *Gene Anal. Techn.*, 3 (1986) 86.
9 J. T. Kadonaga and R. Tjian, *Proc. Natl. Acad. Sci. U.S.A.*, 83 (1986) 5889.
10 A. S. Cohen, S. Terabe, J. A. Smith and B. L. Karger, *Anal. Chem.*, 59 (1987) 1021.
11 A. S. Cohen, D. Najarian, J. A. Smith and B. L. Karger, *J. Chromatogr.*, 458 (1988) 323.
12 Y. Kato, K. Nakamura and T. Hashimoto, *J. High Resolut. Chromatogr. Chromatogr. Commun.*, 8 (1985) 154.
13 D. J. Burke, J. K. Duncan, C. Siebert and G. S. Ott, *J. Chromatogr.*, 359 (1986) 533.
14 K. Kalghati and Cs. Horváth, *J. Chromatogr.*, 398 (1987) 335.
15 L. Varády, K. Kalghatgi and Cs. Horváth, *J. Chromatogr.*, 458 (1988) 207.
16 Y. Kato, J. Kitamura, A. Mitsui and T. Hashimoto, *J. Chromatogr.*, 398 (1987) 327.
17 R. Janzen, K. K. Unger, H. Giesche, J. N. Kinkel and M. T. W. Hearn, *J. Chromatogr.*, 397 (1987) 91.
18 Y.-F. Maa and Cs. Horváth, *J. Chromatogr.*, 445 (1988) 71.
19 H. Rockstroh, W. Wangler and Th. Ackermann, *J. Chromatogr.*, 442 (1988) 401.
20 J. A. Thompson, *BioChromatography*, 1 (1986) 16.
21 Y. Kato, T. Kitamura, A. Mitsui, Y. Yamasaki, T. Hashimoto, T. Murotsu, S. Fukushige and K. Matsubara, *J. Chromatogr.*, 447 (1988) 212.
22 T. Maniatis, E. F. Fritsch and J. Sambrook (Editors), *Molecular Cloning: A Laboratory Manual*, Cold Spring Harbor Laboratory, Cold Spring, NY, 1982.

23 Cs. Horváth and H.-J. Lin, *J. Chromatogr.*, 126 (1976) 401.
24 J.-X. Huang and Cs. Horváth, *J. Chromatogr.*, 406 (1987) 275.
25 J.-X. Huang and Cs. Horváth, *J. Chromatogr.*, 406 (1987) 285.
26 S. Chang, R. Noel and F. Regnier, *Anal. Chem.*, 48 (1976) 1839.
27 D. Scanlon, J. Haralambidis, C. Southwell, T. Turton and C. Tregear, *J. Chromatogr.*336 (1984) 189.
28 F. Antia and Cs. Horváth, *J. Chromatogr.*, 435 (1988) 1.
29 Y. Kato, M. Sasaki and T. Hashimoto, *J. Chromatogr.*, 265 (1983) 342.
30 S. Eriksson, G. Glad, P. Pernemalm and E. Westman, *J. Chromatogr.*, 359 (1986) 265.
31 D. J. Stowers, J. M. B. Keim, P. S. Paul, Y. S. Lyoo, M. Merion and R. M. Benbow, *J. Chromatogr.*, 444 (1988) 47.
32 M. Merion and W. Warren, *BioTechniques*, 7 (1989) 60.
33 J. A. Thompson, *BioChromatography*, 2 (1987) 4.
34 S. M. Cramer, B. Nathanael and Cs. Horváth, *J. Chromatogr.*, 295 (1984) 405.
35 M. Mandelkern, N. Dattagupta and D. M. Crothers, *Proc. Natl. Acad. Sci. U.S.A.*, 78 (1981) 4294.
36 Y. Kato, Y. Yamasaki, A. Onaka, T. Kitamura and T. Hashimoto, *J. Chromatogr.*, 478 (1989) 264.
37 J. A. Thompson, *BioChromatography*, 1 (1986) 68.

Journal of Chromatography, 508 (1990) 75–79
Elsevier Science Publishers B.V., Amsterdam — Printed in The Netherlands

CHROM. 22 275

Improved sample preparation method for high-performance liquid chromatography of deoxyribonucleoside triphosphates from cell culture extracts

JOHAN HARMENBERG
Department of Virology, National Bacteriological Laboratory, S-105 21 Stockholm (Sweden)
and
SUSAN COX* and ANNELIE ÅKESSON-JOHANSSON
Department of Virology, National Bacteriological Laboratory, S-105 21 Stockholm, and Department of Virology, Karolinska Institute, S-105 21 Stockholm (Sweden)
(First received May 1st, 1989; revised manuscript received January 9th, 1990)

SUMMARY

The accurate determination of deoxyribonucleoside triphosphates in cells is difficult owing to the high concentrations of interfering ribonucleoside triphosphates. The latter can be degraded to their respective bases by periodate oxidation of cell extracts. However, the large amount of bases so produced can interfere with subsequent high-performance liquid chromatographic (HPLC) analysis. The use of a weak ion-exchange cartridge to partially purify and concentrate deoxyribonucleoside triphosphates in periodate-treated cell extracts, prior to HPLC, thus allowing accurate determination is described. The recovery of the deoxyribonucleoside triphosphates is >95%, and >90% of the interfering bases are removed.

INTRODUCTION

The measurement of nucleoside triphosphate pools in mammalian cells is of importance in studies on aspects of DNA and RNA synthesis and regulation. Many anticancer and antiviral drugs interfere with DNA and RNA precursors and with DNA and RNA synthesis. High-performance liquid chromatography (HPLC) has been used for the direct separation and quantification of nucleotides in cell extracts. However, the determination of deoxyribonucleoside triphosphates (dNTP) in cell and tissue extracts is difficult because ribonucleoside triphosphates (NTP), which normally co-elute with dNTP, are present in concentrations several orders of magnitude higher than those of dNTP[1].

Attempts have therefore been made to remove NTP from cell extracts prior to HPLC of dNTP. Boronate affinity chromatography has been used to retain NTP selectively in cell extracts, but the procedure is lengthy and a lyophilization step is required prior to HPLC of the dNTP[2].

0021-9673/90/$03.50

The selective degradation of NTP to their corresponding bases by periodate and methylamine has been used to remove interfering NTP prior to HPLC of the remaining unaffected dNTP[1]. The degradation of NTP by the periodate oxidation procedure has been used extensively. Although the method is rapid and efficient, we experienced problems with the separation of the large amount of bases produced from the NTP in the periodate oxidation (which eluted early in the chromatogram) from the dNTP of interest.

The large amount of bases absorbed UV radiation, making accurate measurement of the small dNTP peaks difficult, and also shortened the life of the column. Hence a method for removing these interfering bases and for purifying dNTP in periodate-treated cell extracts prior to HPLC is required.

A number of different procedures for partially purifying dNTP in periodate-treated extracts prior to HPLC have previously been published. These include calcium fluoride coprecipitation[3], acetonitrile precipitation[3], silica cartridge separation[4] and strong anion-exchange (SAX) cartridge separation[3]. All these procedures give good recoveries using standard aqueous solutions of nucleotides but, except for the SAX cartridge procedure, give much poorer recoveries with periodate-treated cell extracts. We have previously shown that the SAX cartridge procedure shows consistently high recoveries of dNTP both using standard aqueous solutions and periodate-treated cell extracts[3]. Unfortunately, the procedure involved elution with 1 *M* hydrochloric acid, which must therefore be quickly neutralized to avoid any acid hydrolysis of the dNTP. A further disadvantage was that the elution volume was between 2 and 5 ml to achieve 100% recovery of the dNTP, which meant that a lyophilization step was necessary prior to HPLC, which might affect the recovery. We have now investigated the use of weak anion-exchange (aminopropyl) cartridges for the partial purification and concentration of dNTP in periodate-treated cell extracts prior to HPLC. The results show that dNTP in periodate-treated cell extracts can be quickly and simply partially purified prior to HPLC using weak anion-exchange cartridges.

EXPERIMENTAL

Chemicals

All nucleotides were of the highest purity available and were purchased from Sigma (St. Louis, MO, U.S.A.). The purity of the standard nucleotides was determined by HPLC as described below. All standard nucleotides used were at least 98% pure.

Chromatographic equipment

All HPLC analyses were performed on a chromatograph from Waters Assoc. (Milford, MA, U.S.A.). The absorbance at 254 and 280 nm was measured with a Model 440 dual-wavelength absorbance detector. Integration of the peaks was performed with a Shimadzu C-R3A integrator with an FDD-IA floppy disc drive.

Chromatographic procedure

Nucleotides were separated isocratically by ion-exchange HPLC using a strong anion-exchange column (Partisil 10 SAX, 250 × 4.6 mm I.D.) (Whatman, Clifton, NJ, U.S.A.). The mobile phase was 0.6 *M* KH_2PO_4 adjusted to pH 3.25 with phosphoric acid. A flow-rate of 2 ml/min was used.

Cell extraction procedure

CEM cells (a human CD4 + lymphocyte cell line) were grown at 37°C in RPMI medium supplemented with 10% heat-inactivated foetal calf serum in a humidified atmosphere of 5% carbon dioxide in air. Cells (1×10^8) were harvested by centrifugation at 1000 *g* for 10 min. The medium was decanted and the pellet completely drained by inversion on tissue paper for 30 s. A volume of cold 12% trichloroacetic acid approximately equal to the volume of the cell pellet (600 μl) was added to the pellet and the solution (total volume *ca.* 1.2 ml) was vortex mixed for 20 s. The extract was kept on ice for 10 min, then mixed again. The precipitate was removed by centrifugation at 1000 *g* for 10 min. The supernatant (volume *ca.* 1 ml) was removed and 1.1 volume of a freshly made 0.5 *M* solution of tri-*n*-octylamine in Freon was added to neutralize the pH of the supernatant[5]. The solution was vortex mixed for 20 s and then centrifuged at 1000 *g* for 2 min to separate the phases. The neutralized aqueous phase (volume *ca.* 1 ml) containing the nucleotides extracted from $1 \cdot 10^8$ cells was carefully decanted and frozen at −20°C.

Periodate oxidation procedure

The ribonucleotides in the neutralized cell extracts were degraded to bases by the periodate oxidation procedure developed by Garrett and Santi[1]. A 40-μl volume of a 0.5 *M* aqueous solution of sodium periodate was added to 1 ml of neutralized extract (containing nucleotides extracted from 1×10^8 cells) and the solution was gently mixed. After incubation at 37°C for 3 min a 50-μl volume of a 4 *M* aqueous solution of methylamine (pH adjusted to 7 by addition of phosphoric acid) was added and the solution gently mixed. The solution was incubated at 37°C for a further 30 min and the reaction was then terminated by the addition of 10 μl of a 1 *M* aqueous solution of rhamnose. The sample (volume *ca.* 1.1 ml) was then put on ice. The entire 1.1-ml sample was applied to the cartridge in the next step.

Weak anion-exchange cartridge procedure

Weak anion-exchange cartridges (Sep-Pak and Sep-Pak Light aminopropyl cartridges) were obtained from Millipore–Waters (Milford, MA, U.S.A.). The cartridge was washed with 3 ml of water before the sample was applied. A 1-ml volume of a standard solution of deoxynucleotides in water (25 μM each of dATP, dGTP, dCTP and dTTP) was then applied to the cartridge. For experiments with cell extracts, 1.1 ml of a periodate-treated extract from $1 \cdot 10^8$ cells was applied to the cartridge instead. When the recovery of the deoxynucleotides was being measured, the cell extract was "spiked" with a predetermined concentration of standard deoxynucleotides in excess of the intracellular concentration (50 μM each of dATP, dGTP, dCTP and dTTP); otherwise, when the intracellular dNTP concentration of CEM cells was being measured the cell extracts were not "spiked". The cartridge was then rinsed with 3 ml of water to remove unretained components. Finally, the cartridge was eluted with 1 ml of 5 *M* sodium chloride solution. A 100-μl volume of the 5 *M* sodium chloride fraction was injected directly onto the HPLC column. The amounts of each dNTP present were determined by integration of the peak at 254 nm and comparison with that given by a known amount of a standard solution of each dNTP injected directly onto the column without use of the cartridge. Peaks were identified by (a) retention time, (b) ratio of absorbance at 280 nm to that at 254 nm and (c) spiking with known

standards. A 300-μl volume of the 3-ml water wash from the cartridge was also injected to check that all the dNTP had been retained on the cartridge prior to the salt elution. The recoveries of each dNTP were determined by calculating the total amount of dNTP eluted in the 1-ml 5 *M* salt fraction and comparing this with the known amount applied to the cartridge in the standard aqueous solution or spiked cell extract. All experiments were performed in triplicate and the mean results with the standard deviations are quoted. The amount of bases present in the sample was determined likewise by integration of the appropriate peaks.

RESULTS AND DISCUSSION

Weak anion-exchange cartridges were used to retain dNTP while the other components of the periodate-treated cell extracts, including the bases that arise from the periodate degradation of NTP, were eluted in the water wash. Only the triply charged dNTP could be expected to have bound to this weak anion-exchange matrix. The NTP cannot bind as they are known to be degraded to bases in the periodate reaction[1]. The dNTP were then eluted with 1 ml of 5 *M* sodium chloride and subjected to HPLC.

The recoveries of each of the four dNTP in the 1-ml salt fraction when applied to the cartridge as an aqueous solution of known concentration and purity were as follows (means of three determinations $\pm$ standard deviation): 97 $\pm$ 0.61% for dATP; 96 $\pm$ 1.4% for dGTP; 98 $\pm$ 2.1% for dCTP; and 98 $\pm$ 0.72% for dTTP. No dNTP was detectable in the 3-ml water wash from the cartridge, indicating that all the dNTP was retained by the cartridge prior to the salt elution. The recoveries of dNTP in the salt fraction when periodate-treated cell extracts were spiked with known amounts of standard dNTP were similar, indicating that there was no decrease in recovery of dNTP when periodate-treated cell extracts were used instead of aqueous solutions.

Fig. 1 shows a typical chromatogram obtained with and without partial purification of the periodate-treated cell extract with the ion-exchange cartridge. Without use of the cartridge (Fig. 1a) the large amount of bases (produced from NTP in the periodate degradation) eluted early in the chromatogram and obscured the dNTP peaks. Only the dGTP peak at 14.4 min was accurately measured. After partial purification of the periodate-treated cell extract with the ion-exchange cartridge (Fig. 1b) most of the bases were removed and the peaks of dCTP, dTTP, dATP and dGTP could be clearly seen and accurately measured. The total absorbance at 254 nm of the interfering bases eluting with the solvent front at 1–10 min (without use of the cartridge, Fig. 1a) or at 1–5 min (after partial purification with the cartridge, Fig. 1b) was determined by integration of the appropriate peaks and the values were compared to determine how much of the interfering bases had been removed by use of the ion-exchange cartridge. The results showed that 93 $\pm$ 6% (mean of three separate determinations $\pm$ standard deviation) of the interfering bases eluting at the solvent front were removed using the ion-exchange cartridge.

Attempts were made to reduce the salt concentration and volume required for elution of the dNTP by the use of sodium chloride in phosphate buffer (0.6 *M* KH_2PO_4 adjusted to pH 3.5 or 2.2 with phosphoric acid). Lowering the pH to 3.5 or 2.2 did not decrease the salt concentration or volume significantly. However, the use of smaller cartridges (Sep-Pak Light) with one third the amount of sorbent did permit a reduction

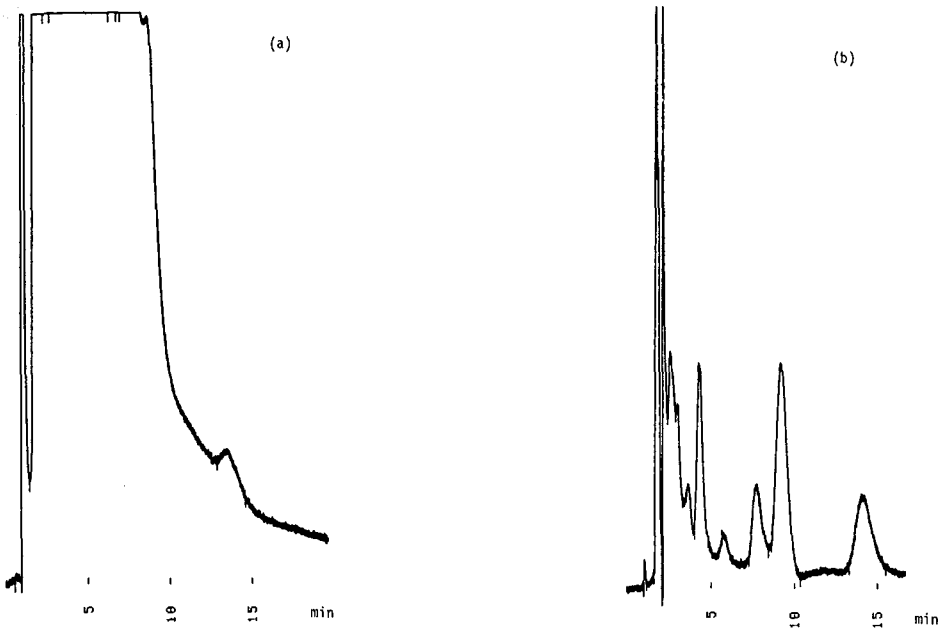

Fig. 1. Chromatogram obtained on injection of a periodate-treated cell extract (a) without further purification and (b) after partial purification on a weak anion-exchange cartridge. Extracts from $2 \cdot 10^7$ cells were injected in each instance. The absorbance at 254 nm was measured. The sensitivity was set at 0.01 a.u.f.s. dCTP, dTTP, dATP and dGTP eluted at 5.9, 7.8, 9.4 and 14.4 min, respectively.

in the elution volume. In this instance the elution volume could be reduced to 0.5 ml without a decrease in recovery. This small volume allowed the concentration of the dNTP in periodate-treated cell extracts and removed the need for lyophilization before HPLC analysis.

Using these cartridges to partially purify the periodate-treated extract, the dNTP content of CEM cells in the late logarithmic phase was measured by HPLC. The dNTP contents in pmol per 10^6 cells of a periodate-treated extract of CEM cells measured by HPLC after partial purification on the ion exchange-cartridge were found to be as follows: dATP, 22.8 $\pm$ 5.2; dGTP, 15.7 $\pm$ 1.1; dCTP, 3.1 $\pm$ 0.7; and dTTP, 18.8 $\pm$ 5.7 (means of four determinations $\pm$ standard deviations).

In conclusion, it has been demonstrated that aminopropyl cartridges provide a rapid and reliable means of partly purifying and concentrating dNTP in periodate-treated cell extracts at neutral pH prior to HPLC. The use of these cartridges removes much of the bases produced in the periodate reaction and thus allows the accurate measurement of the dNTP content of cell extracts by HPLC.

REFERENCES

1 C. Garrett and D. V. Santi, *Anal. Biochem.*, 99 (1979) 268.
2 V. Srivastava, M. L. Pall and A. L. Schroeder, *Mutat. Res.*, 200 (1988) 45.
3 J. Harmenberg, A. H. J. Karlsson and G. Gilljam, *Anal. Biochem.*, 161 (1987) 26.
4 C. D. Lothrop and M. Uziel, *Clin. Chem.*, 26 (1980) 1430.
5 S.-C. Chen, P. R. Brown and D. M. Rosie, *J. Chromatogr. Sci.*, 15 (1977) 218.

Journal of Chromatography, 508 (1990) 81–96
Elsevier Science Publishers B.V., Amsterdam — Printed in The Netherlands

CHROM. 22 322

Characterization of chemically synthesized human relaxin by high-performance liquid chromatography

ELEANOR CANOVA-DAVIS*, IDA P. BALDONADO and GLEN M. TESHIMA
Analytical Chemistry Department, Genentech, Inc., 460 Point San Bruno Boulevard, South San Francisco, CA 94080 (U.S.A.)
(First received June 13th, 1989; revised manuscript received January 2nd, 1990)

SUMMARY

Highly purified human relaxin, produced by combining chemically synthesized A- and B-chains, was analyzed by reversed-phase high-performance liquid chromatography, ion-exchange chromatography and tryptic mapping in order to ascertain purity of the material, presence of uncleaved protecting groups, correctness of disulfide linkages and presence of deamidated or oxidized variants. It was shown by a variety of analytical methods that the product was of high purity; a minimum purity level as judged by the most discriminating assay was greater than 98%. Components of the relaxin preparation removed during the purification were identified to be variants containing deletions arising from incomplete coupling reactions in the solid phase peptide synthesis and/or oxidized methionine residues.

INTRODUCTION

Recent elucidation of the primary structure of relaxin has revealed its homology to insulin essentially by its strikingly similar disulfide bond structure. The relaxin and insulin molecules are each composed of two non-identical peptide chains linked by two disulfide bridges with an additional intrachain disulfide bridge in the smaller A-chain. The amino acid sequences of relaxin are known for a number of species including porcine[1], rat[2], sand tiger shark[3], spiny dogfish shark[4], human[5,6], skate[7], minke whale[8] and Bryde's whale[8]. From protein sequencing data on the purified ovarian hormones and nucleotide sequence analysis data of cDNA clones[9,10] it appears that the relaxins are expressed as single chain peptide precursors with the overall structure: signal peptide–B-chain–C-peptide–A-chain. Since the sites of *in vivo* processing of human prepro relaxin are not identified, they were postulated by analogy to the processing of porcine and rat preprorelaxins[6]. Hence, the human A-chain was chemically synthesized by solid phase methods as a 24-amino acid polypeptide and the B-chain as 33 amino acids in length.

The chemical synthesis of small polypeptide hormones has been extensively described and shown to be invaluable for confirmation of proposed sequences and for

0021-9673/90/$03.50

structure–function studies[11]. In particular, peptide synthesis has been shown to be a very useful technique for studies of the chemical and biological properties of human relaxin since it has not been possible to obtain the natural hormone from human tissue[12]. However, the use of chemical synthesis as opposed to recombinant-DNA techniques for the manufacture of small polypeptides (50 residues or less) for pharmaceutical application is an area of lively debate[13,14]. Examples to date include calcitonin (32 amino acids), pentagastrin and tetracosa adrenocorticotropin peptide[13]. In addition to considerations such as speed, cost, complexity of the technology and yield, the requirement of high purity for human testing is an important aspect, as a product of chemical synthesis has a variety of potential side reactions that are not generated by a biosynthetic process; *e.g.*, racemization, deletions and residual blocking groups.

With the advent of biotechnology and the capability to produce recombinant proteins in good yield with a high degree of purity, has come the requirement for sensitive and varied analytical methods for product characterization[15]. Recommendations issued by the Federal Drug Administration for protein pharmaceuticals have included a specification for the characterization of any variant present at the 1% level. Therefore, this study was an attempt to characterize a chemically synthesized protein in some detail, *i.e.*, using various analytical methods in addition to the routine amino acid and liquid chromatographic analyses generally employed[12] to investigate the relative merits of the two technologies. This is the first instance in which a chemically synthesized protein of the size of relaxin (57 amino acids) has been characterized to conform with the Federal Drug Administration's requirements. Emphasis was placed upon reversed-phase high-performance liquid chromatography (HPLC) analysis as it is a widely accepted high-resolution procedure[16–19]. In addition, the recent technique of fast atom bombardment-mass spectrometry (FAB-MS)[20–21] was utilized to more thoroughly examine the protein for any chemical modifications.

In recombinant DNA-derived protein pharmaceuticals, the potential variants have typically been deamidated, oxidized, proteolytically degraded and aggregated species. In addition to the possibility of these forms existing in a chemically synthesized protein, amino acid deletions, truncations, racemization, incomplete removal of blocking groups and re-acetylation or alkylation can also occur. These side reactions inherent in a chemical synthesis become more significant as the length of the synthesized peptide increases. Since the chemical synthesis method chosen involved the use of *tert.*-butyloxycarbonyl amino acids, the probability of racemization occurring to any extent is minimized[22]. The following investigation is an in-depth study of the chemical characteristics of such a prepared human relaxin molecule.

EXPERIMENTAL

Chemical synthesis of human relaxin

The A- and B-chains and a B-chain analogue of human relaxin were synthesized in the Peptide Group at Genentech by the solid-phase synthesis method of Merrifield[23] using *tert.*-butyloxycarbonyl amino acid derivatives and a phenylacetamidomethyl resin. The side chain protecting groups were as follows: cysteine, 4-methylbenzyl; aspartic and glutamic acid, cyclohexyl; lysine, chlorocarbobenzoxy; asparagine and glutamine, xanthyl; arginine, tosyl; serine and threonine, benzyl and tyrosine,

2,6-dichlorobenzyl. The crude chains were purified, combined to form relaxin and the resultant protein was isolated as previously described[24]. Briefly, the individual chains were purified by reversed-phase HPLC using a Vydac C_4 column with a 0.1% trifluoroacetic acid (TFA)–acetonitrile linear gradient. The isolated chains were subsequently combined in a reaction mixture containing 100 m*M* glycine (pH 10.5), 1 m*M* EDTA, 2.5 m*M* dithiothreitol (DTT), 3% *n*-propanol, 3% acetonitrile and 1 *M* urea. The solution was stirred open to the air for 28 h at ambient temperature. This material was then purified by reversed-phase HPLC using a SynChropak RP-C_4 column with a 0.05% TFA–acetonitrile linear gradient and finally by ion-exchange chromatography in the Process Development Group at Genentech. The purified material was shown to be biologically active in the mouse pubic symphysis ligament *in vivo* bioassay[25] and the rat uterine contractility *in vitro* bioassay[26].

Amino acid and amino terminal sequencing analyses

The acid hydrolysates of 6–8 μg of relaxin preparations were analyzed using a Beckman Model 6300 analyzer with the standard three-buffer elution system and post-column ninhydrin detection. To analyze for cysteine, samples were treated with performic acid according to Hirs[27] prior to acid hydrolysis. Thioglycolic acid (7%) was added to samples before acid hydrolysis in order to quantitate tryptophan.

The A-chain amino terminal of the relaxin molecule was deblocked by treatment with pyroglutamate aminopeptidase (Boehringer Mannheim) as described by Podell and Abraham[28]. The treated protein was chromatographed by reversed-phase HPLC on a Waters gradient liquid chromatography system (connected to a Nelson Analytical 6000 data system) that consisted of two 510 pumps, a 720 controller, a WISP injector and 440 absorbance detector with an extended wavelength module for dual-wavelength detection (214 and 280 nm) fitted with a Vydac C_4 column (250 mm × 4.6 mm I.D., 5 μm, 300 Å). An acetonitrile elution was begun with 15% acetonitrile containing 0.1% TFA for 10 min followed by a 40 min linear gradient to 35% acetonitrile. The recovered peptide-containing fractions were pooled and subjected to Edman degradation using an Applied Biosystems 447A protein sequencer, with on-line phenylthiohydantoin detection (Applied Biosystems 120A analyzer).

Extinction coefficient

The ultraviolet spectrum of relaxin in 10 m*M* sodium citrate, pH 5.0, and isotonic saline was obtained. The extinction coefficient was determined according to Beaven and Holiday[29] as modified by Wetlaufer[30] for a 0.1% solution of the protein and found to be 2.04.

Size-exclusion chromatography

Gel filtration of relaxin (50 μl) was conducted using a TSK G2000 SWXL column (300 mm × 7.5 mm I.D.) equilibrated with 10 m*M* sodium citrate, pH 5.0, in 0.25 *M* sodium chloride. The flow-rate was 0.5 ml/min and the protein was monitored at 214 nm.

Hydrophobic interaction chromatography (HIC)

These separations were done using a Hewlett-Packard 1090M liquid chromatograph. This system consisted of an autoinjector with a 25-μl sample loop and a

photodiode array detector. Ultraviolet absorbance was monitored at 214 nm. The TSK-phenyl-5 PW column was purchased from HP Genenchem. This column was 75 mm × 7.5 mm I.D. and was packed with a resin of 10-μm particle diameter with an average pore diameter of 1000 Å. Buffer A consisted of 0.1 *M* potassium phosphate, pH 7.0, containing 2 *M* ammonium sulfate. Buffer B was 0.1 *M* potassium phosphate, pH 7.0. The column was equilibrated with 50% buffer A and 50% buffer B and a decreasing linear salt gradient was generated to 100% B in 50 min. The flow-rate was maintained at 1 ml/min and the temperature was ambient. Relaxin concentrations were adjusted to 1 mg/ml with buffer B; 50-μl aliquots were injected.

Tryptic mapping

Human relaxin at a concentration of 0.5 mg/ml was digested with L-1-tosylamido-2-phenylethyl chloromethyl ketone (TPCK)-treated trypsin (Cooper Biomedical) at 37°C for 4 h in 10 m*M* Trisacetate, pH 7.3, 0.2 m*M* calcium chloride. Two aliquots (10 μl each) of enzyme–substrate (1:100, w/w) of trypsin were added: the first at zero time, and the second after 2 h of digestion. Samples were frozen at −20° if not analyzed immediately. The peptide peaks collected manually from the Waters HPLC system were characterized by amino acid analysis after acid hydrolysis and by FAB-MS. For FAB-MS the samples (0.5–1.0 nmol) were lyophilized to remove volatile salts. They were then solubilized in a minimum volume of 0.1% acetic acid and analyzed by direct addition to glycerol on the sample probe of a two-sector JEOL HXIIOHF mass spectrometer with a DA 5000 data system. Fast atom bombardment was performed with 6 keV xenon atoms. Data were acquired over a mass range of 100–4300 daltons.

RESULTS AND DISCUSSION

Amino acid analyses

Typical analyses of relaxin and its composite A- and B-chains are shown in Table I. Residues per mol were normalized to the sum of alanine and leucine. These results demonstrate excellent correlation with the theoretical values[6]. As can be seen in this table, the cysteic acid determination for human relaxin is 87% of the expected theoretical value. Humulin (recombinant human insulin) was analyzed at the same time, as a control for these particular cystine linkages. The cysteic acid value obtained was 80% of the expected value. Amino acid analysis can be used for the partial assessment of the primary structure of a polypeptide. With small peptides, such as relaxin, it was a useful technique for the determination of purity[31]. At the very least, this method served as a confirmation of the presence of the correct amino acids in the proper ratios and suggested that the purified product contained minimal levels of deletion peptides.

Amino terminal sequencing

Synthetic human relaxin was analyzed by Edman degradation to determine the amino acid sequence at the N-termini of the two chains present in the molecule. Since the A-chain contains an N-terminal pyroglutamic acid residue, sequence data could be obtained only after treatment of the molecule with pyroglutamate aminopeptidase. The expected sequences for the two chains were found (Table II). No other N-termi-

TABLE I

AMINO ACID COMPOSITION OF HUMAN RELAXIN AND ITS COMPOSITE A- AND B-CHAINS

Amino Acid	*Composition (residues/mol)*[b]		
	Relaxin	*A-chain*	*B-chain*
CyA[a]	5.18 (6)	3.82 (4)	1.92 (2)
Asx	1.99 (2)	0.98 (1)	0.93 (1)
Thr[c]	1.97 (2)	1.00 (1)	0.98 (1)
Ser[c]	5.83 (6)	1.97 (2)	3.90 (4)
Glx	5.02 (5)	0.98 (1)	3.97 (4)
Pro[a]	0 (0)	0 (0)	0 (0)
Gly	3.00 (3)	1.02 (1)	2.01 (2)
Ala	4.96 (5)	2.95 (3)	2.02 (2)
Val[d]	2.93 (3)	0.98 (1)	1.94 (2)
Met	1.86 (2)	0 (0)	1.82 (2)
Ile[d]	2.74 (3)	0 (0)	2.63 (3)
Leu	6.04 (6)	3.05 (3)	2.98 (3)
Tyr	0.98 (1)	0.97 (1)	0 (0)
Phe	1.05 (1)	1.04 (1)	0 (0)
His	0.99 (1)	1.00 (1)	0 (0)
Lys	3.97 (4)	2.00 (2)	1.93 (2)
Trp[e]	2.01 (2)	– (0)	2.03 (2)
Arg	4.98 (5)	2.01 (2)	2.90 (3)

[a] Performic acid oxidized sample.
[b] Theoretical values are in parentheses.
[c] Extrapolation to zero time of hydrolysis.
[d] After a 72-h hydrolysis.
[e] Determined in the presence of thioglycolic acid.

nal sequences were observed, again indicating the absence of any significant deletion peptides arising from the chemical synthesis as present in the purified material. It was possible to detect a secondary sequence in a B-chain preparation estimated to contain 5% des Asp[1]-B-chain by reversed-phase HPLC[32].

Size-exclusion chromatography

When the chemically synthesized relaxin preparation was chromatographed at pH 5.0 at a concentration of 0.4 mg/ml or less it behaved as a monomer. The molecular weight of the monomer was determined by FAB-MS to be 6448.9 as compared to a calculated value of 6449.6. However, when the chromatography was conducted at a concentration of 2 mg/ml, it began eluting from the column as a dimer. This is consistent with the data[33] obtained from sedimentation equilibrium experiments which demonstrated that human relaxin self associates in a reversible manner which is concentration and pH dependent. Analysis with a monomer–dimer association model[34] results in an association constant of 38.2 l/g at pH 5.0.

Reversed-phase HPLC

Relaxin samples were analyzed by reversed-phase HPLC using a shallow gradient of acetonitrile, which resolved relaxin and its component A- and B-chains from

TABLE II

AMINO-TERMINAL SEQUENCE ANALYSIS OF HUMAN RELAXIN AFTER TREATMENT WITH PYROGLUTAMATE AMINOPEPTIDASE

Cycle number	*A-chain*		*B-chain*	
	Sequence	*Yield (pmol)*	*Sequence*	*Yield (pmol)*
1	Leu	120	Asp	64
2	Tyr	67	Ser[a]	–
3	Ser[a]	–	Trp	49
4	Ala	110	Met	76
5	Leu	110	Glu	57
6	Ala	110	Glu	84
7	Asn	47	Val	75
8	Lys	61	Ile	79
9	Cys[b]	–	Lys	62
10	Cys[b]	–	Leu	86
11	His	2.4	Cys[b]	–
12	Val	32	Gly	56
13	Gly	28	Arg	15
14	Cys[b]	–	Glu	36
15	Thr	4.4	Leu	68
16	Lys	23	Val	50
17	Arg	11	Arg	11
18	Ser[a]	–	Ala	66
19	Leu	36	Gln	33
20	Ala	42	Ile	49
21	Arg[c]	–	Ala	89
22	Phe	30	Ile	49
23	Cys[c]	–	Cys[c]	–
24			Gly	32
25			Met	28
26			Ser[c]	–
27			Thr	4.0
28			Trp[c]	–
29			Ser[c]	–
30			Lys[c]	–
31			Arg	3.7
32			Ser[c]	–
33			Leu[c]	–

[a] Identified as the dehydroalanine adduct of dithiothreitol with a concomitant peak in the Ser position.

[b] Identified as the dehydroalanine adduct of dithiothreitol without a concomitant peak in the Ser position.

[c] Not confirmed.

each other. Fig. 1 shows a typical profile of a relaxin preparation obtained before and after reduction with DTT. Relaxin preparations that had been purified by reversed-phase HPLC and cation-exchange chromatography contained greater than 98% of the total integrated area in the main peak when analyzed by reversed-phase HPLC. Recovery from this column was quantitative as judged from the linear response of the total integrated area of relaxin samples from 0–20 μg. The later elution of B-chain as

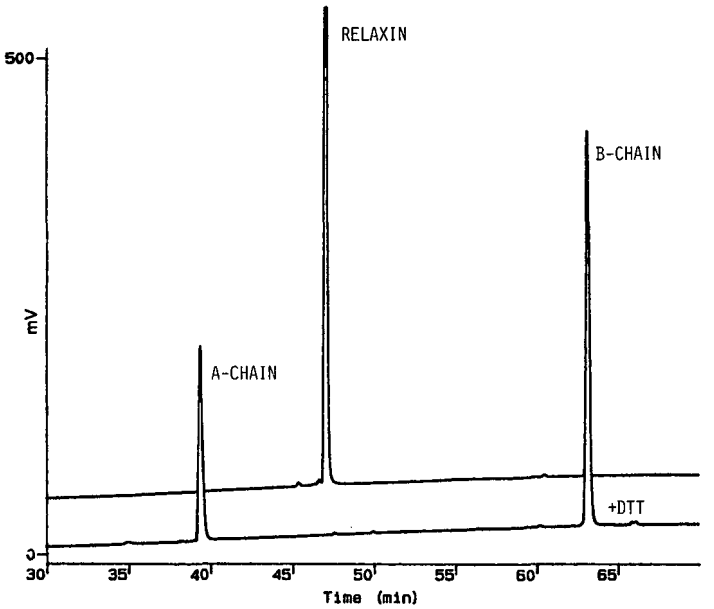

Fig. 1. Reversed-phase HPLC chromatograms of human relaxin before and after reduction with DTT. The chromatography was performed on the Waters HPLC system using a Vydac C_4 column equilibrated with 18% acetonitrile containing 0.1% TFA. Elution was conducted isocratically for 20 min followed by a linear gradient to 50% acetonitrile over 40 min and ending with a 10-min hold at 50% acetonitrile. The flow-rate was 1 ml/min, the protein was monitored at 214 nm, the analog output to the integrator was scaled at 0.5 volts per absorbance unit and the column temperature was maintained at 35°C. An amount of 10 μg of intact relaxin in 5% acetic acid was injected in 50 μl. In addition, relaxin samples were routinely reduced to their component A- and B-chains with 50 m*M* DTT, 4 *M* guanidine in 50 m*M* Tris · HCl, pH 8.5, at ambient temperature. A sample (50 μl) was injected directly onto the column.

compared to the intact hormone suggested greater hydrophobicity for the B-chain. Calculations of the hydrophilicity of the A-chain, the B-chain and relaxin itself yielded values of 1.18, 0.74 and 0.95, respectively[35] consistent with this observation.

Hydrophobic interaction chromatography

Since Gooding *et al.*[36] claimed that substantial changes in retention times and selectivity were seen under HIC conditions and little effect seen with reversed-phase HPLC in analyzing ovalbumin and bovine serum albumin, the HIC of relaxin was investigated. The profiles obtained for relaxin preparations showed less heterogeneity than those that had been observed after reversed-phase chromatography (Fig. 1). Hence, in this case, reversed-phase HPLC was a more discriminating technique than HIC. This is consistent with the recent work of Hoeger *et al.*[37] showing that reversed-phase HPLC is quite efficient in resolving closely related impurities from synthetic polypeptides in the 1500–4200-dalton molecular mass range.

Cation-exchange chromatography

Cation-exchange chromatography profiles of relaxin were generated in 0.05 *M* potassium phosphate at pH 6.0, 6.5 and 7.0. At lower pH values, the protein bound

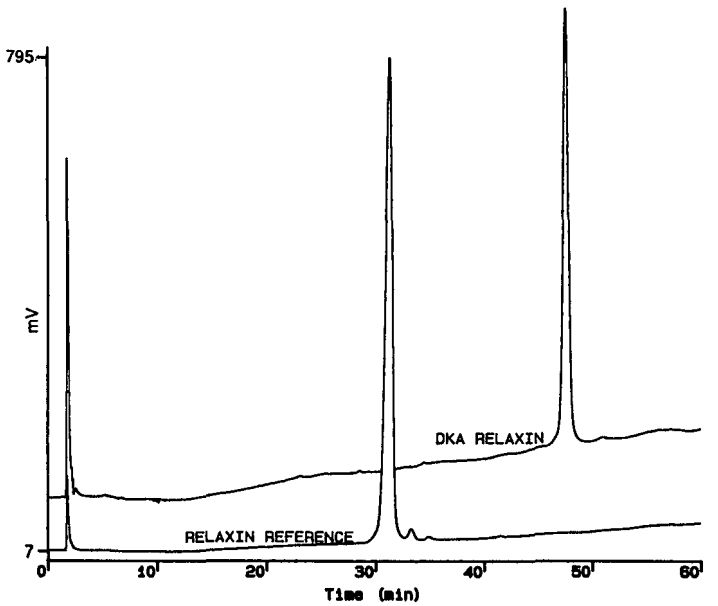

Fig. 2. Comparison of the human DKA relaxin analogue (Lys^{B-4} Ala^{B-25} relaxin) and relaxin by cation-exchange chromatography. The chromatography was performed on a polyaspartic acid (Poly CAT A) column (200 mm × 4.6 mm I.D., 5 μm, 300 Å) purchased from the Nest Group. The buffer used was 0.05 *M* potassium phosphate at pH 7.0 in 25% acetonitrile. A linear gradient was generated with this buffer containing 0.5 *M* sodium chloride at a rate of 5m*M* sodium chloride/min. The flow-rate was maintained at 1 ml/min, the protein was monitored at 220 nm (0.5 volts per absorbance unit), and the temperature was kept at ambient. Relaxin concentrations were adjusted to 0.2 mg/ml with equilibration buffer; 50-μl aliquots were injected.

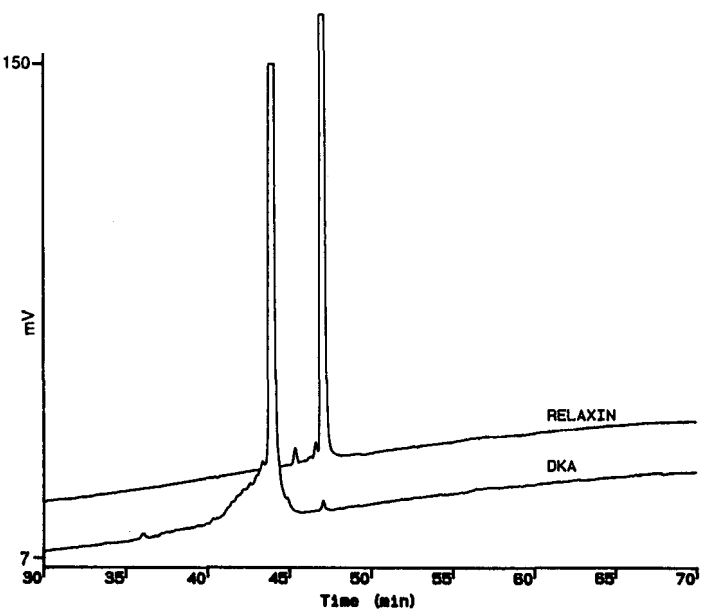

Fig. 3. Comparison of the human DKA relaxin analogue (Lys^{B-4} Ala^{B-25} relaxin) and relaxin by reversed-phase chromatography. The chromatography was performed as described in legend to Fig. 1.

more strongly to the column as expected by virtue of the greater protonation of relaxin at more acidic pH values (data not shown). In all cases, the main peak contained more than 99% of the material by peak area calculations.

An analogue of relaxin (DKA relaxin) was chemically synthesized whereby the methionine residues in the B-chain were replaced by lysine and alanine at positions B-4 and B-25, respectively. As can be seen in Fig. 2 the addition of a basic residue such as lysine results in the elution of the analogue at later retention times. When this analogue is analyzed by reversed-phase HPLC it elutes at an earlier retention time than relaxin itself consistent with its more hydrophilic nature (Fig. 3).

As might be expected, the cation-exchange chromatography was capable of detecting and resolving the charged variant better than reversed-phase chromatography. Cation-exchange chromatography was chosen as opposed to anion-exchange since relaxin has an isoelectric point above 7 (p*I* 10.5) as calculated according to Shire[38], in particular, polyaspartic acid cation-exchange columns were used since they have been reported to be capable of resolving proteins with as little difference as one amino acid[39].

Since this method separates proteins on the basis of their ionic character[40], it is a complementary technique to reversed-phase HPLC which resolves peptides primarily according to their hydrophobicity. Hydrophobic interaction and cation-exchange chromatography were investigated in an attempt to find an analytical procedure that would detect any variants that elude a reversed-phase HPLC step. This was particularly important in view of the preparative reversed-phase HPLC step used to purify the synthetic relaxin.

Tryptic mapping

Although synthetic relaxin was shown to be 98% pure by these different chromatographic techniques it was still possible that deletion peptides could not be detected due to any three dimensional structure of the hormone. Therefore, the tryptic map was a key technique in this study as enzymatic digestion generated nine small peptides that could be readily analyzed by reversed-phase HPLC. In addition, the trypsin digestion could be carried out on the unreduced protein so that information could also be gained concerning the disulfide linkages.

Digestion of the A-chain of human relaxin with trypsin can theoretically result in the release of five fragments (T_1, A1–9; T_2, A10–17; T_3, A18; T_4, A19–22; T_5, A23–24); that of the B-chain in the release of six fragments (T_6, B1–9; T_7, B10–13; T_8, B14–17; T_9, B18–30; T_{10}, B31; T_{11}, B32–33). By analogy with the disulfide pairing established for porcine relaxin[41] peptide T_2 would be expected to be covalently bonded to T_7 and peptide T_5 to T_9, respectively, in human relaxin. A typical tryptic map (digestion at pH 7.3) of relaxin is shown in Fig. 4. The peptide assignments were made after analysis of the peaks by acid hydrolysis for amino acid composition (data not shown) and confirmed by FAB-MS. The observed masses were within ± 0.7 a.m.u. of the theoretical values. Non-tryptic-like cleavages were seen to occur in the T_9 peptide. These peptides were identified as: T_{9a}, B18–25; T_{9b}, B18–28; T_{9c}, B26–30 as determined by their amino acid composition. The expected atomic mass units were observed for the T_5–T_{9a} peptide upon FAB-MS analysis. However, that expected for the T_{9c} peptide was low by 18 a.m.u., suggesting that a dehydration reaction had occurred. One possibility would be that a serine residue may have been converted to

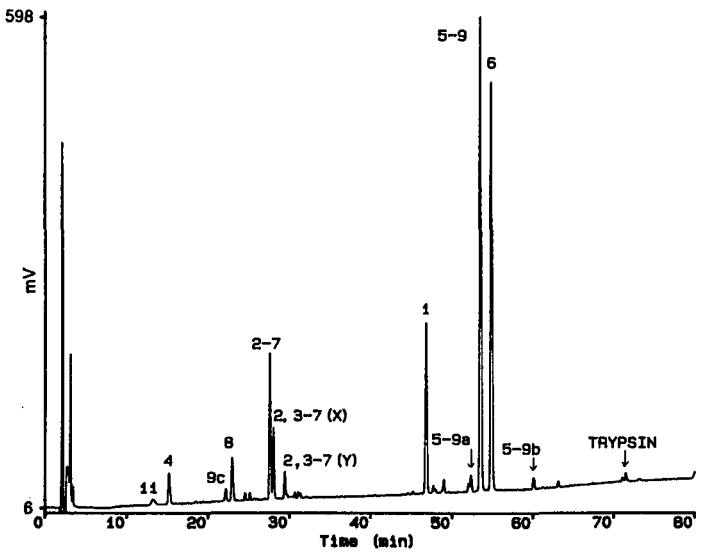

Fig. 4. Tryptic map of human relaxin following enzymatic digestion at pH 7.3. The digestion procedure was conducted as described in the Experimental section. The resulting peptide mixture (200 μl; 0.49 mg/ml) was separated by reversed-phase HPLC and monitored at 214 nm (0.5 volts per absorbance unit). The column was packed with Nucleosil C_{18} resin (150 mm × 4.6 mm I.D., 5μm, 300 Å). Elution was effected with a linear gradient from 3 to 30% acetonitrile containing 0.08% TFA over 54 min then to 70% acetonitrile in 40 min. The flow-rate was 1 ml/min and the column temperature was controlled at 35°C. The tryptic peptides are numbered sequentially from the amino termini of the A- and B-chains as described in the Results and Discussion section.

dehydroalanine. Since the recovery of serine by amino acid analysis is at least 83% in all cases and the FAB-MS spectrum of the intact B-chain shows no evidence for a dehydroalanine-containing peptide (data not shown), it is possible that the T_{9c} peptide underwent dehydration during the FAB-MS analysis. The carboxy terminal amino acid of T_{9b} was presumed to be tryptophan since the peptide T_5–T_{9b} had an appreciable absorbance at 280 nm. This deduction was confirmed by FAB-MS.

No evidence for improperly formed disulfide bonds was found when the tryptic digest was conducted at pH 7.3. However, if digestion was performed at the usual pH of 8.2 additional peptides were observed (Fig. 5). The addition of iodoacetic acid to the digestion reaction at pH 8.2 produced a profile similar to the one obtained when the digestion was conducted at pH 7.3 (Fig. 4). This suggested that disulfide exchanges were responsible for the extra peaks. These peaks were collected and identified by both acid hydrolysis for amino acid composition (data not shown) and by FAB-MS (Table III). It is apparent that a disulfide exchange is occuring during the tryptic digestion at pH 8.2. Not only are new peaks (identified as mixed disulfides) being observed, but the expected T_2–T_7 and T_5–T_9 peaks are decreasing. Dimers of T_2 and T_7 were also identified.

The cystine-containing peaks were isolated and reduced as described in the legend to Fig. 1 before rechromatography by reversed-phase HPLC. In every instance the two cysteine-containing peptides of the individual chains were observed (data not shown). A comparison of the retention times observed for each cysteine-containing

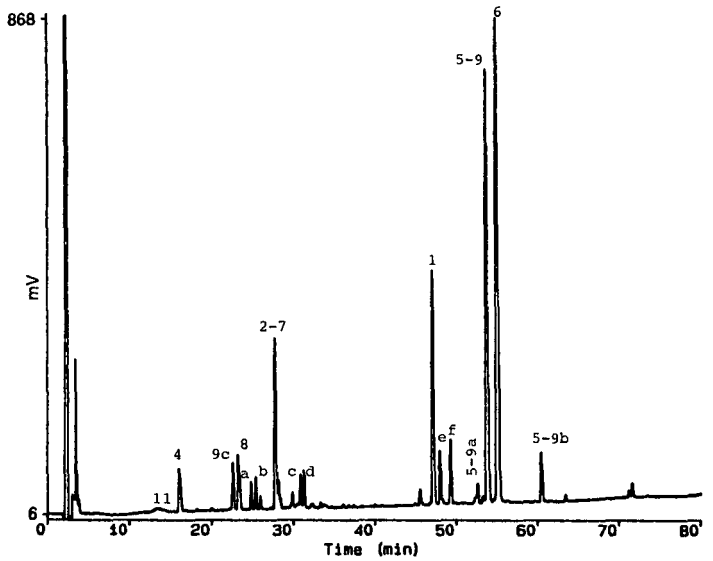

Fig. 5. Tryptic map of human relaxin following enzymatic digestion at pH 8.2. The procedure was conducted as described in the Experimental section and in Fig. 4 legend.

peptide led to the assignment of the component peptides. The identification of the T_2, T_5, T_7 and T_9 peptide peaks was confirmed by amino acid analysis. These cystine-containing peaks were also oxidized by performic acid before amino acid analysis to quantitate the cysteine levels. The correct composition was obtained for each of the peptides indicating that the six cysteine residues are actually present in the intact molecule.

These analyses not only confirmed the correct peptide sequence but also demonstrated the absence of significant coelutions. Thus, synthetic relaxin could be manufactured free of significant amounts of deletion peptides at the threshold of detection

TABLE III

MASS SPECTRAL ANALYSIS OF ADDITIONAL TRYPTIC PEPTIDES OF RELAXIN GENERATED AT pH 8.2.

Peak	*Theoretical mass*	*Observed*	*Assignment*
a	447.6	893.5	T_7
b	1293.8[a]	1293.6	T_2–T_7
		1295.6	
d	848.2[a]	848.2	T_2
		1695.8	
e	2242.1[a]	2243.2	T_2–T_9
f	1841.5	1842.1	T_7–T_9

[a] Molecular ions expected if the $Cys^{A\text{-}10}$–$Cys^{A\text{-}15}$ intrachain disulfide bond is intact.

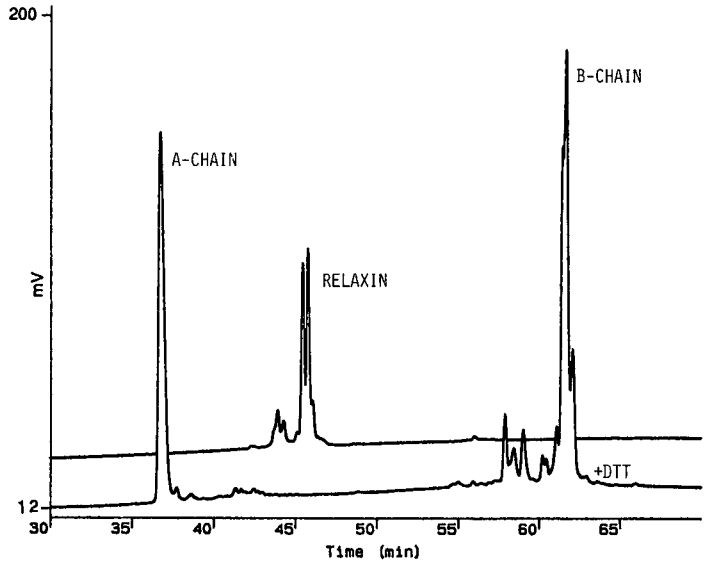

Fig. 6. Reversed-phase HPLC chromatograms of human relaxin side fraction before and after reduction with DTT. The chromatography was performed on a Vydac C_4 column as described in legend to Fig. 1.

in the tryptic map which is approximately 2–5%[42]. In addition, the following disulfide assignments were confirmed: T_2–T_7 and T_5–T_9. This unequivocally established $Cys^{A\text{-}24}$–$Cys^{B\text{-}23}$. The positions of the disulfides in T_2–T_7 will require further analysis to confirm their homology to those of insulin[43].

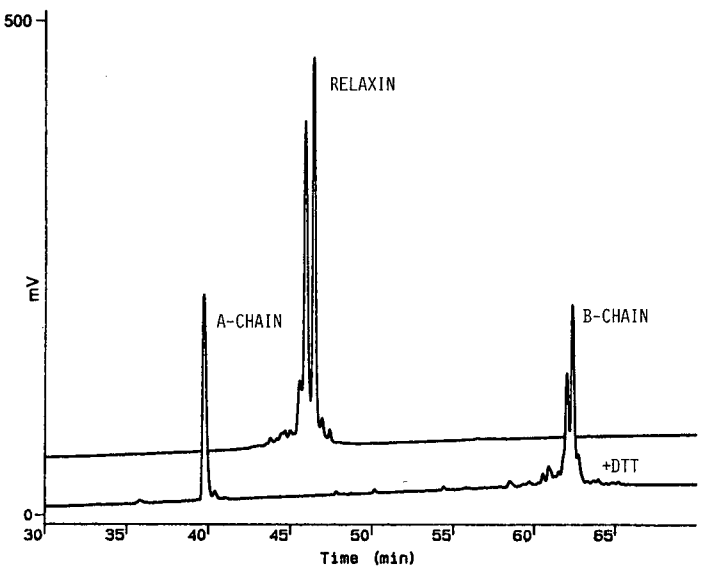

Fig. 7. Reversed-phase HPLC chromatograms of human relaxin preparation after incubation at 40°C before and after reduction with DTT. The chromatography was performed on a Vydac C_4 column as described in legend to Fig. 1.

Since deamidation of asparagine side chains is commonly seen in proteins[44], that at position A-8 was of interest. The T_1 peptide was chemically synthesized with an aspartic acid at position A-8. Its elution position in the tryptic map is as expected, immediately following the T_1 Asn-containing peptide. No detectible amount of the deamidated peptide is visible in the tryptic map of a purified relaxin preparation.

Evaluation of HPLC Techniques

In order to assess the ability of these HPLC methods to discriminate between closely related relaxin molecules, two samples known to be heterogeneous were obtained. One sample was a by-product of the purification procedure. The first step in the purification of relaxin after combination of the A- and B-chains is a reversed-phase HPLC isolation. The leading edge of the relaxin main peak is routinely removed in an effort to produce a homogeneous product. The second sample was generated by incubating a purified relaxin sample at 40°C in 10 m*M* Tris, pH 7.5, and isotonic saline for eight months. The analyses described above were performed on these preparations. Both of these samples contained material which eluted earlier than purified relaxin upon reversed-phase HPLC (Figs. 6 and 7). The profiles obtained from analysis of reduced material suggested that the differences were due to variants of the B-chain.

Although both HIC and cation-exchange chromatography were not effective in demonstrating any heterogeneity in the purified relaxin preparation, these methods did yield profiles of the side fraction and intentionally degraded preparations that consisted of multiple peaks (data not shown). These profiles were distinct from those obtained by reversed-phase HPLC (Figs. 6 and 7) and from each other substantiating the unique discriminating powers of these different chromatographic conditions.

The side fraction from the relaxin purification was also analyzed by tryptic mapping in the manner as described above for the purified fraction. A methionine sulfoxide was found at position B-4 in T_6 and at B-25 in T_9. In addition, four T_6 peptides were identified; namely, des Ser^2 Met^4 SO T_6, des Asp^1 T_6, des Ser^2 T_6 and des (Asp^1 Ser^2) T_6.

The intentionally degraded sample was analyzed similarly. The reversed-phase HPLC profile suggested that the methionine residues may have been oxidized (Fig. 7). As seen in the tryptic map (data not shown) of the side fraction from the relaxin purification a peptide eluted before the T_1 peptide and another just after it. These had been identified as Met^4 SO T_6 and T_5–T_9 Met^{25} SO, respectively, in the tryptic map analysis of the side fraction. By analogy, these assignments were made for the peptides seen in the tryptic map of the degraded sample. An amino terminal sequence analysis of the intact hormone confirmed that the methionine at position B-4 was indeed oxidized. This analysis also revealed that the N-terminus of the B-chain was intact. In addition, a peptide eluting after T_6 was discerned and characterized as T_5–T_9 (B18-29). No peaks which may have corresponded to deamidated peptides were detected.

CONCLUSIONS

It has been possible to chemically synthesize and prepare a complex protein like relaxin that is reproducibly more than 98% pure as judged by reversed-phase HPLC.

Analytical methods including amino acid analysis, reversed-phase HPLC and FAB-MS were utilized during the synthesis of the individual chains to monitor any synthesis-related problems.

The synthesis of the A-chain was reported[12] to be relatively straightforward compared to that of the B-chain. Not only was the B-chain difficult to synthesize[12,14], but it was also difficult to purify mainly due to its solubility characteristics which are a reflection of its high p*I* (11.5) calculated according to Shire[38] and extreme hydrophobicity[12]. Fortunately, the procedure of combining the A- and B-chains resulted in a product that lacked many of the impurities present in the B-chain component. The modifications of the B-chain shown to be present in the crude preparation such as *tert.*-butyl Trp and benzyl Cys[14] were not detected in the purified relaxin; neither were the B-chain deletions at Thr[27], Cys[23] and Gln[19] (ref. 14). The des Asp[1] truncated peptide did combine with the A-chain to form relaxin, but it could be removed during the reversed-phase HPLC purification step. A deletion at Ser[2], which was not previously reported, was also found in the combined relaxin, but was removed along with the des Asp[1] peptide during reversed-phase HPLC used to purify crude relaxin.

Chain combination followed by an optimized recovery process led to a clean profile upon reversed-phase HPLC. In order to demonstrate that this homogeneity is in fact real, and not due to lack of resolution of the technique, a number of tests were applied. The assays typically used for protein characterization, such as amino acid composition and amino terminal sequencing reinforced the conclusion of high purity as suggested by the reversed-phase chromatogram. In addition, degraded and chemically modified relaxin samples were identified in part by their altered retention times upon reversed-phase chromatography. Other chromatographic methods such as HIC and cation-exchange were not as effective as reversed-phase HPLC in detecting any latent heterogeneity.

Since no deamidation at Asn[8] in the A-chain was detected by tryptic mapping, it is not surprising that the purity of relaxin preparations were seen to be higher when determined by ion-exchange as opposed to reversed-phase chromatography. The lack of evidence for deamidation of relaxin preparations is consistent with the absence of Asn–Gly or Asn–Ser sequences[45] in its primary structure (Table II). An ion-exchange chromatography step was included in the purification procedure to guard against such a possibility. Tryptic mapping, which was instrumental in characterizing the oxidized and truncated forms, also suggested that the final product was quite pure. Hence, it has been possible by the judicious choice of selected analytical techniques to monitor the purity of a chemically synthesized relaxin molecule and to use this knowledge to devise a purification scheme leading to a relaxin preparation that is more than 98% pure.

ACKNOWLEDGEMENTS

The authors wish to thank Dr. John Burnier for the synthesis of the relaxin A- and B-chains; Dr. Ernst Rinderknecht for the production and purification of relaxin from its individual chains; Reed Harris for the amino acid analyses; Karen Williams for the N-terminal sequence analysis; and Dr. John Stults for the FAB-MS analyses. Special thanks are due to Dr. William Hancock for helpful discussions in the preparation of the manuscript.

REFERENCES

1 R. James, H. Niall, S. Kwok and G. Bryant-Greenwood, *Nature (London)*, 267 (1977) 544.
2 M. J. John, B. W. Borjesson, J. R. Walsh and H. D. Niall, in G. D. Bryant-Greenwood, H. D. Niall and F. C. Greenwood (Editors), *Relaxin*, Elsevier/North-Holland, New York, 1981, p. 37.
3 L. K. Gowan, J. W. Reinig, C. Schwabe, S. Bedarkar and T. L. Blundell, *FEBS Lett.*, 129 (1981) 80.
4 E. E. Büllesbach, L. K. Gowan, C. Schwabe, B. G. Steinetz, E. O'Byrne and I. P. Callard, *Eur. J. Biochem.*, 161 (1986) 335.
5 P. Hudson, J. Haley, M. John, M. Cronk, R. Crawford, J. Haralambidis, G. Tregear, J. Shine and H. Niall, *Nature (London)*, 301 (1983) 628.
6 P. Hudson, M. John, R. Crawford, J. Haralambidis, D. Scanlon, J. Gorman, G. Tregear, J. Shine and H. Niall, *EMBO*, 3 (1984) 2333.
7 E. E. Büllesbach, C. Schwabe and I. P. Callard, *Biochem. Biophys, Res. Commun.*, 143 (1987) 273.
8 C. Schwabe, E. E. Büllesbach, H. Heyn and M. Yoshioka, *J. Biol. Chem.*, 264 (1989) 940.
9 J. Haley, P. Hudson, D. Scanlon, M. John, M. Cronk, J. Shine, G. Tregear and H. Niall, *DNA*, 1 (1982) 155.
10 P. Hudson, J. Haley, M. Cronk, J. Shine and H. Niall, *Nature (London)*, 291 (1981) 127.
11 G. Losse, H. Stange, W. Naumann and B. Schwenzer, *Z. Chem.*, 20 (1980) 429.
12 G. W. Tregear, Y-C. Du, K-Z. Wang, C. Southwell, P. Jones, M. John, J. Gorman, B. Kemp and H. D. Niall, in M. Bigazzi, F. C. Greenwood and F. Gasparri (Editors) *Biology of Relaxin and its Role in the Human*, Elsevier, Amsterdam, 1983, p. 42.
13 D. T. Liu, N. Goldman and F. Gates, III, in M. Phillips, S. P. Shoemaker, R. D. Middlekauff and R. M. Ottenbrite (Editors), *The Impact of Chemistry on Biotechnology: Multidisciplinary Discussions (ACS Symposium Series*, No. 362), American Chemical Society, Washington, DC, 1988, p. 162.
14 E. Canova-Davis, R. C. Chloupek, I. P. Baldonado, J. E. Battersby, M. W. Spellman, L. J. Basa, B. O'Connor, R. Pearlman, C. Quan, J. A. Chakel, J. T. Stults and W. S. Hancock, *Am. Biotechnol. Lab.*, 6 (1988) 8.
15 W. S. Hancock, E. Canova-Davis, R. C. Chloupek, S.-L. Wu, I. P. Baldonado, J. E. Battersby, M. W. Spellman, L. J. Basa and J. A. Chakel, *Banbury Report 29: Therapeutic Peptides and Proteins: Assessing the New Technologies*, Cold Spring Harbor Laboratory, Cold Spring Harbor, NY, 1988, p. 95.
16 M. T. W. Hearn and W. S. Hancock, *Trends Biochem. Sci.*, 4 (1979) N58.
17 P. E. Petrides, R. T. Jones and P. Bohlen, *Anal. Biochem.*, 105 (1980) 383.
18 J. E. Rivier, *J. Liq. Chromatogr.*, 1 (1978) 343.
19 J. B. Shelton, J. R. Shelton and W. A. Schroeder, *Hemoglobin*, 3 (1979) 353.
20 M. Barber, R. S. Bordoli, R. D. Sedgwick and A. N. Tyler, *J. Chem. Soc., Chem. Commun.*, (1981) 325.
21 K. Biemann, *Anal. Chem.*, 58 (1986) 1288A.
22 J. P. Greenstein and M. Winitz, *Chemistry of the Amino Acids*, Robert E. Krieger Publ., Malabar, FL, 1984, p. 763.
23 R. B. Merrifield, *Adv. Enzymol.*, 32 (1969) 221.
24 J. P. Burnier and P. D. Johnston, *Eur. Pat., 0251615A2*, Bulletin 88/01, January 7, 1988.
25 B. G. Steinetz, V. L. Beach, R. L. Kroc, N. R. Stasilli, R. E. Nussbaum, P. J. Nemith and R. K. Dun, *Endrocinology*, 67 (1960) 102.
26 J. St.-Louis, *Can. J. Physiol. Pharmacol.*, 59 (1981) 507.
27 Hirs, C. H. W., *Methods Enzymol.*, 11 (1967) 59.
28 D. N. Podell, and G. N. Abraham, *Biochem. Biophys. Res. Commun.*, 81 (1978) 176.
29 G. H. Beaven, and E. R. Holiday, *Adv. Protein Chem.*, 7 (1952) 319.
30 D. B. Wetlaufer, *Adv. Protein Chem.*, 17 (1962) 303.
31 R. E. Chance, E. P. Kroeff, and J. A. Hoffmann, in J. L. Gueriguian (Editor), *Insulins, Growth Hormone and Recombinant DNA Technology*, Raven Press, New York, 1981, p. 71.
32 E. Canova-Davis, I. P. Baldonado and G. M. Teshima, unpublished results.
33 S. J. Shire, D. L. Foster and E. Rinderknecht, *Biophys. J.*, 53 (1988) 72a.
34 D. C. Teller, *Methods Enzymol.*, 27 (1972) 346.
35 D. Guo, C. T. Mant, A. K. Taneja, J. M. R. Parker and R. S. Hodges, *J. Chromatogr.*, 359 (1986) 499.
36 D. L. Gooding, M. N. Schmuck and K. M. Gooding, *J. Chromatogr.*, 296 (1984) 107.
37 C. Hoeger, R. Galyean, J. Boublik, R. McClintock and J. Rivier, *BioChromatography*, 2 (1987) 134.
38 S. J. Shire, *Biochemistry*, 22 (1983) 2664.
39 A. J. Alpert, *J. Chromatogr.*, 266 (1983) 23.

40 E. A. Peterson and H. A. Sober, *Methods Enzymol.*, 5 (1962) 3.
41 C. Schwabe and J. K. McDonald, *Science (Washington, DC)*, 197 (1977) 914.
42 W. S. Hancock, E. Canova-Davis, J. Battersby and R. Chloupek, in J. L. Gueriguian, V. Fattorusso and D. Poggiolini (Editors), *Biotechnologically Derived Medical Agents*, Raven Press, New York, 1988, p. 29.
43 A. P. Ryle, F. Sanger, L. F. Smith and R. Kitai, *Biochem. J.*, 60 (1955) 541.
44 A. B. Robinson, and C. J. Rudd, in B. L. Horecker and E. R. Stadtman (Editors), *Current Topics in Cellular Regulation,* Acedemic press, New York, 1974, p. 247.
45 M. Bodanszky and J. Z. Kwei, *Int. J. Pept. Protein Res.*, 12 (1978) 69.

Journal of Chromatography, 508 (1990) 97–107
Elsevier Science Publishers B.V., Amsterdam — Printed in The Netherlands

CHROM. 22 271

One-step 10^4-fold purification of transformed glucocorticoid receptor

Method for purifying receptors associated with M_r *ca.* 90 000 heat-shock protein

MARC DENIS*, PHILIPPE BLANCHARDIE, JEAN-LUC ORSONNEAU and PATRICK LUSTENBERGER

Department of Medical Biochemistry, Nantes University Hospital, 1 Rue G. Veil, F-44035 Nantes (France)

(First received October 3rd, 1989; revised manuscript received January 10th, 1990)

SUMMARY

Chromatography of rabbit glucocorticoid–receptor complexes in the absence of sodium molybdate on a Mono Q anion-exchange column induces the transformation of the receptor and allows the resolution of the transformed and non-transformed molecular species. These abilities were used to design a new purification scheme for the glucocorticoid receptor from rabbit liver in its transformed state. Microgram amounts of receptor were obtained using this single-step procedure in less than 2 h. The purification yield was 50–60%. Immunoblot experiments showed that the glucocorticoid receptor was present as an $M_r \approx 94\,000$ polypeptide in these preparations and represented 20–30% of the eluted proteins as determined by densitometric scanning analysis of silver-stained sodium dodecyl sulphate polyacrylamide gels. Finally, the purified receptor was able to interact quantitatively with bulk DNA.

INTRODUCTION

Glucocorticoid hormone receptors are soluble proteins, present at low concentration in target cells (0.01–0.1‰ of total cytosolic proteins). Two main procedures for glucocorticoid receptor purification have been used. Ligand affinity chromatography is based on the ability of the receptor to bind specifically its ligand (for a review, see ref. 1). The second technique is based on the capacity of the glucocorticoid receptor to be converted into a DNA-binding form following ligand binding and heat treatment[2]. Sequential chromatography on phosphocellulose and DNA–cellulose has been used to purify glucocorticoid–receptor complexes from rat liver[3,4], porcine liver[5] and human HeLa S3 cells[6]. The purified receptor preparations thus obtained have been very useful, *e.g.*, in raising polyclonal[7] and monoclonal antibodies[8], defining the

0021-9673/90/$03.50

domain structure of the glucocorticoid receptor protein[9] and studying the interaction of the receptor with specific DNA sequences[10–13].

The characterization and purification of glucocorticoid–receptor complexes have mainly been performed using conventional low-pressure chromatographic techniques. More recently, high-performance liquid chromatographic methods have been shown to have interesting preparative[14,15] and analytical[16–19] applications. We report here on the use of high-performance ion-exchange chromatography (HPIEC) to purify rapidly and efficiently the transformed glucocorticoid receptor. This new method relied on two aspects: (i) the high resolution of HPIEC, allowing transformed and non-transformed glucocorticoid–receptor complexes to be separated and (ii) the matrix-induced transformation of the immobilized receptor. Characterization of the chromatographic eluates indicated that the purified receptor was a molecular mass, $M_r \approx 94\,000$ protein which was recognized by a monoclonal antibody and was able to interact with DNA.

EXPERIMENTAL

Materials

[1, 2, 4(n)-^{3}H]Dexamethasone (45 Ci/mmol) was obtained from the Radiochemical Centre (Amersham, U.K.), unlabelled dexamethasone from Roussel UCLAF (Romainville, France) and DEAE-Trisacryl M, ss DNA-Ultrogel A4R and HA-Ultrogel from IBF (Villeneuve la Garenne, France). All other chemicals were of analytical-reagent grade from Sigma (St. Louis, MO, U.S.A.).

Preparation of cytosol

Cytosol from adrenalectomized rabbits was prepared in PG buffer [20 m*M* potassium phosphate, 20% (v/v) glycerol, 20 m*M* 2-mercaptoethanol, pH 7.4] or in PGM buffer (10 m*M* sodium molybdate in PG buffer) as described[20]. Receptor was labelled with 20 n*M* [^{3}H]dexamethasone for 16 h at 4°C. Non-specific binding was measured by a parallel incubation with a 1000-fold excess of unlabelled dexamethasone and steroid-binding activity was determined according to Blanchardie *et al.*[20]. The starting cytosol contained *ca.* 3–4 pmol/ml of [^{3}H]dexamethasone-binding sites and 15 mg/ml of proteins.

High-performance ion-exchange chromatography

HPIEC was performed using a Beckman chromatographic system equipped with a Model 420 gradient programmer controlling two Model 110A pumps. Samples were chromatographed on a Mono Q HR 5/5 column (Pharmacia, Uppsala, Sweden). The flow-rate and the composition of the mobile phase were controlled by the gradient programmer. The buffers used were (A) 20 m*M* Tris–HCl–20 m*M* 2-mercaptoethanol–2% (v/v) acetonitrile–0.2 m*M* phenylmethylsulphonyl fluoride (PMSF) (pH 7.4) and (B) 0.5 *M* sodium chloride–10 m*M* sodium molybdate in buffer A. Acetonitrile appeared to accelerate significantly the removal of free dexamethasone during the washing steps without affecting the ligand binding to the receptor (data not shown). Further, it was helpful to dissolve the PMSF, used as a protease inhibitor during the purification procedure. All samples and buffers were filtered through a 0.45-μm filter before use. The programme used to purify the transformed glucocorticoid receptor from rabbit liver is detailed in Table I.

TABLE I

PURIFICATION OF RABBIT LIVER GLUCOCORTICOID RECEPTOR

Step	*Time (min)*	*Buffer B (%)*	*NaCl (mM)*	*Na_2MoO_4 (mM)*
Sample + wash	0→20	50	250	5
Transformation	20→65	0	0	0
Elution	65→90	0→100	0→500	0→10

Sodium dodecyl sulphate–polyacrylamide gel electrophoresis (SDS-PAGE)

Samples were prepared and electrophoresed under denaturing conditions according to Laemmli[21] as described in detail elsewhere[22]. After electrophoresis, the gels were silver stained[23] and scanned on an LKB Ultroscan XL. Calibration was performed using the following prestained standard proteins: myosin ($M_r \approx 200\,000$), phosphorylase *b* ($M_r \approx 92\,000$), bovine serum albumin ($M_r \approx 69\,000$) and carbonic anhydrase ($M_r \approx 30\,000$).

Protein immunoblot

Proteins separated by SDS-PAGE were transferred to nitrocellulose filters[22]. Glucocorticoid receptor immunoreactivity was detected using the monoclonal antibody No. 7 raised against the transformed rat liver glucocorticoid receptor[8] followed by reaction with goat anti-mouse immunoglobins labelled with horseradish peroxidase[22].

Separation of glucocorticoid–receptor complexes

The DNA-binding activity of purified glucocorticoid–receptor complexes was determined using a modification[22] of the procedure described by Holbrook *et al.*[24]. Briefly, three syringes containing 0.2 ml of DNA-Ultrogel (on the top), 0.2 ml of DEAE-Trisacryl (in the middle) and 0.2 ml of HA-Ultrogel (on the bottom) were connected to one other. Samples to be analysed were diluted 5-fold with PGM buffer and loaded on the minicolumns. The gels were then washed with PGM buffer (*ca.* 20 ml) and counted. The results are expressed as the percentage of radioactivity retained on each gel.

Miscellaneous

Quantification of proteins was performed according to the method of Bradford[25] using bovine serum albumin as a standard. Radioactivity was measured in a Beckman LS 2800 liquid scintillation counter. The concentration of chloride ions was determined using an Astra analyser (Beckman).

RESULTS

Binding capacity of receptor to the Mono Q column

We have previously shown that the non-transformed glucocorticoid receptor from rabbit liver, stabilized by sodium molybdate, is retained on a Mono Q anion-

exchange column[18]. In order to determine the capacity of this matrix, we incubated batchwise increasing amounts of labelled liver cytosol (10 μl–1 ml) with 10-mg aliquots of stationary phase. Following incubation, unbound proteins and free ligand were washed away, and the retained glucocorticoid–receptor complexes were eluted with 0.5 *M* sodium chloride solution. The saturation curve obtained after determination of the radioactivity eluted from the aliquots of gel is shown in Fig. 1A. These results were also analysed according to Scatchard[26] as shown in Fig. 1B. The number of binding sites for glucocorticoid–receptor complexes on the matrix was calculated to be 0.78 pmol per 10 mg of stationary phase. Similar results were obtained for anion-exchange matrices used in conventional chromatography (data not shown). Rabbit liver cytosol usually contains 0.2–0.3 pmol of glucocorticoid binding sites per milligram of protein[20]. We were then able to calculate that glucocorticoid–receptor complexes from 8–10 ml of cytosol could be retained on a 1-ml column (Mono Q HR 5/5).

Induction of transformation by the anion exchanger

Chromatography on a Mono Q column allows the complete resolution of transformed complexes generated by heat or salt treatment and non-transformed complexes[18]. When labelled cytosol was chromatographed in the absence of molybdate, a less negatively charged dexamethasone-binding species was eluted by a linear salt gra-

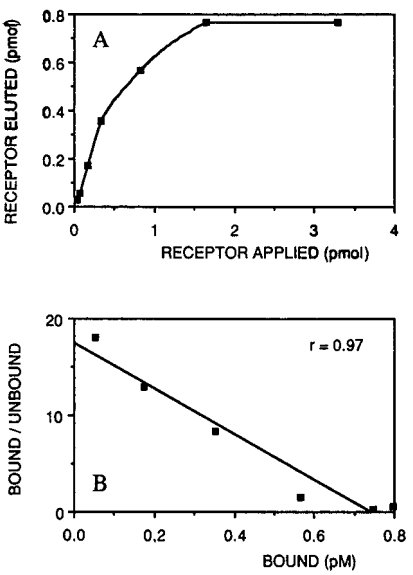

Fig. 1. (A) Binding of [^{3}H]dexamethasone–receptor complexes to the anion exchanger. Aliquots of cytosol (10 μl–1 ml), labelled with [^{3}H]dexamethasone in the absence or presence of a 1000-fold excess of unlabelled dexamethasone, were incubated for 15 min at 4°C with 10 mg of solid phase from a Mono Q column. The solid phase was recovered by centrifugation, washed with 1 ml of buffer A and retained glucocorticoid–receptor complexes were eluted with 0.25 ml of buffer B. The amount of specific radioactivity contained in these eluates was determined by scintillation counting and the number of receptors eluted was plotted against the amount of receptor applied on the gel. (B) Scatchard representation of the experimental results.

dient. This new receptor form, which was not detected when sodium molybdate was included in all the buffers, has been identified as the transformed receptor ($M_r \approx$ 100 000 DNA-binding species[18]).

We then tested the effect of different washing conditions on the yield of the transformation of glucocorticoid–receptor complexes adsorbed on the stationary phase. Labelled cytosol was loaded on the Mono Q column, which was washed with molybdate-free buffer at 4 or 20°C. The [^{3}H]dexamethasone–receptor complexes were then eluted with a linear salt gradient and the two peaks were pooled separately and assayed for radioactivity. The results obtained are shown in Fig. 2, where the percentages of transformation correspond to the ratio of the radioactivity in the peak of transformed receptor to that in the two peaks. In all instances, the percentage of transformation (*i.e.*, the relative abundance of the more acidic species) increased with the length of the washing step (Fig. 2). Half of the steroid–receptor complexes prepared in molybdate-containing buffer were in the transformed state after a 15-min washing period with buffer A at 4°C (Fig. 2, closed squares). Heating the column at 20°C during the washing period considerably accelerated this phenomenon as 70% of the complexes prepared in the presence of molybdate were transformed after only 5 min (Fig. 2, open squares). The same extent of transformation was obtained after 15–20 min when the cytosol applied to the column was prepared without sodium molybdate and washed at 4°C (Fig. 2, closed circles).

Purification of glucocorticoid receptor

While the proteins that were eluted from the Mono Q column below *ca.* 0.25 *M* sodium chloride in the presence of molybdate were washed away during the first step of the purification protocol, the molybdate-stabilized non-transformed glucocorticoid–receptor complexes, normally eluted with *ca.* 0.32 *M* sodium chloride[18], were still retained on the column. Interaction of these complexes with the cationic matrix in the absence of molybdate was shown to induce their transformation, even when the cytosol was prepared in molybdate-containing buffer (Fig. 2). Therefore, the receptors were converted to the more acidic species during the second phase of the purification, *i.e.*, when the column was washed with a mobile phase containing no salt and

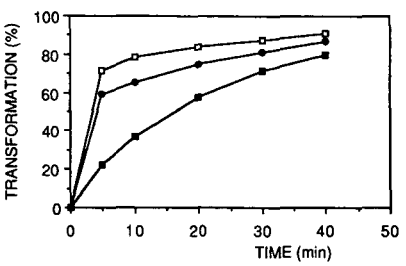

Fig. 2. Transformation of glucocorticoid–receptor complexes induced by the anion exchanger. Cytosol prepared in (●) PG buffer or in (□, ■) PGM buffer was incubated with 20 n*M* [^{3}H]dexamethasone for 16 h. Samples (500 μl) were loaded on a Mono Q column. After washing with buffer A for different times at (●, ■) 4°C or (□) 20°C, elution was carried out with a linear salt gradient (buffer A to buffer B in 25 min). The amount of radioactivity contained in each peak was determined, and the ratio of radioactivity in the peak of transformed receptor (first peak eluted) to total radioactivity eluted was calculated and plotted against the length of the washing step.

no molybdate. The retained proteins were finally eluted with a linear salt gradient (Fig. 3B). An aliquot of each fraction was counted in order to localize glucocorticoid–receptor complexes (Fig. 3A, closed squares). Comparison with the elution profile of proteins (Fig. 3A, open diamonds) indicated that the protein concentration in the fractions containing the transformed receptors was very low. This was not surprising as proteins which eluted below 0.25 *M* sodium chloride have been eliminated during the first phase of the purification, and the final eluate contained exclusively proteins for which the total negative charge had been greatly decreased by the elimination of sodium molybdate during the washing step. It is interesting that the major peak of protein, eluted at 0.3–0.4 *M* sodium chloride, contained large amounts of partially purified $M_r \approx 90\,000$ heat-shock protein, hsp90[22].

Characterization of the purified receptor

The fractions corresponding to the first peak of eluted radioactivity were pooled and the glucocorticoid receptor present in these preparations was characterized by several criteria. The proteins contained in these fractions were precipitated with trichloroacetic acid, dissolved in solubilization buffer and analysed by denaturing PAGE. Following transfer to sheets of nitrocellulose, glucocorticoid receptor was probed using the monoclonal antibody No. 7 raised against the rat receptor[8]. A major band of immunoreactivity was detected on the filter corresponding to an $M_r \approx 94\,000$ protein (Fig. 4, lane 1). This value is in complete agreement with the reported molecular weight determined under similar conditions for rat[4], porcine[5] and human glucocorticoid receptor[6].

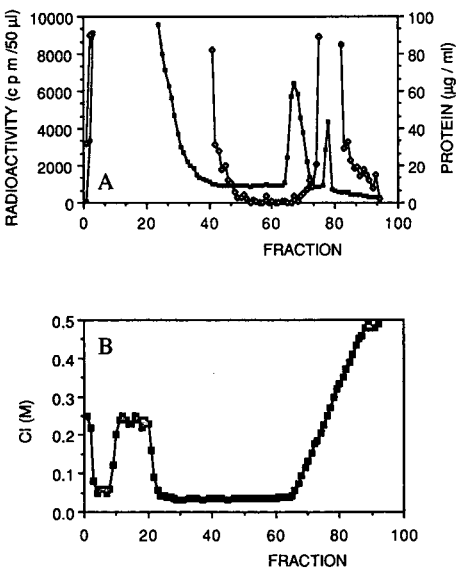

Fig. 3. Chromatographic profile of a typical purification. Cytosol from rabbit liver was incubated with 20 n*M* [^{3}H]dexamethasone for 16 h at 4°C and 8 ml were loaded on a Mono Q column washed with 50% of buffer B for 20 min. The column was then washed with buffer A for 45 min and the elution was initiated. Each fraction collected was assayed for (A, ◇) protein content (A, ■) radioactivity and (B) chloride ion concentration.

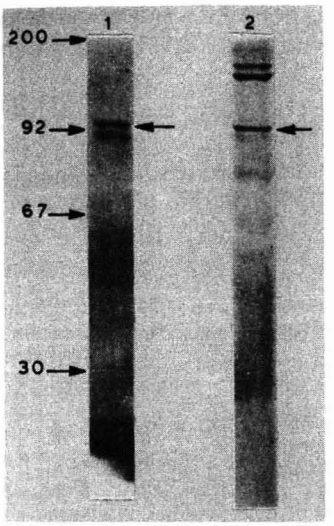

Fig. 4. SDS-PAGE of purified receptor. Samples containing purified receptor (*ca.* 0.5 μg) were analysed under denaturing conditions. Lane 1 shows an immunoblot analysis of the eluate probed with the monoclonal anti-glucocorticoid receptor antibody N. 7. A similar gel was silver stained (lane 2). Positions of standard proteins are shown on the left (molecular weights × 10^{-3}). The arrows on the right indicate the position of the glucocorticoid receptor.

When the polyacrylamide gel was silver stained, a band was clearly seen in the region where the immunoreactivity was detected (Fig. 4, lane 2). Densitometric scanning analysis of such gels revealed that the $M_r \approx 94\,000$ receptor protein represented 20–30% of the eluted proteins (data not shown). Using this technique to determine the purity of the preparation, and assuming one hormone-binding site per receptor molecule, it was possible to calculate that the glucocorticoid–receptor complexes were purified *ca.* 10 000-fold by this single step (Table II). Two other proteins ($M_r \approx$ 140 000 and $M_r \approx$ 155 000) were seen on silver-stained gels. At present, there has been no report indicating the presence of such high-molecular-weight proteins in the non-transformed glucocorticoid receptor. It is possible, however, that these proteins

TABLE II

PURIFICATION OF RABBIT GLUCOCORTICOID RECEPTOR

The binding activity of the cytosol was determined as described under Experimental. The purification was performed using 8 ml of labelled cytosol as starting material.

Step	*Proteins (mg)*	*Receptor (pmol)*	*Purity (%)*	*Purification (fold)*	*Yield (%)*
Cytosol	146	38.5	0.0025[a]	1	100
Mono Q Eluate	–	21.8	28.1[b]	11 336	56.5

[a] Calculated assuming a molecular weight of 94 000.
[b] Determined by densitometric scanning analysis of SDS-PAGE after silver staining.

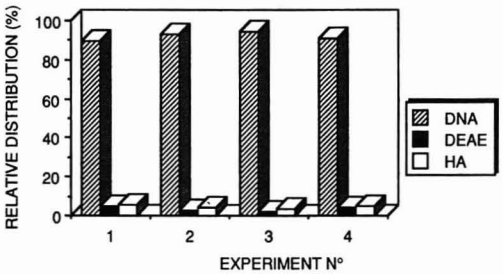

Fig. 5. DNA-binding ability of purified glucocorticoid–receptor complexes. Purified samples eluted from the Mono Q column were diluted with PGM buffer and chromatographed on minicolumns as detailed under Experimental. The retentions on (DNA) DNA-Ultrogel, (DEAE) DEAE-Trisacryl and (HA) HA-Ultrogel of purified complexes from four separate purifications are presented.

also associate with hsp90 to form complexes that are stabilized by sodium molybdate. These complexes might have been dissociated when the Mono Q column was washed with molybdate-free buffer, releasing the monomeric $M_r \approx 140\,000$ and $M_r \approx 155\,000$ proteins.

Characterization of the purified receptor was also performed under non-denaturing conditions. The hydrodynamic parameters determined were similar to those previously reported for the transformed receptor from rabbit liver[18], *i.e.*, a Stokes radius of 5.0–5.2 nm, a sedimentation coefficient of *ca.* 4.5 S and a calculated molecular weight of *ca.* 100 000 (data not shown). Hence, the receptor purified by this procedure appeared to be in a monomeric form, as opposed to the dimeric state recently reported by Wrange *et al.*[27].

The property of DNA binding was studied by the minicolumn procedure originally described by Holbrook *et al.*[24]. The results from four separate experiments are presented in Fig. 5. It is clear from this diagram that most of the purified receptors are present in a DNA-binding form, as expected for a receptor in a transformed state.

Conservation of the purified receptor

The stability of the purified receptor preparations was tested. The eluates were supplemented with 10% (v/v) glycerol, 0.1% (w/v) bacitracin and 10 n*M* [^{3}H]dexamethasone and stored at 4°C or frozen at −70°C. At different times, the number of

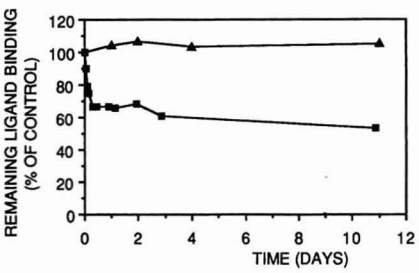

Fig. 6. Ligand-binding stability of the purified receptor. Purified samples were supplemented with 10% glycerol, 0.1% (w/v) bacitracin and 10 n*M* [^{3}H]dexamethasone. Aliquots were assayed for the presence of glucocorticoid–receptor complexes after different times of storage at (■) 4°C or (▲) −70°C.

ligand-binding sites remaining in the samples was determined using the hydroxylapatite assay[28]. The non-specific binding was measured after exposure of the eluates to 100°C for 10 min. At 4°C, the ligand-binding capacity of the purified receptors was decreased to *ca.* 60% after 4 h, but then remained stable for as long as 11 days (Fig. 6). When the samples were stored at −70°C, no decrease in the ligand-binding capacity was seen (Fig. 6), and the purified receptor was still able to interact with DNA (data not shown).

DISCUSSION

Transformation of the glucocorticoid receptor can be induced *in vitro* by a variety of manipulations such as heat treatment, exposure to elevated ionic strength, dilution, ATP or heparin (for a review, see ref. 29). The appearance of DNA-binding activity appears to correlate with the dissociation of the dimer of hsp90 from the M_r 94 000 receptor monomer[30–32]. This transformation also occurs when the receptor is immobilized on an immunoaffinity matrix[2,32] or on an anion exchanger[15,18,33]. The nature of this phenomenon still remains to be elucidated. However, it seems to be well established that most of the hydrodynamic and physico-chemical properties of the non-transformed glucocorticoid receptor are related to the presence of a dimer of hsp90 in the complex. This protein is highly negatively charged[34,35], which is probably responsible for the behaviour of the molybdate-stabilized non-transformed glucocorticoid receptor on anion exchangers[36–38]. When the receptor is adsorbed on the Mono Q column in the absence of molybdate, the hsp90 dissociates and the total negative charge of the glucocorticoid–receptor complex dramatically decreases.

We combined the high resolution of HPIEC with this transformation process to develop a new purification scheme. This protocol, as opposed to the purification techniques routinely used (see Introduction and the references cited there), does not rely on the properties of ligand and DNA binding of the receptor. The purified receptor appeared to be intact as judged by its molecular weight determined under denaturing conditions. It also contained the three functional domains first described at the protein level by Carlstedt-Duke *et al.*[39]. Thus, the C-terminal third of the purified receptor was bound to the ligand, the DNA-binding domain was accessible since the receptor could be retained on immobilized DNA and the purified protein was recognized by a monoclonal antibody raised against the N-terminal "immunodominant" domain[39]. The function of the glucocorticoid receptor is to regulate the transcription of specific genes[40]. However, there has so far been no report describing an *in vitro* transcription system that we could use to determine whether the glucocorticoid receptor purified according to our procedure is functional or not. Finally, the purified material was stable, especially at −70°C, and the preparations could be stored until further use.

The different sequences of the purification (washing with 0.25 *M* sodium chloride and 5 m*M* sodium molybdate, washing with no salt and no molybdate, salt gradient) were automatically controlled by the gradient programmer. No manual operation was required after injection of the cytosolic preparation. The purified receptor was eluted only *ca.* 70 min after the injection, and a new purification could be performed every 90 min. Starting with 8–10 ml of rabbit liver cytosol, we routinely obtained microgram amounts of purified receptor. Similar results were obtained us-

ing triamcinolone acetonide-labelled rat liver glucocorticoid receptor as starting material[41]. As 5- and 10-ml Mono Q columns are available larger amount of purified receptor can be obtained using this protocol.

We also tried to extend this purification technique to other steroid hormone receptors that are also found associated with the $M_r \approx 90\,000$ heat-shock protein in cytosol[42]. Preliminary experiments indicated that progesterone receptors from human T47D cells and estrogen receptors from human MCF7 cells are also transformed by interaction with the cationic matrix[43], and therefore can be purified using a similar scheme. The purification protocol described here and its straightforward application to other steroid hormone receptors would be of great convenience for experiments requiring microgram amounts of potentially functional receptor.

ACKNOWLEDGEMENTS

This work was supported by grants from INSERM, from the Association pour la Recherche contre le Cancer (ARC) and by U.F.R. of Medicine. We thank A.-C. Wikström and J.-Å. Gustafsson for the gift of monoclonal antibodies.

REFERENCES

1 P. Formstecher and P. Lustenberger, in V. K. Moudgil, (Editor), *Recent Advances in Steroid Hormone Action*, Vol. 2, Walter de Gruyter, Berlin, 1987, pp. 499–535.
2 M. Denis, L. Poellinger, A.-C. Wikström and J.-Å. Gustafsson, *Nature (London)*, 333 (1988) 686–688.
3 Ö. Wrange, J. Carlstedt-Duke and J.-Å. Gustafsson, *J. Biol. Chem.*, 254 (1979) 9284–9290.
4 Ö. Wrange, S. Okret, M. Radojcic, J. Carlstedt-Duke and J.-Å. Gustafsson, *J. Biol. Chem.*, 259 (1984) 4534–4541.
5 A. R. Marks, D. D. Moore, D. I. Buckley, B. Gametchu and H. M. Goodman, *J. Steroid Biochem.*, 24 (1986) 1097–1103.
6 M. Brönnegard, L. Poellinger, S. Okret, A.-C. Wikström, Ö. Bakke and J.-Å. Gustafsson, *Biochemistry*, 26 (1987) 1697–1704.
7 S. Okret, J. Carlstedt-Duke, Ö. Wrange, K. Carlstrom and J.-Å. Gustafsson, *Biochim. Biophys. Acta*, 677 (1981) 205–219.
8 S. Okret, A.-C. Wikström, Ö. Wrange, B. Andersson and J.-Å. Gustafsson, *Proc. Natl. Acad. Sci. U.S.A.*, 81 (1984) 1609–1613.
9 J. Carlstedt-Duke, P.-E. Strömstedt, Ö. Wrange, T. Bergman, J.-Å. Gustafsson and H. Jörnvall, *Proc. Natl. Acad. Sci. U.S.A.*, 84 (1987) 4437–4440.
10 F. Payvar, D. DeFranco, G. L. Firestone, B. Edgar, Ö. Wrange, S. Okret, J.-Å. Gustafsson and K. R. Yamamoto, *Cell*, 35 (1983) 381–392.
11 Ö. Wrange, J. Carlstedt-Duke and J.-Å. Gustafsson, *J. Biol. Chem.*, 261 (1986) 11770–11778.
12 S. Okret, L. Poellinger, Y. Dong and J.-Å. Gustafsson, *Proc. Natl. Acad. Sci. U.S.A.*, 83 (1986) 5899–5903.
13 A. Hecht, A. Berkenstam, P.-E. Strömstedt, J.-Å. Gustafsson and A. Sippel, *EMBO J.*, 7 (1988) 2063–2073.
14 P. Lustenberger, P. Blanchardie, M. Denis, P. Formstecher and S. Bernard, *Biochimie*, 67 (1985) 1267–1278.
15 T. Idziorek, P. Formstecher, P. M. Danze, B. Sablonnière, P. Lustenberger, C. Richard, V. Dumur and M. Dautrevaux, *Eur. J. Biochem.*, 153 (1985) 65–74.
16 M. C. LaPointe, C. H. Chang and W. V. Vedeckis, *Biochemistry*, 25 (1986) 2094–2101.
17 B. Sablonnière, P. Lefebvre, P. Formstecher and M. Dautrevaux, *J. Chromatogr.*, 403 (1987) 183–196.
18 M. Denis, F. Guendouz, P. Blanchardie, S. Bernard and P. Lustenberger, *J. Steroid Biochem.*, 30 (1988) 281–285.
19 M. Denis, J.-Å. Gustafsson and A.-C. Wikström, *J. Biol. Chem.*, 263 (1988) 18520–18523.

20 P. Blanchardie, P. Lustenberger, J. L. Orsonneau and S. Bernard, *J. Steroid Biochem.*, 18 (1983) 789–799.
21 U. K. Laemmli, *Nature (London)*, 227 (1970) 680–685.
22 M. Denis, *Anal. Biochem.*, 173 (1988) 405–411.
23 C. R. Merril, D. Goldman, S. A. Sedman and M. H. Ebert, *Science (Washington, D.C.)*, 211 (1981) 1437–1438.
24 N. J. Holbrook, J. E. Bodwell, M. Jeffries and A. Munck, *J. Biol. Chem.*, 258 (1983) 6477–6485.
25 M. M. Bradford, *Anal. Biochem.*, 72 (1976) 248–254.
26 G. Scatchard, *Ann. N.Y. Acad. Sci.*, 51 (1949) 660–672.
27 Ö. Wrange, P. Eriksson and T. Perlmann, *J. Biol. Chem.*, 264 (1989) 5253–5259.
28 P. Blanchardie, P. Lustenberger, J. L. Orsonneau and S. Bernard, *Biochimie*, 66 (1984) 505–511.
29 T. J. Schmidt and G. Litwack, *Physiol. Rev.*, 62 (1982) 1132–1192.
30 E.-E. Baulieu, *J. Cell. Biochem.*, 7 (1987) 164–174.
31 W. B. Pratt, *J. Cell. Biochem.*, 3 (1987) 51–68.
32 M. Denis and J.-Å. Gustafsson, *Cancer Res.*, 49 (1989) 2275–2281.
33 F. Svec and D. Tate, *J. Receptor Res.*, 7 (1987) 859–870.
34 S. Koyasu, E. Nishida, T. Kadowaki, F. Matsuzaki, K. Iida, F. Harada, M. Kasuga, H. Sakaiand I. Yahara, *Proc. Natl. Acad. Sci. U.S.A.*, 83 (1986) 8054–8058.
35 M. Denis, A.-C. Wikström and J.-Å. Gustafsson, *J. Biol. Chem.*, 262 (1987) 11803–11806.
36 T. Nemoto, Y. Ohara-Nemoto and M. Ota, *J. Biochem.*, 102 (1987) 513–523.
37 E. R. Sanchez, S. Meshinchi, W. Tienrungroj, M. J. Schlesinger, D. O. Toft and W. B. Pratt, *J. Biol. Chem.*, 262 (1987) 6986–6991.
38 M. Denis, A.-C. Wikström, S. Cuthill, H. Jörnvall and J.-Å. Gustafsson, *Biochem. Soc. Trans.*, 16 (1988) 688–690.
39 J. Carlstedt-Duke, S. Okret, Ö. Wrange and J.-Å. Gustafsson, *Proc. Natl. Acad. Sci. U.S.A.*, 79 (1982) 4260–4264.
40 K. R. Yamamoto, *Annu. Rev. Genet.*, 19 (1985) 209–252.
41 M. Denis, A.-C. Wikström and J.-Å. Gustafsson, unpublished results.
42 M. G. Catelli, N. Binart, I. Jung-Testas, J. M. Renoir, E.-E. Baulieu, J. R. Welch and W. J. Feramisco, *EMBO J.*, 4 (1985) 3131–3135.
43 A. Berkenstam, P.-E. Strömstedt, M. Denis and J.-Å. Gustafsson, unpublished results.

Journal of Chromatography, 508 (1990) 109–125
Elsevier Science Publishers B.V., Amsterdam — Printed in The Netherlands

CHROM. 22 366

Design and applications of biomimetic anthraquinone dyes

III. Anthraquinone-immobilised C.I. Reactive Blue 2 analogues and their interaction with horse liver alcohol dehydrogenase and other adenine nucleotide-binding proteins

STEVEN J. BURTON[a]
Institute of Biotechnology, University of Cambridge, Downing Street, Cambridge CB2 3EF (U.K.)
C. VIVIAN STEAD[a]
Research Department, Imperial Chemical Industries plc, Organics Division, P.O. Box 42, Blackley, Manchester M9 3DA (U.K.)
and
CHRISTOPHER R. LOWE*
Institute of Biotechnology, University of Cambridge, Downing Street, Cambridge CB2 3EF (U.K.)
(First received August 11th, 1989; revised manuscript received February 1st, 1990)

SUMMARY

C.I. Reactive Blue 2 analogues were bonded onto an agarose support matrix by a novel method which entailed immobilisation by the anthraquinone ring 1-amino group as opposed to the usual triazine ring coupling methods. Dyes with spacer arms attached to the anthraquinone ring 1-amino group were synthesised by reacting methoxytriazine analogues of C.I. Reactive Blue 2 with chloroacetyl chloride and ethylenediamine. Unlike the blue parent dyes, all C.I. Reactive Blue 2 analogues with derivatised anthraquinone ring 1-amino groups were of a characteristic red colour. This change of chromaticity was entirely expected since the anthraquinone ring 1-amino group is an important component of the C.I. Reactive Blue 2 chromophore. Chromatographic studies indicated that, in comparison to adsorbents comprising triazine ring-immobilised dyes, adsorbents formed from C.I. Reactive Blue 2 analogues immobilised by the anthraquinone ring were better suited to the isolation of horse liver alcohol dehydrogenase and other adenine nucleotide-requiring enzymes. Similarities between C.I. Reactive Blue 2 analogues immobilised by the anthraquinone ring and N^6-(6-aminohexyl)adenine nucleotide derivatives could be identified which may account for these observations. These studies confirm that highly effective affinity ligands based on synthetic textile dyes can be designed in a rational manner.

[a] Present address: Affinity Chromatography Ltd., 307 Huntingdon Road, Girton, Cambridge CB3 0JX, U.K.

0021-9673/90/$03.50

INTRODUCTION

Immobilised reactive textile dyes have been used to purify a vast number of proteins by affinity chromatography[1–4]. Despite the success of reactive dyes as affinity ligands, relatively little is known about the interaction of these compounds with their complementary binding sites on proteins. One would surmise that a greater understanding of the interactions between synthetic dyes and proteins could subsequently lead to the identification of dye ligands with improved binding selectivities.

In a previous publication[5], the effect of modifications to the terminal aminobenzenesulphonate ring of C.I. Reactive Blue 2 on the interaction of the dye with horse liver alcohol dehydrogenase was reported. Analogues of C.I. Reactive Blue 2 with various neutral, anionic and cationic groups located on the terminal phenyl ring displayed large variations in affinity for the enzyme. However, the effects of these modifications on the binding of alcohol dehydrogenase were masked when the C.I. Reactive Blue 2 analogues were immobilised by the triazine ring moiety to an agarose support matrix. This observation suggested that the method of dye immobilisation did not promote optimal dye–protein interaction, despite the use of a spacer arm coupling regime.

From X-ray crystallographic studies on the binding of C.I. Reactive Blue 2 by horse liver alcohol dehydrogenase[6], it is apparent that the triazine ring of the dye is bound within a deep cleft situated at the junction of the coenzyme and catalytic domains of the enzyme. This region of the protein is normally associated with binding the pyrophosphate bridge of NAD^+ or NADH. Thus, for steric reasons, immobilisation of C.I. Reactive Blue 2 via the triazine ring is not conducive to optimal interaction with horse liver alcohol dehydrogenase. The anthraquinone ring 1-amino group represents a more suitable point of dye attachment, since this group, like the exocyclic adenine N^6-amino group of bound NAD^+, is exposed to the exterior solvent[6,7]. Thus, the synthesis of affinity adsorbents composed of C.I. Reactive Blue 2 analogues immobilised by a spacer arm attached to the 1-amino group of the anthraquinone ring is reported here. These adsorbents displayed improved properties for the purification of horse liver alcohol dehydrogenase and were found to be effective in binding other adenine nucleotide-requiring enzymes.

EXPERIMENTAL

Materials

p-Dimethylaminobenzaldehyde, 1,1′-carbonyldiimidazole (CDI), cyanogen bromide (CNBr) and glucose 6-phosphate were purchased from Sigma (Poole, U.K.). N-2-Hydroxyethylpiperazine-N′-2-ethanesulphonic acid (HEPES) and ethylenediaminetetraacetic acid (EDTA) were supplied by BDH (Poole, U.K.), whilst chloroacetyl chloride and ethylenediamine were obtained from Fisons (Loughborough, U.K.).

The following biochemicals were purchased from Boehringer (Lewes, U.K.): nicotinamide-adenine dinucleotide (NAD^+); reduced nicotinamide-adenine dinucleotide (NADH); nicotinamide-adenine dinucleotide phosphate ($NADP^+$); phosphoenolpyruvate (PEP); adenosine 5′-diphosphate (ADP); adenosine 5′-triphosphate (ATP); horse liver alcohol dehydrogenase (alcohol:NAD^+ oxidoreductase; EC

1.1.1.1; 2.7 U mg^{-1}); yeast glucose-6-phosphate dehydrogenase (D-glucose-6-phosphate: $NADP^+$ 1-oxidoreductase; EC 1.1.1.49; 140 U mg^{-1}); rabbit muscle lactate dehydrogenase (L-lactate:NAD^+ oxidoreductase; EC 1.1.1.27; 550 U mg^{-1}); yeast hexokinase (ATP:D-hexose 6-phosphotransferase; EC 2.7.1.1; 140 U mg^{-1}) and rabbit muscle pyruvate kinase (ATP:pyruvate 2-O-phosphotransferase; EC 2.7.1.40; 200 U mg^{-1}).

The chromatographic materials Sepharose 4B and Sephadex LH-20 were obtained from Pharmacia (Milton Keynes, U.K.). Intermediates used in the synthesis of C.I. Reactive Blue 2 analogues were donated by ICI Organics Division. All other reagents and solvents were of analytical grade and purchased from the usual sources.

Synthesis of C.I. Reactive Blue 2 analogues with anthraquinone-linked spacer arms

Methoxylated C.I. Reactive Blue 2 analogues II–IV (Fig. 1) were synthesised, as described previously[8], by reacting 1-amino-4-(4′-amino-3′-sulphoanilino)anthraquinone-2-sulphonic acid with 2,4-dichloro-6-methoxy-*s*-triazine, followed by reaction of the product with the relevant substituted phenylamine derivative.

Chloroacetylated C.I. Reactive Blue 2 analogues V–VIII (Fig. 1) were synthesised by stirring a solution of the methoxylated dyes I–III (25 mmol) in dimethylformamide (DMF; 150 ml) with chloroacetyl chloride (250 mmol) for 30 min at 20–25°C. The reaction end-point was established by analytical thin-layer chromatography (TLC), whereupon saturated NaCl solution (800 ml) was added and the red chloroacetyl product filtered, washed with 10–15% (w/v) NaCl solution (300 ml), re-suspended in acetone (1 l), filtered and dried under vacuum at 50°C.

Dyes with β-aminoethylaminoacetylamino spacer arms (VIII–X; Fig. 1) were formed by reacting chloroacetyl dyes V–VII (15 mmol in 75 ml DMF) with ethylenediamine (150 mmol) for 25 min at 20–25°C. The reaction end-point was determined by analytical TLC, whereupon the mixture was diluted with saturated NaCl solution (800 ml) and the product suspension adjusted to pH 7.0 with concentrated HCl. The red precipitate was filtered, washed with 10% (w/v) NaCl solution (500 ml), acetone (100 ml) and dried under vacuum at 50°C.

Analysis of C.I. Reactive Blue 2 analogues

Analytical TLC was performed using silica foils (Schleicher & Schuell, Dassel, F.R.G.) and a propan-2-ol–ammonia-water (7:2:1, v/v/v) solvent. The presence of dyes which contained a primary amine was confirmed by treating dried TLC foils with Ehrlich's reagent, a solution of *p*-dimethylaminobenzaldehyde (1 g) in methanol–concentrated HCl (9:1, v/v) (100 ml).

Visible absorption spectra of purified C.I. Reactive Blue 2 analogues were recorded (800–400 nm) from 0.1 m*M* aqueous solutions in 10 mm path-length cells. The dyes were purified to near homogeneity by lipophilic chromatography on Sephadex LH-20 as described previously[9]. Infrared spectra were recorded from paraffin oil mulls of purified dye.

Immobilisation of C.I. Reactive Blue 2 analogues to beaded agarose

Purified dyes VIII–X were immobilised to CDI-activated Sepharose 4B according to established procedures[5]. Immobilised dye concentrations were determined by acid hydrolysis and spectrophotometric estimation of the solubilised dye[5]. For the

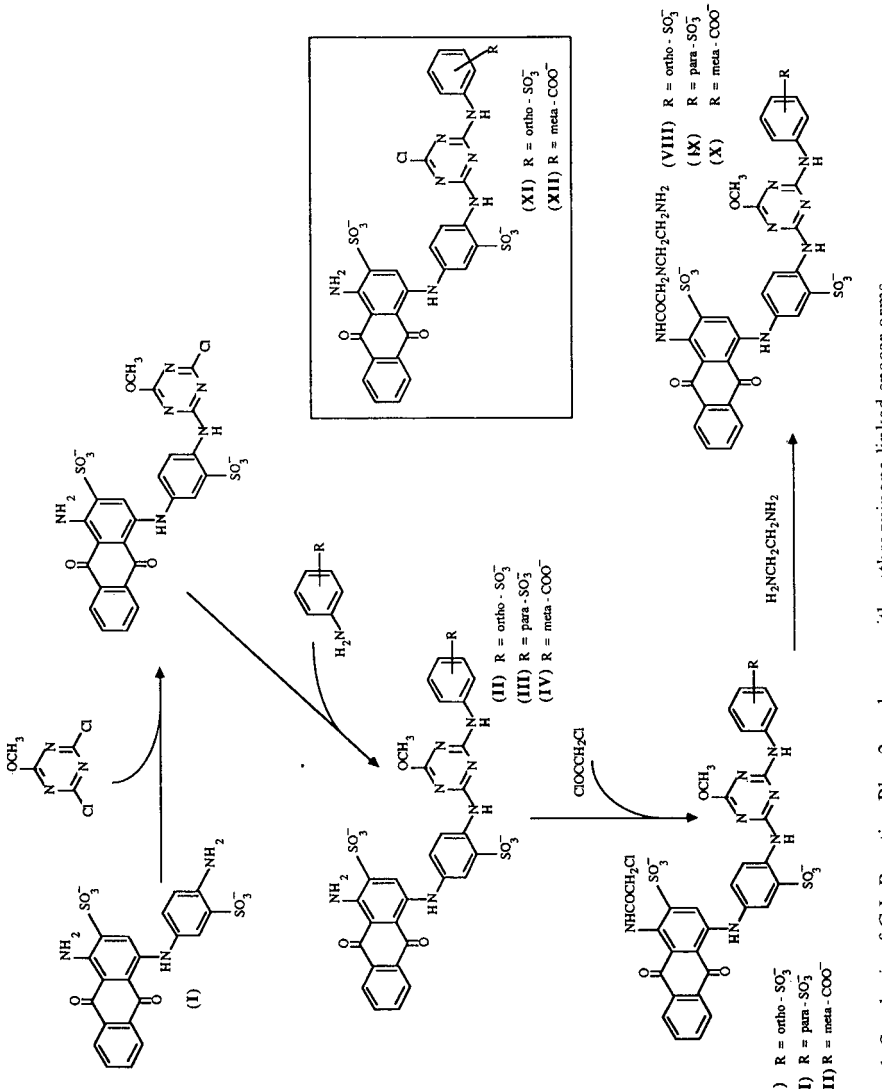

Fig. 1. Synthesis of C.I. Reactive Blue 2 analogues with anthraquinone-linked spacer arms.

purposes of immobilised dye determination, molar extinction coefficients of purified dyes VIII–X were determined following the incubation of aqueous dye solution (0.2 m*M*; 100 μl) with 5 *M* HCl (200 μl) for 5 min at 60°C. The solution was neutralised by adding NaOH (10 *M*; 100 μl) and potassium phosphate buffer (1 *M*; 600 μl), whereupon the absorbance of the solution was measured at 516 nm against a no-dye blank.

Trial immobilisations to CNBr-activated agarose were also performed. Activated Sepharose 4B (2 g moist gel; synthesised according to Lowe[10]) was added to a solution of dye (25 mg) in sodium carbonate buffer, pH 9.5 (0.4 *M*; 5 ml) and tumbled for 16 h at 4°C. Dyed gels were washed sequentially with water (100 ml), 1 *M* NaCl solution (100 ml), water (100 ml), 50% (v/v) dimethylsulphoxide (DMSO) solution (20 ml), water (100 ml) and stored in 0.02% (w/v) sodium azide solution (4°C) until required.

Preparation of crude horse liver extract

A cell-free horse liver extract was prepared by a method based on a previous report[11]. All procedures were performed at 4°C.

Fresh horse liver (1 kg) was washed with distilled water and ground in a meat grinder. The liver pulp was stirred (16 h; 4°C) in 10 m*M* HEPES–NaOH buffer, pH 7.0 (500 ml) and debris removed by screening through a nylon mesh. The retained liver pulp was re-slurried in 500 ml buffer and screened a second time. The crude extracts were combined, centrifuged (4 h; 23 000 *g*; average distance from the centre of rotation: 8.9 cm), the lipid layer was removed and the supernatant decanted to yield 900 ml cell-free extract. The extract was dialysed (3 days) against 64 volumes potassium phosphate buffer, pH 7.0 (20 m*M*) containing reduced glutathione (1 m*M*) before use.

Affinity chromatography of horse liver alcohol dehydrogenase on immobilised C.I. Reactive Blue 2 analogues

The interaction of purified horse liver alcohol dehydrogenase with dyes VIII–X immobilised to CDI-activated agarose was established by analytical affinity chromatography as described previously[5]. The enzyme was purified from a crude horse liver extract as follows.

Glass columns (10 × 0.5 cm I.D.) were slurry packed with adsorbent (1.0 g moist gel) and the gel bed was equilibrated with HEPES–NaOH buffer, pH 7.5 (20 m*M*) containing reduced glutathione (1 m*M*). Horse liver extract was dialysed (16 h; 4°C) against 150 volumes equilibration buffer, and 2 ml (130 mg protein) were chromatographed at a flow-rate of 30 ml h^{-1} cm^{-2}. The column was flushed with equilibration buffer (10 ml) and bound enzyme eluted with equilibration buffer containing 1 *M* KCl. Fractions (1 ml) were collected throughout the procedure and 20-μl samples removed for assay of enzyme activity and protein concentration.

Interaction of adenine-nucleotide-binding proteins with immobilised C.I. Reactive Blue 2 analogues

The interaction of various dehydrogenases and kinases with immobilised C.I. Reactive Blue 2 analogues was investigated by affinity chromatography at 4°C. Columns of adsorbent were equilibrated with HEPES–NaOH buffer, pH 7.5 (20 m*M*) containing $MgCl_2$ (5 m*M*), EDTA (0.4 m*M*) and 2-mercaptoethanol (2 μ*M*). Suspensions of pure enzyme were dialysed (16 h; 4°C) against 2000 volumes equilibration

buffer, and 5–10 U were applied to the columns at a flow-rate of 30 ml h^{-1} cm^{-2}. Buffer flow was interrupted for 10 min following which the adsorbent was washed with equilibration buffer (6 ml) and bound enzyme displaced by a linear 0–1.0 *M* KCl elution gradient. Fractions (1 ml) were collected, from which 20-μl samples were removed for assay of enzyme activity.

Enzyme and protein assays

Glucose-6-phosphate dehydrogenase was assayed by following the reduction of $NADP^+$ at 340 nm (25°C). In a total volume of 1 ml were: triethanolamine–NaOH buffer, pH 7.6 (86 μmol); $MgCl_2$ (6.6 μmol): glucose 6-phosphate (1.2 μmol); and $NADP^+$ (360 nmol). 1 U of activity is defined as the amount of enzyme required to reduce 1 μmol $NADP^+$ per min at 25°C. Alcohol dehydrogenase was assayed as described previously[5].

Hexokinase activity was followed with a glucose-6-phosphate dehydrogenase-linked assay. In a total volume of 3 ml were: triethanolamine–NaOH buffer, pH 7.6 (250 μmol); $MgCl_2$ (20 μmol); glucose (660 μmol); ATP (8.1 μmol); $NADP^+$ (2.2 μmol); and glucose-6-phosphate dehydrogenase (50 μg; 2.5 U). 1 U of hexokinase activity is defined as the amount of enzyme required to effect the reduction of 1 μmol $NADP^+$ per min at 25°C.

Pyruvate kinase activity was determined with a lactate dehydrogenase-linked assay. In a total volume of 3 ml were: triethanolamine–KOH buffer, pH 7.6 (0.26 mmol); $MgSO_4$ (7.5 μmol); KCl (30 μmol); PEP (1.6 μmol); ADP (14 μmol); NADH (0.6 μmol); and lactate dehydrogenase (50 μg; 15 U). 1 U of pyruvate kinase activity is defined as the amount of enzyme required to promote the oxidation of 1 μmol NADH per min at 25°C.

Alcohol dehydrogenase concentration was determined by absorbance at 280 nm (ε_{280} = 0.455 ml mg^{-1} cm^{-1})[12]. Protein concentrations of crude mixtures were determined by the method of Warburg and Christian[13].

RESULTS

Triazine dyes are commonly immobilised to chromatographic support materials by direct reaction between the chlorotriazine group of the dye and nucleophilic groups (frequently hydroxyl ions) on the surface of the matrix. To prevent a similar reaction occurring with C.I. Reactive Blue 2 analogues possessing anthraquinone-linked spacer arms, unreactive methoxylated triazine dyes were synthesised (Fig. 1). This was achieved by reacting the blue chromophore of C.I. Reactive Blue 2 (I; Fig. 1) with 2,4-dichloro-6-methoxy-*s*-triazine, a procedure which also eliminated any reaction between ethylenediamine and the triazine ring in the final stage of synthesis.

Three methoxylated C.I. Reactive Blue 2 analogues were produced which possessed *o*-sulphonate, *p*-sulphonate and *m*-carboxylate groups on the terminal aminobenzene ring of the dye (Fig. 1). Reaction of dyes II–IV with chloroacetyl chloride was accompanied by a colour change from royal blue to burgundy red. The reaction occurred readily in DMF but did not occur in water or aqueous DMF mixtures. Reaction of chloroacetyl dyes V–VIII with ethylenediamine also proceeded smoothly in DMF, although appreciable product hydrolysis was observed if the reaction was allowed to proceed for longer than 30 min. This was readily apparent since as a result

of amide bond hydrolysis in the alkaline reaction mixture, the precursory blue methoxy dye was regenerated, thus causing the reaction mixture to darken.

Spectrophotometric analysis of purified dyes VIII–X (Table I; Fig. 2) revealed maximal light absorption in the region of 520 nm. This represented a hypsochromic shift of approximately 100 nm relative to the λ_{max} of the *o*-sulphonate isomer of C.I. Reactive Blue 2 (XI; Fig. 1). The shift in absorption maximum from 617 to 520 nm was also accompanied by a reduction in extinction (Table I). These spectral changes were entirely expected since the anthraquinone ring 1-amino group is a principal electron-donating group of the C.I. Reactive Blue 2 chromogen[14,15]. Consequently, any alteration of the electronic distribution of the 1-amino group will be manifested as a change in the amount of energy required for electronic transition. Therefore the wavelength and intensity of light absorption will be altered following reactions involving the anthraquinone ring 1-amino group. Chloroacetyl dyes had a λ_{max} marginally lower (approximately 10 nm) than dyes with β-aminoethylaminoacetylamino spacer arms (Table I). This discrepancy may reflect differences in electronegativity between chlorine and substituted nitrogen atoms.

Blue 1,4-diaminoanthraquinone dyes are readily protonated by mineral acids to form quaternary amine salts[15,16]. A large hypsochromic shift is associated with this process. The visible absorption spectrum of the *o*-sulphonate terminal ring isomer of C.I. Reactive Blue 2 (XI) recorded in 4.5 *M* HCl resembled the absorption spectra of C.I. Reactive Blue 2 analogues with modified anthraquinoid 1-amino groups (Fig. 2). The absorption peak of the protonated dye was shifted 91 nm relative to the λ_{max} of the dye in distilled water (526 *versus* 617 nm). However the λ_{max} of V in 4.5 *M* HCl was very similar to that recorded in distilled water (502 *versus* 508 nm; Fig. 2). This observation suggested that the 1-amino group of chloroacetylated dyes was not susceptible to protonation, presumably since this group had been derivatised. Additional evidence of the formation of a 1-chloroacetylamino group was obtained by infrared spectroscopy. Dye V clearly showed the presence of an absorption peak at 1660 cm^{-1} which is indicative of an amide carbonyl group. This peak was absent in the spectrum of the blue precursor dye (II).

Successful coupling of chloroacetyl dyes to ethylenediamine was confirmed using Ehrlich's reagent. Dye VIII rapidly turned an orange colour on exposure to Ehrlich's reagent, confirming the presence of a primary amine. No reaction was observed with compound V, the chloroacetyl precursor of compound VIII.

TABLE I

SPECTRAL DATA DETERMINED FOR C.I. REACTIVE BLUE 2 ANALOGUES

C.I. Reactive Blue 2 analogue[a]	λ_{max}[b] *(nm)*	ε_{λ}[b] *(l mol^{-1} cm^{-1})*
V	508	5800
VII	516	5500
IX	520	5400
X	520	4900
XI	617	12600

[a] For structures, see Fig. 1.

[b] Data obtained from 100 μM aqueous solutions.

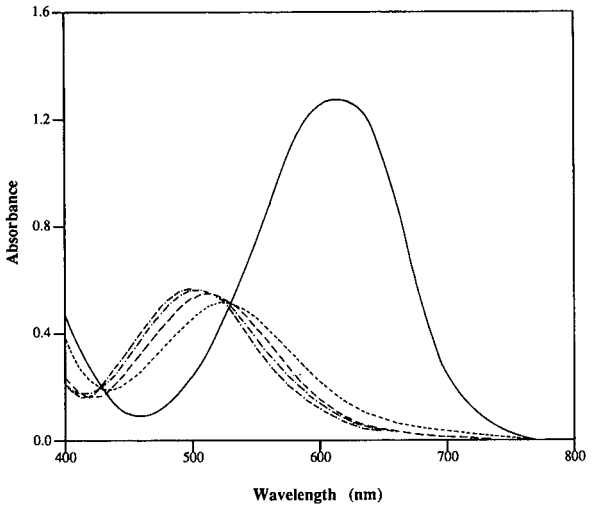

Fig. 2. Absorption spectra of C.I. Reactive Blue 2 analogues. Spectra were recorded from 0.1 m*M* aqueous dye solutions in 10 mm path length cells (25°C) against a distilled water–4.5 *M* HCl blank:— = XI in distilled water; . . . . . = XI in 4.5 *M* HCl; – . – . – = V in distilled water; – . – . – . – = V in 4.5 *M* HCl; - - - - = VIII in distilled water.

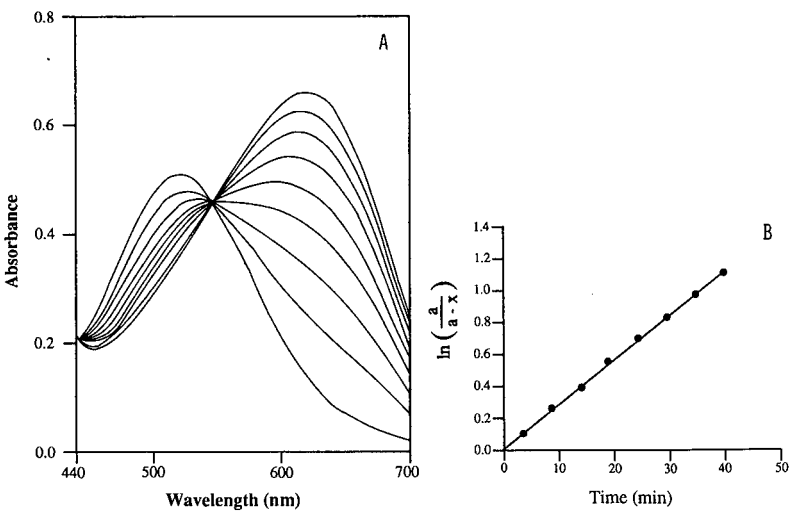

Fig. 3. Base-catalysed hydrolysis of C.I. Reactive Blue 2 analogue V. (A) Visible absorption spectra of a solution containing, in 1 ml total volume, 100 nmol of compound V and 100 μmol of NaOH, were recorded at 5-min intervals against a distilled water blank; path length 10 mm. (B) Plot of ln [initial dye concentration (a)/dye concentration at time t ($a - x$)] against time; values were determined from the absorbance at 516 nm (ε_{516} = 2400 l mol^{-1} cm^{-1}). The slope of the line gives an estimate of the pseudo-first-order rate constant (k_1).

C.I. Reactive Blue 2 analogues with anthraquinone-linked spacer arms were rapidly hydrolysed in strongly alkaline solutions. A time-dependent reduction in absorbance at 518 nm and a concomitant increase in absorbance at 618 nm was observed when compound VIII was treated with 0.1 *M* NaOH (Fig. 3). An isosbestic point at 545 nm was clearly visible, indicating direct conversion of compound V to the blue compound absorbing at 618 nm. Absorbance at 618 nm reached a steady maximum after 4 h. Analysis of the hydrolysate by TLC revealed the blue species had an identical R_F value to precursor compound II. Thus, the initial 1-aminoanthraquinone dye is regenerated as a result of alkaline hydrolysis. The reaction was found to observe typical pseudo-first-order kinetics with a first-order rate constant of $4.64 \cdot 10^{-4}$ s^{-1} (Fig. 3).

Dyes with anthraquinone ring-linked spacer arms (VIII–X) were immobilised to CDI-activated Sepharose 4B to yield red gels. Dye hydrolysis in the mildly alkaline coupling medium (pH 10.0) was not observed spectrophotometrically over a period of 14 h at 15°C. Immobilised dye concentrations were determined as described in the Experimental section in an effort to account for potential acid-catalysed dye hydrolysis during gel dissolution with 5 *M* HCl. However, under these conditions dye hydrolysis was limited. Determined ε_{515} values were 4600, 4600 and 4400 l mol^{-1}, cm^{-1} for compounds VIII, IX and X, respectively. A trial immobilisation of compound V to CDI-activated Sepharose 4B was also performed. As expected, a very weakly substituted gel was produced (immobilised dye concentration 0.1 μmol g^{-1} of moist gel), the low level of coupling being attributable to reaction between the chloroacetyl group of the dye and unsubstituted hydroxyl groups on the matrix.

A number of published reports describe the direct immobilisation of C.I. Reactive Blue 2 to activated matrices, supposedly by reactions involving the anthraquinone ring 1-amino group[17–19]. However, in view of our findings, we were surprised to find no mention of a colour change upon immobilisation by this method. Thus, a number of C.I. Reactive Blue 2 analogues were reacted with CNBr-activated Sepharose 4B, essentially as described by Jankowski *et al.*[17]. Immobilised dye concentrations were determined by a previously reported method[5]. Purified II did not immobilise to CNBr-activated Sepharose 4B, whilst purified XI coupled to give a very weakly substituted gel (Table II). However, significant immobilisation of the blue chromophoric base compound I and commercial-grade C.I. Reactive Blue 2 (supplied by ICI Organics Division) was observed (Table II). In all instances blue gels were produced as opposed to the characteristically red gels obtained when dyes VIII–X were immobilised. These findings suggested that C.I. Reactive Blue 2 does not couple directly to

TABLE II

IMMOBILISATION OF C.I. REACTIVE BLUE 2 ANALOGUES TO CNBr-ACTIVATED AGAROSE

C.I. Reactive Blue 2 analogue	*Immobilised dye concentration (μmol g^{-1} of moist gel)*
Pure I	0.3
Pure II	0.0
Pure XI	0.1
Crude C.I. Reactive Blue 2	0.6

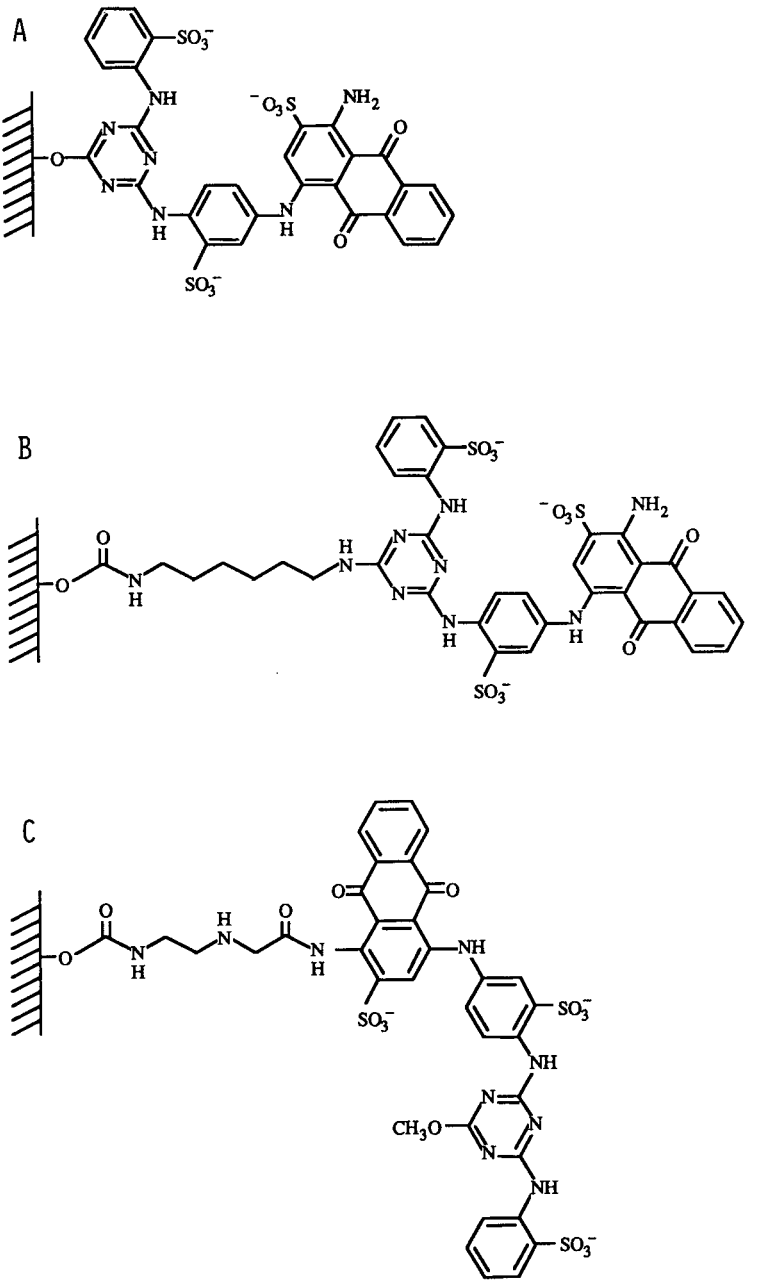

Fig. 4. Structures of immobilised C.I. Reactive Blue 2 analogues. (A) Compound XI coupled directly to agarose; (B) compound XI coupled to CDI-activated agarose by a triazine ring-coupled 6-aminohexyl spacer arm; (C) compound VIII immobilised to CDI-activated agarose.

activated matrices by the anthraquinone ring 1-amino group. The low level of substitution observed for compound XI is probably due to reaction of the chlorotriazine ring with free hydroxyl groups on the matrix. Therefore, the higher level of substitution observed for crude C.I. Reactive Blue 2 is most likely to be attributable to immobilisation of chromophoric contaminants known to be present in commercial dye preparations[9].

Affinity chromatography of pure horse liver alcohol dehydrogenase was performed using C.I. Reactive Blue 2 analogues VIII–X coupled to CDI-activated Sepharose 4B (Fig. 4). All three dyes bound the enzyme, compound X exhibiting the highest affinity (Table III). The concentration of NADH required to elute adsorbed alcohol dehydrogenase correlated directly with the apparent dissociation constant (K_d) of the dye in free solution (determined by difference spectroscopy[5] using methoxylated dyes II–IV). The concentration of NADH required for elution from immobilised X (K_d 0.27 μM) was almost double that required for elution from immobilised IX (K_d 5.7 μM). When compound XI is immobilised to beaded agarose by a 1,6-diaminohexane spacer arm attached to the triazine ring of the dye, an unduly high concentration of NADH is required to displace bound horse liver alcohol dehydrogenase[5]. Steric factors associated with terminal phenyl ring structure and the point of spacer arm attachment were thought to be responsible. Elution of the enzyme from immobilised VIII (which possesses an equivalent terminal ring structure to compound XI) was achieved in a manner entirely consistent with the observed K_d of the dye in free solution. This suggested that immobilisation of C.I. Reactive Blue 2 analogues by the anthraquinone ring 1-amino group was advantageous when using analytical affinity chromatography to investigate the effects of terminal phenyl ring modifications on enzyme binding.

Horse liver alcohol dehydrogenase was effectively purified from a crude liver extract by affinity chromatography on anthraquinone ring-immobilised C.I. Reactive Blue 2 analogues. A non-selective desorption technique was adopted (1 *M* KCl) so that an indication of adsorbent specificity could be gained. On the basis of previous work[1,2], one would predict that considerably higher degrees of purification would be achieved by use of a selective eluent such as NADH. Immobilised C.I. Reactive Blue 2 analogue VIII gave the highest degree of enzyme purification with a 10.3-fold increase in specific activity (Table IV; Fig. 5). Dye IX gave the lowest degree of purification, a

TABLE III

AFFINITY CHROMATOGRAPHY OF HORSE LIVER ALCOHOL DEHYDROGENASE ON IMMOBILISED C.I. REACTIVE BLUE 2 ANALOGUES

Immobilised C.I. Reactive Blue 2 analogue	K_d (μM)[b]	*Immobilised dye concentration* ($\mu mol\ g^{-1}$ *of moist weight gel*)	*NADH concentration required for elution* (μM)[a]	*Activity recovered* (%)
VIII	0.66 ± 0.05	2.1	108	87
IX	5.7 ± 0.5	2.2	68	91
X	0.27 ± 0.07	2.3	113	69

[a] pH 7.5, 4°C.
[b] Determined for the methoxylated precursor dyes II–IV.

TABLE IV

PURIFICATION OF HORSE LIVER ALCOHOL DEHYDROGENASE FROM A CRUDE LIVER EXTRACT BY AFFINITY CHROMATOGRAPHY ON IMMOBILISED C.I. REACTIVE BLUE 2 ANALOGUES

C.I. Reactive Blue 2 analogue	*Immobilised dye concentration (μmol g^{-1} of moist gel)*	*Specific activity of applied sample (U mg^{-1})*	*Specific activity of eluted enzyme (U mg^{-1})*	*Purification (fold)*	*Yield (%)*
VIII	2.1	0.018	0.185	10.3	86
IX	2.2	0.019	0.058	3.1	36
X	2.3	0.015	0.085	5.6	74
XI[a]	2.1	0.015	0.065	4.3	87
XI[b]	2.2	0.014	0.103	7.3	84

[a] Direct coupling through chlorotriazine group.
[b] 6-Aminohexyl coupling.

possible reflection of the relatively low affinity of this analogue for horse liver alcohol dehydrogenase. Similar purification experiments were also performed with adsorbents composed of XI coupled directly to Sepharose 4B (synthesised according to Lowe *et al.*[20]) and 6-aminohexyl-XI coupled to CDI-activated Sepharose 4B (synthesised as described previously[5]). The method of dye immobilisation (Fig. 4) was found to have a profound effect on adsorbent specificity (Table IV). The commonly

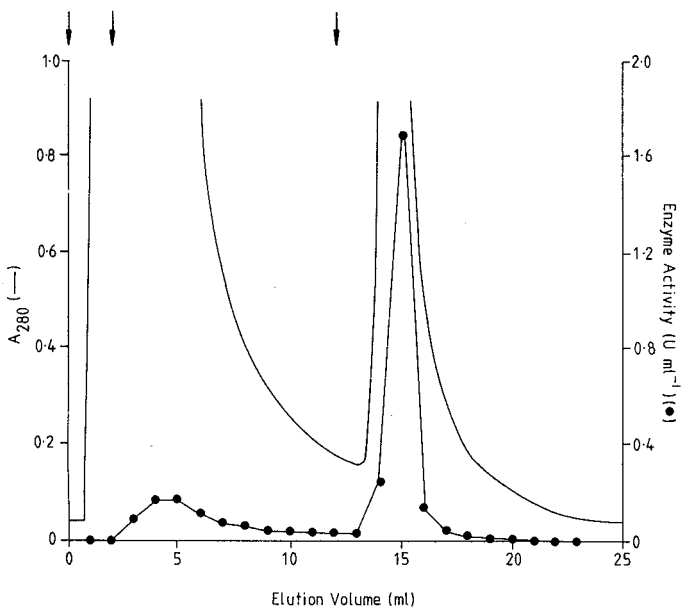

Fig. 5. Purification of alcohol dehydrogenase from horse liver extract by affinity chromatography on agarose-immobilised C.I. Reactive Blue 2 analogue VIII. Dialysed horse extract (2 ml; 130 mg protein) was applied at a linear flow-rate of 30 ml min^{-1} cm^{-2} to a 10 cm × 0.5 cm I.D. glass column packed with 1.0 g of adsorbent equilibrated in HEPES–NaOH buffer, pH 7.5 (20 m*M*) containing glutathione (1 m*M*). The column was flushed with equilibration buffer (10 ml) and bound protein eluted with buffer containing 1 *M* KCl. Fractions (1 ml) were collected and assayed for enzyme activity.

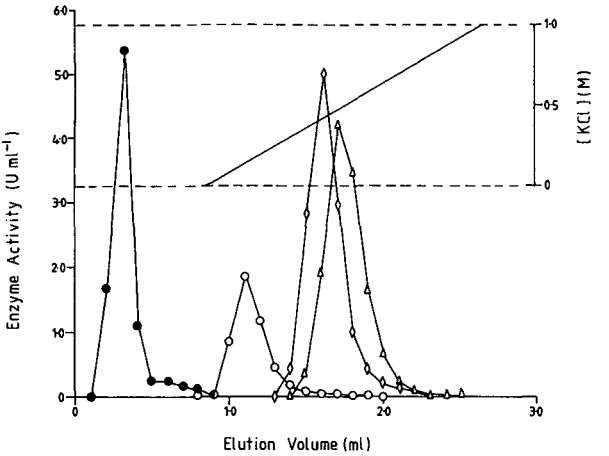

Fig. 6. Affinity chromatography of dehydrogenases and kinases on immobilised C.I. Reactive Blue 2 analogue X. Glass columns (10 cm × 0.5 cm I.D.) containing Sepharose 4B-immobilised X (1.0 g moist gel; total column volume, 2.2 ml) was equilibrated with HEPES–NaOH buffer, pH 7.5 (20 m*M*) containing 2-mercaptoethanol (2 μM), EDTA (0.4 m*M*) and $MgCl_2$ (5 m*M*). Dialysed enzyme [yeast hexokinase, 10 U (●); rabbit muscle pyruvate kinase, 10 U (△); horse liver alcohol dehydrogenase, 5 U (○); or yeast glucose-6-phosphate dehydrogenase, 10 U (◇)] was applied to the columns at a flow-rate of 30 ml h^{-1} cm^{-2} and incubated with the adsorbent for 10 min. The columns were flushed with equilibration buffer (6 ml) and adsorbed enzyme was eluted with a KCl gradient (0–1.0 *M*; 20 ml). Fractions (1 ml) were collected and samples (20 μl) assayed for enzyme activity.

adopted direct immobilisation technique resulted in a low degree of enzyme purification (4.3-fold). Spacer arm-coupled dyes gave notably higher degrees of purification, linkage to the anthraquinone ring proving the most effective method of immobilisation.

Investigations with immobilised nucleotides show that the point of spacer arm attachment can dramatically affect the affinity of the immobilised ligand for nucleotide-binding proteins[21–23]. Consequently, affinity chromatography was used to investigate the interaction of selected dehydrogenases and kinases with compounds X and 6-aminohexyl-XII (synthesised as reported previously[5]), immobilised to CDI-

TABLE V

AFFINITY CHROMATOGRAPHY OF DEHYDROGENASES AND KINASES ON C.I. REACTIVE BLUE 2 ANALOGUES IMMOBILISED TO SEPHAROSE 4B BY SPACER ARM COUPLING TO THE ANTHRAQUINONE RING (X) OR THE TRIAZINE RING (6-AMINOHEXYL-XII)

Enzyme	*Concentration of KCl required for elution (M)*	
	Immobilised X	*Immobilised XII*
Horse liver alcohol dehydrogenase	0.15	0.12
Yeast glucose-6-phosphate dehydrogenase	0.44	0.47
Rabbit muscle pyruvate kinase	0.45	0.30
Yeast hexokinase	—[a]	—[a]

[a] Enzyme eluted in void volume.

activated Sepharose 4B (Fig. 6). Rabbit muscle pyruvate kinase bound more tightly to compound X than to 6-aminohexyl-XII (as adjudged by the concentration of KCl required for elution), whilst horse liver alcohol dehydrogenase and yeast glucose-6-phosphate dehydrogenase were bound by both adsorbents with approximately equal affinity (Table V). Yeast hexokinase was unretarded by both adsorbents as might have been deduced from previous dye-binding studies[24]. Thus C.I. Reactive Blue 2 analogues immobilised by the anthraquinone ring 1-amino group retain their ability to interact with nucleotide-binding proteins. In he case of rabbit muscle pyruvate kinase, binding is favoured by this method of immobilisation.

DISCUSSION

The interaction of affinity ligands with the ligand binding sites of proteins is frequently enhanced by the provision of a spacer arm between the ligand and the support matrix[10]. In addition, the orientation of the immobilised ligand can also influence its affinity for proteins. Studies with immobilised nucleotides such as adenosine 5′-monophosphate (AMP) or NAD^+ have shown that spacer arm linkage and ligand orientation can have a profound effect on protein adsorption[21–23]. Rather surprisingly, such considerations are seldom applied to reactive dye ligands, despite the fact that these commonly used compounds have been applied to the purification of a large number of nucleotide-binding proteins[1–4]. The predominant immobilisation technique adopted for reactive dyes, regardless of application, parallels the direct reaction of chlorotriazine dyes with cellulose textiles[4].

From previous investigations on the interaction of C.I. Reactive Blue 2 analogues with horse liver alcohol dehydrogenase, we concluded that immobilisation by the triazine ring was responsible for interferences with dye binding[5]. A more suitable point of attachment appeared to be the anthraquinone ring 1-amino group, since this component is exposed to the exterior solvent when dye is bound to the enzyme[5,6]. We find that immobilisation of C.I. Reactive Blue 2 analogues by a spacer arm linked to the anthraquinone ring 1-amino group, as opposed to the chlorotriazine ring, not only increases the affinity of the immobilised analogues for horse liver alcohol dehydrogenase, but also improves their specificity.

Previously, an immobilised C.I. Reactive Blue 2 analogue with an *m*-orientated carboxyl group on the terminal phenyl ring of the dye (K_d 0.06 μM) bound horse liver alcohol dehydrogenase with an affinity such that 90 μM NADH was required for elution[5]. In this work, analogue X (which also possessed an *m*-orientated terminal ring carboxyl group; K_d 0.27 μM) immobilised by the anthraquinone ring, as opposed to the triazine ring, bound the enzyme more tightly so that 113 μM NADH was required for desorption (Table III). Since both experiments were performed under identical conditions, the results suggest that immobilisation by the anthraquinone ring 1-amino group promotes the interaction of C.I. Reactive Blue 2 analogues with horse liver alcohol dehydrogenase. Presumably steric hindrance in the vicinity of the triazine ring is reduced on immobilising the dye by the anthraquinone ring.

The increase in immobilised dye specificity was particularly marked for compound VIII. Following alcohol dehydrogenase purification from a crude liver extract, a 2.4-fold increase in enzyme specific activity was achieved over the level of purification obtained with essentially the same dye (XI) immobilised by direct coupling

(Table IV). Enzyme recovery upon elution was virtually identical for both adsorbents (86–87%). Spacer arm coupling, by the anthraquinone ring or the triazine ring, resulted in a higher degree of enzyme purification as compared to the performance of directly coupled dyes (Table IV). Confirmation was provided by additional chromatographic data (not presented) determined for other immobilised C.I. Reactive Blue 2 analogues. This finding suggests that immobilisation of reactive dyes by a spacer arm linkage may enhance selective dye–protein interactions at the expense of non-selectgive binding, thereby promoting an overall increase in adsorbent selectivity. Similar conclusions may be reached from binding studies performed with blue dextran Sepharose. Human fibroblast and leucocyte interferons have greater affinity for Cibacron Blue F3G-A immobilised by a dextran linker, as opposed to dye coupled directly to beaded agarose[17]. Conversely, rat brain hexokinase and pigeon liver NAD^+ kinase display a reduced affinity for blue dextran Sepharose[24,25]. Thus dye specificity may be modulated by the use of spacer arm linkage regimes.

C.I. Reactive Blue 2 analogues immobilised by the anthraquinone ring 1-amino group were capable of interacting with a number of dehydrogenases and kinases (Fig. 6). Interestingly, the anthraquinonoid 1-amino group of C.I. Reactive Blue 2 bound to horse liver alcohol dehydrogenase is located in a similar position to the adenyl N^6-amino group of bound NAD^+[6] (ref. 6). Both NAD^+ and AMP immobilised by a hexyl spacer arm attached to the adenyl N^6-amino group often provide very effective adsorbents for the purification and resolution of dehydrogenases and kinases. Therefore, C.I. Reactive Blue 2 immobilised by the anthraquinone ring may bind a variety of adenine nucleotide-requiring proteins, possibly with an affinity and specificity greater than the conventionally immobilised dye.

Reaction of the C.I. Reactive Blue 2 anthraquinone ring 1-amino group with electrophiles is hindered due to the close proximity of the quinone oxygen and 2-sulphonate groups. In addition, the $2P_z$ electrons of the 1-amino group conjugate with the anthraquinone ring π electron cloud, causing a reduction in basicity of the 1-amino group. For these reasons, the 1-amino group is not particularly reactive towards electrophiles, accounting for its lack of reactivity with cyanuric chloride in aqueous solution[9]. However, reactivity of the 1-amino group probably increases in DMF due to suppression of anthraquinone-2-sulphonate group ionisation. This factor, coupled with the absence of water, may allow reaction of the anthraquinone ring 1-amino group with chloroacetyl chloride to yield an amide bond.

Conjugation of the 1-amino group $2P_z$ electrons with the electron cloud of the anthraquinone ring gives rise to a charge-transfer absorption peak in the visible region of the spectrum, brought about by $2P_z$–π^* transition[14]. Addition of a second electron donor group in the 4-position causes a bathochromic shift and increase in extinction[14,16]. Thus, 1-amino anthraquinone absorbs at 475 nm with a molar extinction coefficient of 6300 l mol^{-1} cm^{-1}, whilst 1,4-diaminoanthraquinone absorbs at 550–590 nm with an extinction coefficient of 15 850 l mol^{-1} cm^{-1} (values determined in methanol)[15,16]. If the electron density of the amino groups are reduced in any way (by acetylation for example), a hypsochromic shift and reduction in extinction are observed[14,26]. Reactions involving the anthraquinone ring 1-amino group will therefore result in marked spectral changes.

The spectral perturbations observed upon chloroacetylation of C.I. Reactive Blue 2 analogues (Fig. 2) are entirely consistent with the known behaviour of ami-

noanthraquinone chromophores[14,16]. However, our findings are at odds with a number of reports in the biochemical literature which infer that C.I. Reactive Blue 2 may be coupled to activated matrices via the anthraquinone ring 1-amino group without significant changes of chromaticity[17–19,25]. We find that purified C.I. Reactive Blue 2 couples very poorly to CNBr-activated Sepharose, the coupling observed probably being attributable to reaction of the chlorotriazine moiety with matrix hydroxyl groups. Significant blue coloration was observed if impure dye was immobilised, suggesting that chromophoric contaminants (probably compounds I and 2,4-dichloro-*s*-triazin-6-yl-I) were immobilised on previous occasions and not C.I. Reactive Blue 2. A possible consequence of this may be the reportedly low affinity of C.I. Reactive Blue 2 towards protein when supposedly immobilised by the anthraquinone ring 1-amino group[17–19,25]. These findings have also been reported in several review articles[1,2,27]. In fact, C.I. Reactive Blue 2 analogues genuinely immobilised by the 1-amino group are very effective affinity ligands. It is worthwhile noting that analogue X bound yeast glucose-6-phosphate dehydrogenase avidly, whereas an adsorbent formed by reacting Cibacron Blue F3G-A with succinyl-polyacrylic hydrazide agarose did not bind the enzyme[18]. Thus, great care must be exercised when interpreting chromatographic results obtained on using affinity adsorbents constructed from heterogeneous commercial dye preparations.

As with most small affinity ligands, the protein binding selectivity of reactive dyes is influenced by the immobilisation technique adopted and the point of attachment to the matrix. Such considerations should not be overlooked when designing chromophoric ligands for the chromatographic purification of proteins. Optimally immobilised biomimetic dyes, with structures designed to interact with selected proteins, should therefore have considerably improved specificities to conventional textile dyes.

ACKNOWLEDGEMENTS

We would like to thank the Biotechnology Directorate of the Science and Engineering Research Council and ICI plc for their financial support.

REFERENCES

1 C. R. Lowe, in A. Wiseman (Editor), *Topics in Enzyme and Fermentation Biotechnology*, Vol. 9, Ellis Horwood, Chichester, 1984, pp. 78–161.
2 G. Kopperschläger, H.-J. Böhme and E. Hoffman, in A. Feichter (Editor), *Advances in Biochemical Engineering*, Vol. 25, Springer, Berlin, Heidelberg, 1982, pp. 101–138.
3 C. R. Lowe and J. C. Pearson, *Methods Enzymol.*, 104 (1984) 97–113.
4 Y. D. Clonis, A. A. Atkinson, C. J. Bruton and C. R. Lowe (Editors), *Reactive Dyes in Protein and Enzyme Technology*, Macmillan, Basingstoke, 1987.
5 S. J. Burton, C. V. Stead and C. R. Lowe, *J. Chromatogr.*, 455 (1988) 201–216.
6 J.-F. Biellman, J.-P. Samama, C.-I. Branden and H. Eklund, *Eur. J. Biochem.*, 102 (1979) 107–110.
7 H. Eklund, J.-P. Samama and T. A. Jones, *Biochemistry*, 23 (1984) 5982–5996.
8 J. C. Pearson, S. J. Burton and C. R. Lowe, *Anal. Biochem.*, 158 (1986) 382–389.
9 S. J. Burton, S. B. McLoughlin, C. V. Stead and C. R. Lowe, *J. Chromatogr.*, 435 (1988) 127–137.
10 C. R. Lowe, in T. S. Work and E. Work (Editors), *Laboratory Techniques in Biochemistry and Molecular Biology*, Vol. 7, North-Holland, Amsterdam, 1979, pp. 267–522.
11 L. Andersson, H. Jornvall, A. Akeson and K. Mosbach, *Biochim. Biophys. Acta*, 364 (1974) 1–8.
12 D. J. Cannon and R. H. McKay, *Biochem. Biophys. Res. Commun.*, 35 (1969) 403–409.

13 O. Warburg and W. Christian, *Biochem. Z.*, 310 (1941) 384–421.
14 V. Y. Fain, in R. W. A. Oliver (Editor), *The Electronic Spectra of Anthraquinones*, 1970.
15 P. F. Gordon and P. Gregory, *Organic Chemistry in Colour*, Springer, Berlin, Heidelberg, 1983.
16 R. H. Peters and H. H. Summer, *J. Chem. Soc.*, (1953) 2101–2110.
17 W. I. Jankowski, W. Muenchhausen, E. Sulkowski and W. A. Carter, *Biochemistry*, 15 (1976) 5182–5187.
18 R. S. Beissner and F. B. Rudolph, *J. Chromatogr.*, 161 (1978) 127–135.
19 R. J. Leatherbarrow and P. D. G. Dean, *Biochem. J.*, 189 (1980) 27–34.
20 C. R. Lowe, M. Hans, N. Spibey and T. W. Drabble, *Anal. Biochem.*, 104 (1980) 23–28.
21 M. J. Harvey, C. R. Lowe, D. B. Craven and P. D. G. Dean, *Eur. J. Biochem.*, 41 (1974) 335–340.
22 C. R. Lowe, *Pure Appl. Chem.*, 51 (1979) 1429–1441.
23 C. R. Lowe, I. P. Trayer and H. R. Trayer, *Methods Enzymol.*, 66 (1980) 192–208.
24 J. E. Wilson, *Biochem. Biophys. Res. Commun.*, 72 (1976) 816–823.
25 D. K. Apps and C. D. Gleed, *Biochem. J.*, 159 (1976) 441–443.
26 Z. Yoshida and F. Takabayashi, *Tetrahedron*, 24 (1968) 913–943.
27 F. Quadri, *Trends Biotechnol.*, 3 (1985) 7–12.

Journal of Chromatography, 508 (1990) 127–132
Elsevier Science Publishers B.V., Amsterdam — Printed in The Netherlands

CHROM. 22 306

Chromatographic behaviour of cyclodextrin complexes of NADH and NADP

MANABU SENO*, MEILING LIN and KAZUTOSHI IWAMOTO
Institute of Industrial Science, University of Tokyo, 7-22-1, Roppongi, Minato-ku, Tokyo 106 (Japan)
(Received January 2nd, 1990)

SUMMARY

The retention behaviour of NADH and NADP on an ODS-C_{18} reversed-phase column was investigated by using a 0.05 *M* phosphate buffer (pH 6) containing α-, β- or γ-cyclodextrin (CD) as the mobile phase. Three reversible processes were assumed and the partition coefficients, k_2, of inclusion complexes and their stability constants, *K*, were calculated. The value of k_2 is clearly dependent on the molecular weight of the CD. It was established from the calculated values of *K* that NADH and NADP are liable to form more stable inclusion complexes with β-CD than α- and γ-CDs. NADP has a higher stability constant than NADH owing to the formation of hydrogen bonds between the phosphate moieties of NADP and the hydroxyl groups of CDs.

INTRODUCTION

α-, β- and γ-cyclodextrins (CDs) are cyclic oligosaccharides containing six, seven and eight glucose units, respectively. Because of the dimensions of their non-polar central cavities, CDs act as "hosts", forming stable inclusion complexes with a variety of "guest" species. The formation of an inclusion complex is based on the ability of the CD to incorporate hydrophobic molecules in its cavity and to form hydrogen bonds between hydroxyl groups at the entrance of the CD cavity and the hydrophilic moieties of the guest molecule[1–3]. For example, a chiral molecule forms a hydrogen bond with the 2-hydroxyl groups at the entrance of the CD cavity[4,5]. In addition, many other factors such as Van der Waals force, dipole–dipole interactions and hydrophobic interactions also play important roles in governing the stability of the complex[6].

In recent years, CD inclusion phenomena have been utilized in high performance liquid chromatographic (HPLC) techniques in two ways: the use of CD-bonded stationary phases as reported by Issaq[7] and the use of CD as one component of the mobile phase in reversed-phase liquid chromatography (RP-LC)[8–11]. Cline Love and Arunyanart[12] dealt with the latter method and calculated the stability constants, *K*, of benzene, phenol, *o*, *m*- and *p*-nitrophenol, naphthalene and biphenyl with β-CD.

This paper reports the results of further studies on the determinations of the

0021-9673/90/$03.50

capacity factors, k'_2, of inclusion complexes formed between NADH or NADP and CDs, and their stability constants, K, based on a model consisting of three reversible processes[13,14]. The elution behaviour of NADH and NADP in RP-LC was also investigated by using a 0.05 M phosphate buffer (pH 6) containing α-, β- or γ-CD as the mobile phase.

EXPERIMENTAL

Reagents

NADP (nicotinamide adenine dinucleotide phosphate) and NADH (nicotinamide adenine dinucleotide) were obtained from Sigma and α-, β- and γ-CDs from Tokyo Kasei. All the materials were used without further purification.

Apparatus and procedures

A Bionert LC system (Japan Spectroscopic) equipped with a Model 875-UV Intelligent UV–VIS detector operating at 254 nm, an SIC Chromatocorder 12 and a Model 880-PU Intelligent pump were employed. A Hitachi Gel 3056 ODS-C_{18} reversed-phase column (150 × 4 mm I.D.; 5 μm particle diameter) was used.

The CD mobile phase was prepared by dissolving the appropriate weight of CD in 0.05 M phosphate buffer (pH 6) (Na_2HPO_4–NaH_2PO_4) and filtering through a poly(vinylidene fluoride) membrane filter (Millipore, pore size 0.65 μm). All the chromatographic experiments were carried out at a constant flow-rate of 1.0 ml/min and at room temperature. A 3-μl sample volume containing 50 μg/ml of solute was injected into the column.

The void volume of the column with a mobile phase containing different concentrations of the CDs was determined by using analytical-reagent grade potassium nitrate[13].

RESULTS AND DISCUSSION

The elution behaviour of NADH and NADP can be analysed by using a model consisting of three reversible reactions: a reversible reaction of guest molecule A and CD in the mobile phase to form an inclusion complex A · CD, and two reversible adsorption processes of A and A · CD on the stationary phase of the ODS-C_{18} column. A and A · CD adsorbed on the ODS-C_{18} column are represented by A_s and A · CD_s, respectively.

$$A + CD \overset{K}{\rightleftharpoons} A \cdot CD \tag{1}$$

$$A \overset{k_1}{\rightleftharpoons} A_s \tag{2}$$

$$A \cdot CD \overset{k_2}{\rightleftharpoons} A \cdot CD_s \tag{3}$$

where K is the stability constant of the inclusion complex A · CD and k_1 and k_2 are the partition coefficients of A and A · CD, respectively, between the mobile phase and the stationary phase.

The capacity factors of A and A · CD, k'_1 and k'_2, are given as follows[15]:

$$k'_1 = \varphi k_1 = \varphi \frac{[A_s]}{[A]} \tag{4}$$

$$k'_2 = \varphi k_2 = \varphi \frac{[A \cdot CD_s]}{[A \cdot CD]} \tag{5}$$

where φ is the phase ratio, *i.e.*, the ratio of the volume of the stationary phase, V_s, to the void volume of the mobile phase, V_0, in the column.

The capacity factor k' of the guest molecule A, which is experimentally determined, is represented by[15]

$$k' = \varphi \frac{[A_s] + [ACD_s]}{[A] + [ACD]} \tag{6}$$

Combination of eqns. 1, 4, 5 and 6 yields the following expression for the capacity factor:

$$k' = \frac{k'_1 + k'_2 K[CD]}{1 + K[CD]} \tag{7}$$

where [CD] is the molar concentration of CD. Eqn. 7 is similar to that derived by Uekama *et al.*[16] for the determination of the stability constants of the CD complexes of various ionic species measured by ion-exchange chromatography.

If k'_2 is small enough to be ignored, the following expression is obtained:

$$k' = \frac{k'_1}{1 + K[CD]} \tag{8}$$

By taking the reciprocal of both sides of eqn. 8 and plotting $1/k'$ *vs.* [CD], one can obtain a straight line and the value of the stability constant K is obtained as the slope/intercept ratio.

If k'_2 cannot be neglected, eqn. 7 can be linearized by a simple transformation:

$$\frac{k'_1 - k'_2}{k' - k'_2} = 1 + K[CD] \tag{9}$$

When one takes an appropriate value of k'_2 in eqn. 9, the plot of $(k'_1 - k'_2)/(k' - k'_2)$ *vs.* [CD] should be linear and the value of the stability constant K is obtained from the slope of the line.

The retention volumes of NADP and NADH were measured at different concentrations of α-, β- or γ-CD in the 0.05 *M* phosphate buffer (pH 6). The capacity factor k' for each guest molecule was calculated from the retention data by using the ratio $(V_R - V_0)/V_0$, where V_R is the elution volume of the guest molecule and V_0 is the void volume of the column. The relationships between the capacity factor k' of NADP

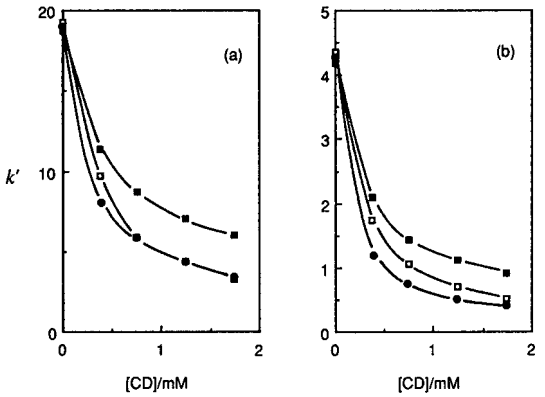

Fig. 1. Relationships between the experimental capacity factors k' of (a) NADH and (b) NADP to the concentrations of (□) α-CD, (●) β-CD and (■) γ-CD in 0.05 *M* phosphate buffer (pH 6) mobile phase.

and NADH and the concentration of α-, β- or γ-CD in the mobile phase are shown in Fig. 1. With increasing concentration of α-, β- or γ-CD, the k' values of NADH and NADP are reduced. It is evident that α-, β- and γ-CD form inclusion complexes with NADH and NADP. Addition of β-CD reduces the k' value more than addition of α- or γ-CD, and the effect decreases in the order β-CD > α-CD > γ-CD. On the other hand, the k' values of NADP are reduced more than those of NADH, NADP is considered to form more stable complexes than NADH with CDs.

Fig. 2 shows the relationships between the reciprocal capacity factors of (a) NADH and (b) NADP and the concentration of α-, β- or γ-CD in the 0.05 *M* phosphate buffer (pH 6) mobile phase. The $1/k'$ of NADH and NADP *vs.* [α-CD] plots satisfy a linear relationship. This shows that the value of k'_2 is adequately small for α-CD. The stability constant K for α-CD was calculated from this plot as shown in Table I. For β- and γ-CD, the plots of $1/k'$ *vs.* [CD] were not linear, indicating that the capacity factor k'_2 of β- and γ-CD cannot be neglected. Therefore, values of k'_2 were

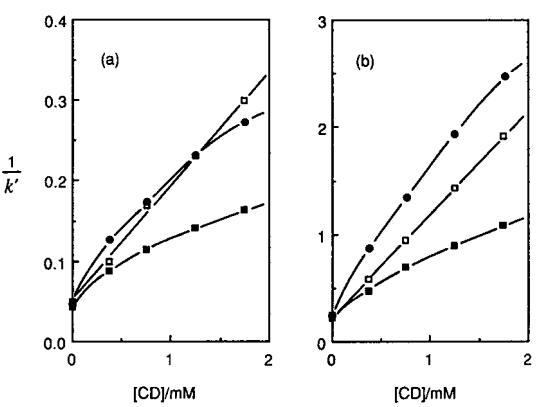

Fig. 2. Relationships between the reciprocal capacity factor of (a) NADH and (b) NADP and the concentration of (□) α-CD, (●) β-CD and (■) γ-CD in the 0.05 *M* phosphate buffer (pH 6) mobile phase. In the case of α-CD, the solid straight lines were obtained.

TABLE I

PARTITION COEFFICIENTS k_1 AND k_2 AND STABILITY CONSTANTS K (mmol l^{-1}) OF NADH AND NADP WITH α-, β- AND γ-CD

Compound	*α-CD*			*β-CD*			*γ-CD*		
	k_1	k_2	K	k_1	k_2	K	k_1	k_2	K
NADH	34.86	0.0	2.80	34.86	2.96	4.42	34.86	5.48	2.37
NADP	7.73	0.0	4.36	7.73	0.18	7.15	7.73	0.58	3.10

assigned to give a linear relationship between $(k'_1 - k'_2)/(k' - k'_2)$ and the concentration of β- or γ-CD in the mobile phase according to eqn. 9. The resulting relationships are shown in Fig. 3. The stability constants K for β-CD and γ-CD were determined from the slopes.

The results are summarized in Table I. The k'_1 and k'_2 values are converted to the k_1 and k_2 values, respectively, by using eqns. 4 and 5. The stability constants K of β-CD with NADP and NADH are large compared with those of α- and γ-CD. This means that NADP and NADH are liable to form stable inclusion complexes with β-CD. Moreover, the K value of NADP is always larger than that of NADH.

The formation of the inclusion complexes is due to the ability of CDs to incorporate hydrophobic molecules in their cavities and to form hydrogen bonds between the hydroxyl groups at the entrance of the CD cavity and the polar groups of the guest molecule[1–5]. It is considered that NADH and NADP form inclusion complexes with CD by incorporating their adenine moiety in the CD cavity, as shown schematically in Fig. 4. The cavity size of β-CD matches well the size of the adenine moiety, because the inner diameters of α-, β- and γ-CD are 0.57, 0.78 and 0.95 nm, respectively[17], and the lateral maximum size of the adenine moiety of NADH and NADP was estimated from the bond length and bond angles of the adenine molecule to be *ca.* 0.62 nm.

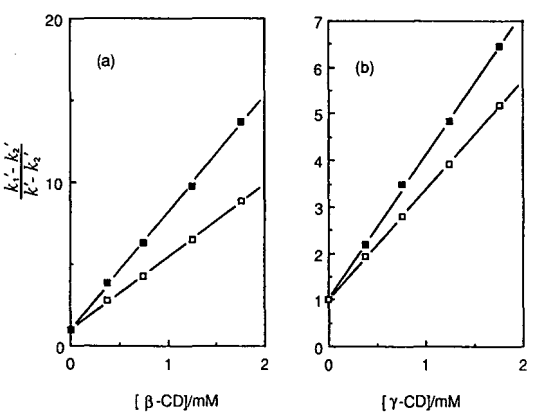

Fig. 3. Relationships between $(k'_1 - k'_2)/(k' - k'_2)$ and the concentrations of (a) β-CD and (b) γ-CD in the mobile phase for (□) NADH and (■) NADP. Solid lines were obtained by plotting eqn. 9.

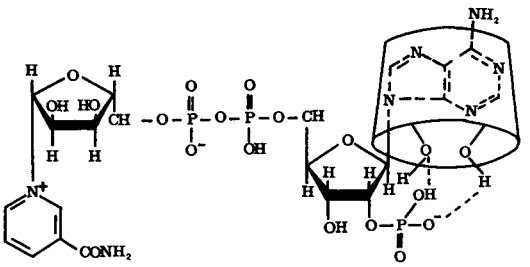

Fig. 4. Schematic representation of the NADP–CD inclusion complex. The dashed lines represent the hydrogen bonds.

The partition coefficients k_2 of γ-CD complexes are larger than those of β-CD complexes, and the partition coefficients k_2 of α-CD complexes are nearly zero in this instance. The value of k_2 is clearly dependent on the molecular weight of the CD and an increase in the molecular weight enhances the hydrophobicity and therefore the column affinity of CD complexes. Lastly, it can be noted that NADP forms hydrogen bonds between its phosphate moiety and the hydroxyl groups of CD, as shown in Fig. 4, resulting in a larger stability constant K than for NADH.

REFERENCES

1 F. Cramer, *Rev. Pure Appl. Chem.*, 5 (1955) 143.
2 C. Van Hooidonk and J. C. A. E. Breebaart-Hansen, *Recl. Trav. Chim. Pays-Bas*, 90 (1971) 680.
3 F. Cramer and W. Dietsche, *Chem. Ber.*, 92 (1959) 1739.
4 J. Debowski, J. Jurczak and D. Sybilska, *J. Chromatogr.*, 282 (1983) 83.
5 D. W. Armstrong, *J. Liq. Chromatogr.*, 7 (1984) 353.
6 W. L. Hinze, *Sep. Purif. Methods*, 10 (1981) 159.
7 H. J. Issaq, *J. Liq. Chromatogr.*, 11 (1988) 2131.
8 M. Gadag, G. Szepesi and L. Huszar, *J. Chromatogr.*, 436 (1988) 31.
9 B. Luděk and W. Milan, *J. Chromatogr.*, 445 (1988) 337.
10 C. A. Chang, Q. Wu and L. Tan, *J. Chromatogr.*, 316 (1986) 199.
11 K. Shimada, T. Masue, K. Toyoda, M. Takani and T. Nambara, *J. Liq. Chromatogr.*, 11 (1988) 1475.
12 L. J. Cline Love and M. Arunyanart, *ACS Symp. Ser.*, 297 (1986) 226.
13 J. Zukowski, D. Sybilska and J. Jurczak, *Anal. Chem.*, 57 (1985) 2215.
14 J. Debowski and D. Sybilska, *J. Chromatogr.*, 353 (1986) 409.
15 A. Manop and L. J. Cline Love, *Anal. Chem.*, 56 (1984) 1557.
16 K. Uekama, F. Hirayama, S. Nasu, N. Matsuo and T. Irie, *Chem. Pharm. Bull.*, 26 (1978) 3477.
17 J. Szejtli, *Cyclodextrins and Their Inclusion Complexes*, Akadémiai Kiadó, Budapest, 1982, p. 25.

Journal of Chromatography, 508 (1990) 133–140
Elsevier Science Publishers B.V., Amsterdam — Printed in The Netherlands

CHROM. 22 308

2-(2,3-Naphthalimino)ethyl trifluoromethanesulphonate as a highly reactive ultraviolet and fluorescent labelling agent for the liquid chromatographic determination of carboxylic acids

YUTA YASAKA*, MINORU TANAKA and TOSHIYUKI SHONO
Department of Applied Chemistry, Faculty of Engineering, Osaka University, Yamada-oka, Suita, Osaka 565 (Japan)
and
TADAHIRO TETSUMI and JUN'ICHI KATAKAWA
Faculty of Pharmaceutical Sciences, Setsunan University, Nagaotoge, Hirakata, Osaka 571-01 (Japan)
(First received October 24th, 1989; revised manuscript received January 26th, 1990)

SUMMARY

The use of 2-(2,3-naphthalimino)ethyl trifluoromethanesulphonate in the preparation of 2-(2,3-naphthalimino)ethyl ester derivatives of carboxylic acids for ultraviolet and fluorescent detection in high-performance liquid chromatography is described. The reagent is easily synthesized in two steps from 2,3-naphthalenedicarboxylic anhydride and is stable at least for 6 months at room temperature. Reactions of carboxylate potassium salts (10^{-5} *M*) with a 10-fold equivalent excess amount of the reagent proceed to completion within 10 min in acetonitrile at room temperature in the presence of 18-crown-6 as a catalyst. The derivatization procedure with this reagent has been applied succesfully to the determination of some carboxylic acids in mouse brain. The detection limits (signal-to-noise ratio = 3) with ultraviolet and fluorescent detection are 100 fmol (at 259 nm) and 4 fmol (λ_{ex} = 259 nm, λ_{em} = 394 nm), respectively.

INTRODUCTION

Carboxylic acids are widely distributed in nature and play important roles as nutritional substrates and metabolites in the living body. The carboxyl functional group is only weakly chromophoric, so carboxylates with no other adequately chromophoric structural feature must be derivatized for their sensitive detection by high-performance liquid chromatography (HPLC). Of the detection methods currently available for HPLC, fluorimetric detection is one of the most selective and sensitive. Several fluorescent labelling agents, *e.g.*, 4-bromomethyl-7-methoxycoumarin[1], 1-bromoacetylpyrene[2], 9-aminophenanthrene[3], 9-anthryldiazomethane[4] and 3-bromomethyl-6,7-dimethoxy-1-methyl-2(1*H*)-quinoxalinone[5], have been developed for the determination of carboxylic acids by HPLC. The reactions of carboxylic

0021-9673/90/$03.50

acids with these reagents are slow and/or require elevated temperatures for complete derivatization because of the poor reactivity of the carboxyl groups. Longer reaction times at elevated temperatures are unfavourable not only for simplicity in the derivatization procedures but for the determination of thermolabile substances such as α-ketocarboxylic acids.

On the other hand, the powerful alkylating abilities of perfluoromethanesulphonates are well known in the field of organic synthesis. Ingalls *et al.*[6] developed 4′-bromophenacyl trifluoromethanesulphonate as a highly reactive UV-labelling agent for carboxylic acids for HPLC determination. This reagent can derivatize the acids completely to the corresponding derivatives within 5 min in acetonitrile at room temperature in the presence of N,N-diisopropylethylamine. Recently, we have also reported the UV-labelling of carboxylic acids with 2-(phthalimino)ethyl trifluoromethanesulphonate at room temperature[7].

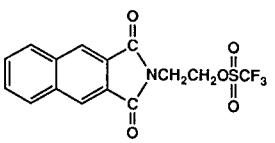

NE-OTf

In this work, 2-(2,3-naphthalimino)ethyl trifluoromethanesulphonate (NE-OTf) was developed as a highly reactive ultraviolet and fluorescent labelling agent for carboxylic acids in HPLC. Myristic acid was chosen as a representative carboxylic acid and the reactivity of NE-OTf towards the acid was investigated under various conditions. An attempt was made to apply the reagent to small-volume biological samples and some carboxylic acids in mouse brain were successfully determined.

EXPERIMENTAL

Apparatus

The HPLC system consisted of a JASCO 880-PU pump, a Rheodyne Model 7125 injector valve, a JAI Model 3702 UV detector operating at 259 nm or a Hitachi F-1000 spectrofluorimeter operating at 394 nm emission and 259 nm excitation and a Shimadzu Chromatopac C-R6A integrator. Two types of analytical columns were used, a Chemcosorb 5C8 (5 μm; 150 × 4.6 mm I.D.) obtained from Chemco (Osaka, Japan) for the analysis of mouse brain samples and a Wakosil 5C18-200T (5 μm; 150 × 4.6 mm I.D.) obtained from Wako (Osaka, Japan) for all the other experiments. A Hitachi 850 spectrofluorimeter and a Hitachi 304 spectrophotometer were used for the measurements of fluorescence and ultraviolet spectra. Melting points were measured with a Yanaco melting point apparatus and were uncorrected. A Hitachi 05P-21 centrifuge and an NS-310E micro-homogenizer (Nichion Medical Instruments, Japan) were used in the preparation of mouse brain samples. An Erma ERC-3510 degasser was utilized for continuous degassing of the mobile phase.

Reagents and materials

2,3-Naphthalenedicarboxylic anhydride was obtained from Tokyo Kasei

(Tokyo, Japan). HPLC-grade methanol was purchased from Wako and used in the preparation of the mobile phases. All other chemicals were of special grade. Water was purified with a Milli-Q water purification unit (Millipore, Bedford, MA, U.S.A.). Eppendorf Safe-Lock microcentrifuge tubes (2.0 ml) were used as reaction tubes. Male ddy (7–8-week-old) mice were purchased from Shimizu Laboratory Supplies (Kyoto, Japan).

Authentic 2-(2,3-naphthalimino)ethyl ester of myristic acid was prepared by reaction between N-(2-hydroxyethyl)-2,3-naphthalimide and myristoyl chloride according to the literature method[8] and identified by mass spectrometry, IR spectrophotometry and elemental analysis. This ester was used in spectrophotometric studies and in optimization studies of derivatization reaction conditions as an external reference standard.

Synthesis of NE-OTf

NE-OTf was prepared in two steps from commercially available precursors. N-(Hydroxyethyl)-2,3-naphthalimide was synthesized by modifying the literature method[9]. Thus, in a 500-ml flask fitted with a water separator and a reflux condenser were placed 9.9 g (0.05 mol) of 2,3-naphthalenedicarboxylic anhydride, 3.1 g (0.051 mol) of 2-aminoethanol and 300 ml of dry toluene. The mixture was heated for 3 h under vigorous reflux on an oil-bath. After cooling, the solid product was filtered off on a G-3 glass filter and washed with three 50-ml portions of cold water. Recrystallization from ethanol gave transparent needles of the naphthalimide: yield, 85%; m.p., 192–195°C. Analysis: calculated for $C_{14}H_{11}NO_3$, C 69.71, H 4.56, N 5.81; found, C 69.89, H 4.54, N 5.75.

To a solution of trifluoromethanesulphonic anhydride (5 g, 0.018 mol) in dichloromethane (100 ml) was carefully added dropwise a mixture of pyridine (1.4 g, 0.018 mol) and the naphthalimide (3.9 g, 0.016 mol) suspended in warm dichloromethane (100 ml) at a rate such as to keep the temperature of the reaction mixture below −5°C; the addition required about 1 h. After the addition, stirring was continued for 2 h. The resulting solution was washed three times with cold deionized water and then dried over anhydrous magnesium sulphate. After removing dichloromethane under reduced pressure, the crude product was recrystallized twice from a mixture of dichloromethane and tetrachloromethane. NE-OTf was obtained as transparent flakes: yield, 53%; m.p., 138–140°C. Analysis: calculated for $C_{15}H_{10}NSO_5F_3$, C 48.26, H 2.68, N 3.75; found, C 48.06, H 2.68, N 3.74. IR, 1200 and 1400 cm^{-1} (–O–SO_2–); MS, m/z = 374 (MH^+).

Derivatization procedure

A typical derivatization procedure was as follows. To 0.5 ml of a test solution of fatty acids in acetonitrile placed in a reaction tube were added 0.1 ml of 18-crown-6 (10^{-3} *M*) in acetonitrile and *ca.* 5 mg of anhydrous potassium fluoride. After vortex mixing the tube slightly, 0.1 ml of NE-OTf (10^{-3} *M*) in acetonitrile was combined with it. The mixture was vortex mixed for 10 min at room temperature. The resulting solution was allowed to stand for 30 s and an aliquot (10 μl) of the supernatant was injected directly into the chromatograph.

Preparation of mice brain samples

To the cerebrum dissected from a mouse was added margalic acid (0.1 ml) as an internal standard, and this sample was homogenized in methanol (3 ml) and centrifuged for 10 min (5000 *g*). The supernatant was removed and the residual pellet was rehomogenized in methanol. This extraction process was repeated three times. The supernatants were combined and evaporated *in vacuo*, then the residue was dissolved in acetonitrile (0.2 ml), followed by the above-mentioned derivatization procedure.

RESULTS AND DISCUSSION

It is well known that trifluoromethanesulphonate possesses an excellent alkylating ability towards nucleophilic species. However, as far as we know, there only one report has been published on the use of 4′-bromophenacyl trifluoromethanesulphonate as a UV-labelling agent for the determination of carboxylic acids by HPLC. This omission might be due to the difficulties in the synthesis and isolation of trifluoromethanesulphonate-bearing substances suitable for HPLC detection. We found that NE-OTf could be easily synthesized from commercially available materials and is stable at room temperature.

Fluorescence properties of carboxylic acid derivatives

Fig. 1 shows the excitation and fluorescence spectra of the 2-(2,3-naphthalimino)ethyl ester of myristic acid (NE-C_{14} ester) in methanol–water (9:1). The excitation and the emission maxima were at 259 and 394 nm, respectively. The effect of water concentration on the fluorescence intensity was examined. The fluorescence intensity of NE-C_{14} ester in aqueous methanol was almost constant at water concentrations of 0–30% (v/v), but decreased slightly with increasing water concentration over 30%.

Optimization of derivatization reaction conditions

Potassium carbonate is frequently used to convert free carboxylic acids into their

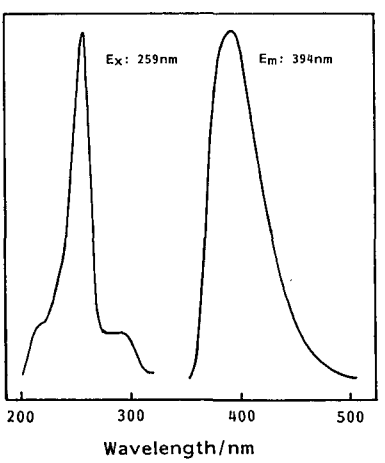

Fig. 1. Fluorescence spectra of 2-(2,3-naphthalimino)ethyl myristate in methanol–water (9:1).

carboxylate anions in derivatization systems using halogenoalkyl-type reagents. Preliminary experiments indicated that the use of potassium carbonate caused many endogenous peaks, some of which overlapped the derivative peaks of interest in sensitive detection. Shimada *et al.*[10] reported that potassium fluoride could be used in place of the carbonate for the conversion of free carboxylic acids into the carboxylate anions. We examined its use in the present derivatization system and found that the appearance of the interfering peaks was suppressed. Potassium fluoride was therefore adopted in this derivatization system.

We investigated some parameters that affect the rate of reaction and the derivatization yield, such as the reaction time and the amounts of the reagent and the catalyst. Myristic acid was chosen, owing to the suitable retention time of its derivative, as a model monocarboxylic acid in the subsequent studies. The effect of the reaction time on the derivatization yield was examined for the acid (10^{-5} *M*) both with and without 18-crown-6 as a catalyst. The reaction was completed within 10 min at room temperature with a 10-fold excess of NE-OTf in the presence of 18-crown-6. On the other hand, without 18-crown-6, it took 40 min to reach a derivatization yield of 96%. Hence a reaction time of 10 min in the presence of 18-crown-6 was adopted in the subsequent experiments.

To optimize the amounts of NE-OTf and 18-crown-6, the reactions were carried out with various equivalent ratios of each to the acid. The reaction proceeded to completion with a 5-fold excess of NE-OTf in the presence of a 10-fold excess of 18-crown-6. The effect of the relative concentrations of NE-OTf to 18-crown-6 on the derivatization yield was also examined, as shown in Fig. 2. A large excess of NE-OTf with respect to 18-crown-6 obviously brought about a decrease in the yield. On the other hand, with a ratio of 1:1, a complete derivatization yield was obtained even when a 300-fold excess of NE-OTf with respect to the acid was used in the derivatization reaction. It is therefore essential for this derivatization system to use equivalent or excess amounts of 18-crown-6 with respect to NE-OTf.

The application of the method to the determination of saturated fatty acids (C_6–C_{16}) was examined. The results indicated good linearity for the determination of

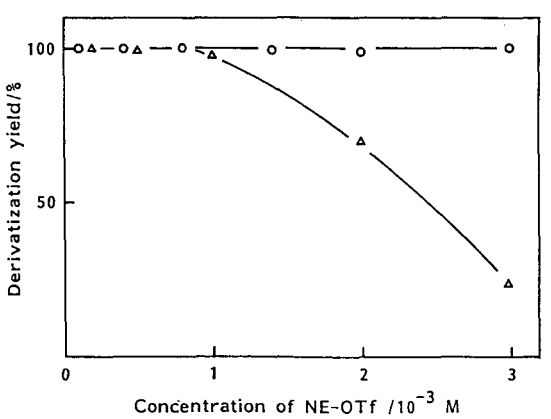

Fig. 2. Effect of concentration of NE-OTf relative to 18-crown-6 on the derivatization of myristic acid (10^{-5} *M*). ○ = 18-Crown-6 concentration = NE-OTf concentration; △ = 18-crown-6 concentration = 10^{-4} *M*.

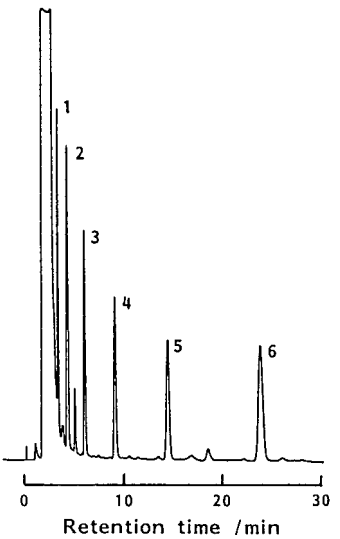

Fig. 3. Typical chromatogram of six fatty acid derivatives. Each peak corresponds to 1.0 pmol of a fatty acid. Column, Wakosil 5C18-200T; mobile phase, methanol–water (9:1); flow-rate, 1.0 ml/min; detection, fluorescence (λ_{ex} = 259 nm, λ_{em} = 394 nm). Peaks: 1 = *n*-caproic acid; 2 = *n*-caprylic acid; 3 = *n*-capric acid; 4 = lauric acid; 5 = myristic acid; 6 = palmitic acid.

each acid at seven different concentrations. The linear regression equation obtained for C_{14} acid, for instance, was $y = 0.868x + 0.471$ with a correlation coefficient $r = 0.9996$ ($2 \cdot 10^{-8}$–$1.2 \cdot 10^{-7}$ *M*), where y and x are the peak area and the concentration of the acid, respectively. A typical chromatogram of the derivatives of the acids is shown in Fig. 3.

Determination of carboxylic acid in mouse brain

As an application of this reagent to the analysis of real samples, five carboxylic acids in mouse brain were simultaneously determined according to the above procedure (Table I). The recovery of these acids in the extraction process was estimated from that of added margalic acid, which does not occur naturally in mouse brain, and

TABLE I

RESULTS OF THE DETERMINATION OF CARBOXYLIC ACIDS IN MOUSE BRAIN

Acid	*Concentration (nmol/g wet weight)*[a]	*R.S.D. (%)*[b]
Docosahexaenoic acid	18.1 ± 0.4	2.0
Arachidonic acid	79.6 ± 1.4	1.7
Palmitic acid	36.2 ± 0.7	1.9
Oleic acid	46.0 ± 1.0	2.1
Stearic acid	75.4 ± 1.6	2.1

[a] Mean ± S.D. (n = 7).
[b] Relative standard deviation (n = 7).

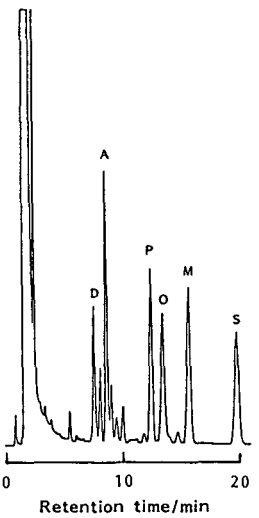

Fig. 4. Chromatogram for the determination of carboxylic acids in mouse brain. Column, Chemcosorb 5C8; mobile phase, methanol–water (87:13); flow-rate, 1.0 ml/min; detection as in Fig. 3; injection volume, 10 μl corresponding to 1/250 portions of the whole sample. Peaks: D = docosahexaenoic acid; A = arachidonic acid; P = palmitic acid; O = oleic acid; M = margaric acid (internal standard); S = stearic acid.

was consistently 95%. These derivatives were well separated from each other within 20 min on the C_8 column with methanol–water (87:13) as the eluent (Fig. 4). The values obtained for the cerebrum (0.33 g wet weight) are summarized in Table I. All the acids could be determined with relative standard deviations of *ca.* 2%.

Stability of the reagent

Solid NE-OTf was stable for at least 6 months in a light-protected desiccator at room temperature. The stability of NE-OTf in acetonitrile (10^{-2} *M*) was examined by periodically chromatographing the solution. Half of the initial peak heights were lost in 3 h at room temperature (32°C), but it was possible to keep the loss to 8% after 6 days by keeping the solution below −20°C.

In conclusion, NE-OTf can be easily synthesized from commercially available starting materials in two steps and is stable at room temperature. The labelling reaction proceeds rapidly to completion simply by mixing the reagents at room temperature, which also makes it possible to label thermolabile carboxylic acids without isomerization and decomposition. The resulting derivatives possess good chromatographic properties, strong UV absorptivity (λ_{max} = 259 nm, ε_{max} = 62 000) and intense fluorescence (λ_{ex} = 259 nm, λ_{em} = 394 nm); the detection limits (signal-to-noise ratio = 3) are 100 fmol with UV detection and 4 fmol with fluorescence detection.

ACKNOWLEDGEMENT

We thank Professor Takayuki Matsushita of Ryukoku University for valuable discussions on the synthesis of NE-OTf.

REFERENCES

1 S. Lam and E. Grushka, *J. Chromatogr.*, 158 (1978) 207.
2 S. Kamada, M. Maeda and A. Tsuji, *J. Chromatogr.*, 272 (1983) 29.
3 M. Ikeda, K. Shimada, T. Sakaguchi and U. Matsumoto, *J. Chromatogr.*, 305 (1984) 261.
4 N. Nimura and T. Kinoshita, *Anal. Lett.*, 13 (1980) 191.
5 M. Yamaguchi, S. Hara, R. Matsunaga, M. Nakamura and Y. Ohkura, *Anal. Sci.*, 1 (1985) 295.
6 S. T. Ingalls, P. E. Minkler, C. L. Hoppel and J. E. Nordlander, *J. Chromatogr.*, 299 (1984) 365.
7 Y. Yasaka, M. Tanaka, T. Matsumoto, J. Katakawa, T. Tetsumi and T. Shono, *Anal. Sci.*, 6 (1990) 49.
8 E. C. Horning (Editor), *Organic Syntheses*, Coll. Vol. 3, Wiley, New York, 1955, p. 390.
9 H. E. Baumgarten (Editor), *Organic Syntheses*, Coll. Vol. 5, Wiley, New York, 1973, p. 973.
10 K. Shimada, C. Sakayori and T. Nambara, in *Proceedings of 36th Annual Meeting of the Japan Society for Analytical Chemistry*, Japan Society for Analytical Chemistry, Tokyo, 1987, p. 484.

Journal of Chromatography, 508 (1990) 141–147
Elsevier Science Publishers B.V., Amsterdam — Printed in The Netherlands

CHROM. 22 277

High-performance liquid chromatographic determination of glycoalkaloids in potato products

KOICHI SAITO*, MASAKAZU HORIE, YOUJI HOSHINO and NORIHIDE NOSE
Saitama Institute of Public Health, 639-1, Kamiokubo, Urawa-shi, Saitama 338 (Japan)
and
HIROYUKI NAKAZAWA
National Institute of Public Health, 4-6-1, Shirokanedai, Minato-ku, Tokyo 108 (Japan)
(First received October 23rd, 1989; revised manuscript received January 15th, 1990)

SUMMARY

A method for the determination of α-solanine and α-chaconine, two major potato glycoalkaloids, in commercial potato products by high-performance liquid chromatography (HPLC) was developed. The glycoalkaloids were extracted with methanol and then purified using Sep-Pak C_{18} or Sep-Pak NH_2 cartridges. A Nucleosil 5-NH_2 column was employed for HPLC with acetonitrile–20 m*M* potassium dihydrogenphosphate (75:25, v/v) as the mobile phase. The calibration graph was linear in the range 1–50 μ g/ml for both α-solanine and α-chaconine. The average recoveries were 82.4–92.6% for α-solanine and 86.5–97.4% for α-chaconine added to various commercial potato products at a level of 5 mg per 100 g. The proposed method is applicable to all commercially available potato products and potato starch.

INTRODUCTION

The two major glycoalkaloids present in potato tubers are the steroidal triglycosides α-solanine and α-chaconine, which possess the same aglycone, solanidine, but differ in their sugar moiety. They account for more than 95% of the total glycoalkaloid content found in the potato tubers[1,2]. They are haemolitically active like saponin, fungitoxic[3] and highly toxic to humans. The toxicity of potato glycoalkaloids (PGAs) generally involves gastrointestinal disturbances and neurological disorders[4,5]. Sprouted cull and green potatoes which contain over 20 mg of total PGAs per 100 g are considerd toxic to humans[6]. A few cases of PGA intoxication have occurred and have been reported[7].

Although increasing numbers of commercial potato products, such as potato chips, fried potatoes and croquettes, are now on the market, very little information for evaluating their quality is available. Therefore, there was a need to develop a simple method for determining their PGA content in order to control the quality and evaluate the safety of commercial potato products.

0021-9673/90/$03.50

A number of methods, such as spectrophotometry[8], titrimetry[9], thin-layer chromatography[10], gas chromatography[11], high-performance liquid chromatography (HPLC)[12–14] and enzyme-linked immunosorbent assay (ELISA)[15], have been used for the determination of individual or total PGAs in potato tissues. HPLC is now becoming the most widely used method because it is rapid, accurate and reproducible and can be used to determine both individual and total PGAs. However, most studies have involved the detection of PGAs in fresh potato tissues and not in commercial products, except for Bushway and Ponnampalam's LC method[12]. Their technique, although of great value, included an ammonium precipitation clean-up step that was complicated and very time consuming.

This paper proposes a more sophisticated HPLC method that is simple and precise for the determination of PGAs in commercial potato products using combined Sep-Pak C_{18} and NH_2 cartridges for the sample preparation procedure.

EXPERIMENTAL

Chemicals and reagents

A glycoalkaloid stock standard solution (1 mg/ml) was prepared by dissolving 10 mg of α-solanine and α-chaconine (Sigma, St. Louis, MO, U.S.A.) in 10 ml of methanol. Working standarad solutions were prepared by dilution with methanol.

The HPLC mobile phase was prepared by mixing acetonitrile and 20 m*M* potassium dihydrogenphosphate (KH_2PO_4) buffer solution (75:25, v/v).

The clean-up columns were Sep-Pak C_{18} and Sep-Pak NH_2 cartridges (Millipore, Milford, MA, U.S.A.). The Sep-Pak C_{18} cartridge was preconditioned by elution with 10 ml of methanol and then 10 ml of water prior to use, and the Sep-Pak NH_2 cartridge was conditioned with 10 ml of methanol and then 10 ml of acetonitrile.

Acetonitrile and methanol were of HPLC grade (Kanto Kagaku, Tokyo, Japan). Water was glass distilled and deionized. All other chemicals were of analytical-reagent grade and used without further purification.

Apparatus

HPLC was carried out using a Shimadzu LC-6A system (Shimadzu, Kyoto, Japan) equipped with a Model SPD-6A spectrophotometer. The analytical column was Nucleosil 5-NH_2 (250 mm × 4.6 mm I.D.) (Machery, Nagel & Co., Düren, F.R.G.). The mobile phase was run isocratically at 30°C at a flow-rate of 0.7 ml/min. The detection wavelength and the sensitivity were set at 208 nm and at 0.04 a.u.f.s., respectively.

Sample preparation

Products with low lipid levels (potato tubers, mashed potato and potato starch). A 5-g sample was homogenized with 30 ml of methanol for 2 min, followed by filtration through a suction filter containing a Toyo Roshi No. 4 filter-paper. The residue was rinsed with *ca.* 10 ml of methanol and the rinsings were combind with the original filtrate. The filtrate was brought to a final volume of 50 ml with methanol. A 5-ml aliquot of the extract (when potato starch was treated, 50 ml of the extract were concentrated to *ca.* 5 ml using a rotary evaporator) was mixed with 8 ml of water. The mixture was applied to the Sep-Pak C_{18} cartridge, which was then washed with 5 ml of

40% methanol, and was subsequently eluted with 15 ml of methanol. The eluate was evaporated to dryness *in vacuo*, and the residue formed was dissolved in 1 ml of methanol. An aliquot (20 μl) of the solution was injected into the HPLC system.

Products with high lipid levels (potato chips, fried potatoes, croquettes and potato salad). A 5-g sample was treated in a manner similar to that already described. The final 1 ml of methanol solution obtained was mixed with 19 ml of acetonitrile. The mixture was applied to the Sep-Pak NH_2 cartridge, which was then washed with 5 ml of acetonitrile, and was subsequently eluted with 10 ml of methanol. The eluate was evaporated to dryness *in vacuo* and the residue was dissolved in 1 ml of methanol. An aliquot (20 μl) of the solution was injected into the HPLC system.

Calibration graph

A 20-μl volume of the PGA standard solution (1–50 μg/ml each of α-solanine and α-chaconine) was injected into the HPLC system. A calibration graph was prepared by measuring the peak heights of α-solanine and α-chaconine.

RESULTS AND DISCUSSION

Chromatographic conditions

As for the separation of PGAs by HPLC, the use of a reversed-phase column was not appropriate, because α-solanine and α-chaconine have the same aglycone, solanidine, in their structures. Although Carman *et al.*[14] separated PGAs by using an ion-pair technique with a C_{18} column, the resolution was poor.

On the other hand, Bushway and co-workers[12,13] employed an NH_2 column with a mixture of tetrahydrofuran, acetonitrile and phosphate buffer as the mobile phase. However, according to the method described by Carman *et al.*[14], because of the lack of inhibitors in HPLC-grade tetrahydrofuran, the formation of decomposition products such as peroxides caused the background absorbance to become so high that the solvent mixture was not usable.

Therefore, a mixture of acetonitrile and phosphate buffer without tetrahydrofuran was employed for the resolution of PGAs with a Nucleosil 5-NH_2 column. The parameters examined, which were varied in order to effect the required separation, were the concentration of the KH_2PO_4 and water in the mobile phase, its pH and the column temperature.

Fig. 1A shows the effect of the water concentration in the mobile phase on the capacity factor (k'). The k' values of both α-solanine and α-chaconine decreased with increase in the concentration of water (22–30%). This phenomenon suggested that the PGAs were chromatographed in the normal-phase mode. A 25% water concentration, approximately the middle of the range examined, was chosen for subsequent work.

The effect of the KH_2PO_4 concentration in the mobile phase on the k' values is shown in Fig. 1B, and revealed a convex shape for α-solanine and α-chaconine over the range 5–50 m*M* KH_2PO_4. Relatively constant k' values were obtained in the range 20–30 m*M*. A symmetrical shape peak and a good baseline separation of the PGAs were also observed in this range.

The k' values of the PGAs showed a dependence on the pH of the mobile phase, as shown in Fig. 1C. A good baseline separation was achieved in the pH range 2–7. As the pH of the acetonitrile–20 m*M* KH_2PO_4 (75:25, v/v) mobile phase was *ca.* 6, no additional pH adjustment was employed.

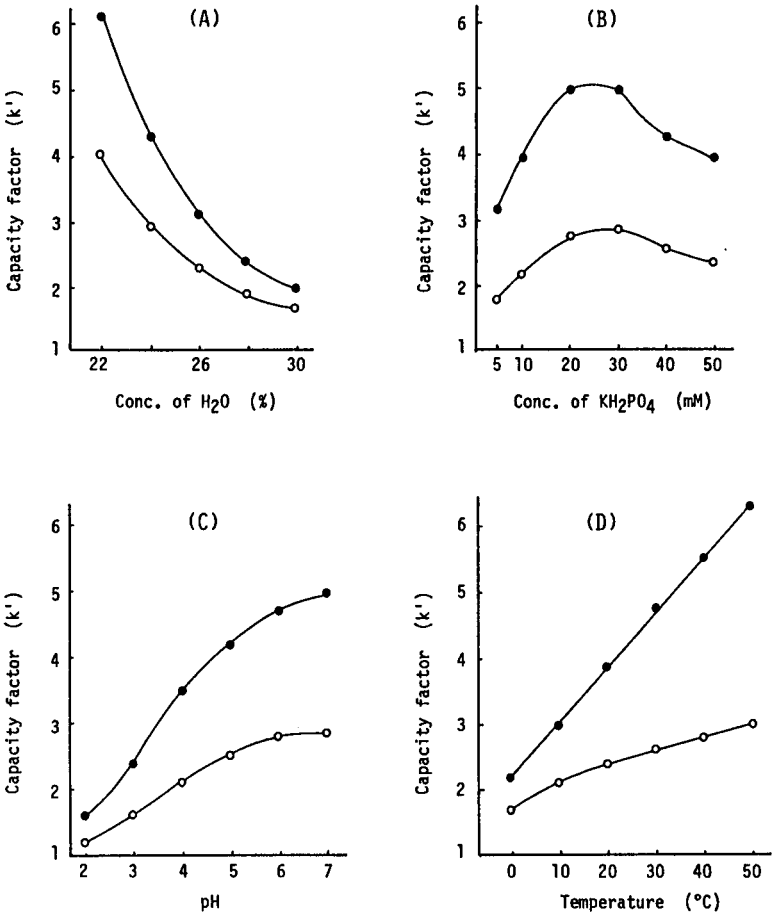

Fig. 1. Effect of (A) water concentration, (B) KH_2PO_4 concentration, (C) pH of the mobile phase and (D) column temperature on capacity factor of (●) α-solanine and (○) α-chaconine.

Preliminary experiments revealed that the column temperature affected the reproducibility of the retention times of the PGAs and the stability of the baseline. Therefore, the effect of the column temperature in the range 0–50°C on the k' values were examined. The dependence on column temperature is illustrated in Fig. 1D. The k' values, especially for α-solanine, increased with increase in temperature. Above 30°C, the elution of α-solanine was markedly slower than that of α-chaconine. Therefore, the column temperature was maintained at 30 ± 0.5°C in subsequent work.

The calibration graphs of peak height *versus* alkaloid concentration were linear in the range 1.0–50.0 μg/ml for both α-solanine and α-chaconine. The detection limit was 20 ng (signal-to-noise ratio = 3) for each alkaloid at a sensitivity of 0.04 a.u.f.s.

Clean-up

Carman *et al.*[14] used a Sep-Pak C_{18} cartridge for the sample preparation procedure. The Sep-Pak C_{18} cartridge was applied to potato tubers[16] and to the

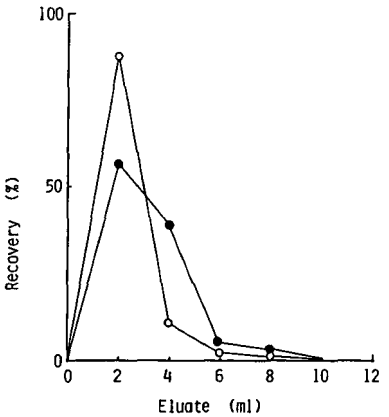

Fig. 2. Elution pattern of (●) α-solanine and (○) α-chaconine from the Sep-Pak NH_2 cartridge. Amounts of 200 μg of α-solanine and α-chaconine were applied to Sep-Pak NH_2 cartridge. Eluent: methanol.

various potato products, such as potato chips and fried potatoes. However, the clean-up of the potato products was insufficient because of their high lipid contents. The HPLC traces showed interferences from impurities, which may lead to a decrease in the ability of the HPLC column to separate the compounds of interest.

Attempts were made to clean up samples using Sep-Pak NH_2 cartridge, which revealed an interaction in the normal-phase mode similar to that with the Nucleosil 5-NH_2 column used for the HPLC analysis. When a methanolic solution of the PGAs was placed on the Sep-Pak NH_2 cartridge, the PGAs were not retained because of the high polarity of the solvent. Addition of acetonitrile to the methanolic solution of the PGAs in order to lower the methanol concentration below 10% resulted in good retention of the PGAs. Fig. 2 shows the elution patterns of α-solanine and α-chaconine

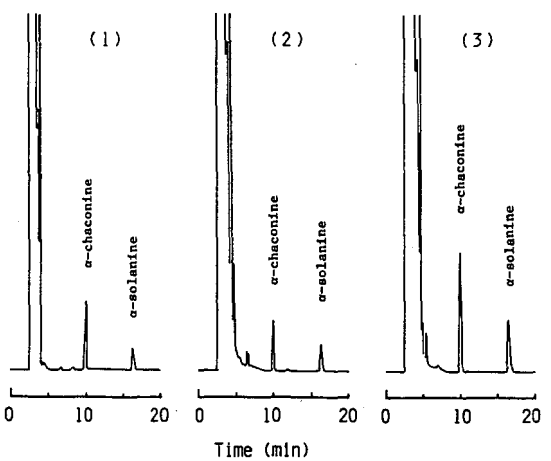

Fig. 3. Typical chromatograms of α-solanine and α-chaconine from various potato products. Volumes of 20 μl were injected into the chromatograph. (1) Potato starch (3.0 μg/ml of α-solanine, 6.0 μg/ml of α-chaconine); (2) mashed potato (4.3 μg/ml of α-solanine, 5.3 μg/ml of α-chaconine); (3) potato chips (7.4 μg/ml of α-solanine, 13.1 μg/ml of α-chaconine).

TABLE I

RECOVERIES OF α-SOLANINE AND α-CHACONINE ADDED TO VARIOUS POTATO PRODUCTS

Sample[a]	*Recovery (%)*[b]	
	α-Solanine	*α-Chaconine*
Potato tuber	90.8 ± 3.5	93.8 ± 3.6
Potato starch	91.9 ± 3.5	97.4 ± 7.7
Mashed potatoes	89.1 ± 3.1	94.2 ± 2.0
Potato chips	92.6 ± 9.1	90.0 ± 8.3
Fried potatoes	82.7 ± 3.2	86.5 ± 5.2
Croquettes	89.2 ± 3.0	95.0 ± 2.2
Potato salad	82.4 ± 1.8	90.0 ± 2.1

[a] α-Solanine and α-chaconine were added to each sample at the level of 5 mg per 100 g.
[b] Mean ± S.D. (n = 5).

from the Sep-Pak NH_2 cartridge with methanol as the eluent. All of the α-solanine and α-chaconine were found in the first 10 ml of the eluate. Typical chromatograms are shown in Fig. 3 for potato starch, mashed potatoes and potato chips after removal of impurities.

TABLE II

CONTENTS OF α-SOLANINE AND α-CHACONINE IN VARIOUS POTATO PRODUCTS

Sample	*Content (mg per 100 g)*		
	α-Solanine	*α-Chaconine*	*Total PGAs*[a]
Potato starch A	0.12	0.23	0.35
Potato starch B	0.06	0.12	0.18
Potato starch C	0.03	0.08	0.11
Sweet potato starch	ND[b]	ND	ND
Wheat starch	ND	ND	ND
Corn starch	ND	ND	ND
Arrowroot starch	ND	ND	ND
Potato chips D	1.5	2.6	4.1
Potato chips E	0.6	1.1	1.7
Potato chips F	1.6	3.8	5.4
Potato chips G	1.3	2.4	3.7
Potato chips H	0.5	0.6	1.1
Potato chips I	0.5	0.9	1.4
Fried potatoes	1.7	1.6	3.3
Frozen fried potatoes	1.5	1.6	3.1
Croquettes	0.9	1.5	2.4
Frozen croquettes	2.7	4.0	6.7
Mashed potatoes	0.9	1.1	2.0
Potato tuber J	1.9	2.1	4.0
Potato tuber K	0.9	1.3	2.2
Potato tuber L	0.7	1.0	1.7

[a] Total PGAs = α-solanine + α-chaconine.
[b] ND = not detected.

Recovery study and analysis of commercial samples

Various commercial potato products fortified at a level of 5 mg per 100 g each of α-solanine and α-chaconine were used for the recovery study. Table I demonstrates that the mean recoveries were 82.4–92.6% for α-solanine and 86.5–97.4% for α-chaconine. The detection limits of both PGAs by the proposed method were 0.02 mg per 100 g for potato starch and 0.2 mg per 100 g for other potato products.

Table II shows that the total PGAs found in all commercial potato products and three brands of potato starch varied from 0.11 to 6.7 mg per 100 g, all below the critical level of 20 mg per 100 g which is used as the upper limit when screening new potato varieties for human consumption. On the other hand, PGAs were found not to be present in other kinds of starches such as wheat, sweet potato, corn and arrowroot. The reason why PGAs were found only in the potato starch is thought to be due to their imperfect purification during production of the starch from potato tubers. Therefore, it is considered that the PGAs were contaminants in almost all potato starches commercially available as foodstuffs.

CONCLUSIONS

The clean-up using Sep-Pak C_{18} and NH_2 cartridges gave excellent recovery, sensitivity and reproducibility. The chromatograms were significantly cleaner than those obtained by other HPLC methods. The determination of α-solanine and α-chaconine can be evaluated in terms of quality control and safety assessment of various potato products. Further, the proposed method can be applied as a confirmation method for a particular potato starch among the various kinds of starches by monitoring the PGAs.

REFERENCES

1 A. R. Guseva and V. A. Paseshnickenko, *Biochemistry*, 22 (1957) 792.
2 S. L. Sinden and R. E. Webb, *U.S. Dep. Agric. Tech. Bull.*, (1974) 1492.
3 E. A. Allen and J. Kuc, *Phytopathology*, 58 (1968) 776.
4 R. R. Dalvi and W. C. Bowie, *Vet. Human Toxicol.*, 23 (1983) 13.
5 S. G. Willimott, *Analyst (London)*, 58 (1933) 431.
6 N. Sapeika, *Food Pharmacology*, Thomas, Springfield, IL, 1969, pp. 67–68.
7 H. Iwasaki, *J. Food Hyg. Soc. Jpn.*, 25 (1984) 466.
8 W. W. A. Bergers, *Potato Res.*, 23 (1980) 105.
9 R. J. Bushway, A. M. Wilson and A. A. Bushway, *Am. Potato J.*, 57 (1980) 561.
10 R. Jellema, E. T. Elema and T. M. Malingre, *J. Chromatogr.*, 210 (1981) 121.
11 S. F. Herb, T. J. Fitzpatrick and S. F. Osman, *J. Agric. Food Chem.*, 23 (1975) 520.
12 R. J. Bushway and R. Ponnampalam, *J. Agric. Food Chem.*, 29 (1981) 814.
13 R. J. Bushway, J. L. Bureau and J. King, *J. Agric. Food Chem.*, 34 (1986) 277.
14 A. S. Carman, Jr., S. S. Kuan, G. M. Ware, O. J. Francis, Jr. and G. P. Kirschenheuter, *J. Agric. Food Chem.*, 34 (1986) 279.
15 M. R. A. Morgan, D. T. Coxon, S. Bramham, H. W.-S. Chan, W. M. J. van Gelder and M. J. Allison, *J. Sci. Food Agric.*, 36 (1985) 282.
16 K. Saito, M. Horie, N. Nose and H. Iwasaki, *Annu. Rep. Saitama Inst. Publ. Health*, 19 (1985) 45.

Journal of Chromatography, 508 (1990) 149–158
Elsevier Science Publishers B.V., Amsterdam — Printed in The Netherlands

CHROM. 22 274

Examination of organic trace contamination and thermo-oxidative deterioration of ε-caprolactam by high-performance liquid chromatography

GÜNTER EPPERT*, GERT LIEBSCHER and CLAUS STIEF
VEB Leuna-Werke, 4220 Leuna (G.D.R.)
(First received September 1st, 1989; revised manuscript received December 28th, 1989)

SUMMARY

Technical ε-caprolactam, used in the manufacture of polyamides, can be examined using high-performance liquid chromatography on silica gel with acetonitrile as the mobile phase and UV detection at 200 nm in order to determine organic impurities that affect the quality of the final product. A linear correlation was found between the adipimide content of the caprolactam samples, which acts as a measure of their deterioration by oxidation, and the quality index "volatile basis" and also between the aniline content and the so-called "permanganate extinction number". On the basis of the proposed method, a thermo-oxidation value can be defined.

INTRODUCTION

ε-Caprolactam is an important starting material in the production of polyamides (Dederon, Perlon L, nylon 6, etc.). However, certain organic impurities in monomeric ε-caprolactam reduce the quality of the final products[1,2]. Partial thermo-oxidative reaction of ε-caprolactam during processing, storage and transport can also occur forming oxidation products that have an adverse effect on the quality of the polymerizate and the polyamide fibres (*e.g.*, chain breakage, discoloration, embrittlement).

Chemical characteristics are commonly determined, *e.g.*, "permanganate extinction number", "UV extinction" and "volatile bases"[3].

For the determination of the permanganate extinction number (PEZ), according to ref. 3, 20 g of caprolactam are dissolved in 25 ml of 0.5 *M* sulphuric acid and treated with 1.00 ml of 0.02 *M* potassium permanganate solution at 25.0 ± 0.5°C. The extinction *E* at 545 nm is determined after 600 s, and the permanganate extinction number is calculated as PEZ = $Ef \cdot 100$, where *f* is the factor of the photometer correction[3]. To determine the so-called volatile bases according to ref. 3, 20 g caprolactam are dissolved in 100 ml of distilled water and 100 ml of 1 *M* sodium hydroxide solution are added. By means of a special distillation assembly[3], 10 ml of the solution are distilled into a calibrated vessel containing 10 ml of 0.01 *M* hydrochloric

0021-9673/90/$03.50

acid, 100 ml of distilled water and 5 droplets of methyl red–methylene blue indicator mixture. The excess of the acid is titrated with 0.01 *M* sodium hydroxide and corrected by a blank. The base number can be calculated as mequiv./kg. However, in view of the above, the determination of individual impurities in ε-caprolactam is clearly of major importance.

Chromatographic methods are particularly useful in identifying and determining organic impurities in ε-caprolactam, and especially gas chromatography has often been applied[4–15]. However, high-performance liquid chromatography (HPLC) is in principle more promising for less volatile substances[16]. So far HPLC has only been used to separate and identify cyclic oligomers of ε-caprolactam[17,18], and there has also been a report on the determination of ε-caprolactam and its metabolites using HPLC[19].

The aim of this paper is to show the possibilities of using HPLC for determining organic trace impurities in technical ε-caprolactam. We mainly examined the determination of aniline (the origin of which is discussed in ref. 20), cyclohexanone oxime and adipimide. The last compound should also allow the determination of the oxidative deterioration of ε-caprolactam.

EXPERIMENTAL

Equipment

A Hewlett-Packard HP 1090 M liquid chromatography system with a diode-array detector and an 7999 A HPLC workstation, consisting of an HP 310 computer, HP 9153 A Winchester disc drive, HP 2225 A ink-jet printer and HP 7440 plotter, was used.

Solvents

Water was distilled and filtered over a G-4 frit prior to chromatography. Acetonitrile, extra pure for UV spectroscopy (PCK, Schwedt, G.D.R.) with a water content of 0.35% (w/w) was used.

Test substances, calibration solution and test mixture

The purity of the test substances used was determined by liquid chromatography.

A stock solution of 7 mg of aniline, 42 mg of cyclohexanone oxime, 13 mg of adipimide and 50 mg of octahydrophenazine in 100 ml of acetonitrile was used for the determination of individual components. The stock solution was diluted 1:100 to give a working standard solution.

The chromatographic separation system was optimized using a test mixture of 40 mg of aniline, 65 mg of cyclohexanone oxime, 34 mg of adipimide, 70 mg of octahydrophenazine, 65 mg of *n*-valeramide, 25 mg of ε-methylcaprolactam, 250 mg of N-methylcaprolactam, 300 mg of acetamide and 120 mg of ε-caprolactam in 100 ml of acetonitrile.

Samples

Original samples from various caprolactam manufacturers and also oxygen-impaired products prepared by aeration of pure molten caprolactam at 100°C were used as solutions of 10 g of sample in 25 ml of acetonitrile.

Chromatographic conditions

The separation columns were each 200 mm × 2 mm I.D., containing ES-Gel 10 spherical silica (4 μm) from Leuna-Werke (Leuna, G.D.R.). The column filling was prepared by the balanced-density technique with dioxane and 1,2-dibromoethane. The mobile phase[a] was acetonitrile–water (99:1, v/v) at a flow-rate of 0.42 ml/min. The column temperature was 40°C, detection wavelength 200 nm (band width 4 nm), reference wavelength 550 nm (band width 100 nm) and injection volume 2 μl (*ca.* 800 μg of sample substance).

RESULTS AND DISCUSSION

Determination of a suitable separation system

At the start of the experiments reversed-phase (RP) systems were tested for their suitability for the determination of impurities in caprolactam, based on RP-8 and RP-18 materials with aqueous–organic mobile phases. The retention properties of the test substances demonstrated the general suitability of such systems. In this manner, for example, the adipimide from the thermo-oxidation of ε-caprolactam is eluted before the main component ε-caprolactam and can be determined using an RP-8 column (200 × 4.6 mm I.D.) and methanol–water (65:15 v/v) as the mobile phase with a detection wavelength of 205 nm. However, the disadvantage of this system is that some quality-affecting impurities, *e.g.*, aniline and cyclohexanone oxime, are eluted after the main component, which results in non-optimum conditions for the determination of trace amounts.

The separation problem was solved by using silica gel and acetonitrile, with which all the test substances examined eluted before the caprolactam peak. The addition of *ca.* 1% of water to the acetonitrile was found to improve the chromatographic resolution and analysis time (Fig. 1). A further decrease in the water content (*e.g.*, down to 0.1%) prolonged the analysis time. Occasionally, this can be advantageous because changes in selectivity also occur. The retention values show good reproducibility (relative standard deviation, R.S.D. = 0.5%).

The excellent separation selectivity of the chosen system is shown by the chromatogram of a test mixture of possible caprolactam impurities in Fig. 2. Table I gives the overall retention times (t_R) of several test substances. Some compounds cannot be separated from each other. Aniline and cyclohexanone, for example, are eluted together. Because of the considerably smaller molar absorptivity of cyclohexanone ($\varepsilon_{200} \approx 40$ l mol^{-1} cm^{-1}) compared with that of aniline ($\varepsilon_{200} \approx 31\,000$ l mol^{-1} cm^{-1}), the determination of aniline is only affected at a large excess of cyclohexanone, which is not to be expected in pure caprolactam.

Examination of caprolactam samples

Fig. 3 shows the chromatogram of ε-caprolactam with a serious deterioration of quality and a permanganate extinction number of zero. The size of the aniline peak should be noted. Cyclohexanone oxime and adipimide were identified as further

[a] Contrary to the internationally accepted nomenclature, which is followed in the *Journal of Chromatography*, the authors prefer the terms "compact phase" and "fluid phase", which correspond to the accepted terms "stationary phase" and "mobile phase", respectively. They feel that the former are generally applicable because the "stationary phase" is not always stationary but is moving during some well-known chromatographic processes, whereas the "mobile phase" does not have to be moved to realize the chromatographic phenomenon[30]. For further information, see ref. 31.

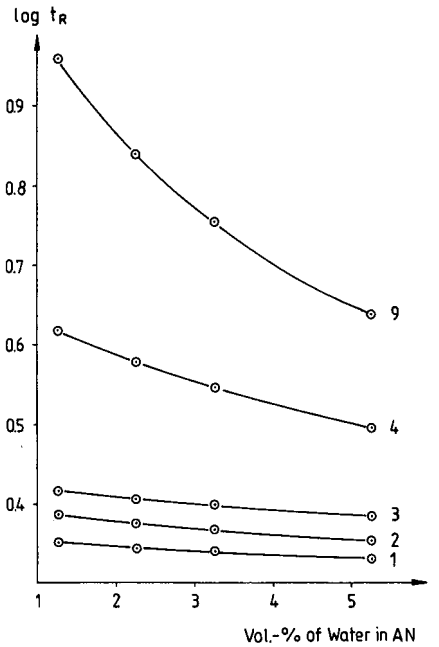

Fig. 1. Influence of the water content of acetonitrile on the overall retention time, t_R, of selected compounds. Conditions: stationary phase, Es-Gel 10; mobile phase, acetonitrile (AN) with a water content of 1.27, 2.27, 3.27 and 5.26% (v/v); one separation column; flow-rate, 0.25 ml/min; UV detection at 200 nm. 1 = Aniline; 2 = cyclohexanone oxime; 3 = adipimide; 4 = octahydrophenazine; 9 = ε-caprolactam.

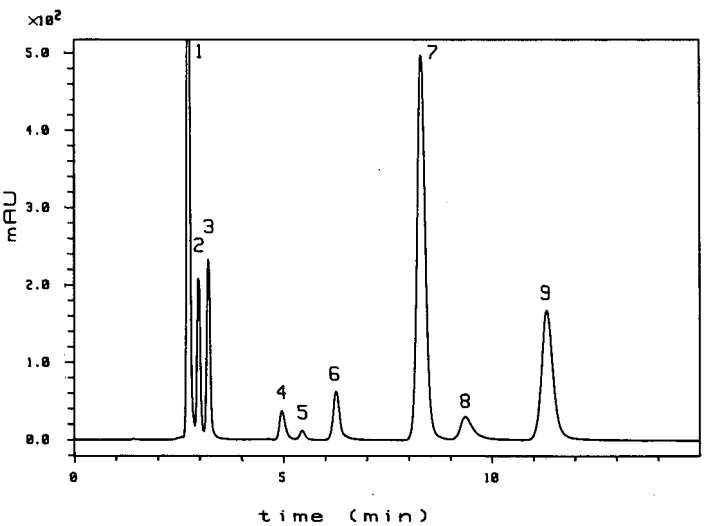

Fig. 2. Chromatogram of a test mixture of caprolactam impurities. Conditions: stationary phase, ES-Gel 10; mobile phase: acetonitrile–water (99:1, v/v); two separation columns in series; flow-rate, 0.42 ml/min; volume of test mixture, 0.5 μl; other conditions as under Experimental. Peaks: 1 = aniline (0.2 μg); 2 = cyclohexanone oxime (0.33 μg); 3 = adipimide (0.17 μg); 4 = octahydrophenazine (0.35 μg); 5 = *n*-valeramide (0.33 μg); 6 = ε-methyl-ε-caprolactam (0.13 μg); 7 = N-methyl-ε-caprolactam (1.25 μg); 8 = acetamide (1.5 μg); 9 = ε-caprolactam (0.6 μg).

TABLE I

RETENTION OF MODEL SUBSTANCES

Compound	t_R *(min)*[a]	*Compound*	t_R *(min)*[a]
Nitrobenzene	2.51	*n*-Capronamide	5.12
Dicyclohexanone	2.52	*n*-Valeramide	(5) 5.46
Tetrahydrobenzofurazan	2.55	N-*n*-Pentylacetamide	5.47
Dicyclohexanone oxime	2.59	N-Isobutylacetamide	5.69
Aniline	(1) 2.73	ε-Methyl-ε-caprolactam	(6) 6.38
Cyclohexanone	2.78	N-Methyl-ε-caprolactam	(7) 8.30
Cyclohexanone oxime	(2) 2.98	Acetamide	(8) 9.37
Adipimide	(3) 3.21	ε-Caprolactam	(9) 11.73
Octahydrophenazine	(4) 4.96		

[a] t_R = Overall retention time. The numbers in parentheses refer to the peaks on the chromatograms.

impurities. A deviation from the baseline at a retention time of 3.8 min, visible in some chromatograms, occurs when there are minor differences in the water content between the mobile phase and the sample solution.

Fig. 4 shows the chromatogram of pure caprolactam with a permanganate extinction number of 91. Only trace amounts of aniline and adipimide can be found. Adipimide had previously been found in all caprolactam samples examined.

Various spectra recorded with the diode-array detector are shown in Figs. 5a–c. Fig. 5a shows the reference spectrum of aniline, and Fig. 5d its spectrum recorded on the sample peak in the chromatogram in Fig. 3.

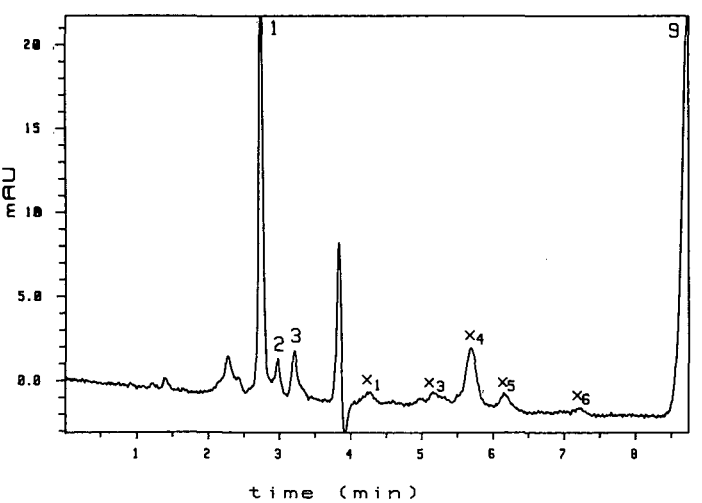

Fig. 3. Chromatogram of quality-reduced ε-caprolactam. Conditions: stationary phase, ES-Gel 10; mobile phase, acetonitrile–water (99:1, v/v); two separation columns in series: flow-rate, 0.42 ml/min; sample volume, 2 μl of solution from 10 g of sample in 25 ml of acetonitrile; other conditions as under Experimental. Peaks: 1 = aniline; 2 = cyclohexanone oxime; 3 = adipimide; 9 = ε-caprolactam; x_1–x_4, x_6 = unknowns; x_5 corresponds to C-methylcaprolactam.

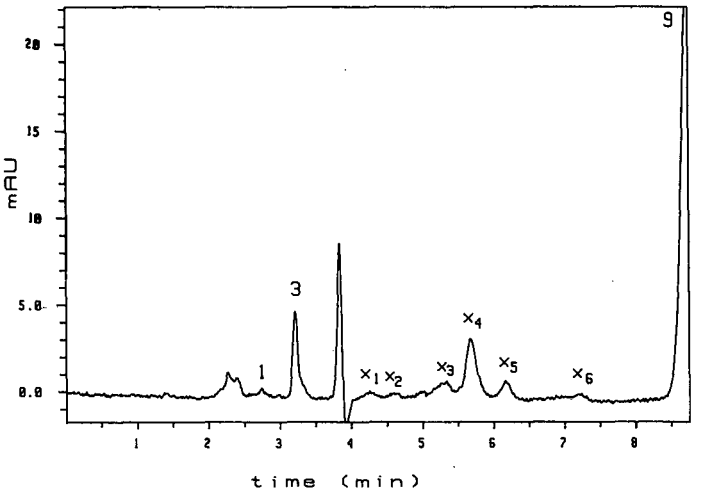

Fig. 4. Chromatogram of pure caprolactam. Conditions: stationary phase, ES-Gel 10; mobile phase, acetonitrile–water (99:1, v/v); two separation columns in series; flow-rate, 0.42 ml/min; sample volume, 2 μl of solution from 10 g of sample in 25 ml of acetonitrile; other conditions as under Experimental. Peaks: 1 = aniline; 3 = adipimide; 9 = ε-caprolactam; x_1–x_4, x_6 = unknowns; x_5 corresponds to C-methyl-caprolactam.

Quantitative analysis

The external standard method was used to evaluate the chromatograms. In Table II, the slope m of the linear calibration function and the limit of determination c_m, measured as three times the noise level, are listed for some caprolactam impurities. The calibration slope represents the response factor, dependent on the substance used. If m is set to equal 1 for octahydrophenazine, the peak areas for equal amounts of

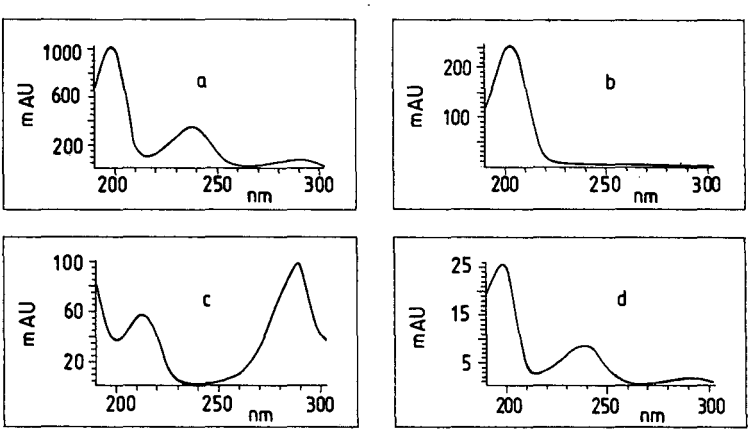

Fig. 5. UV spectra using the diode-array detector for peak identification. Conditions as under Experimental. (a) Peak 1 from Fig. 2 (aniline); (b) peak 3 from Fig. 2 (adipimide); (c) peak 4 from Fig. 2 (octahydrophenazine); (d) peak 1 from Fig. 3.

TABLE II

CONSTANTS OF THE CALIBRATION FUNCTION $y = mx$ OF INDIVIDUAL IMPURITIES AND THE MINIMUM AMOUNTS DETERMINED AFTER REGRESSION ANALYSIS[21]

Substance	*m (area/amount)*	*Limit of determination, c_m (ppm)*	*Correlation coefficient, r*
Aniline	21.4	0.1	0.998
Cyclohexanone oxime	3.4	0.5	0.999
Adipimide	6.6	0.5	0.999
Octahydrophenazine	2.0	1.0	0.999

octahydrophenazine, cyclohexanone oxime, adipimide and aniline are in the ratio 1:1.6:3.5:10.9. Some results for the determination of caprolactam impurities are given in Table III. As can be seen from Fig. 6, the content of aniline correlates with the permanganate extinction number according to ref. 3.

TABLE III

QUANTITATIVE EXAMINATION OF CAPROLACTAM SAMPLES FROM DIFFERENT MANUFACTURERS (I–IV)

Sample	*Aniline (ppm)*	*Cyclohexanone oxime (ppm)*	*Adipimide (ppm)*
Pure caprolactam I	0.1	<0.5	5.5
Pure caprolactam II	0.2	<0.5	3.4
Pure caprolactam III	<0.1	<0.5	3.2
Pure caprolactam IV	0.8	0.6	6.3
Depolymerization caprolactam	1.1	<0.5	71.7

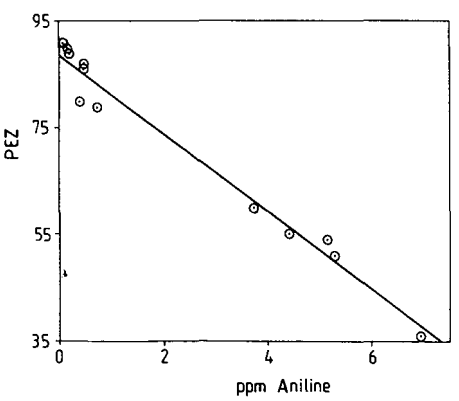

Fig. 6. Correlation between aniline content and permanganate extinction number (PEZ)[3] for caprolactam samples of different quality. Condition as under Experimental. Correlation coeffcient $r = -0.9891$; probability $P = 95.0\%$.

Thermo-oxidative deterioration

ε-Caprolactam is easily oxidized at high temperatures owing to its amide bond. As commercially it is stored, transported and further processed in a molten form, considerable attention must be paid to this point. Previous experiments showed that on exposure to oxygen, caprolactam (I) is converted primarily to the N-vicinal caprolactam hydroperoxide (II) and then to adipimide (III) (eqn. 1)[22–28]. Apart from adipimide, numerous other oxidation products, *e.g.*, valeramide, formyl-ε-caprolactam and cyclohexenecarboxylic lactam (1-[*H*]-7-oxo-4,5-dihydroazepine) can also be formed[27].

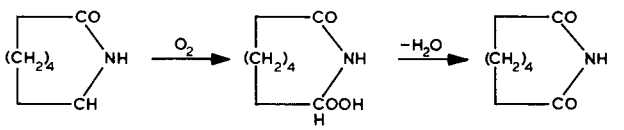

I II III

Gas chromatography has been applied to the characterization of thermo-oxidatively impaired ε-caprolactam. Under the preferred, alkaline conditions however, adipimide was not eluted and the degree of oxidation was concluded from the existence of an "oxidation peak"[6]. The fluorescence of the compounds with a ketoimide structure formed by thermo-oxidation of monomeric and polymeric ε-caprolactam has als been proposed as a measure of oxidative deterioration[29]. No significant differences could be detected in the samples of pure caprolactam using the latter method. The adipimide formed as the main product of thermo-oxidation of ε-caprolactam shows no fluorescence and so is not detected in this instance.

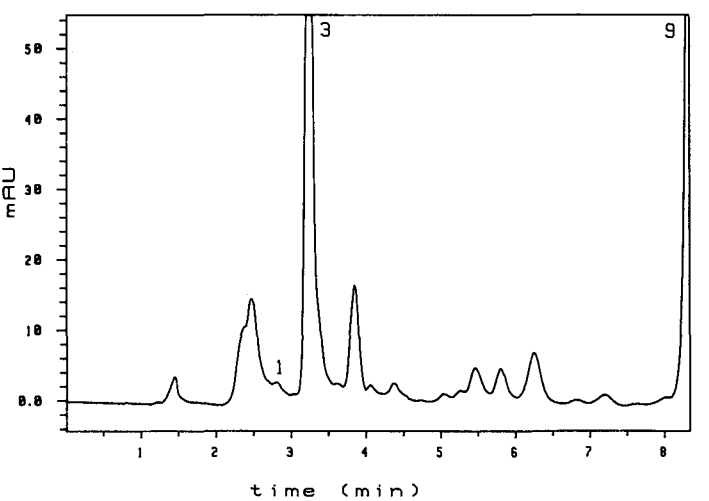

Fig. 7. Chromatogram of caprolactam from depolymerization. Conditions: stationary phase, ES-Gel 10; mobile phase, acetonitrile–water (99:1, v/v); one separation column; flow-rate, 0.21 ml/min; sample volume, 2 μl of solution of 10 g of sample in 25 ml of acetonitrile; other conditions as under Experimental. Peaks: 1 = aniline; 3 = adipimide; 9 = ε-caprolactam; other peaks unknowns. •

Using the HPLC method with silica and acetonitrile, a rapid, simple and sensitive means is available for measuring the oxidative deterioration of caprolactam. The slightest contamination can be accurately evaluated (compare Table II and Fig 4).

Fig 7 shows the chromatogram of a depolymerization caprolactam. The high adipimide content indicates a very strong oxidative action. The significant increase in the content of adipimide and of volatile bases on aeration of pure caprolactam can be seen in Table IV.

TABLE IV

RELATIONSHIP BETWEEN TIME OF AERATION, BASE NUMBER AND AMOUNT OF ADIPIMIDE DURING THERMO-OXIDATIVE DETERIORATION OF ε-CAPROLACTAM

Pure caprolactam was aerated at 100°C with 6.7 l/h of air.

Sample	*Aeration time (h)*	*Base number*[3] *(mmol/kg)*	*Adipimide (ppm)*
Pure caprolactam	0	0.17	8.5
Aerated samples	3	5.2	131.9
	3.5	8.6	214.1
	4	8.2	180.1
	4	8.6	224.6
	5	10.3	266.3

As further reaction products from the thermo-oxidation of ε-caprolactam, in addition to the key component adipimide, can be included in the determination of the volatile bases, *e.g.*, amines and ammonia of other origins, it was of interest to examine the connection between the adipimide content and the base number according to ref. 3. Fig. 8 shows that there is a linear correlation. The correlation was confirmed with samples of pure caprolactam of different origins. This demonstrates that the base number generally results from thermo-oxidative deterioration.

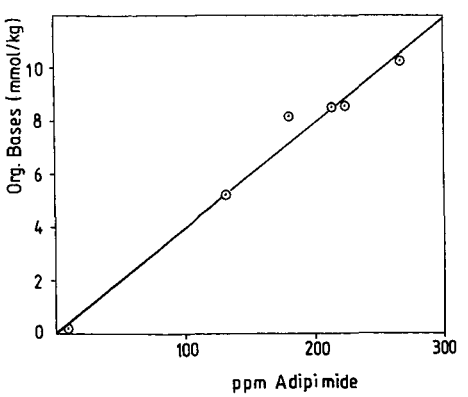

Fig. 8. Correlation between adipimide content and base number for samples of thermo-oxidative deteriorated ε-caprolactam. Conditions as in Table IV. Correlation coefficient $r = 0.9903$; probability $P = 95.0\%$.

The adipimide content determined by liquid chromatography can be defined as the thermo-oxidation value (TOV). The TOV lies in the range 1–100, corresponding to ppm or mg levels adipimide per kg of caprolactam.

CONCLUSIONS

This work has shown that HPLC on silica gel is well suited for the examination of caprolactam samples for technically relevant impurities. The conditions were found to be both simple and easily reproduced, and the previous history of the products can be derived from the chromatograms.

REFERENCES

1 J. Střešinka and J. Mokrý, *Chem. Prum.*, 24 (1974) 299.
2 J. Králiček, J. Kondelíková, V. Kubánek, Z. Zámostný and Le Thuan Anh, *Chem. Prum.*, 24 (1974) 620.
3 *Caprolactam*, G. D. R. Standard, TGL 7430, Verlag für Standardisierung, Leipzig, 1989.
4 C. Pavel, *Chem. Prum.*, 17 (1967) 73.
5 G. C. Ongemach and A. C. Moody, *Anal. Chem.*, 39 (1967) 1005.
6 L. P. Friz, G. L. Bertuzzi and E. Bovetti, *J. Chromatogr.*, 39 (1969) 253.
7 S. Mori, M. Furusawa and T. Takeuchi, *Anal. Chem.*, 42 (1970) 661.
8 E. I. Grushova, *Zh. Prikl. Khim.*, 51 (1978) 689.
9 L. Yankov, K. Lekova, G. Simeonov and L. Kardieva, *Khim. Ind. (Sofia)*, 50 (1978) 58.
10 L. Yankov, G. Simeonov, P. Rusev, K. Lekova and L. Kardieva, *Khim. Ind. (Sofia)*, 51 (1979) 359.
11 W. Czerwiński, M. Wiejcka, H. Malikowska and S. Dyjas, *J. Chromatogr.*, 208 (1981) 27.
12 L. G. Jodra, A. Romero, F. Garcia-Ochoa and J. Aracil, *J. Appl. Polym. Sci.*, 26 (1981) 3271.
13 L. G. Jodra, A. Romero, F. Garcia-Ochoa and J. Aracil, *Ind. Eng. Chem., Prod. Res Dev.*, 20 (1981) 562.
14 W. Czerwiński, M. Wiejcka and S. Dyjas, *Chem. Anal. (Warsaw)*, 28 (1983) 337.
15 R. N. Nikolov, D. I. Pishev and A. D. Stefanova, *J. Chromatogr.*, 365 (1986) 435.
16 G. Eppert, *Einführung in die Schnelle Flüssigchromatographie (Hochdruckflüssigchromatographie)*, Akademie-Verlag, Berlin, and Vieweg, Braunschweig/Wiesbaden, 2nd ed., 1988.
17 J. Brodilová, J. Rotschová and J. Pospíšil, *J. Chromatogr.*, 168 (1979) 530.
18 V. Krajník, P. Božek, J. Kondeliková and J. Králiček, *J. Chromatogr.*, 240 (1982) 539.
19 P. D. Unger and M. A. Friedman, *J. Chromatogr.*, 187 (1980) 429.
20 A. Schäffler and W. Ziegenbein, *Chem. Ber.*, 88 (1955) 767.
21 K. Doerffel, *Statistik in der Analytischen Chemie*, VEB Deutscher Verlag für Grundstoffindustrie, Leipzig, 1966. p. 191.
22 A. Rieche and M. Schulz, *Angew. Chem.*, 70 (1958) 694.
23 A. Rieche and W. Schön, *Z. Chem.*, 3 (1963) 443.
24 A. Rieche, *Chem. Ber.*, 99 (1966) 3238.
25 A. Rieche and W. Schön, *Kunststoffe*, 57 (1967) 49.
26 W. Schön and A. Rieche, *Chem. Ber.*, 100 (1967) 4052.
27 A. R. Doumaux and D. J. Trecker, *J. Org. Chem.*, 35 (1970) 2121.
28 G. J. Dege and H. K. Reimschüssel, *J. Polym. Sci., Polym. Chem. Ed.*, 11 (1973) 873.
29 E. I. Smirnova, G. N. Vetschkanov, L. N. Aleksejeva and E. B. Kremer, *Khim. Volokna*, No. 5 (1985) 30.
30 A. Lowman, *Science (Washington, D.C.)*, 96 (1942) 211.
31 G. Eppert, *Chem. Technol.*, 37 (1985) 294.

Journal of Chromatography, 508 (1990) 159–178
Elsevier Science Publishers B.V., Amsterdam — Printed in The Netherlands

CHROM. 22 302

Gas chromatographic analysis and gas chromatographic–mass spectrometric identification of components in the cyclohexane-extractable fraction from contaminated sediment samples

MIKAEL REMBERGER, PER-ÅKE HYNNING and ALASDAIR H. NEILSON*
Swedish Environmental Research Institute, Box 21060, S-100 31 Stockholm (Sweden)
(Received September 20th, 1989)

SUMMARY

A comprehensive investigation was carried out on the cyclohexane-soluble extracts from three sediment samples. Elemental analysis of the residue after careful removal of solvent showed that nitrogen was absent, sulphur accounted for 10–20% of the residue and the carbon/chlorine ratio was high. Gas chromatography and gas chromatography–mass spectrometry confirmed that a substantial fraction of the extracts consisted of non-chlorinated long-chain alkenoic and alkanoic acids, terpenes and plant steroids and that the free organochlorine compounds were dominated by chlorinated long-chain alkanoic acids and chlorinated resin acids, whereas chloroform, chemically bound phenolic compounds, and polychlorinated biphenyls made only a small contribution. The chemical structures of constituents of the extractable organic chlorine fraction and of the corresponding methanolic alkali extracts from whole sediments were completely different; the former did not have a major contribution from products originating in chlorinated guaiacyl-C_3 residues. Only *ca.* 8% of the organically bound chlorine could be accounted for in terms of known compounds which originated in bleachery effluents. Three hypotheses may be put forward for the nature of the unidentified components: they may not be constituents of bleachery effluents, they may not hitherto have been characterized in such effluents or they may be transformation products formed in the sediment phase. It was not possible in the light of current evidence to access which of these was correct. It was concluded that procedures used for characterization which rely heavily on gas chromatographic separation must be substantially improved to enable an acceptable level of indentification to be attained.

INTRODUCTION

A wide range of structurally diverse chlorinated compounds[1–5] is formed during the production of bleached pulp by conventional processes. Ultimately, a substantial

0021-9673/90/$03.50

fraction of this organically bound chlorine reaches the aquatic environment even after treatment. Considerable effort has therefore been directed to evaluating the impact of such discharge on the biota[6]. In addition, environmental monitoring for exposure to bleachery effluents has utilized sum parameters such as extractable organic chlorine (EOCl)[7,8] and analysis for specific compounds has been used in both field[9] and laboratory studies[10].

It is generally recognized that the persistence, the toxicity or the potential for bioconcentration of a compound may present a potential environmental hazard[11]. The bioconcentration potential is generally assessed from the octanol–water partition coefficient or some suitable surrogate, so that compounds extractable with cyclohexane and therefore components of the EOCl fraction are clearly lipophilic and putatively have a high bioconcentration potential. Substantial interest has therefore centred on the nature of the compounds contained in this cyclohexane-extractable fraction[12,13].

It has been shown, however, that at least as far as the sediment phase is concerned, the total amount of cyclohexane-EOCl significantly exceeds the sum of the concentrations of chloroguaiacols, chlorocatechols and chlorovanillins which can be extracted from sediments, even using relatively aggressive procedures[14]. On the basis of the results of a comparison of various extraction methods, we have postulated that a hitherto undetermined fraction of these compounds is bound to organic components of the sediment phase and is not chemically, and probably not biologically, accessible[14]. It is therefore important to identify the compounds responsible for this discrepancy.

As a prerequisite to achieving a realistic environmental hazard assessment of compounds originating in bleachery effluents and subsequently entering the environment, it is important to characterize the precise nature of the compounds in the EOCl fraction of both sediments and biota. Characterization of the organochlorine components of whole bleachery effluents have relied heavily, indeed almost exclusively, on application of gas chromatographic (GC) and gas chromatographic–mass spectrometric (GC–MS) procedures[1,2,15–17]. Clearly, then, these should be applied to the cyclohexane-EOCl fraction; this was the specific object of this investigation, which was directed at sediment samples from areas in the neighbourhood of the discharge of bleachery effluents. In this investigation, it was found that, in spite of considerable effort, only *ca.* 8% of the EOCl could be identified in terms of known compounds, and it is therefore suggested that attention be directed to analytical procedures that do not depend exclusively on the use of GC.

EXPERIMENTAL

Solvents and reagents

The solvents cyclohexane, benzene, methanol, acetonitrile, dichloromethane, 1,2-dichloroethane, carbon tetrachloride were obtained from LabScan (Stillorgan, Ireland), *tert.*-butyl methyl ether, pentane and hexane from Burdick & Jackson Labs. (Muskegon, MI, U.S.A.) and diethyl ether from Fisons (Loughborough, U.K.).

Octadec-9-enoic acid, octadec-9,12-dienoic acid, hexadec-7-enoic acid, glyceryl trihexadecanoate, octadecanyl octadecanoate, cholesteryl octadecanoate, cholesterol, lupeol and betulin were obtained from Sigma (St. Louis, MO, U.S.A.), abietic acid and

dehydroabietic acid from K & K Labs. (Plainview, NY, U.S.A.), β-sitosterol from Serva (Heidelberg, F.R.G.), even-membered straight-chain alkanoic acids (C_{10-22}) from Alltech (Dearfield, IL, U.S.A.), tetrahydroabietic acid and pimaric acid from Hercules Powder (Wilmington, DE, U.S.A.), acetic anhydride from Fluka (Buchs, Switzerland), N-methyl-N-nitroso-*p*-toluenesulphonamide and boron tribromide–dimethyl sulphide complex from Janssen (Beerse, Belgium), hydrogen chloride in methanol from Tokyo Kasai (Tokyo, Japan) and methoxamine hydrochloride in pyridine and trimethylsilylimidazole (TMSI) from Pierce (Rockford, IL, U.S.A.). Silica gel 60 (70–230 mesh, aluminium oxide (70–230 mesh), acidic and basic, and sulphur (puriss. cryst.) were purchased from Merck (Darmstadt, F.R.G.). All other reagents were of analytical-reagent grade.

Synthesis of reference compounds

7,8-Dichlorohexadecanoic acid and 9,10-dichlorooctadecanoic acid were prepared by chlorination of hexadec-7-enoic acid and octadec-9-enoic acid with chlorine in dichloromethane at room temperature. Solvent was removed to give a white, low-melting waxy material whose methyl esters were >99% pure (GC–MS). No attempt was made to resolve the mixture of diastereoisomers. The mass spectra [electron impact (EI)] of the methyl esters had extremely weak parent ions (*m/z* 338 and 366, corresponding to $C_{17}H_{32}O_2Cl_2$ and $C_{19}H_{36}O_2Cl_2$), which gave rise to daughter ions with *m/z* 266 ($M^+ - 2$ HCl) and 294 ($M^+ - 2$ HCl).

9,10,12,13-Tetrachlorooctadecanoic acid was prepared in a similar way from octadec-9,12-dienoic acid by chlorination with a stoichiometric amount of chlorine in dichloromethane. Solvent was removed and the residue extracted several times with hexane to give a white powder which was free from compounds other than the desired product. The mass spectrum (EI) of the methyl ester had a weak parent ion (*m/z* 434, corresponding to $C_{19}H_{34}O_2Cl_4$), which gave rise to a daughter ion with *m/z* 326 ($M^+ - 3$ HCl).

9,10-Dibromooctadecanoic acid was prepared as for the corresponding chloro compound. The mass spectrum (EI) of the methyl ester had an extremely weak parent ion (*m/z* 454, corresponding to $C_{19}H_{36}O_2Br_2$), which gave rise to a daughter ion with *m/z* 295 ($M^+ - 2$ HBr).

The synthesis of 12-chloro-, 14-chloro- and 12,14-dichlorodehydroabietic acid has been described[18], but in attempting to repeat this work we encountered two serious problems: inclusion of the free-radical scavenger 2,3-dichloro-5,6-dicyanobenzoquinone brought about ring dehydrogenations[19] to products that were difficult to remove, and separation of the two monochloro isomers through formation of the amides was unreliable in our hands. The following modifications were therefore adopted. Only the $FeCl_3$–SiO_2 catalyst was used; the monochloro isomers were prepared by chlorination in dichloromethane at 0°C with slightly over one molar equivalent of chlorine, and the products were separated by semi-preparative high-performance liquid chromatography (HPLC). A Nucleosil C_{18} column (250 × 10 mm I.D., particle size 5 μm) (Jones Chromatography, U.K.) was used at a flow-rate of 4 ml min^{-1}, and the products were detected by their absorption at 280 nm. Two mobile phases were prepared by mixing 6% (v/v) acetic acid with acetonitrile in the ratios 30:70 (system A) and 40:60 (system B). Purification of the chlorinated resin acids was carried out first with system A and further purification of the product with system B.

The mass spectra of the methyl esters had *m/z* 348, corresponding to $C_{21}H_{29}O_2Cl$. The dichloro compound was prepared using excess of chlorine in dichloromethane at room temperature for 2 h and the product was purified by semi-preparative HPLC using system A. The mass spectrum of the methyl ester had *m/z* 382, corresponding to $C_{21}H_{28}O_2Cl_2$.

The procedure for the synthesis of 5,6-dichloro-β-sitosterol O-benzoate was first evaluated using the more readily available cholesterol, which was benzoylated with benzoyl chloride in pyridine[20]. After the reaction was complete, potassium carbonate solution (8 ml, 0.8 *M*) was added and the mixture shaken for 5 min. The precipitate was filtered and washed with hydrochloric acid and water. The dried product was crystallized from *tert.*-butyl methyl ether, chlorinated with chlorine at 0°C in carbon tetrachloride and the product purified first by semi-preparative HPLC using a Nucleosil C_{18} column with acetonitrile as the mobile phase and the detector set at 232 nm, and then finally recrystallized from acetonitrile. The direct probe mass spctrum had *m/z* 560, corresponding to $C_{34}H_{50}O_2Cl_2$. Pure β-sitosterol was benzoylated in the same way, and the EI mass spectrum, which lacked a parent ion (typical of Δ^5-steroids) had a principal peak at *m/z* 105 ($C_6H_5CO^+$) which showed that benzoylation had occurred. The O-benzoate was chlorinated at 0°C in carbon tetrachloride, the solvent removed and the product purified by semi-preparative HPLC on a Nucleosil C_{18} column with 100% methanol (6 ml/min) as the mobile phase and with the detector set at 232 nm. The direct-probe mass spectrum had a parent peak at *m/z* 588, corresponding to $C_{36}H_{54}O_2Cl_2$.

Source of sediments

All the samples were recovered from within 2 km of bleachery discharges, samples A and B from the Gulf of Bothnia, Sweden, and sample C from Oslo Fjord, Norway. Determinations of dry weight and ignition loss were carried out by procedures already described[15].

Extraction procedures for EOCl

These were carried out by established procedures[7]. The following experiment was carried out to exclude the possibility of interference from inorganic chloride. Cyclohexane was spiked with octadecanyl octadecanoate, glyceryl trihexadecanoate, dehydroabietic acid (all at three concentrations, 25, 75 and 225 μg/ml) and cholesteryl octadecanoate (5, 15 and 45 μg/ml), and chloride was added to the water–propan-2-ol phase to give a concentration of 0.7%. The extraction with cyclohexane was then carried out by the standard procedure used for sediment samples and the organic phase analysed for EOCl.

Elemental analysis

The extracts were evaporated to dryness *in vacuo* under a stream of nitrogen and dried in a vacuum desiccator over phosphorus pentoxide. These residues were analysed by ICI Agrochemicals (Jealotts Hill, U.K.).

Chemical treatment of samples

Analyses of polychlorinated biphenyls (PCBs) were carried out with extract residues prepared as above for elemental analysis. The residues were dissolved in

a small volume of *n*-hexane, chromatographed on silica gel deactivated with 5% (w/w) water, the hexane eluates collected, elemental sulphur removed[21], the extracts shaken repeatedly with concentrated sulphuric acid, washed with water and finally chromatographed on a column of acidic alumina overlayered with basic alumina. The hexane eluate was discarded and the PCBs were eluted with benzene, the extracts concentrated and used for analysis.

The following chemical modifications were carried out with *ca.* 2 mg of residue:

(i) The sample was treated with sulphuric acid (85%, w/w) overnight at room temperature, diluted with water and extracted twice with *tert.*-butyl methyl ether–hexane (1:1), the extracts dried (sodium sulphate), solvent removed and the residues derivatized as below.

(ii) Alkali treatment was carried out with 1 *M* aqueous methanolic (1:1) potassium hydroxide overnight at room temperature, the sample diluted with water, acidified, extracted and derivatized as below.

(iii) Treatment with $BBr_3 \cdot (Me_2S)$ (100 mg) was carried out in 1,2-dichloroethane for 1 h at 80°C in a closed tube. Excess of reagent was destroyed by adding water and the products were extracted with *tert.*-butyl methyl ether–hexane and derivatized as below.

(iv) The residue was dissolved in *tert.*-butyl methyl ether, anhydrous sodium methoxide added to give a final concentration of 0.2 *M* and the mixture was shaken vigorously for 1 min, acidified with dilute hydrochloric acid and the organic phase was used directly for analysis. Except for simple lipid esters, it was necessary to use *tert.*-butyl methyl ether as solvent for the transesterification.

(v) The residue was treated with 3 *M* aqueous potassium hydroxide and $CuSO_4$ $5H_2O$ (300 mg) at 100°C for 1 h. The sample was acidified, extracted and analysed for chlorophenolic compounds as described below.

(vi) The residue was dissolved in propan-2-ol, hydrobromic acid (0.1 ml, 48%) was added and the mixture was heated for 1 h at 100°C, diluted, extracted with *tert.*-butyl methyl ether–hexane and esterified as below.

Preparation of derivatives of standards and of EOCl extracts for GC and GC–MS analysis

Acetylation of phenolic compounds was carried out by standard procedures[14]. Free alkanoic acids were methylated with diazomethane or methanolic hydrogen chloride and resin acids with diazomethane[22], and non-chlorinated sterols and pentacyclic triterpenes were trimethylsilylated[23]. For quantification in EOCl extracts, these samples were used directly; for identification, however, they were first purified. The derivatized samples were evaporated to dryness, dissolved in hexane and purified by chromatography on a column of silica gel; the hexane eluate was discarded and the desired compounds eluted with benzene. Benzoylation of EOCl extracts was carried out as described for the synthesis of β-sitosterol benzoate except that after destruction of excess of reagent, the product was extracted with hexane (2 × 1.5 ml) and the extracts were washed with hydrochloric acid and dried (sodium sulphate). The extracts were chromatographed on silica gel and the product was eluted with benzene. Solvent was removed, and the product rechromatographed twice by semi-preparative HPLC as described for the synthesis of dichloro-β-sitosterol benzoate.

Gas chromatography–mass spectrometry

GC–MS analysis was carried out as described[24] with the modifications that the injector temperature was 260°C and the temperature programming was continued to 300°C and held for 20 min. For direct-probe analysis, the following temperature programme was used: 50°C (30 s isothermal), increased at 150°C/min to 450°C, which was maintained for 3 min.

Gas chromatography

Analysis of chlorophenolic compounds was carried out as described previously[14]. For the analysis of chloroform, samples were extracted with pentane and the following temperature programme was used: 35°C (6 min isothermal), increased at 10°C/min to 265°C. Attention is drawn to serious interference in the analysis of chloroform resulting from compounds released from PTFE-coated screw-cap liners, the use of which must therefore be avoided.

Analysis of PCBs was carried out using splitless injection with a Varian 3700 gas chromatograph fitted with an electron-capture detector, and the following temperature programme: 50°C isothermal for 1 min, increased at 4°C/min to 295°C, which was held for 5 min. Quantification was carried out using authentic standards (IUPAC Nos. 28, 31, 40, 52, 53, 101, 105, 138, 153, 180 and 209).

Analysis of elemental sulphur was carried out by GC with electron-capture detection (ECD) using the same temperature programme as for chlorophenolic compounds described above.

For the analysis of all other compounds, splitless injection was used with a flame ionization detection (FID) system and a Hewlett-Packard Model 5880 gas chromatograph using the following temperature programme: 50°C (2 min isothermal), increased at 15°C/min to 215°C, then at 8°C/min to 300°C, which was maintained for 30 min. The injector temperature was 250°C and the detector temperature 275°C. A DB-5 fused-silica capillary column (30 m × 0.25 mm I.D., film thickness 0.25 μm) (J & W Scientific, Folsom, CA, U.S.A.) was used with a column head pressure of 70 kPa. Quantification was carried out as follows: surrogate standards [dibromooctadecanoic acid for the carboxylic and resin acids and cholesterol for the sterols (100 μg of each)] were added to the extracts (1.0 ml) and the extracts were evaporated to dryness under nitrogen, esterified with diazomethane, again evaporated to dryness and silylated with TMSI. Hexane–*tert.*-butyl methyl ether (1:1) (1.0 ml) containing naphthalene (50 μg/ml) as internal standard was added and the organic phase analysed as above. Quantification was made using authentic standard compounds.

RESULTS AND DISCUSSION

General characteristics of the EOCl extract

In order to avoid confusion, it is important at the outset to appreciate that the term EOCl (extractable organic chlorine) is, by itself, an imprecise specification. The values obtained, together with the nature of the substances extracted, clearly depend critically on the choice of solvent. Cyclohexane was originally selected not primarily on account of its effectiveness as a solvent, but because it does not dissolve appreciable amounts of water. In this way, interference from inorganic chloride during neutron activation analysis of organic chlorine is minimized[25]. In the following discussion, we

TABLE I

LOSSES ON DRYING AND ON IGNITION OF DRIED SEDIMENT SAMPLES

Loss	*Sample*		
	A	*B*	*C*
Loss on drying (%)	85	67	52
Loss on ignition (%)	15	6	6

use the term EOCl exclusively for the fraction obtained by extraction of a sediment with propan-2-ol followed by back-extraction with cyclohexane. However, as the extracts contained high concentrations of non-chlorinated surface-active compounds, it was imperative to eliminate conclusively the possibility that the EOCl analyses were compromised by an artefact resulting from inadvertently introduced inorganic chloride. The experiments using the three "model" substances clearly showed that there was no interference from inorganic chloride.

The gross characteristics of the sediments are given in Table I and the elemental analysis of the residues after evaporation of the solvent showed that they contained no nitrogen and a high percentage of sulphur (Table II). GC and GC–MS confirmed the sulphur analysis, and showed that it was in the form of elemental sulphur. Organic nitrogen and sulphur compounds therefore made only a negligible contribution to the organic components of the extracts.

Quantification of organochlorine compounds

There were two main types of chlorinated compounds whose GC relative retention times and response factors are given in Table III.

The first consisted of a group of carboxylic acids. The concentrations obtained by treatment with diazomethane are designated "free"; treatment with sodium methoxide, however, which brings about transesterification of lipid esters[26], resulted in the release of a further contribution from chloroalkanoic acids, designated "bound", although not from the chlorinated resin acids (Table IV). In a separate experiment, it was shown that the treatment with methoxide did not result in any destruction of the chloroalkanoic acids, which were sensitive to treatment with aqueous methanolic alkali. The latter reagent did not release concentrations of the chlorinated resin acids exceeding those designated "free", so that it was assumed that these resin acids occurred only in the free form. The quantification of these compounds

TABLE II

MEAN DUPLICATE ELEMENTAL ANALYSES FOR RESIDUES AFTER EVAPORATION OF EOCl EXTRACTS

Sample	*C (%)*	*H (%)*	*Cl (%)*	*S (%)*
A	65.3	9.5	1.87	13.5
B	71.8	9.9	1.83	11.0
C	67.0	9.5	0.99	11.4

TABLE III

RETENTION TIMES AND RESPONSE FACTORS OF CHLORINATED CARBOXYLIC ACID METHYL ESTERS RELATIVE TO THAT OF 9,10-DIBROMOOCTADECANOIC ACID METHYL ESTER

Methyl ester	*Relative retention time*	*Relative response factor*
7,8-Dichlorohexadecanoic	0.782	0.74
9,10-Dichlorooctadecanoic	0.931	0.89
9,10,12,13-Tetrachlorooctadecanoic	1.064	0.90
12-Chlorodehydroabietic	0.956	0.93
14-Chlorodehydroabietic	0.972	1.44
12,14-Dichlorodehydroabietic	1.040	1.27

presented a technical problem as all of them have only low GC electron-capture responses and quantification was carried out using an FID system. Quantification of the chlorinated resin acids was carried out by both GC with FID and GC–MS procedures, and the results were in excellent agreement.

The second group of compounds, consisting of chlorophenolic compounds in the free form, constituted only a small fraction of the extracts, although this was increased by chemical modification; these components are therefore designated "bound" (Table V). There was also a minor contribution from chloroform, although the precise value depends critically on the details of the extraction procedure, and in particular the temperatures used during working up.

The chlorinated dehydroabietic acids and chlorinated octadecanoic acids, which clearly accounted for the greater fraction of the identified organochlorine compounds (Table VI), even though their total concentrations represented only a small fraction

TABLE IV

CONCENTRATIONS (mg/kg ORGANIC C) OF MAJOR ORGANOCHLORINE COMPONENTS OF EOCl; THE VALUES IN PARENTHESIS ARE GIVEN IN mg Cl/kg ORGANIC C

Compound	*Locality*		
	A	*B*	*C*
9,10-Dichlorooctadecanoic acid:			
Free	148 (28)	102 (20)	44 (8.3)
Bound	154 (30)	66 (13)	19 (3.6)
9,10,12,13-Tetrachlorooctadecanoic acid:			
Free	13 (10)	51 (14)	49 (16)
Bound	<[a]	44 (14)	19 (6)
12-Chlorodehydroabietic acid	28 (6.4)	32 (15)	31 (5)
14-Chlorodehydroabietic acid	70 (9)	66 (8)	66 (7)
12,14-Dichlorodehydroabietic acid	350 (90)	181 (31)	35 (8.8)
Chloroform	1.5 (1.3)	1.8 (1.6)	0.6 (0.33)
EOCl	(2180)	(2260)	(780)

[a] < = Lower than the limit of quantification.

TABLE V

CONCENTRATIONS (mg/kg ORGANIC C) OF CHLOROPHENOLIC COMPOUNDS RELEASED FROM EXTRACTS OF SAMPLE A AFTER CHEMICAL MODIFICATION

Modification	*Component*[a]					
	3,4,5-CG	*3,4,5-CC*	*TCG*	*TCC*	*2,4,5-CP*	*Penta-CP*
Untreated	0.64	0.13	0.39	1.78	<[b]	<
KOH	1.78	0.06	0.64	0.32	<	0.13
BBr_3 $(Me)_2S$	<	1.93	1.28	1.93	4.49	1.93

[a] CG = Chloroguaiacol; CC = chlorocatechol; CP = chlorophenol.
[b] < = Lower than the limit of quantification.

of the organically bound chlorine, are an environmentally important group of compounds because even the non-chlorinated derivatives of dehydroabietic acids are toxic[27–29], and both groups of compounds were apparently persistent in the sediment phase.

In addition, careful attention was directed to the possible presence of any compound that had been identified in bleachery effluents, or that was suspected of having a global distribution. Although a range of chlorinated thiophenes have been identified in bleachery effluents[5], and tetrachlorothiophene was the dominant thiophene in an effluent from the same factory in the neighbourhood of which the sediment sample was collected, none of these compounds could be identified in the EOCl fraction in spite of their ready extractability with cyclohexane. Chlorinated quinones, which have been putatively identified in bleachery effluents[30] and which might be environmental chemical modification products of chlorinated catechols, were also absent. An examination was also made for the presence of PCBs and other pesticides, but the contribution of all of these was extremely low. The identity of the PCB congeners was carried out by selected ion monitoring mass spectrometry of the parent ions taking into account the characteristic chlorine isotope patterns, but the only congener which occurred in sufficient concentration for conclusive identification was 2,3,2′,3′-tetrachlorobiphenyl (IUPAC No. 40), which occurred in samples B and C at concentrations of 2.9 and 0.1 mg/kg organic C.

TABLE VI

SUMMARY OF CONCENTRATIONS (mg Cl/kg ORGANIC C) OF IDENTIFIED COMPONENTS IN THE EOCl FRACTION IN SAMPLE A

Component	*Concentration*	*Component*	*Concentration*
Total chlorinated resin acids	105	Chloroform	1.3
Total chlorinated fatty acids	68	PCBs	0.4
Total phenolic compounds	9.5	EOCl	2180

"Free" and "bound" residues

Since chemical treatment of the extracts released additional amounts of chloroalkanoic acids (Table IV) and chlorophenolic compounds (Table V), a significant fraction of these compounds has been designated as "bound", and we have hypothesized that these compounds were covalently linked to organic components either in the sediment phase or to those originating in the effluents. We suggest that the chloroalkanoic acids existed as lipids, and emphasize that care must be taken in the choice of reagent for the release of "bound" residues. For example, the chlorinated alkanoic acids were rapidly destroyed by treatment with aqueous methanolic alkali which was used for release of the chlorophenolic compounds, but were stable to anhydrous sodium methoxide. The chlorocatechols were clearly demethylation products of the initially released chloroguaiacols, so that the latter group of substances were quantitatively the more significant. All these observations are consistent with the previously established fact that whereas chlorocatechols can be recovered from sediment samples by direct solvent extraction, the chloroguaiacols are apparently "bound" in some hitherto unknown manner so that they are effectively extractable only by more aggressive procedures[14].

These apparently "bound" residues were clearly extractable with cyclohexane, in contrast to the "bound" chlorophenolic compounds in whole sediments which were not effectively removed with water-immiscible solvents[14]. Whereas the essential nature of this covalent binding of the phenolic components in the cyclohexane extracts might have been similar to that in the bulk sediment, significant differences have now clearly emerged. Treatment of whole sediment samples with alkaline copper sulphate[31] effectively released amounts of chlorovanillins comparable to those of the phenolic compounds after treatment with methanolic alkali (Table VII). In addition, these values do not take into account the presence of substantial concentrations of the de-O-methylated vanillins whose presence was conclusively demonstrated by mass spectrometric examination. By contrast, application of similar procedures to the EOCl produced only low concentrations of chlorovanillins. We interpret the results from whole sediments as involving oxidative degradation of high-molecular-weight chlorinated lignin with initial fission into guaiacyl-C_3 entities, and subsequent loss of the side-chain with formation of the vanillins. These entities were presumably part of the polymeric chlorolignin structure, and these results are consistent with the fact that

TABLE VII

CONCENTRATIONS (mg/kg ORGANIC C) OF CHLOROPHENOLIC COMPOUNDS RELEASED FROM WHOLE SEDIMENT SAMPLE A AFTER CHEMICAL MODIFICATION

Modification	*Component*[a]			
	6-CV	*5,6-DCV*	*3,4,5-CG*	*TCG*
Untreated	<[b]	<	3	2
Methanolic KOH	13	15	77	61
Cu^{2+}–KOH	59	32	79	57

[a] CV = chlorovanillin; DCV = dichlorovanillin; CG = chloroguaiacol; TCG = tetrachloroguaiacol.

[b] < = Lower than the limit of quantification.

substantial amounts of unchlorinated vanillins were also released, presumably from lignin itself. Comparable polymerized entities were apparently of relatively minor significance in the EOCl fractions. In agreement with this is the fact that oxidation of EOCl residues with $KMnO_4$ and KIO_4, which has been used successfully for chlorolignin[32], yielded negligible amounts of chlorinated aromatic fragments.

Mass spectrometric identification of EOCl components

In a matrix as complex as that encountered in heavily contaminated sediment samples, identification of organic components clearly cannot be based solely on comparison of GC retention times with those of reference compounds[33]. All of these components were therefore conclusively identified by EI-MS comparison with reference compounds (Figs. 1 and 2). To facilitate identification, and eliminate as far as possible interfering compounds, all samples were purified by chromatography on silica gel before GC–MS analysis. A serious technical difficulty emerged because, under EI conditions, the chlorinated alkanoic acid esters had extremely weak parent ions, and readily formed daughter ions lacking chlorine atoms[34]; this considerably exacerbated their conclusive identification in complex mixtures of organic compounds and indeed the presence of chlorine in the compounds could readily have been overlooked. These results emphasize the necessity for access to pure samples of reference compounds. Although these chlorinated alkanoic acids and resin acids have been identified in bleachery effluents[22,35], we are not aware of their recovery from environmental samples prior to this study.

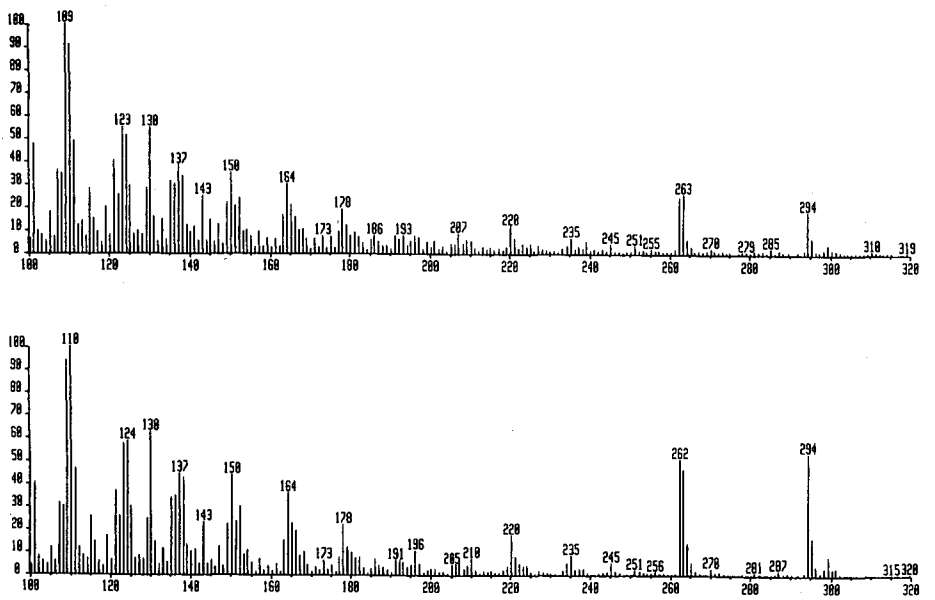

Fig. 1. Comparison of EI mass spectra of derivatives of compounds isolated from EOCl extracts (top) with those of authentic reference compounds (bottom): 9,10-dichlorooctadecanoic acid methyl ester.

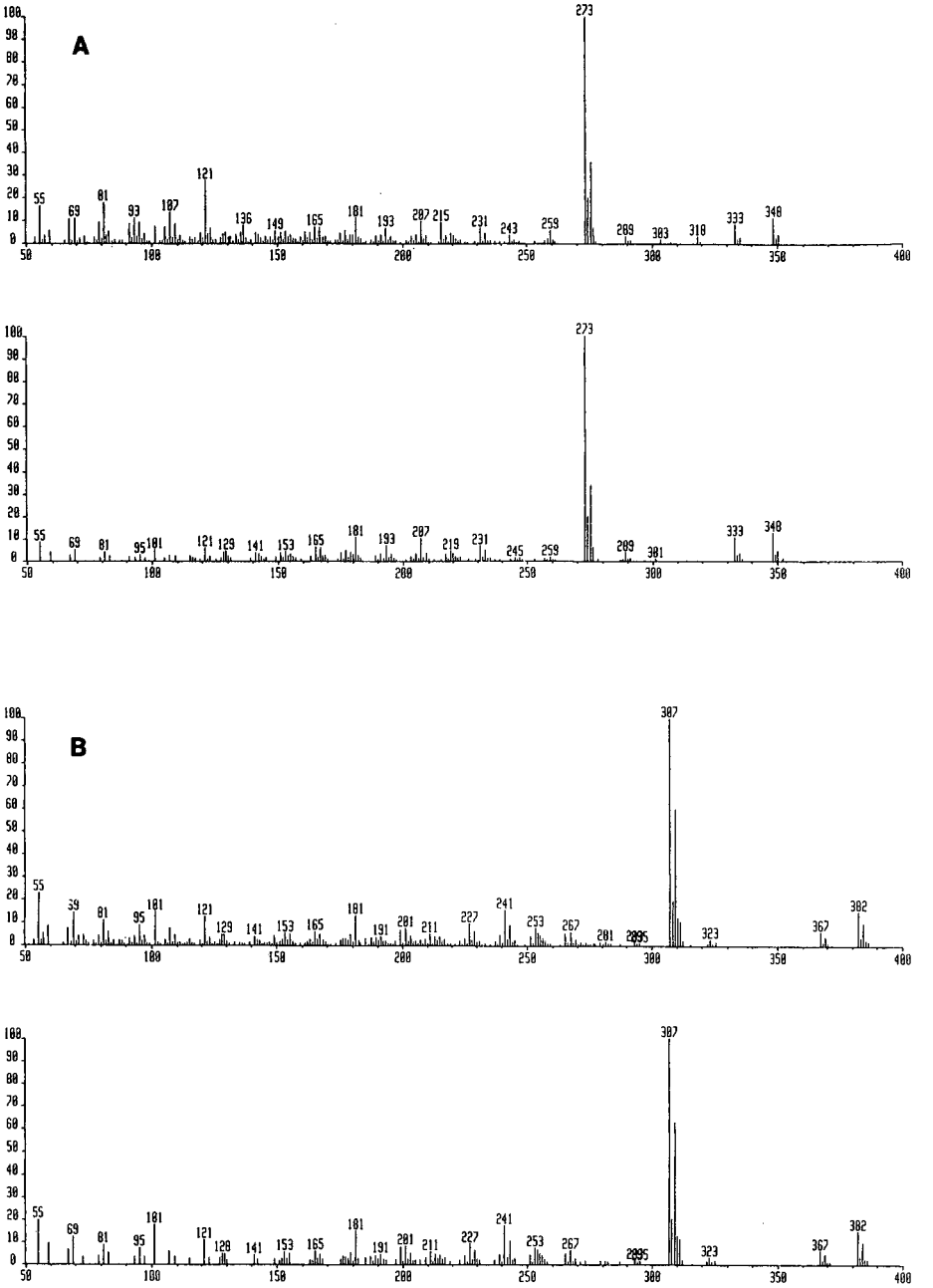

Fig. 2. Comparison of EI mass spectra of derivatives of compounds isolated from EOCl extracts (top) with those of authentic reference compounds (bottom): (A) 14-chlorodehydroabietic acid methyl ester; (B) 12,14-dichlorodehydroabietic acid methyl ester.

Origin and nature of the organochlorine compounds in the EOCl fraction

All the compounds identified above, with the exception of the PCBs, have been reported in bleachery effluents so that there can be little doubt as to their origin. It should be appreciated, however, that our samples were collected in the close proximity of the discharge of such effluents, so that a point discharge source could be clearly identified. Although less than 10% of the organically bound chlorine compounds in the EOCl fractions have been identified in terms of specific compounds, we feel that the comprehensive nature of this investigation, which employed procedures effectively used for analysis of bleachery effluents[1,2,15–17], reasonably excludes any major contribution from other compounds hitherto identified in such effluents. Three hypotheses concerning the origin of the unidentified compounds may be put forward: they do not originate in bleachery discharge and have a hitherto unknown origin, they have not yet been identified in bleachery effluents or they are transformation products of the original compounds contained in the effluents. In the light of current knowledge, it is impossible to decide between these alternatives.

Problems in identifying the components of the EOCl fraction in biota have been encountered by other workers[12,13] so that this may be assumed to be a general issue. It is important to realize, however, that the EOCl in biota from remote locations may be entirely different; possibly the major components are neutral, free organochlorine compounds transported via the atmosphere[36,37]. The possible confusion resulting from the uncritical use of sum parameters is therefore again emphasized.

The data presented clearly show that the use of sum parameters such as EOCl in environmental hazard assessment of bleachery effluents is unsatisfactory since such a substantial fraction remains unidentified in spite of intensive efforts. Among the more critical issues are (i) it is impossible to determine unambiguously the source of the contamination and (ii) it is not realistic to attempt an environmental impact assessment when the cardinal issues of persistence, bioavailability and potential toxicity cannot be addressed. The use of parameters such as adsorbable organic halogen (AOX) is fraught with even greater uncertainty, since a distinction between chloro- and bromo-organics clearly cannot be made.

Application of alternative analytical procedures

A compound was recovered from extracts whose benzoate after purification by HPLC had a mass spectrum identical with that of the benzoate of 5ξ,6ξ-dichloro-β-sitosterol (Fig. 3). However, as it co-chromatographed with another substance, identifiable by its mass spectrum as dihydro-β-sitosterol benzoate, quantification was not possible. Because, however, it was identified in sub-samples from the same sediment on two separate occasions, we feel confident of its occurrence and identification. This presented an interesting example of a compound whose existence had not hitherto been reported in bleachery effluents although its presence is eminently reasonable by analogy with the occurrence of the chlorinated long-chain alkanoic acids and that cannot be analysed by GC–MS owing to apparent disintegration on injection or during GC. This appears to be a general problem with chlorinated steroids (and probably also chlorinated triterpenoids) as GC analysis of the related 5ξ,6ξ-dichlorocholesterol acetate was unsuccessful even using on-column injection. Application of HPLC to the purification of the derivatized (benzoylated) extracts before direct probe mass analysis was clearly successful, so that further exploitation of this

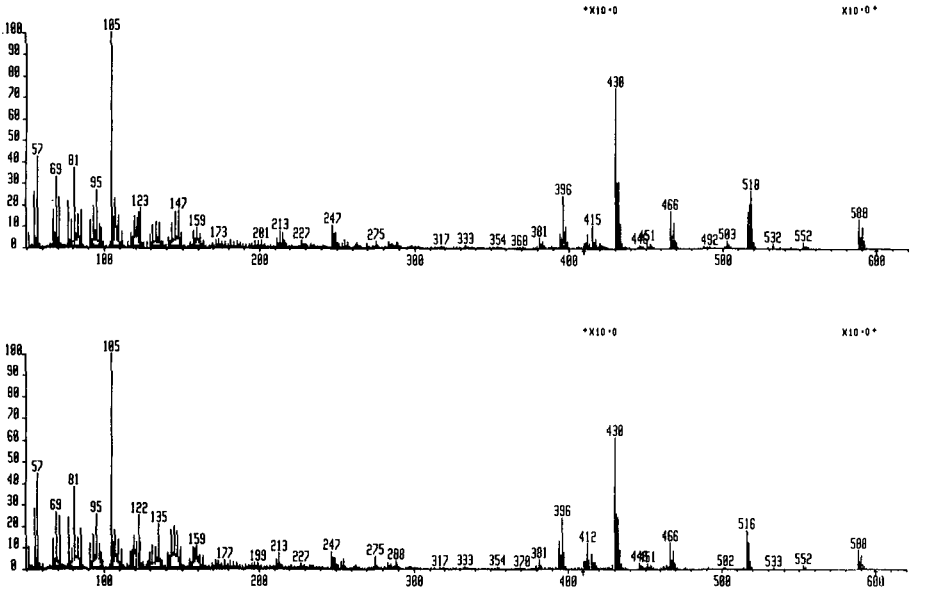

Fig. 3. Comparison of EI mass spectra of derivatives of compounds isolated from EOCl extracts (top) with those of authentic reference compounds (bottom): 5ξ,6ξ-dichloro-β-sitosterol benzoate.

technique opens new horizons for the characterization of hitherto unidentified compounds in EOCl extracts.

Non-chlorinated organic compounds

The preceding discussion has considered only organochlorine compounds. The elemental analyses (Table II) clearly illustrated, however, the high C–Cl ratio which could be rationalized on the basis either of a low degree of chlorination of the components or the presence of unchlorinated analogues. The latter conclusion finds support in the results of mass spectrometric examination of the derivatized extracts, which showed a range of unchlorinated aliphatic long-chain alkenoic and alkanoic acids, β-sitosterol and its reduction product and a range of terpenes including a few pentacyclic triterpenes (Table VIII, Figs. 4–6). The GC relative retention times and response factors of these compounds are given in Table IX.

As with the chlorinated analogues, only the alkanoic acids occurred in the form of lipid esters. These non-chlorinated compounds were found at concentrations often ten times greater than those of the chlorinated analogues, and their recovery suggests a substantial persistence. Many of the terpenes and sterols were sensitive to chemical modification by the procedures adopted for the chlorophenolic compounds so that these methods cannot be employed to assess their existence as "bound" residues. Some of the compounds such as the terpenes are toxic to aquatic organisms[27–29], and as it may plausibly be assumed that all compounds in this fraction have a high bioconcentration potential, attention should probably be directed to all these compounds, and also to the organochlorine compounds discussed above. As the relative fraction of identified organochlorine compounds in the EOCl extracts and of

TABLE VIII

CONCENTRATIONS (mg/kg ORGANIC C) OF PRINCIPAL NON-CHLORINATED COMPOUNDS IN EOCl EXTRACTS WITH CONCENTRATION OF LIPID-BOUND FATTY ACIDS IN PARENTHESES

Compound	*A*	*B*	*C*
Fatty acids:			
C_{14}	160 (135)	58 (102)	49 (141)
C_{16}	353 (263)	459 (379)	234 (127)
C_{18}	109 (45)	262 (102)	58 (24)
C_{20}	1136 (128)	1283 (235)	653 (205)
C_{16}:$\Delta 7$	340 (295)	58 (262)	49 (141)
C_{18}:$\Delta 9$	230 (116)	182 (226)	175 (73)
Terpenes and sterols:			
Abietic acid	539	488	385
Dehydroabietic acid	3126	5051	1946
Pimaric acid	565	1108	63
Tetrahydroabietic acid	725	488	385
β-Sitosterol	2277	2693	1513
Dihydro-β-sitosterol	841	1179	439
Lupeol	<[a]	924	29
Betulin	380	7278	<
Methylcycloartenol	165	718	344

< = Lower than the limit of quantification.

TABLE IX

RETENTION TIMES OF NON-CHLORINATED CARBOXYLIC ACID METHYL ESTERS AND TRIMETHYLSILYL ETHERS OF STEROLS AND TRITERPENES RELATIVE TO THAT OF 9,10-DIBROMOOCTADECANOIC ACID METHYL ESTER

Compound	*Relative retention time*	*Relative response factor*
Methyl esters:		
Dodecanoic	0.536	0.81
Tetradecanoic	0.612	0.99
Hexadecenoic	0.682	0.98
Hexadecanoic	0.689	1.05
Octadeca-8,10-dienoic	0.759	1.03
Octadecenoic	0.762	1.07
Octadecanoic	0.770	1.23
9,10-Epoxyoctadecanoic	0.777	1.16
Eicosanoic	0.854	1.63
Docosanoic	0.937	1.47
Pimaric	0.760	—[a]
Tetrahydroabietic	0.872	—[a]
Dehydroabietic	0.876	1.34
Abietic	0.897	—[a]
O-Trimethylsilyl ethers:		
Cholesterol	1.178	1.42
β-Sitosterol	1.287	1.06
5,6-Dihydro-β-sitosterol	1.297	—[b]
Lupeol	1.332	1.36
Betulin	1.419	0.96

[a] Response factors assumed to be the same as for dehydroabietic acid.
[b] Response factor assumed to the same as for β-sitosterol.

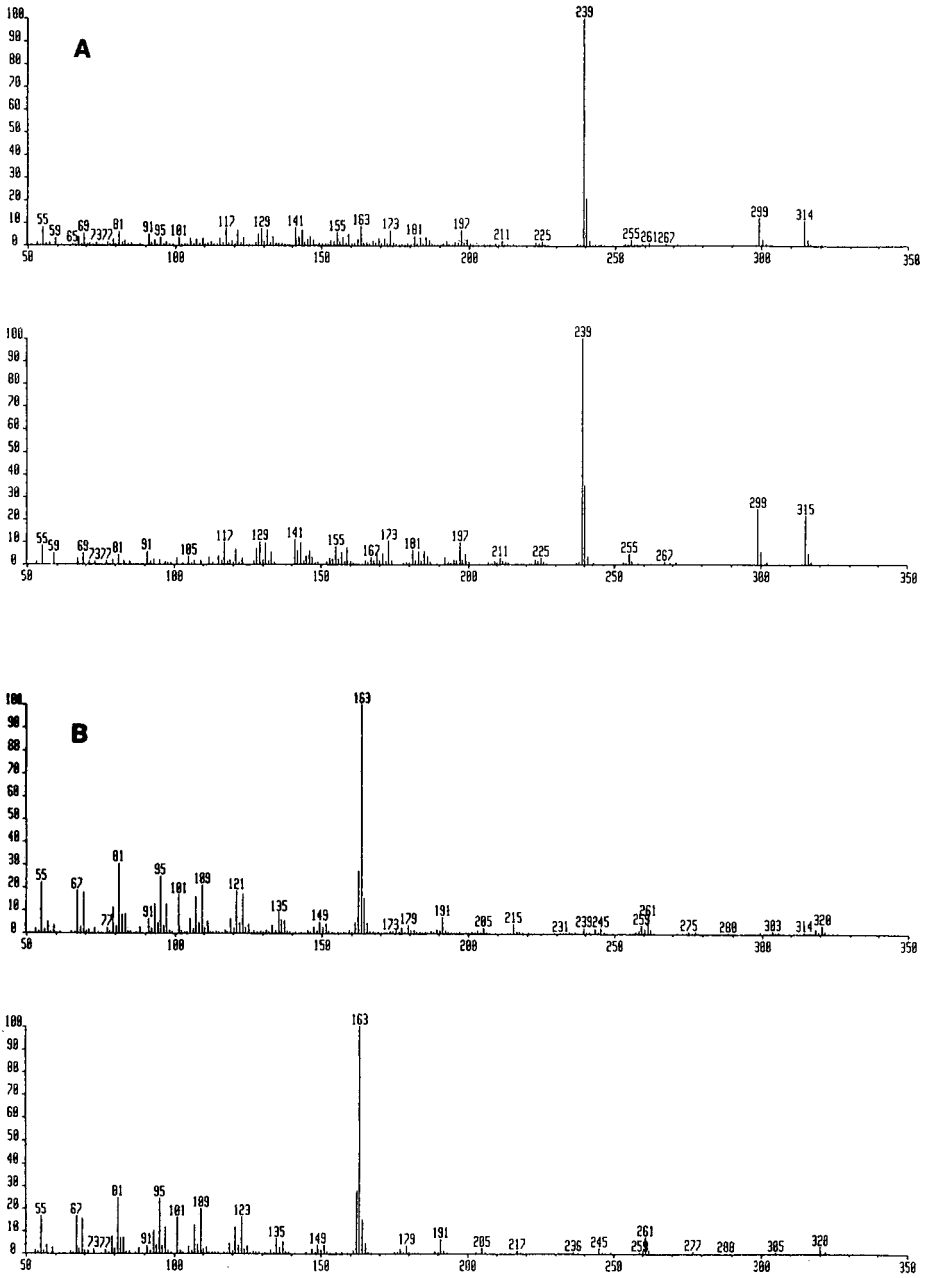

Fig. 4. Comparison of EI mass spectra of derivatives of compounds isolated from EOCl extracts (top) with those of authentic reference compounds (bottom): (A) dehydroabietic acid methyl ester; (B) tetrahydroabietic acid methyl ester.

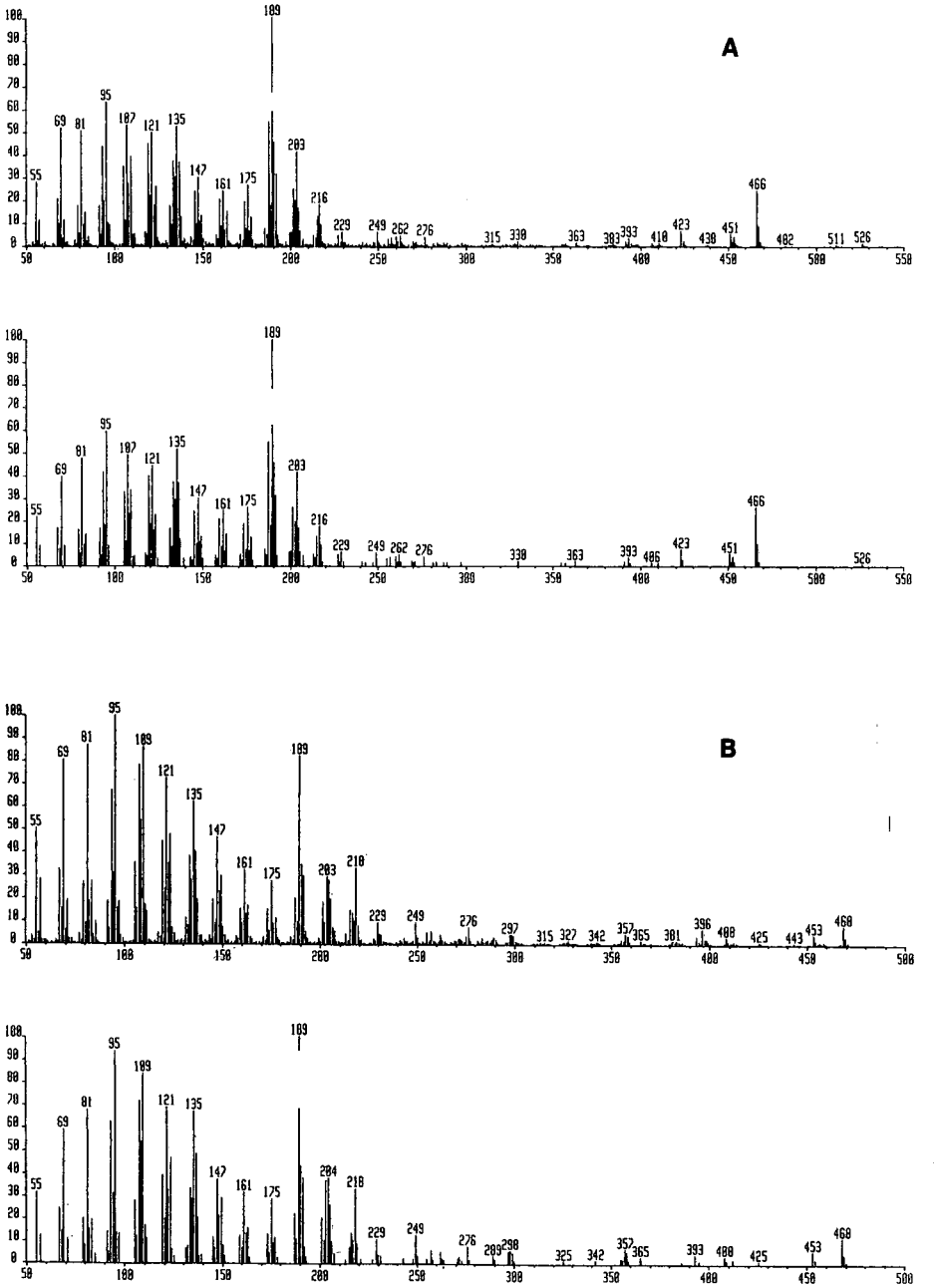

Fig. 5. Comparison of EI mass spectra of derivatives of compounds isolated from EOCl extracts (top) with those of authentic reference compounds (bottom): (A) betulin O-acetate; (B) lupeol O-acetate.

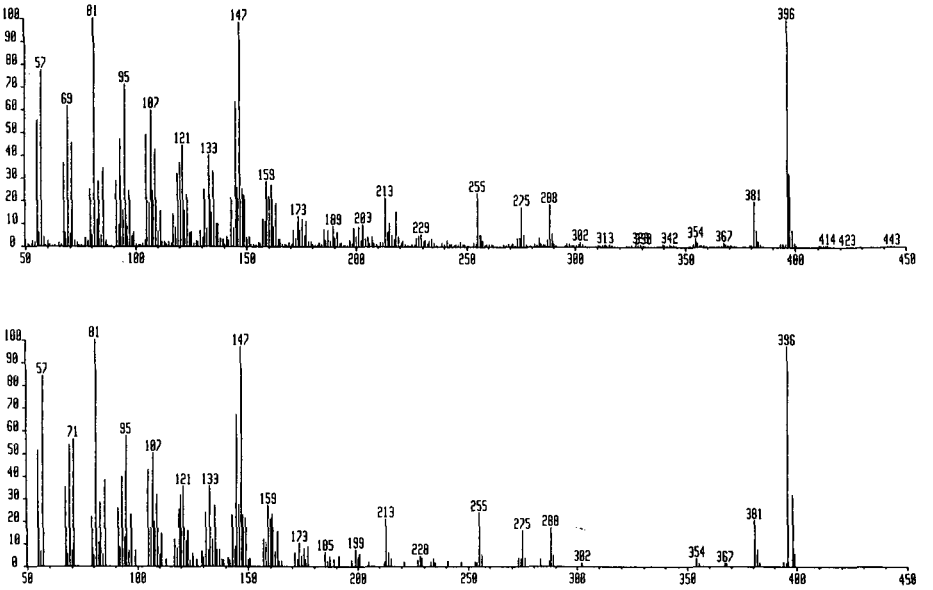

Fig. 6. Comparison of EI mass spectra of derivatives of compounds isolated from EOCl extracts (top) with those of authentic reference compounds (bottom): β-sitosterol O-acetate.

identified non-chlorinated compounds in the total organic fraction of the sediments was comparable (*ca.* 10%), we hypothesize that the unidentified components belong to classes of compound structurally distinct from those identified in this study. This emphasizes our conclusion from examination of the organochlorine compounds that analytical procedures based exclusively on application of GC methodologies are inadequate for analysis and identification of these constituents.

CONCLUSIONS

The major organic fraction of the cyclohexane-extractable fraction from sediment samples consisted of non-chlorinated compounds, including long-chain alkenoic and alkanoic acids, terpenes and some plant steroids. The free organochlorine compounds which could be identified by GC–MS were dominated by chlorinated long-chain alkanoic acids and chlorinated resin acids; chloroform and PCB isomers comprised a minor fraction. Free chlorinated phenolic compounds made a minor contribution, although such compounds were released in greater amounts after chemical modification.

In spite of intensive efforts, not more than *ca.* 8% of the EOCl fraction has been identified in terms of known compounds; with the exception of the PCBs, all were established constituents of bleachery effluents. It is concluded, therefore, that sum parameters such as EOCl do not provide an acceptable base for environmental hazard assessments of bleachery effluents and that, in addition, attention should be directed not only to chlorinated phenolic compounds but also to apparently persistent chlorinated and non-chlorinated compounds such as resin acids, steroids and long-chain alkenoic and alkanoic acids.

Application of chemical degradative procedures to the EOCl fraction and to whole sediments established that the major constituents of the two were significantly different; the unidentified EOCl components were probably not structurally related to chlorinated C_3-guaiacyl residues.

It is concluded that current procedures based on GC and GC–MS analysis are inadequate for revealing the identity of the major organochlorine constituent(s) of EOCl, and are unlikely to increase significantly the level of identification of the organochlorine components. It is suggested that attention be directed instead to HPLC methods and direct-probe mass spectrometric analysis.

ACKNOWLEDGEMENTS

We thank K. Martinsen and G. Carlberg, Senter for Industriforskning, Oslo, Norway, for the EOCl analyses, and D. J. Austin and M. L. Jamieson, ICI Agrochemicals, Jealotts Hill, U.K., for the elemental analyses. Funding for purchase of the mass spectrometer was provided by the Knut and Alice Wallenberg Foundation, and partial financial support was received from the Swedish Forest Industry Water and Air Pollution Research Foundation within the project "Environment 90, Bleaching Effluents".

REFERENCES

1 K. P. Kringstad and K. Lindström, *Environ. Sci. Technol.*, 18 (1984) 236A.
2 K. Lindström and F. Österberg, *Environ. Sci. Technol.*, 20 (1986) 133.
3 L. M. Strömberg, F. de Sousa, P. Ljungqvist, B. McKague and K. P. Kringstad, *Environ. Sci. Technol.*, 21 (1988) 754.
4 A. B. McKague, F. de Sousa, L. M. Strömberg and K. P. Kringstad, *Holzforschung*, 41 (1988) 191.
5 G. Carlberg, S. Johnsen, L. H. Landmark, B.-E. Bengtsson, B. Bergström, J. Skramstad and H. Storflor, *Water Sci. Technol.*, 20(2) (1988) 37.
6 A. Södergren, B.-E. Bengtsson, P. Johnsson, S. Lagergren, Å. Larsson, M. Olsson and L. Renberg, *Water Sci. Technol.*, 20(1) (1988) 49.
7 K. Martinsen, A. Kringstad and G. E. Carlberg, *Water Sci. Technol.*, 20(2) (1988) 13.
8 L. Håkansson, P. Johnsson, P. Johnson and K. Martinsen, *Water Sci. Technol.*, 20(2) (1988) 25.
9 T.-M. Xie, K. Abrahamsson, E. Fogelqvist and B. Josefsson, *Environ. Sci. Technol.*, 20 (1986) 457.
10 F. Österberg, A. Kierkegaard, L. Renberg and B.-E. Bengtsson, *Chemosphere*, 17 (1988) 1117.
11 L. Landner (Editor), *Chemicals in the Aquatic Environment*, Springer, Berlin, 1989.
12 C. Wesen, *Water Sci. Technol.*, 20(2) (1988) 185.
13 J. Hemming and K.-J. Lehtinen, *Nordic Pulp Paper Res. J.*, 4 (1988) 185.
14 M. Remberger, P.-Å. Hynning and A. H. Neilson, *Environ. Toxicol. Chem.*, 7 (1988) 795.
15 K. Lindström and J. J. Nordin, *J. Chromatogr.*, 128 (1976) 13.
16 G. Eklund, B. Josefsson and A. Björseth, *J. Chromatogr.*, 150 (1978) 161.
17 J. Knuutinen, *J. Chromatogr.*, 248 (1982) 289.
18 J. P. Kutney and E. Dimitriadis, *Helv. Chim. Acta*, 65 (1982) 1351.
19 E. A. Braude, L. M. Jackman, R. P. Linstead and G. Lowe, *J. Chem. Soc.*, (1960) 3123.
20 F. A. Fitzpatrick and S. Siggia, *Anal. Chem.*, 45 (1973) 2310.
21 S. Jensen, L. Renberg and L. Reutergårdh, *Anal. Chem.*, 49 (1977) 316.
22 B. Holmbom, *Pap. Puu*, 62 (1980) 523.
23 C. G. W. Brooks, E. C. Horning and G. S. Young, *Lipids*, 3 (1968) 391.
24 P.-Å. Hynning, M. Remberger and A. H. Neilson, *J. Chromatogr.*, 467 (1989) 99.
25 J. Gether, G. N. Lunde and E. Steinnes, *Anal. Chim. Acta*, 108 (1979) 137.
26 H. T. Badings and C. de Jong, *J. Chromatogr.*, 249 (1983) 493.
27 J. J. Tana, *Water Sci. Technol.*, 20(2) (1988) 77.
28 L. Matsoff and M. Nikinmaa, *Ecotoxicol. Environ. Saf.*, 14 (1987) 157.

29 B. Holmbom and K.-J. Lehtinen, *Pap. Puu*, 62 (1980) 673.
30 B. S. Das, S. G. Reid, J. L. Betts and K. Patrick, *J. Fish. Res. Board Can.*, 26 (1969) 3055.
31 S. Steinberg, M. E. Venkatesan and E. R. Kaplan, *J. Chromatogr.*, 298 (1984) 427.
32 M. Erickson and C. W. Dence, *Sven. Papperstidn.*, 10 (1976) 316.
33 A. H. Neilson, in L. Landner (Editor), *Chemicals in the Aquatic Environment*, Springer, Berlin, 1989, p. 74.
34 J. L. LaBrosse and R. J. Anderegg, *J. Chromatogr.*, 314 (1984) 83.
35 J. M. Leach and A. N. Thakore, *J. Fish. Res. Board Can.*, 32 (1975) 1249.
36 D. L. Swackhamer, B. D. McVeety and R. A. Hites, *Environ. Sci. Technol.*, 22 (1988) 664.
37 D. J. Gregor and W. D. Gummer, *Environ. Sci. Technol.*, 23 (1989) 561.

Journal of Chromatography, 508 (1990) 179–186
Elsevier Science Publishers B.V., Amsterdam — Printed in The Netherlands

CHROM. 22 325

Gas chromatographic assay for 3,9-diethylidene-2,4,8,10-tetraoxaspiro[5.5]undecane

STEFANO A. POGÁNY* and RODNEY A. DEEKEN
INTERx Research Corp., Merck Sharp & Dohme Research Laboratories, 2201 West 21st Street, Lawrence, KS 66047 (U.S.A.)
and
GAYLEN M. ZENTNER
INTERx Research Corp., Merck Sharp & Dohme Research Laboratories, 2201 West 21st Street, Lawrence, KS 66047 (U.S.A.), and Department of Pharmaceutical Chemistry, University of Kansas, Lawrence, KS 66045 (U.S.A.)
(First received November 13th, 1989; revised manuscript received February 2nd, 1990)

SUMMARY

A gas chromatographic method was developed, based on a reference standard, for analysis of the reactive diketene acetal 3,9-diethylidene-2,4,8,10-tetraoxaspiro[5.5]undecane (DETOSU). The method is based on the conversion of DETOSU to 3,9-diethyl-3,9-dimethoxy-2,4,8,10-tetraoxaspiro[5.5]undecane, a stable *ortho* ester.

INTRODUCTION

Ketene acetals react with alcohols to generate ortho esters[1]. 3,9-Diethylidene-2,4,8,10-tetraoxaspiro[5.5]undecane (DETOSU)[2] is a bifunctional ketene acetal used in reactions with diols to synthesize polymeric ortho esters which are hydrolytically unstable and have applications in the area of controlled drug release[3]. DETOSU is a reactive electrophile. Some of its known reactions[1,4,5] are hydrolysis, acid catalyzed self-polymerization, base catalyzed double bond migration, partial hydrolysis followed by intramolecular cyclization and nucleophilic attack by hydroxylic compounds such as alcohols and carboxylic acids. The reaction of DETOSU with polyols to produce polymeric *ortho* esters [poly(ortho ester)s] is a step-reaction (condensation polymerization) in which accurate stoichiometry and high purity monomeric starting materials are critical to obtain high degrees of polymerization[6,7]. It is, therefore, necessary to know accurately the purity of the polyols and the DETOSU. The determination of DETOSU purity presents a special problem because of its highly reactive nature and attendant lack of a reference standard. In the past, DETOSU purity was estimated by an area% gas chromatographic (GC) assay[8,9] that was not based on a reference standard. Non-volatile contaminants (*e.g.* oligomers) would not be detected and inaccurate purity results were possible. This paper presents a

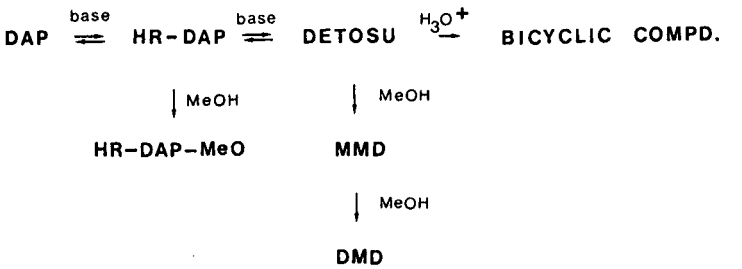

Fig. 1. Synthesis of DETOSU. Me = Methyl.

quantitative GC assay method for DETOSU purity based on the conversion of DETOSU to a stable derivative, dimethoxyDETOSU, that may be isolated for use as a reference standard.

To understand the origin of the peaks in the chromatograms a brief review of DETOSU's synthesis is helpful (Fig. 1). DETOSU is obtained from diallylidene pentaerythritol (DAP) by base catalyzed isomerization of the two double bonds of the diallyl acetal. The isomerization reaction does not lead quantitatively to DETOSU; instead an equilibrium mixture is established the composition of which is unaffected by longer reaction times and/or higher temperatures. The three main constituents of the final reaction mixture are DETOSU, the half-rearranged material (HR-DAP) in which only one double bond is shifted and a bicyclic ortho ester that presumably originates from the reaction of DETOSU with one molecule of water producing a hydroxymethyl group which adds to the residual ketene acetal moiety within the same DETOSU molecule. The reaction of HR-DAP with one molecule of methanol produces HR-DAP-CH_3O. The reaction of DETOSU with one or two molecules of methanol generates monomethoxyDETOSU (MMD) or dimethoxyDETOSU (DMD), respectively.

MATERIALS AND METHODS

The diketene acetal DETOSU was provided by Merck. Methanol (Burdick & Jackson high-purity brand) and methyl myristate (Aldrich, 99% purity) were used as received. Helium, nitrogen and hydrogen (ultra-high-purity grades; Linde Specialty Gases) and compressed air (hydrocarbon-free grade; Linde Specialty Gases) were used as received.

3,9-Diethyl-3,9-dimethoxy-2,4,8,10-tetraoxaspiro[5.5]undecane (DMD) was synthesized by heating DETOSU in methanol at reflux for 1 h, purifying by vacuum distillation (0.1 mmHg, 120°C) and recrystallization [0°C, from light petroleum (b.p. 30–60°C)]. Fourier transform infrared (FT-IR) (Nicolet 5DX FT-IR; KBr pellet), proton NMR (Bruker ACE-200; tetramethylsilane internal standard) and elemental (Schwarzkopf Microanalytical Labs, N.Y., U.S.A.) analyses were performed to verify the molecular structure of DMD. The melting point and purity of DMD were determined by differential scanning calorimetry (DSC) (Perkin-Elmer DSC-4). The DSC celll was calibrated using an indium standard. Dry nitrogen was used to purge the cell for all measurements. Sealed DSC pans with sample sizes ranging from 2 to 5 mg were used in all measurements. To insure good thermal contact between sample and pan,

each sample was briefly heated to 70°C (melted) and then rapidly cooled to −25°C and allowed to stand for 1 h to permit complete recrystallization. The temperature was then raised (100°C/min) to 35°C and the purity runs performed at 2°C/min over the temperature range of 35 to 70°C.

A gas chromatograph (Hewlett-Packard 5840A) equipped with a flame ionization detector, split/splitless capillary inlet port and a fused-silica capillary column (J & W Scientific DB-1 Megabore™, 15 m × 0.530 mm I.D.) with a cross-linked 100% methyl silicone stationary phase (1.5-μm film thickness) was used. The carrier gas was helium (flow-rate: 10 ml/min) and the detector was supplied with the appropriate flows of hydrogen, air and nitrogen as a make-up gas. The temperatures of the inlet port and detector were 250°C. The column temperature was 150°C isothermal. The volume injected was approximately 2 μl with a split ratio of 1:10.

The GC–mass spectrometric (MS) experiments were performed with a gas chromatograph (Hewlett-Packard 5890) equipped with a mass selective detector (Hewlett-Packard 5970B). The mass spectrometer source was operated at 70 eV with electron impact (EI) ionization. A fused-silica capillary column (HP-1 cross-linked 100% methyl silicone, film thickness 0.33 μm, 12 m × 0.20 mm I.D.) with a split/splitless capillary inlet port was used. The carrier gas was helium (flow-rate: 1 ml/min). The injection volume was approximately 0.5 μl with a split ratio of 1:10. Other chromatographic conditions were the same as described previously.

An internal standard solution (ISS) was prepared by dissolving 4.1 g of methyl myristate in 1000 ml of methanol. A reference standard stock solution (PSS) was prepared by dissolving 0.5184 g of DMD in 25 ml methanol. Three standards were prepared by transferring via pipette 1, 2 and 3 ml, respectively, of the PSS into 25-ml volumetric flasks containing 10 ml of ISS, then filling to volume with methanol.

DETOSU samples were prepared by accurately weighing approximately 50 mg into 25-ml volumetric flasks containing 10 ml methanol then heating at 60°C for 5 h, routinely, with longer equilibration times also investigated. After cooling to room temperature, 10 ml of ISS were added and the flasks were filled to volume with methanol.

RESULTS

Analysis of the synthetic DMD by several methods confirmed its identity. The proton NMR spectra (taken in [$^2H_6$]benzene and in [^{2}H]chloroform) were consistent with its structure. The FT-IR spectrum revealed bands at 2978, 2969, 2948, 2913, 2879, 1465, 1458, 1357, 1204, 990, 956, 943 and 926 cm^{-1}. Elemental analysis of DMD ($C_{13}H_{24}O_6$, mol.wt. 276.33) yielded values for carbon and hydrogen of 56.59% and 8.78%, respectively (theoretical values: 56.51% and 8.75%). The melting point of DMD was 51.2°C and the purity (DSC) was 98.2 ± 0.2 mole% ($n=6$). DMD (solid) was stable for > 1 year as indicated by DSC analysis when stored at −25°C in glass bottles.

Injection of authentic samples and GC–MS analysis were used to assign various peaks in the DETOSU sample chromatograms. Authentic samples of DAP, DETOSU and DMD were available and exhibited elution times of 2.22, 3.26 and 6.87 min, respectively. The identities of the other peaks were determined by GC–MS. The peak at 2.72 min had the same molecular ion (m/z = 212) as DAP. This was consistent with

the DAP isomer, HR-DAP, since both compounds have the same molecular weight. The peak at 3.17 min (an impurity in the internal standard) was identified as methyl decanoate by a probability-based library match of the GC–MS data (UNIX Chemstation™ software; Hewlett-Packard). The peak at 3.53 min was previously identified[5] as the bicyclic ortho ester 1-propanoyloxymethyl-4-ethyl-2,6,7-trioxabicyclo[2.2.2]octane and exhibited a weak molecular ion at m/z = 230 and a prominent fragment ion from ester cleavage at m/z = 57 due to $CH_3CH_2CO^+$. Although the peak eluting at 3.84 min was not always discernible due to its low concentration, this peak may be assigned with some confidence to HR-DAP-CH_3O. The addition of methanol to impure DETOSU containing HR-DAP resulted in the disappearance of the HR-DAP peak (2.72 min) and the corresponding appearance of the peak at 3.84 min. The peak at 4.84 min was assigned to MMD. As the reaction of DETOSU with methanol proceeded, this peak first increased then decreased in size, as expected in an A → B → C reaction.

The peak at 4.84 min never disappeared completely and was directly proportional to the DMD concentration in both standards and samples as illustrated in Fig. 2. Variation of the inlet temperature from 150 to 300°C in an attempt to alter the amount of MMD formed during a possible *in situ* breakdown process, resulted in no change in the MMD peak size. Lowering the column temperature resulted in peak tailing, while increasing the column temperature above 150°C resulted in loss of resolution. The mass spectrum associated with this peak showed that it consisted of a single component and exhibited a molecular ion at m/z = 244 (molecular weight of MMD) and an $[M+1]^+$ ion at m/z 213 (molecular weight of DETOSU) attributable to loss of one molecule of methanol from MMD. The remaining fragmentation pattern could be recognized as that of DETOSU. The peak at 7.71 min was methyl myristate, the internal standard.

The structures of the various species and the respective GC retention times are summarized in Table I.

A plot of the DMD–internal standard peak-area ratio *versus* the DMD concentration was linear (r^2 = 0.99) over the concentration range of 0.9 to 4.6 mg/ml. Periodic GC analysis of standard solutions (stored at −25°C) indicated stability for at least two months; linear least squares regression slopes and intercepts of cali-

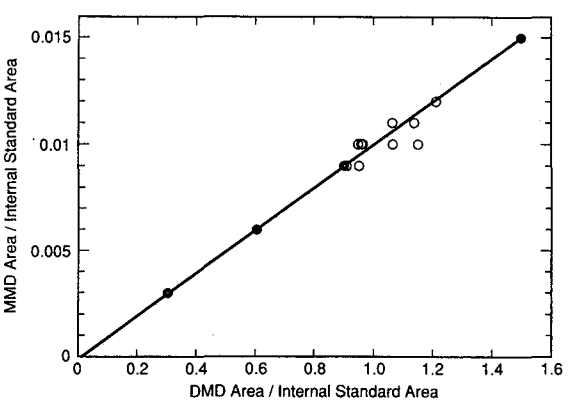

Fig. 2. MMD proportionality to DMD (r^2 = 0.9999). ● = standards; ○ = samples.

TABLE I

IDENTIFIED COMPOUNDS AND CORRESPONDING RETENTION TIMES

Compounds		*Retention time (min)*	
1	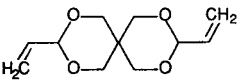	DAP	2.22
2	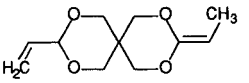	HR-DAP	2.72
3	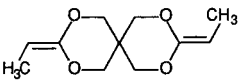	DETOSU	3.26
4	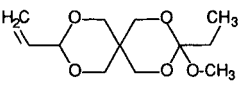	HR-DAP-CH_3O	3.88
5	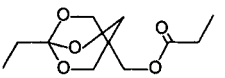	Bicyclic compound	3.53
6	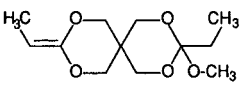	MMD	4.84
7	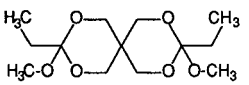	DMD	6.87
8	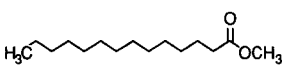	Methyl myristate	7.71

TABLE II

STABILITY OF STANDARD SOLUTION CALIBRATION CURVES

Time (months)	*Slope*	*Intercept*
0	0.2908	0.0042
	0.2915	0.0037
	0.2967	0.0040
Average	0.2930 ± 0.0032	0.0040 ± 0.0003
2	0.2975	0.0047
	0.2959	0.0072
	0.2961	0.0086
Average	0.2965 ± 0.0009	0.0068 ± 0.0020

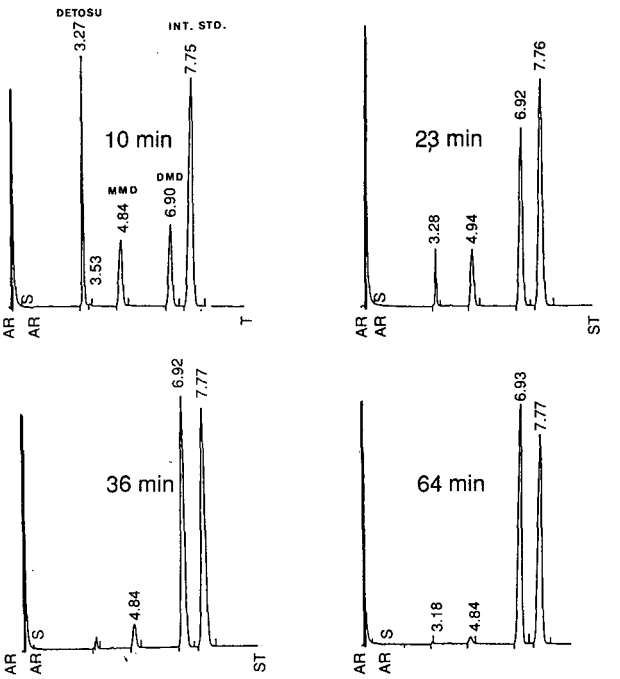

Fig. 3. Chromatograms illustrating the conversion of DETOSU to DMD when heating at 60°C for 10, 23, 36 and 64 min.

bration curves generated from the same standard solutions at time-zero and at time-two months were essentially the same (Table II).

The intraday precision of the assay, defined as the % coefficient of variation (C.V.) was 0.33%. This number, based on ten replicate injections of the same sample, was calculated by dividing the value of the standard deviation by the mean value (n = 10) of the DMD–Internal Standard peak-area ratio and expressing the quotient as a percentage.

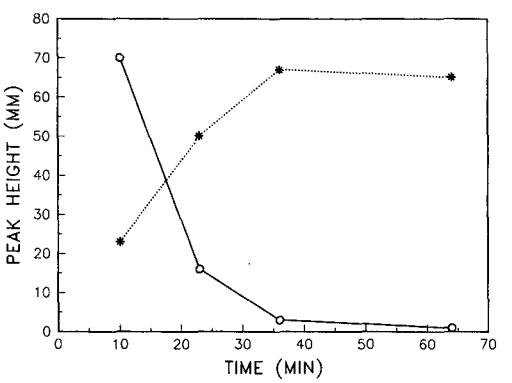

Fig. 4. Kinetics of DMD (*) formation from DETOSU (o).

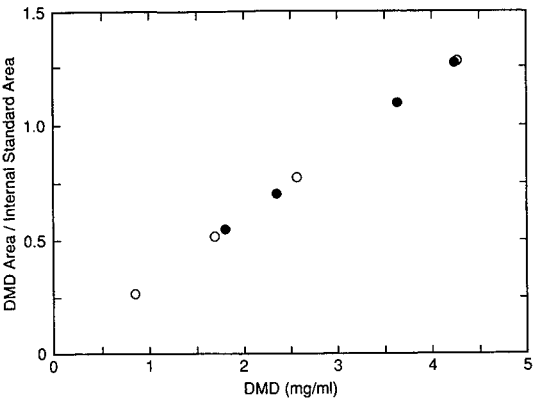

Fig. 5. Extent of conversion of DETOSU to DMD. ● = DETOSU converted to DMD; ○ = DMD standards.

The formation of DMD from DETOSU was followed as a function of time by GC (Figs. 3 and 4). Complete reaction had occured within 1 h as evidenced by the disappearance of the DETOSU peak and stable values for the DMD peak. Longer reaction times (2, 6, 18 and 48 h) at 60°C did not result in further increase of the DMD peak area.

To validate the accuracy of the assay, the extent of conversion of DETOSU to DMD was examined. The data are summarized in Fig. 5. The standard curve was obtained by injection of four DMD standards. This was compared to the sample curve obtained from four DETOSU samples that had been derivatized with methanol as described previously. The following two assumptions were made: (1) the DETOSU was 100% pure and (2) the conversion of DETOSU to DMD was 100%. The sample curve is the plot of the GC area response *versus* the theoretical concentration of DMD that would be obtained if 100% pure DETOSU converted quantitatively to DMD. The standard and sample curves have similar slopes and intercepts (slopes: 0.2982, 0.2961; intercepts: 0.0029, 0.0086) indicating a quantitative conversion of DETOSU to DMD. These data were analyzed by Student's *t*-test method[10] and no significant difference ($p > 0.5$) was found between the slopes of the two curves.

DISCUSSION

The results of this study indicate that the conversion of DETOSU to DMD is quantitative despite the persistence in both the sample and standard chromatogram of a minor peak at 4.84 min identified as MMD by GC–MS. The reason why this residual amount of MMD should not convert to the dimethoxy derivative under the sample preparation conditions of the assay could not be determined. It is proposed that the small peak persisting at 4.84 min is due to an equilibrium between MMD and DMD established inside the injector or column of the gas chromatograph. This hypothesis was corroborated by the fact that the amount of MMD was directly proportional to the amount of DMD injected and that repeated recrystallizations of DMD standards were not effective in reducing the MMD residue peak. The quantitative conversion of DETOSU to DMD, a stable material that can be isolated in high purity

and stored for long periods of time without degradation, can be used in a quantitative assay of DETOSU based on a reference standard.

REFERENCES

1 S. M. McElvain, *Chem. Rev.*, 45 (1949) 453.
2 J. Heller, R. F. Helwing and D. W. Penhale, *U.S. Pat.*, 4 304 767 (1981).
3 J. Heller, *J. Controlled Release*, 2 (1985) 167.
4 D. Borrmann, in E. Muller (Editor), *Houben-Weyl, Methoden der Organischen Chemie*, Vol. VII, Part 4, Thieme, Stuttgart, 1968, Ch. 14, p. 340.
5 G. Rork, J. Alexander and C. Shih, *Pharm. Res.*, 5 (1988) S1–S270.
6 F. W. Billmeyer, Jr., *Textbook of Polymer Science*, Wiley, New York, 3rd ed., 1984, p. 39.
7 J. Heller, D. W. H. Penhale, B. K. Fritzinger and S. Y. Ng, in G. I. Zatuchni, A. Goldsmith, J. D. Shelton and J. Sciarra (Editors), *Long Acting Contraceptive Delivery Systems*, Harper & Row, Philadelphia, PA, 1984, p. 113.
8 J. Heller, D. W. H. Penhale and R. F. Helwing, *J. Polym. Sci., Polym. Lett. Ed.*, 18 (1980) 82–83.
9 S. Y. Ng, D. W. H. Penhale and J. Heller, *Macromol. Synth.*, in press.
10 R. A. Fisher, *Metron*, 5 (1926) 90.

Journal of Chromatography, 508 (1990) 187–192
Elsevier Science Publishers B.V., Amsterdam — Printed in The Netherlands

CHROM. 22 385

Note

Comparison of discharge tubes for deuterium-specific gas chromatographic detection with a microwave-induced plasma

WALTER K. GAVLICK[a], JOHN R. STUFF[b] and PETER C. UDEN*
Department of Chemistry, Lederle Graduate Research Towers, University of Massachusetts, Amherst, MA 01003 (U.S.A.)
(First received July 24th, 1989; revised manuscript received February 20th, 1990)

Atomic spectroscopy has developed as a powerful method for interfaced chromatographic detection because of its capacity to monitor any element selectively in the eluate[1–3]. For gas chromatography (GC), such element-specific detection has been most often accomplished by means of a microwave-induced atmospheric pressure helium plasma (MIP)[4]. The plasma spectrometer system acts as an element-specific detector by monitoring the emission wavelength of a particular element and thus selectively detects compounds which contain the element of interest. Some of the advantages of such a detector are the ability to speciate directly or by derivatization, to tolerate non-ideal elution of components, to achieve high elemental sensitivity and to detect more than one element simultaneously. The most frequently employed GC–MIP system uses plasma discharges maintained within cavities based upon the Beenakker[5] TM_{010} design, which facilitates operation of a helium plasma at atmospheric pressure, allowing simple direct interfacing of a capillary gas chromatograph to the MIP system[6].

Although spectroscopic resolution is not generally adequate to dicriminate between emission lines from different isotopes of the same element, one instance in which this can be accomplished is for the hydrogen isotope deuterium. Deuterium-specific detection studies using various MIP detectors have been reported in the literature[7–9]; the Beenakker cavity has been evaluated for deuterium detection[10]. Recently, Hagen *et al.*[11] described various functional derivatization techniques using deuterium and GC–MIP. Derivatized compounds were monitored with deuterium-specific detection or further derivatization was done with reagents incorporating other elements so that more than one element could be monitored and greater analytical information obtained.

The study now described compares quartz and a boron nitride (BN) discharge tubes for deuterium-specific detection. The latter has proven useful in a number of

[a] Present address: Searle Research and Development, Division of G.D. Searle & Co., c/o Monsanto Company, 800 North Lindbergh Boulevard, St. Louis, MO 63167, U.S.A.
[b] Present address: Frank J. Seiler Research Laboratory, U.S. Air Force Academy, CO 80840, U.S.A.

0021-9673/90/$03.50

studies for elements such as silicon[12]. The BN tube was sealed inside a larger quartz tube to improve the transfer efficiency of microwaves from the generator to the BN tube, and thus allow the operation of a stable helium plasma in the 40–50 W range needed for deuterium-specific detection[12].

Deuterium is used in the study of organic reaction mechanisms, the labeling of biological samples and the alteration of the biological properties of drugs. Such modification of the metabolic pathway of drugs is particularly interesting but relatively undeveloped. If one or more hydrogen atoms are replaced by deuterium, a drug molecule exhibits minimal steric change or changes in its physicochemical properties. The increased bond stability may, however, cause changes in the biological properties of the drug, usually by retarding certain metablic pathways[13]. Since the metabolic pathway is altered, the drug activity is also altered; this may provide benefits, such as the avoidance of formation of toxic metabolites. Despite the promise of this deuterium isotope effect, work in this area has been limited due to the cost of toxicological testing and clinical trials. Gas chromatography–mass spectrometry (GC–MS) is a favored method of analysis for deuterated compounds, but it can be demanding and expensive since unit mass resolution will not be adequate to discriminate deuterated from undeuterated analogues in many instances. A GC–MIP system could serve as a viable alternative in clinical monitoring and testing, thereby extending the utility of the deuterium isotope effect.

EXPERIMENTAL

Instrumentation

A Varian (Walnut Creek, CA, U.S.A.) Model 1200 gas chromatograph modified for capillary column and split injection use was used. The detection system consisted of a Heath 703 Czerny-Turner configuration monochromator (McPherson Instruments, Acton, MA, U.S.A.) (0.35 m, f 6.8 capable of 0.1 nm resolution), a TM_{010} microwave cavity (J & D, Lexington, MA, U.S.A.) which was able to induce and sustain a helium plasma at atmospheric pressure, a microwave generator (Model HV15A, Scintillonics, Fort Collins, CO, U.S.A.) and a heated interface–transfer line. A coaxial stubstretcher (Model SL-10N tuner, Microlab/FXR, Livingston, NY, U.S.A.) was attached to the cavity to act as an impedance matching device and thus minimize reflected power. The photocurrent from the photomultiplier tube (Hamamatsu R928, 1100 V) was monitored with an electrometer (Model 600A, Keithley Instruments, Cleveland, OH, U.S.A.). The resultant signal was displayed on a strip-chart recorder (Omniscribe, Houston Instruments, Houston, TX, U.S.A.).

Materials

[$^2H_8$]Toluene, [$^2H_3$]acetonitrile, [$^2H_6$]acetone, [$^2H_6$]benzene and [$^2H_2$]dichloromethane were obtained from Aldrich (Milwaukee, WI, U.S.A.). A 30 m × 0.25 mm I.D. DB-5 (5% phenylmethylsilicone bonded phase) fused-silica capillary column with a film thickness of 0.25 μm (J & W Scientific, Folsom, CA, U.S.A.) was used. A 6 mm O.D. × 1 mm I.D. fused-quartz discharge tube and a BN discharge tube were used. The BN tube (1 mm I.D.) was sealed inside a larger quartz tube (6.2 mm O.D. × 4 mm I.D.) by means of a high temperature, chemically resistant sealant (Sauereisen Adhesive No. 1, Sauereisen Cements, Pittsburgh, PA, U.S.A.) to prevent flow leakage

between the two tubes. The plasma gas came into contact only with the BN tube while the outside quartz tube, because of its favorable dielectric properties, improved the transfer efficiency of microwaves from the generator to the BN discharge tube.

Analytical method

The microwave detection system was optimized with respect to total plasma gas flow, power, slit width and axial viewing location. The deuterium atomic emission line (656.1 nm) was found by bleeding a deuterated solvent such as [$^2H_6$]acetone into the plasma and then scanning with the monochromator until the wavelength was located. The focussing lens was then adjusted to give the greatest response. The slit width was optimized for the best signal-to-noise ratio by repeated injections of a deuterium-containing compound. The plasma gas flow-rate and power were optimized by simplex optimization[14].

After optimization, calibration curves for the deuterated compounds were prepared. Detection limit and linear dynamic range information was obtained from these plots. Selectivity values were also calculated.

RESULTS AND DISCUSSION

The optimum conditions for deuterium-specific detection were at a helium plasma gas flow-rate of 60 ml/min, a plasma power of 45 W and a 50-μm slit width for the quartz discharge tube. Values for the BN discharge tube involved a flow-rate of 53 ml/min, a plasma power of 55 W and a 50-μm slit width. Calibration curves for various deuterated compounds were constructed using both the BN and quartz discharge tubes, a summary of these data being found in Table I. Deuterium *versus* carbon selectivity values against hexane or heptane for the two different tubes are also given.

The detection limit and most notably the linear dynamic range values are much better for the quartz discharge tube than for the BN tube. Deuterium detection limits of *ca.* 50 pg and the wide linear dynamic range are encouraging features for further

TABLE I

ANALYTICAL DATA FOR DEUTERIUM-SPECIFIC DETECTION

Compound	*Detection limit (pg)*		*Selectivity of deuterium versus carbon*	*Slope*	*Correlation*	*Linear dynamic range*	*Number of points*
	Deuterium	*Compound*					
Quartz discharge tube							
[$^2H_8$]Toluene	28	174	88	0.984	0.9981	5176	8
[$^2H_3$]Acetonitrile	55	402	92	1.182	0.9974	3940	5
[$^2H_6$]Acetone	59	314	84	1.171	0.9974	480	5
[$^2H_6$]Benzene	51	357	78	1.039	0.9958	5130	5
BN discharge tube							
[$^2H_5$]Dichloromethane	43	937	87	0.932	0.9976	135	4
[$^2H_3$]Acetonitrile	233	1710	95	1.008	0.9958	135	5
[$^2H_6$]Acetone	153	815	78	1.237	0.9945	135	5
[$^2H_6$]Benzene	116	813	79	1.183	0.9943	112	5

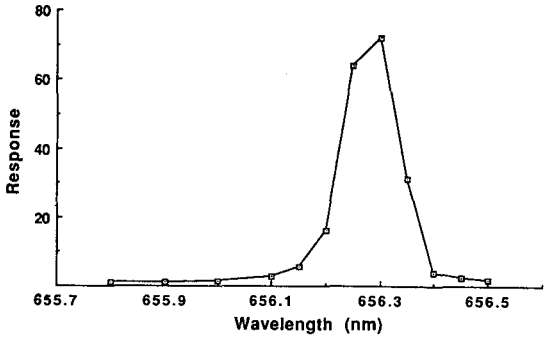

Fig. 1. Helium MIP background response with a quartz discharge tube.

application. However, the deuterium *versus* carbon selectivity is only *ca.* 100 for either discharge tube. It may be that true deuterium to carbon selectivity was not measured because of the contributing response from hydrogen emission at 656.3 nm. In the selectivity determination it was necessary to inject a compound containing carbon and hydrogen along with the deuterated sample, and to measure their responses as they eluted almost simultaneously. This procedure was used for two reasons: to measure responses under virtually identical elution conditions and to make observations for a pair of deuterated and undeuterated species as might be encountered in a practical determination. Since the hydrogen emission line is so close to the deuterium line (656.1 nm), it is possible that the hydrogen emission adds to the emission credited to carbon, thus reducing the measured deuterium *versus* carbon selectivity value, since the calculation does not take into effect such a close and strong interference. Since the hydrogen emission line is so close to the deuterium line, the selectivity value between them would be expected to be low. A selectivity value for deuterium over hydrogen of *ca.* 25 was calculated in this study, from chromatograms such as that shown in Fig. 3; in comparison a value of 50 has recently been reported for measurements at these wavelengths, giving credibility to the above conclusion[15].

Fig. 1 shows the background response of the helium MIP for the mono-

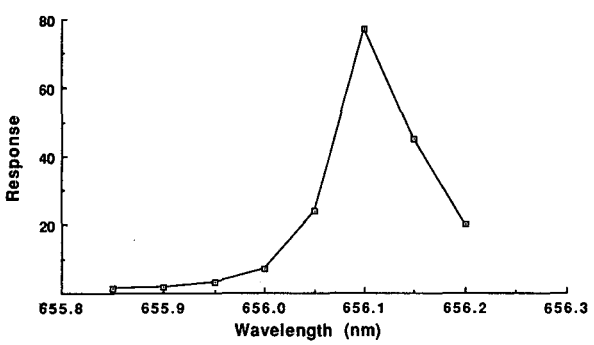

Fig. 2. Helium MIP response with [$^2H_6$]acetone bleed and a quartz discharge tube.

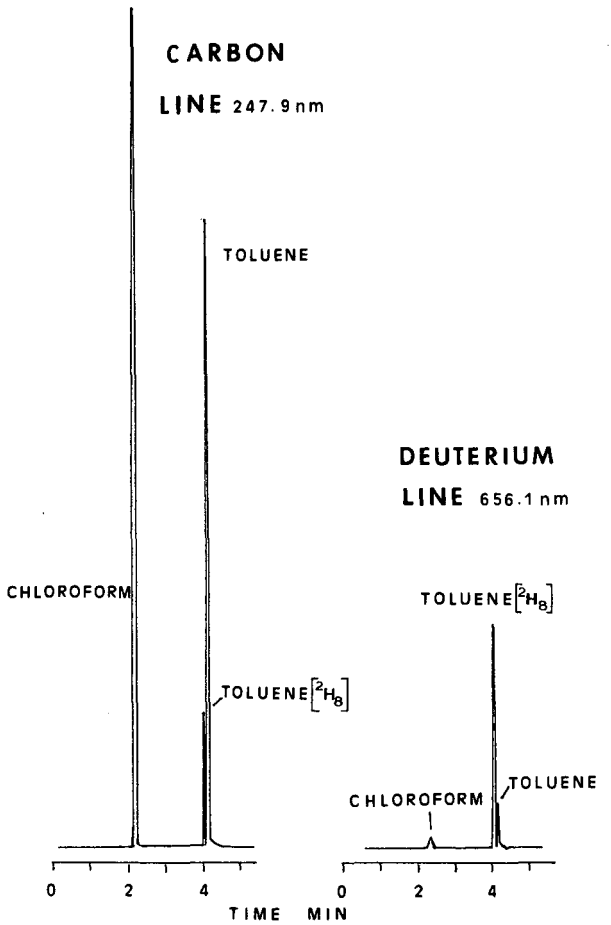

Fig. 3. GC separation of toluene and [$^2H_8$]toluene monitored at the carbon (247.9 nm) and deuterium (656.1 nm) emission lines. Helium column flow-rate, 1.4 ml/min; injection volume, 0.1 μl; inlet split ratio, 53:1; injector temperature, 230°C; detector transfer line temperature, 250°C; column temperature, 57°C isothermal.

chromator used; at 656.1 nm some response is observed. If impurities in the plasma gas are responsible, then a hydrocarbon sample would also be expected to give an enhanced response and thus reduce the selectivity value. Fig. 2 shows the response seen when [$^2H_6$]acetone was bled into the plasma. There is a marked decrease in response away from the 656.1-nm emission line and thus no way to avoid the background emission by moving to another measurement wavelength without sacrifice in detectability.

While selectivity between deuterium and carbon is only moderate, Fig. 3 demonstrates that deuterium-specific detection with the MIP system is a useful tool in distinguishing deuterated compounds in a chromatogram. The separation of toluene and [$^2H_8$]toluene in a chloroform solution (50:10:500, v/v/v) is shown for two indepedent chromatograms, monitoring at the carbon emission line (247.9 nm) and at

the deuterium emission line (656.1 nm). Deuterium detection plasma conditions were as noted above while carbon was monitored at 247.9 nm with a plasma power of 65 W and a plasma gas flow-rate of 88 ml/min. The relative responses are as predicted for the response at the carbon line, based upon the amounts of each component in the sample. The deuterium line response demonstrates the selective detection of the deuterated compound, [$^2H_8$]toluene showing a marked increase in response over toluene. The ability to carry out such selective monitoring can simplify the task of finding the deuterated component in complex matrixes, utilizing carbon- and hydrogen-specific chromatograms to gain further information.

The study showed that the quartz discharge tube gave a better detection limit and linear dynamic range for deuterium detection than did the BN tube which, however, has a longer effective operating life since it suffers less from etching of the walls by the plasma. Although the selectivity of deuterium *versus* carbon and hydrogen are both only moderate, GC–MIP shows potential as a useful tool to monitor deuterated compounds.

ACKNOWLEDGEMENTS

The support of the Dow Chemical Company and of Merck, Sharp and Dohme Research Laboratories is gratefully acknowledged.

REFERENCES

1 L. Ebdon, S. Hill and R. W. Ward, *Analyst (London)*, 111 (1986) 1113.
2 L. Ebdon, S. Hill and R. W. Ward, *Analyst (London)*, 112 (1987) 1.
3 P. C. Uden, *Trends Anal. Chem.*, 6 (1987) 238.
4 T. H. Risby and Y. Talmi, *CRC Crit. Rev. Anal. Chem.*, 14 (1983) 231.
5 C. I. M. Beenakker, *Spectrochim. Acta*, 31B (1976) 483.
6 S. A. Estes, P. C. Uden and R. M. Barnes, *Anal. Chem.*, 53 (1981) 1336.
7 P. M. Houpt, *Anal. Chim. Acta*, 86 (1976) 129.
8 F. P. Schwarz, *Anal. Chem.*, 50 (1978) 1006.
9 W. L. Yu, Q. Y. Qu, K. H. Zeng and G. C. Wang, in R. E. Kaiser (Editor), *Proceedings of the Fourth International Symposium on Capillary Chromatography*, Hüthig, Heidelberg, 1981, p. 445.
10 S. A. Estes, P. C. Uden and R. M. Barnes, *Anal. Chem.*, 53 (1981) 1829.
11 D. F. Hagen, L. C. Haddad and J. S. Marhevka, *Spectrochim. Acta*, 42B (1987) 253.
12 K. J. Slatkavitz, P. C. Uden and R. M. Barnes, *J. Chromatogr.*, 355 (1986) 117.
13 A. B. Forster, *Trends Pharmacol. Sci.*, 12 (1984) 524.
14 C. L. Shavers, M. L. Parsons and S. N. Deming, *J. Chem. Ed.*, 56 (1979) 307.
15 R. L. Firor, *Am. Lab.*, 21, No. 5 (1989) 40.

Journal of Chromatography, 508 (1990) 193–198
Elsevier Science Publishers B.V., Amsterdam — Printed in The Netherlands

CHROM. 22 284

Note

Modified sorbents in binary stationary phase systems in gas chromatography

N. T. KARABANOV, Z. P. VETROVA*, L. A. IVANOVA, T. N. SCHUVALOVA and Ya. I. YASHIN
N. J. Lobachevski Gorkovskii State University, Prospekt Gagarina, 603600 Gorkii (U.S.S.R.)
(Received November 8th, 1989)

The properties of liquid stationary phases used in gas chromatography (GC) are changed stepwise. Studies carried out by Kemula and Buchowski[1] on the distribution of microcomponents between two immiscible liquids established a theoretical basis for the application of binary stationary phases in GC. The equations that they proposed for the distribution of a microcomponent in a liquid–liquid system were used by Waksmundski *et al.*[2] for its distribution between a gas and a mixture of two liquid phases. They suggested a relationship between the partition coefficient in a mixture of two phases and their values in the pure components. They also stated that the excess free energy of mixing characterizes only the interaction between components in the binary liquid phase.

Vigdergauz and Pomasanov[3] showed that the excess free energy is composed of two components, one of which characterizes the interaction between the components in the system and the other the specific interaction of the sorbate used with a binary system.

The following equation was suggested[3]:

$$\ln V_{mm} = X_1 \ln V_{mm,1} + X_2 \ln V_{mm,2} + \frac{\Delta f'}{RT} + \frac{\Delta f''}{RT} \quad (1)$$

where

V_{mm} = molar retention of sorbate at the binary phase;
$V_{mm,1}$, $V_{mm,2}$ = molar retention of sorbate in the first and second pure components of the binary phase, respectively;
X_1, X_2 = molar fraction of the binary phase components;
$\Delta f'$ = excess free energy of mixing for the binary phase components;
$\Delta f''$ = value characterizing the specific interaction of sorbate with a binary phase.

However, eqn. 1 is in fact unsuitable for mixtures of liquid stationary phases and for high-molecular-weight and polymeric compounds and also for modified sorbents, where the notion of molecular weight is inapplicable. Therefore, in this work it is proposed to use eqn. 1 in a different form and also to replace the molar fraction by the weight fraction, and the molar retention by the specific retention volume;

0021-9673/90/$03.50

$$\log V_g = w_1 \log V_{g,1} + w_2 \log V_{g,2} + \frac{g_1^{IE}}{2.3\ RT} + \frac{g_2^{IE}}{2.3\ RT} \quad (2)$$

where

V_g, $V_{g,1}$, $V_{g,2}$ = specific retention volumes for the binary system and the first and second components, respectively;

w_1, w_2 = weight fractions for the components of the binary system;

g_1^{IE} = a value proportional to the excess free energy of mixing of the binary phase components;

g_2^{IE} = a value characterizing the specific interaction of the sorbate with the binary phase.

In the theory of the non-electrolyte solutions, the value of the excess free energy of mixing is expressed through the activity coefficients of the components of the binary solution with the Dewgem–Margules equation:

$$\frac{g^E}{2.3\ RT} = X_1 \log \gamma_1 + X_2 \log \gamma_2 \quad (3)$$

where

γ_1, γ_2 = activity coefficients of the binary solution components;

X_1, X_2 = molar fractions of the binary solution components.

Various expressions have been given in the literature[4] for the g^E value dependence in eqn. 3. One such dependence, suggested by Redlich and Kister[5], has the following form:

$$\varphi = \frac{g^E}{2.3\ RT} = X_1(1 - X_1)[B + C(2\ X_1 - 1) + D(2\ X_1 - 1)^2 + \ldots] \quad (4)$$

where B, C and D are constants and X_1 is the molar fraction of one of the components.

In this work it is suggested that the ratio from the theory of non-electrolyte solutions is used to describe the retention dependence on the composition of any binary system with eqn. 2, but g_1^{IE} and g_2^{IE} values with eqn. 4:

$$\varphi_1 = \frac{g_1^{IE}}{2.3\ RT} = w_1(1 - w_1)[B_w + C_w(2\ w_1 - 1) + D_w(2\ w_1 - 1)^2 + \ldots] \quad (5)$$

$$\varphi_2 = \frac{g_2^{IE}}{2.3\ RT} = w_1(1 - w_2)[B_s + C_s(2\ w_1 - 1) + D_s(2\ w_1 - 1)^2 + \ldots] \quad (6)$$

where B_w, C_w, D_w are constants characterizing deviations in the behavior of the binary system from ideality and B_s, C_s, D_s are constants characterizing the specific interaction of the sorbate with the binary system.

To find B_w, C_w and D_w, the dependence of $\log V_g$ for *n*-decane on the composition of binary system was used with the assumption that the retention of *n*-decane is not characterized by a specific interaction, that is, $\varphi_s = 0$. To determine B_s,

C_s, D_s, we used the dependence of the relative retained volume of sorbates (by decane) on the composition of the binary system:

$$\log r = w_1 \log r_1 + (1 - w_1) \log r_2 + w_1(1 - w_1)[B_s + C_s(2\,w_1 - 1) + D_s(2\,w_1 - 1)^2] \quad (7)$$

where r_1 and r_2 are the relative retention volumes of the sorbate by *n*-decane. To limit the number of constants in equations such as eqns. 2 and 5–7 to two (linear dependence) and for the possible use of relative concentrations, the following empirical equation for Z_1, which is a reduced variable, is suggested:

$$Z_1 = [b(w_{1,i} - w_{1,0})]^a \quad (8)$$

where

a = the empirical constant which was found experimentally to be equal to 0.25–4.00;

b = reciprocal of the concentration range used;

$w_{1,i}$, $w_{1,0}$ = variable values at the beginning of the range used and the current value of the same variable, respectively.

The value of Z_1 is varied from 0 to 1, and it should be noted that the value of Z_2 is calculated as the difference $1-Z_1$.

The influence of the constant a in eqn. 8 on the dependence of log V_g on the composition of binary systems is illustrated by the example of the retention of diphenyl on the hydroxylated Silochrom–polyethylene glycol adipate (PEGA) system (Fig. 1). In this instance the number of constants in eqn. 1 is limited to only two. According to the experimental data (Fig. 1, curve 2) a linear dependence of the $f(Z_1)$ function (Fig. 2) was found, and the least-squares method gave $B = -1.323$ and $C = -0.483$.

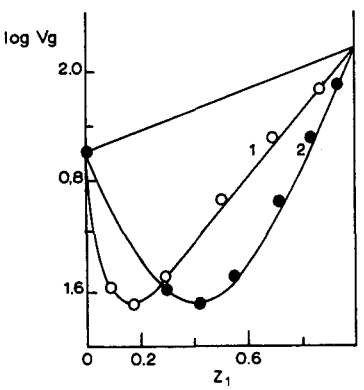

Fig. 1. Logarithmic dependence of the specific retention volume of diphenyl in the binary system hydroxylated Silochrom C-80–PEGA at 200°C on the relative mass fraction of stationary phase (1) and on the relative mass fraction raised to the power 0.5 (2).

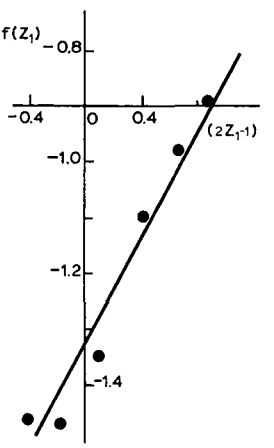

Fig. 2. The $f(Z_1)$ function for diphenyl in the binary system Silochrom C-80–PEGA.

The log V_g dependence for diphenyl was obtained by the equation

$$\log V_g = Z_1 \cdot 2.0495 + (1 - Z_1) \cdot 1.8555 + Z_1(1 - Z_2)[-1.323 + 0.483\ (2\ Z_1 - 1)] \quad (9)$$

where $Z = [3\ C/(100 + C)]^{0.5}$ and C is the PEGA mass fraction from Silochrom weight percent, %; 2.0496 and 1.8555 are the log V_g values at the point C(50%) and for the initial hydroxylated Silochrom, respectively.

We now consider the binary system: *p-n*-dioctyloxybenzene–liquid crystal. As the initial part of the log V_g dependence has a complicated form, we took 3% as the starting point and 20% as the final point. All the points within this range were considered in the relative weight percent.

According to the data in Table I, the dependence of V_g for *n*-decane on the composition of the binary system can be described by

$$\log V_g = Z_1 \cdot 2.0224 + (1 - Z_1) \cdot 2.2188 + Z_1(1 - Z_1)[-0.2822 + 0.0740\ (2\ Z_1 - 1) + 0.1435\ (2\ Z_1 - 1)^2] \quad (10)$$

where $B_w = -0.2822$, $C_w = 0.0740$ and $D_w = 0.1435$; 2.0224 and 2.2188 are the log V_g values at the points 20 and 3 wt.-%, respectively; $Z_1 = [(C - 3)/17]^{0.81}$; C is the mass fraction of the liquid crystal from the Silochrom weight percent.

For specifically retained sorbates such as benzene, ethanol, methyl ethyl ketone and nitromethane, eqns. 6–9 were obtained, together with those describing the dependence of V_g on the composition of the binary system by the $f_w(Z_1)$ function for *n*-decane and also by the constants B_s, C_s and D_s. The equations have the following forms:

for benzene,

$$\log V_g = 1.1072\ Z_1 + 1.4579\ (1 - Z_1) + Z_1(1 - Z_1)\ f_w(Z_1) + Z_1(1 - Z_1)[-0.5701 + 0.4992\ (2\ Z_1 - 1) - 0.1435\ (2\ Z_1 - 1)^2] \quad (11)$$

TABLE I

RELATIVE (TO *n*-NONANE) RETENTION VOLUMES FOR SORBATES AT 100°C ON HYDROXYLATED SILOCHROM C-80 (80 m^2/g) MODIFIED WITH 0–20% *p-n*-DIOCTYLOXYBENZENE

Sorbate	*p-n-Octyloxybenzene content (%)*							
	0	*1*	*3*	*6*	*9*	*12*	*15*	*20*
Benzene	0.541	0.528	0.353	0.229	0.205	0.212	0.225	0.242
Ethanol	10.40	8.18	4.66	2.23	1.66	1.55	1.47	1.42
Methyl ethyl ketone	22.60	22.60	21.00	10.70	4.00	2.39	2.09	1.89
Nitromethane	2.28	2.32	1.45	0.870	0.758	0.733	0.672	0.713
n-Hexane	0.136	0.133	0.125	0.118	0.114	0.116	0.122	0.124
n-Decane	1.94	1.97	2.04	2.05	1.97	1.98	1.98	1.98
n-Nonane[a]	77.80	57.80	81.30	63.80	59.10	55.10	54.50	53.00

[a] The specific retention volume is given in ml/g.

for ethanol,

$$\log V_g = 1.1874\ Z_1 + 2.5786\ (1 - Z_1) + Z_1(1 - Z_1)\, f_w(Z_1) + \\ + Z_1(1 - Z_1)[-0.8040 + 0.4855\ (2\ Z_1 - 1) - 0.1435\ (2\ Z_1 - 1)^2] \quad (12)$$

for methyl ethyl ketone,

$$\log V_g = 2.000\ Z_1 + 2.9395\ (1 - Z_1) + Z_1(1 - Z_1)\, f_w(Z_1) + \\ + Z_1(1 - Z_1)[-1.1960 + 0.4839\ (2\ Z_1 - 1) + 0.3546\ (2\ Z_1 - 1)^2] \quad (13)$$

and for nitromethane,

$$\log V_g = 1.5775\ Z_1 + 2.0719\ (1 - Z_1) + Z_1(1 - Z_1)\, f_w(Z_1) + \\ + Z_1(1 - Z_1)[-0.4979 + 0.3015\ (2\ Z_1 - 1) - 0.6939\ (2\ Z_1 - 1)^2] \quad (14)$$

where

$$f_w(Z_1) = -0.2822 + 0.0740\ (2\ Z_1 - 1) + 0.1435\ (2\ Z_1 - 1)^2.$$

Eqns. 6–9 allow the contribution of the specific interaction of the sorbate with a binary system to be quantified and its influence on the separation coefficient (relative retention) to be estimated. A comparison of the data calculated using eqns. 6–9 with the experimental results shows that the deviation does not exceed 5–6%.

The calculation of V_g for *n*-nonane and *n*-hexane was effected using eqn. 10 with substitution of the values 2.0224 and 2.2188 by the relevant data for *n*-nonane and *n*-hexane at the points of 20 and 3% (w/w). The calculated and experimental data are given in Table II.

Similar calculations for binary systems of Silochrom C-80 with cholesterol pelargonate (liquid crystal), phthalocyanine dilithium and vinyl acetate–ethylene copolymer were also made.

Hence the possibility of using thermodynamic principles from the theory of non-electrolyte solutions to express the retention from the composition of a binary system through the activity coefficients of the constituents and also through the activity coefficients that characterize the specific interaction of a sorbate with a binary system has been demonstrated.

TABLE II

DATA CALCULATED USING EQNS. 6–9 AND THE CORRESPONDING EXPERIMENTAL VALUES

V_g values for various sorbates on dehydroxylated Silochrom C-80 modified with *p-n*-dioctyloxyazoxybenzene at 100°C are given.

C (%, w/w)	Z_1	*Benzene*		*Ethanol*		*Methyl ethyl ketone*		*Nitromethane*		*n-Hexane*		*n-Nonane*	
		$V_g^{calc.}$	$V_g^{exp.}$	$V_g^{calc.}$	$V_g^{exp.}$	$V_g^{calc.}$	$V_g^{exp.}$	$V_g^{calc.}$	$V_g^{exp.}$	$V_g^{calc.}$	$V_g^{exp.}$	$V_g^{calc.}$	$V_g^{exp.}$
6	0.245	14.0	14.6	143.0	142.0	255	255	55.8	55.5	8.12	7.50	64.9	63.8
9	0.430	12.4	12.1	98.9	98.2	143	141	45.3	44.8	7.18	6.72	57.4	59.1
12	0.597	11.9	11.7	84.2	85.2	113	115	40.0	40.4	6.80	6.40	54.4	55.1
15	0.754	12.5	12.3	82.2	80.0	108	108	36.3	36.6	6.72	6.67	53.9	54.5

EXPERIMENTAL

The gas chromatographic measurements were made with the Tsvet-152 chromatograph under isothermal conditions. Glass columns (200 × 0.3 cm I.D.) and a flame ionization detector were used. The oven temperature was maintained constant within ±0.1°C. The relative error of the retention volume ($P = 0.95$) was 2.5–3.5%.

Binary systems of Silochrom C-80 with cholesterol pelargonate[6], *p-n*-dioctyloxyazoxybenzene, phthalocyanine dilithium[7], polyethylene glycol adipate and ethylene–vinyl acetate copolymer[8] were studied.

REFERENCES

1 W. Kemula and H. Buchowski, *Roczn. Chem.*, 29 (1955) 718–729.
2 A. Waksmundski, E. Soczewinski and Z. Suprynowicz, *Collect. Czech. Chem. Commun.*, 27 (1962) 2001–2006.
3 M. S. Vigdergauz and V. V. Pomasanov, *Izv. Akad. Nauk SSSR, Ser. Khim.*, 12 (1971) 2835–2837.
4 V. B. Kogan, *Heterogeneous Equilibrium*, Khimiya, Moscow, 1968, p. 432.
5 O. Redlich and A. T. Kister, *Ind. Eng. Chem.*, 40 (1948) 345–348.
6 Z. P. Vetrova, N. T. Karabanov and Ya. I. Yashin, *Dokl. Akad. Nauk SSSR*, 250 (1980) 1165–1167.
7 Z. P. Vetrova, N. T. Karabanov and Ya. I. Yashin, *Colloid J. USSR*, 37 (1975) 946–949.
8 A. I. Brock, Z. P. Vetrova, D. A. Vyakhierev, N. T. Karabanov and Ya. I. Yashin, *Colloid J. USSR*, 37 (1975) 118–122.

Journal of Chromatography, 508 (1990) 199–202
Elsevier Science Publishers B.V., Amsterdam — Printed in The Netherlands

CHROM. 22 361

Note

Gas–liquid chromatographic analysis of ethyl fenthion in tissues of native birds

W. J. ALLENDER

Chemistry Branch, Biological and Chemical Research Institute, P.M.B. 10, Rydalmere, 2116 N.S.W. (Australia)

(First received November 22nd, 1989; revised manuscript received February 2nd, 1990)

Ethyl fenthion (O,O-diethyl-O-4-methylthio-*m*-tolyl phosphorothioate) is the active component of the pesticide Luci-jet. It is a contact and stomach insecticide and possesses a useful penetrant and persistent action similar to that of the methyl ester (fenthion)[1]. Luci-jet is formulated as a dip and drench and has been used to control blowfly strike (*Lucilia cuprina*) in sheep[2–4]. It is significantly more toxic than the methyl ester with an acute oral LD_{50} for male rats of 45 mg/kg compared to 190–315 mg/kg for fenthion[1,4].

In recent years, deliberate ethyl fenthion poisoning of wildlife has occurred in New South Wales. Determination by semi-quantiative thin-layer chromatography, based on acetylcholinesterase inhibition[5,6] did not allow sufficiently low detection limits for ethyl fenthion in the liver and kidney tissues, but did provide a useful screening procedure for stomach contents.

The purpose of the present work was to develop a specific, sensitive and robust gas chromatographic method for determining ethyl fenthion poisoning of native wildlife.

EXPERIMENTAL

Extraction and clean-up procedure

The liver, stomach plus contents and kidney tissues dissected from the poisoned birds were cut into small pieces. The tissues were then accurately weighed (5–15 g) into a Sorvall cup and 25 ml of an acetone–dichloromethane (1:1) solvent mixture were added. The mixtures were then blended at medium speed for about 2 min and then filtered through a Whatman No. 1 filter into a Kuderna-Danish flask. The samples were re-extracted with a further 25 ml of solvent and the residue was washed several times with the same solvent and passed through the filter in the flask. The combined solvent extracts were then concentrated to a low volume. A 1-ml volume of 1% (v/v) acetic acid in hexane was added and the remainder of the solvent removed under a gentle stream of nitrogen to a final volume of *ca.* 1 ml. The residues were transferred with two 1-ml volumes of 1% (v/v) acetic acid in hexane onto silica gel 60 (particle size 0.063–0.200 mm, E. Merck) clean-up columns. The columns were pre-

0021-9673/90/$03.50

pared by adding 3.5 h of deactivated silica gel [deactivated by addition of 20% (w/w) distilled water], followed by 2 g anhydrous sodium sulphate (granular) to a 200 mm × 6 mm I.D. glass column plugged with glass wool. The columns were washed with 10 ml of 1% (v/v) acetic acid in hexane. After the addition of the sample residues the columns were eluted with 10 ml of 1% (v/v) acetic acid in hexane and the eluent was discarded. The ethyl fenthion was eluted with 30 ml of 5% (v/v) diethyl ether in hexane into a 50-ml volumetric flask. This fraction was subsequently concentrated or diluted depending on initial screening of eluate.

Chromatography

The eluate (2 μl) was injected into a Varian 3700 gas chromatography equipped with a thermionic specific (ceramic-alkali) detector and a 1.5 m × 2.0 mm I.D. glass column containing 7% OV-210 and 3.5% OV-101 on Chromsorb Q HP (100–120 mesh) operating at 185°C. Detector and inlet oven temperatures were 300 and 220°C, respectively. Gas flow-rates were as follows: nitrogen (carrier), 50 ml/min; hydrogen, 5.0 ml/min; air, 170–175 ml/min. Ethyl fenthion concentrations were determined by external quantitation with standard solutions of ethyl fenthion using a Hewlett-Packard Model 3390A integrator interfaced to the gas chromatograph and attenuated at 16 mV full scale deflection.

RESULTS AND DISCUSSION

The method described is sensitive and efficient for extraction and clean-up of ethyl fenthion residues in tissues of poisoned birds of prey. The method detection limit for ethyl fenthion in liver and kidney was 0.02 μg/g. Average recoveries from liver and kidney fortified with ethyl fenthion were greater than 91%.

Typical chromatograms of the reference standard ethyl fenthion and a cleaned stomach contents extract from a poisoned magpie (*Gymonorhina tibicen*) obtained with thermionic specific detection are shown in Figs. 1 and 2.

Table I shows the tissue concentrations of ethyl fenthion in two species of birds of prey. The ethyl fenthion had been extensively metabolished in all the bird livers, probably to the corresponding sulphoxide and sulphone, both of which are also toxic[7]. Ethyl fenthion residues in the magpie (*Gymonorhina tibicen*) were greater than those found in the currawong (*Strepera melanoptera*). This may be due to variation in species sensitivity to the pesticide and/or metabolic rates prior to death.

The use of ethyl fenthion appeared to be limited to mainly meat baits. Birds of prey such as crows, magpies and currawongs were probably the primary target, particularly during the lambing season; however, dogs, including sheep dogs, can also be at risk. The misuse of pesticides to poison vertebrates can put at risk both the person laying the bait and the general public.[8]

The method has proved useful for the analysis of samples derived from a number of instances of ethyl fenthion poisoning of wildlife. Several ethyl fenthion intoxications have been confirmed involving native granivorous birds in addition to birds of prey. The silica gel clean-up method has been successfully used on a variety of substrates. It eliminated co-extractives and provided adequate sensitivity. However, as most baits contained large amounts of the toxic chemical, the method is generally suitable without the clean-up procedure.

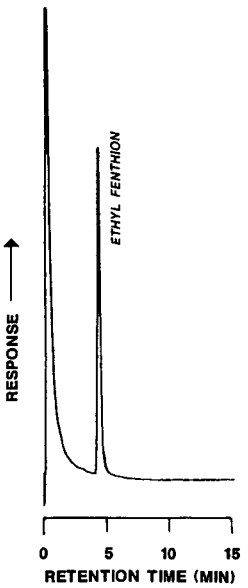

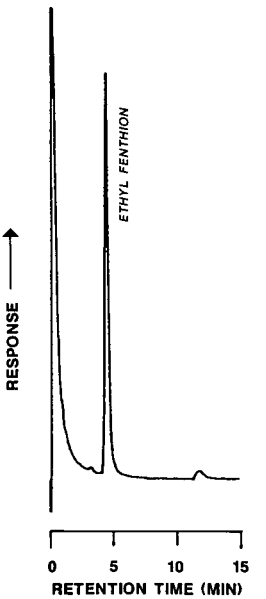

Fig. 1. Chromatogram of 2 μl of 0.5 μg/ml ethyl fenthion references standard (retention time, 4.42 min).

Fig. 2. Chromatogram of a cleaned extract of stomach contents of an ethyl fenthion-intoxicated magpie.

In summary, this method is a useful tool for screening purposes and for quantitation of suspected ethyl fenthion intoxication of wildlife.

TABLE I

ETHYL FENTHION RESIDUES FOUND IN TISSUES OF BIRDS OF PREY

Species	*Tissue*	*Ethyl fenthion content (mg/kg)*
Magpie	Liver	<0.02
(*Gymonorhina tibicen*)	Kidney	0.08
	Stomach contents	199
Magpie	Liver	0.03
(*Gymonorhina tibicen*)	Kidney	0.11
	Stomach contents	99
Currawong	Liver	<0.02
(*Strepera melanoptera*)	Kidney	0.12
	Stomach	<0.02
Currawong	Liver	<0.02
(*Strepera melanoptera*)	Kidney	0.06
	Stomach	0.04

REFERENCES

1 C. R. Worthing (Editor), *The Pesticide Manual — A World Compendium*, British Crop Protection Council, London, 7th ed., 1983, p. 269.
2 G. J. Shanahan and P. B. Hughes, *Vet. Rec.*, 102 (1978) 582.
3 J. H. Viljoen, *Onderstepoort J. Vet. Res.*, 45 (1978) 155.
4 Technical Information Service, *Lu-jet (Bayer S. 1751)*, H. H. York & Co., Sidney, 1962, p. 2.
5 H. Ackermann, *J. Chromatogr.*, 36 (1968) 309.
6 H. Ackermann, *J. Chromatogr.*, 44 (1969) 414.
7 K. D. Rainsford, *Pestic. Biochem. Physiol.*, 8 (1978) 302.
8 W. Bourne and S. Bourne, *Birds*, 15 (1974) 31.

Journal of Chromatography, 508 (1990) 203–207
Elsevier Science Publishers B.V., Amsterdam — Printed in The Netherlands

CHROM. 22 338

Note

Purity control of riboflavin-5′-phosphate (vitamin B_2 phosphate) by capillary zone electrophoresis

ERNST KENNDLER* and CHRISTINE SCHWER
Institute for Analytical Chemistry, University of Vienna, Währingerstrasse 38, A-1090 Vienna (Austria)
and
DUSAN KANIANSKY
Department of Analytical Chemistry, Comenius University, Bratislava (Czechoslovakia)
(First received December 27th, 1989; revised manuscript received February 9th, 1990)

The control of the specified purity of commercial chemicals is an important task in chemical analysis. Often high demands are made on the analytical method because in many instances chemically very similar constituents have to be determined. For riboflavin-5′-phosphate the purity of the products investigated is specified by the producers based on high-performance liquid chromatography (HPLC) or spectrophotometry. Because the most important impurities are riboflavin and the different riboflavin phosphates, the latter method has the disadvantage that the particular riboflavin derivatives (showing similar optical properties) cannot be determined individually, and their total is measured. Therefore, this is not a very suitable technique for the determination of such impurities. Apart from the note on the product label refering to the analytical method applied, no detailed procedures concerning the purity control of riboflavin-5′-phosphate were found in the literature. Only its determination in different matrices, *e.g.*, in pharmaceutical preparations, drinks, foodstuffs, plasma, urine, animal tissues etc., has been described[1–12]. Capillary zone electrophoresis, which has a high separation efficiency, seems to be a very suitable method for the determination of impurities in riboflavin-5′-phosphate. Using conditions under which electroosmotic flow occurs, it is possible to control the purity of riboflavin-5′-phosphate in the presence not only of other ionic but also of neutral sample components such as riboflavin.

EXPERIMENTAL

Chemicals

All chemicals used for the preparation of the buffers were of analytical-reagent grade (E. Merck, Darmstadt, F.R.G.) and were used without further purification. Water was distilled twice from a quartz apparatus.

Riboflavin-5′-phosphate and riboflavin were purchased from different sources (Merck; Serva, Heidelberg, F.R.G.; Fluka, Buchs, Switzerland). The purity of the

0021-9673/90/$03.50

TABLE I

BUFFERING ELECTROLYTES WITH DIFFERENT pH VALUES USED FOR THE ZONE ELECTROPHORETIC SEPARATIONS

pH	*Composition*	*Concentration (mol/l)*
6.0	Morpholinoethanesulphonic acid–histidine	0.01
7.0	Sodium phosphate	0.01
8.2	Sodium phosphate	0.01
9.1	Sodium borate–boric acid	0.01

riboflavin-5′-phosphates was specified as follows: "for biochemistry", 99–101% (Merck); "pure" (Serva); and >89% (Fluka).

The samples were dissolved in the buffer electrolytes at a concentration of about 0.5 mg/ml. The compositions of the buffering electrolytes are given in Table I.

Apparatus

Zone electrophoresis was carried out on a laboratory-made instrument, consisting of a fused-silica separation capillary (100 cm × 100 μm I.D.) (Scientific Glass Engineering, Ringwood, Victoria, Australia), which was mounted in an HPLC fluorescence detector (Model F-1050, Merck-Hitachi). The high-voltage power supply unit (Tachophor 2020; LKB, Bromma, Sweden) was operated in the constant-voltage mode at 17.5 kV. Injection was carried out by electromigration with 10 kV for 5 s. The detector signal was recorded by an integrator (Model D-2500; Merck).

RESULTS AND DISCUSSION

Variation of the pH of the buffering electrolyte

Two parameters, which are decisive for the electromigration of the sample components, are affected by varying the pH of the buffer electrolyte: the electroosmotic flow of the bulk liquid, which is directed towards the cathode under the given conditions, and contributes to the migration of all components to the same extent, independent of the sign and amount of their charge; and the electrophoretic migration of the substances, which is dependent on the pH of the buffer electrolyte via the degree of dissociation.

The different electrophoretic patterns of a riboflavin-5′-phosphate sample, obtained at different pH values of the buffer, are shown in Fig. 1. There is an increase in the migration time of the analytes with decrease in pH. The longer migration time of the first-eluting substance (neutral riboflavin, detected, *e.g.*, at 5.02 min at pH 9.1 or at 7.18 min at pH 6), but also of the other analytes, is caused by the reduction in the electroosmotic flow: lowering the pH leads to a decrease in the number of negative charges on the silica surface (which originate from the dissociation of silanol groups) and therefore reduces the zeta potential. It follows that a high pH is of advantage when the time of analysis is of interest.

On the other hand it can be seen from the electropherograms in Fig. 1 that the separation of the analytes is enhanced on lowering the pH of the buffer. At pH 8.2 one

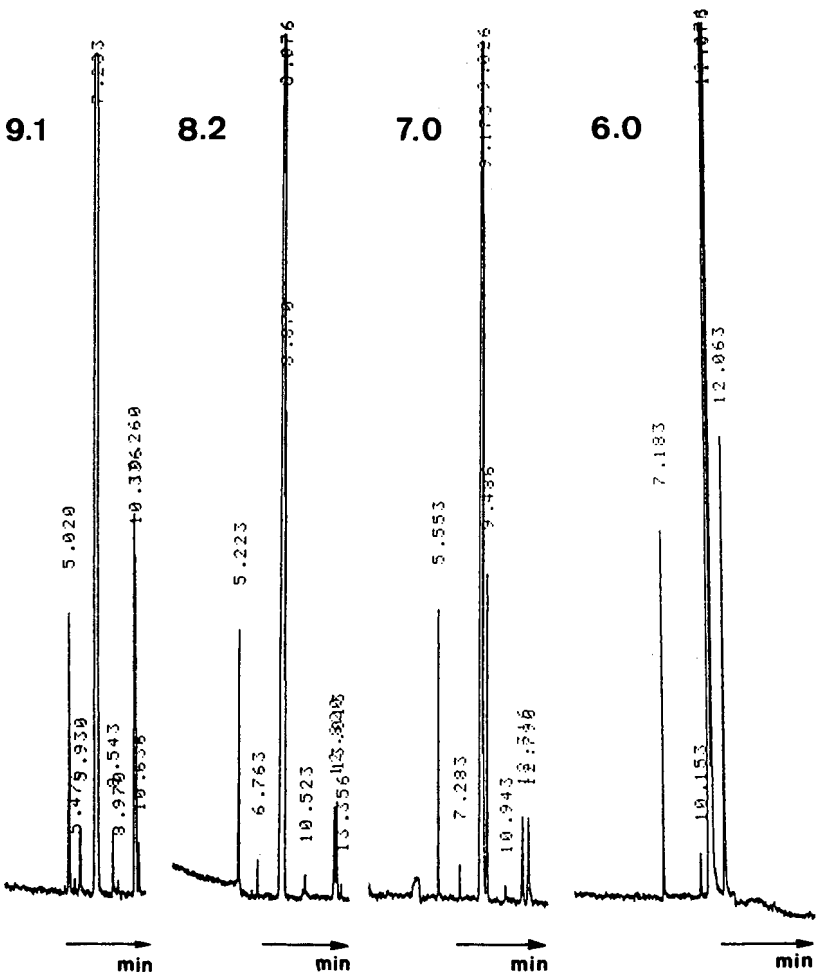

Fig. 1. Electropherograms of a sample of riboflavin-5′-phosphate at different pH values of the buffering electrolyte. Capillary: fused silica, 100 cm × 100 μm I.D., 55 cm distance to detector. Detection: fluorescence (350/520 nm). pH values are indicated by the numbers at the top of the electropherograms. The compositions of the buffers are given in Table I. The main peak is riboflavin-5′-phosphate; the first-eluting compound (*e.g.*, with a migration time of 5.02 min at pH 9.1) is riboflavin. Components with migration times longer than that of riboflavin-5′-phosphate are other riboflavin mono- and diphosphates.

additional peak (at 8.87 min) and a pH 7.0 two additional peaks (at 9.17 and 9.48 min, respectively) are resolved from the largest peak (riboflavin-5′-phosphate). The improved resolution is caused by the increase in selectivity due to changes in the effective mobilities of the analytes, caused by the different extents of dissociation.

Under the given conditions these components migrate as anions like the main component, riboflavine-5′-phosphate, showing similar fluorescence characteristics. Because of the nearly identical mobilities of the fully dissociated species, which are observed at high pH (9.1), it can be assumed that all these analytes are riboflavin

monophosphates, being isomers with respect to the position of the phosphate group on the saccharide.

A further decrease in the pH to 6.0 results in a better separation of the monophosphates, but the two anionic components with migration times of about 12 min at pH 7.0 (according to their electrophoretic behaviour they are probably riboflavin diphosphates) cannot be determined within a reasonable analysis time, because at pH 6 their electrophoretic velocities are too high compared with the electroosmotic velocity of the bulk liquid. It can therefore be concluded that the buffer of pH 7 will give the best results for quantitative analysis.

Precision of the migration time

The reproducibility of the migration times in capillary electrophoresis often depends on the nature of the sample. Especially with proteins, poor reproducibility is observed for subsequent injections, caused by changes in the electroosmotic flow due to interactions of sample components with the silica surface of the capillary, leading to variations of the zeta potential. In these instances, the reproducibility is enhanced by regeneration of the surface on rinsing the capillary with sodium hydroxide solution.

However, for the riboflavin-5′-phosphate samples no such interactions were observed. This is reflected by the excellent precision of the migration times obtained even without rinsing the capillary after the analytical run; a value of 0.6% was found, *e.g.*, for the relative confidence interval of the migration time of riboflavin-5′-phosphate at pH 9.1 (relative standard deviation 1.2%, 16 measurements). This is a typical value found with short term usage.

Quantification

Normalization of the analyte concentrations to 100% is usually applied for the specification of the purity of chemicals or drugs. In general, this method of calibration requires the determination of the individual response factors of the particular analytes. However, for the special analytical problem considered it can be assumed that the different riboflavin derivatives are all detected with equal response. Therefore, no individual calibration functions need to be determined.

When injection is carried out using electromigration, the components are not transferred into the separation capillary with the same mass ratios as in the original sample. Discrimination occurs, whereby the injected amounts are proportional to the sum of the velocity vectors of the electroosmotic and the electrophoretic migration. As electroosmosis causes a flow that is directed towards the cathode under given conditions, the resulting velocity for anions is given by the differences in the scalar velocities of electrophoresis and electroosmosis. The relative amounts of anionic analytes in the separation capillary are therefore always lower than those in the original sample. However, this discrimination by injection is counterbalanced, at least when the concentration of the sample components is significantly lower than that of the buffer in which they are dissolved, by the different migration velocities through the detector cell, which are also proportional to the sum of the vectors mentioned. Given equal fluorescence properties of the analytes, the peak areas (which are based on time, but not on length) can therefore be used directly for quantification.

With this assumption, the content of riboflavin-5′-phosphate was found to be between 72 and 75% in all samples, with a typical value of 1.5% for the relative

confidence interval (five measurements, 95% confidence level). The difference from 100% is caused by the presence of riboflaving (about 7%), other riboflavin monophosphates (about 16%) and riboflavin diphosphates (about 4%).

The deviations of the riboflavin-5′-phosphate contents from those given by the producers can be attributed to the different methods of determination. With spectrophotometric measurements the sum of all riboflavin derivatives and not riboflavin-5′-phosphate specifically is determined. The differences in the quantitative results obtained by (RP-)HPLC and capillary zone electrophoresis probably occur because in HPLC, in contrast to electrophoresis, only a group separation is achieved. Riboflavin and the riboflavin mono- and diphosphates can easily be separated, but the particular monophosphates are probably not resolved. Therefore, their individual contents are not determined.

ACKNOWLEDGEMENT

The authors acknowledge financial support and the donation of a fluorescence detector from E. Merck, Darmstadt, F.R.G.

REFERENCES

1 M. K. Park and J. H. Cho, *Arch. Pharmacol. Res.*, 11 (1988) 45.
2 I. Kamada and T. Adachi, *Kyoto-fu Eisei Kogai Kenkyusho Nenpo*, 33 (1988) 36.
3 K. D. Altria and C. F. Simpson, *J. Pharm. Biomed. Anal.*, 6 (1988) 801.
4 A. Lopez-Anaya and M. Mayersohn, *J. Chromatogr.*, 423 (1987) 105.
5 T. Perez-Ruiz, M. C. Martinez-Lozano and U. Tomas, *Analyst (London)*, 112 (1987) 237.
6 F. L. Lam and A. Lowande, *J. Pharm. Biomed. Anal.*, 6 (1988) 87.
7 R. Roeben and K. Rubach, presented at *Anal. Prep. ITP, Fourth International Symposium on ITP, Hradec Kralove, 1984.*
8 D. C. Wollard, *J. Chromatogr.*, 301 (1984) 470.
9 I. D. Lumley and R. A. Wiggins, *Analyst (London)*, 106 (1981) 1103.
10 K. Shimura and T. Kamada, *Mie-ken Eisei Kenkyusho Nenpo*, 32 (1987) 105.
11 S. P. E. Reyes, K. M. Norris, C. Taylor and D. Potts, *J. Assoc. Off. Anal. Chem.*, 71 (1988) 16.
12 P. Nielsen, P. Rauschenbach and K. Bacher, *Anal. Biochem.*, 130 (1983) 359.

Journal of Chromatography, 508 (1990) 208–211
Elsevier Science Publishers B.V., Amsterdam — Printed in The Netherlands

CHROM. 22 356

Note

Direct chromatographic separation of the enantiomers of oxiracetam

PATRICK CAMILLERI*, JOSÉ A. MURPHY and CHRISTOPHER THORPE
Smith Kline and French Research Ltd., The Frythe, Welwyn, Hertfordshire AL6 9AR (U.K.)
(First received January 23rd, 1990; revised manuscript received February 16th, 1990)

Oxiracetam (4-hydroxy-2-oxo-1-pyrolidineacetamide) (**1**) is a new drug that has neurochemical properties mostly expressed in the improvement of both learning and memory[1,2].

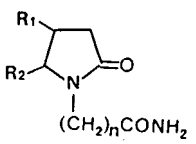

(**1**) $R_1 = OH$, $R_2 = H$, $n = 1$
(**2**) $R_1 = H$, $R_2 = OH$, $n = 1$
(**3**) $R_1 = OH$, $R_2 = H$, $n = 2$

As oxiracetam has a chiral centre, a detailed investigation of both its pharmacokinetic and pharmacodynamic properties could require a knowledge of the individual behaviour of each of the enantiomers under a variety of biological conditions. As a first step of achieving this a method has to be developed that would allow the chromatographic separation of these optical isomers, preferably without derivatisation. In this paper we describe the direct separation and characterisation of the enantiomers of **1** on a chiral stationary phase. We also compare this chromatographic separation with that of two of its closely related molecules, namely, 5-hydroxy-2-oxo-1-pyrolidineacetamide (**2**) and 4-hydroxy-2-oxo-1-propionemide pyrolidine (**3**) in order to collect information about the possible mechanism of retention and chiral recognition.

EXPERIMENTAL

n-Hexane (Rathburn) and absolute ethanol (James Burrough) were degassed with helium before use. Oxiracetam (**1**) and its derivatives **2** and **3** were supplied by Dr. M. Pinza (ISF, Trezzano sul Naviglio, Italy).

High-performance liquid chromatography (HPLC)

HPLC analysis of compounds **1–3** was carried out on a Perkin-Elmer Series 4 liquid chromatograph. A Chiralcel OC (cellulose triphenylcarbamate) column (250 mm × 4.6 mm I.D.) gave the best resolution of the optical isomers of **1** and **3**, using hexane-ethanol at ratios 75:25, 80:20 and 85:15 (as appropriate, see Table I) flowing

0021-9673/90/$03.50

TABLE I

VARIATION IN RETENTION TIMES OF **1**, **2** AND **3** WITH VARIATION IN THE RATIO OF HEXANE TO ETHANOL AT 1 ml min^{-1}

Compound	*Hexane–ethanol*	*Retention times (min)*	*Separation factor*
1	75:25	39.4, 44.1	1.15
2		32.7	
3		34.1, 35.1	1.03
1	80:20	60.2, 67.2	1.13
2		50.1	
3		48.3, 50.1	1.04
1	85:15	113.3, 126.4	1.12
2		88.1	
3		92.6, 96.2	1.04

at a rate of 1 ml min^{-1}. The chromatography column was operated at ambient temperature and compounds were detected at 205 nm.

RESULTS AND DISCUSSION

The chromatographic resolution of the optical isomers of oxiracetam (**1**) is shown in Fig 1a, using a Chiralcel OC column and hexane–ethanol (75:25) as eluent. This column was the only one that gave excellent separation of the enantiomers. No resolution was obtained using a variety of other columns, such a Chiralcel OJ or OF, β-cyclodextrin and α_1-acid glycoprotein.

The separation factor α from the data in Fig. 1a was calculated as 1.15. The first and second peaks were assigned as $S(-)$ and $R(+)$ by comparison to authentic samples of the respective enantiomers (kindly supplied by Dr. M. Pinza, ISF).

Oxiracetam (**1**) is a relatively simple molecule. The absence of one or more aromatic groups in this molecule precludes the occurence of any π–π interactions with the phenyl carbamate residues on the cellulose adsorbed on the column silica gel support. However, the abundance of polar groups, the pyrolidone ring itself and the polar substituents –OH and $-CH_2\ CONH_2$, increases the possibility of chiral discrimination taking place due to "three-point" interaction(s)[3] solely involving hydrogen bonding and/or dipole interactions between **1** and the ciral stationary phase. Such interactions are expected to be stronger when the eluting solvent is relatively non-polar.

Fig. 1b shows the chromatogram of **2**, and isomer of oxiracetam, where the hydroxy substituent on the 2-pyrolidone ring (and hence the chiral centre) is closer to the nitrogen of the lactam moiety. No chiral resolution of the optical isomers of **2** could be obtained as shown in Table I. It is also clear from this table that the retention time of **2** is considerably shorter than that of either of the optical isomers of **1** under the same chromatographic conditions. These differences in retention behaviour are almost certainly due to differences in the hydrophobic nature of the two positional isomers. It is only in the case of molecule **2** that hydrogen bonding is possible between the hydroxy group and the carbonyl moiety in the substituent attached to the lactam nitrogen (Fig. 2).

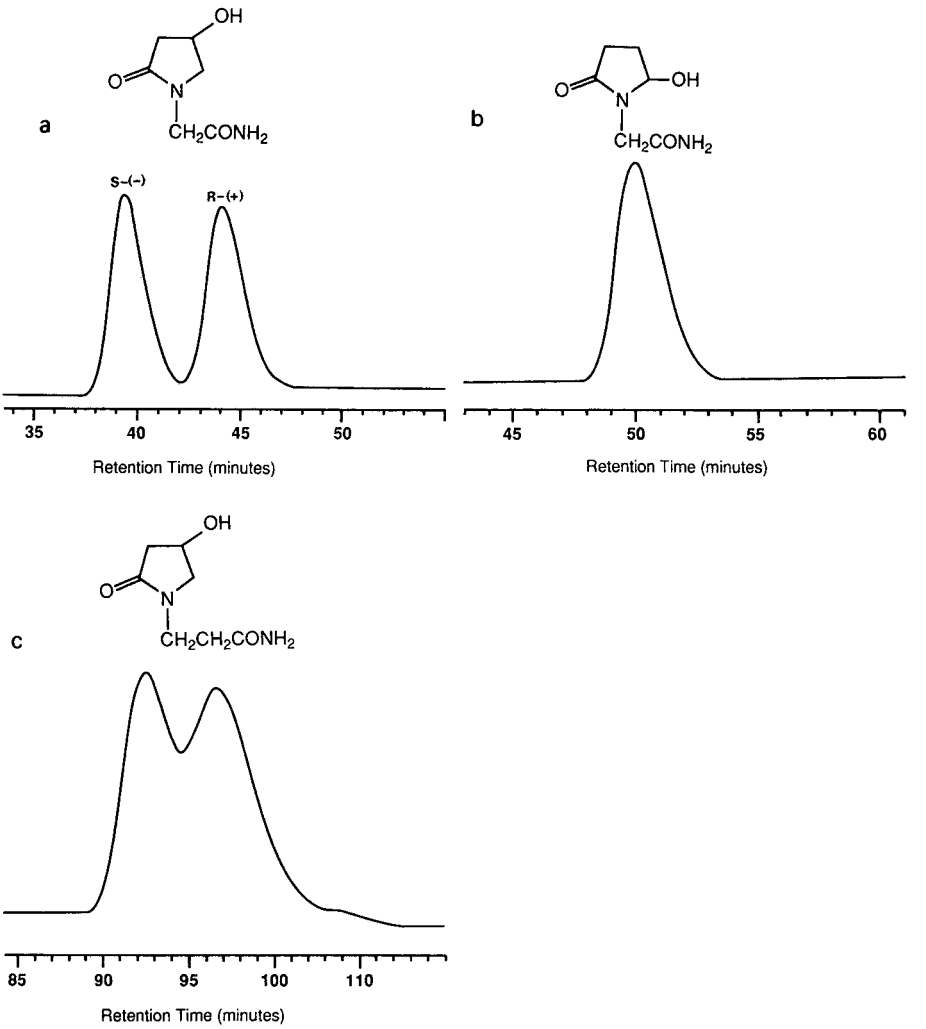

Fig. 1. (a) Chromatographic resolution of oxiracetam (**1**). Eluent, hexane–ethanol (75:25, v/v). (b) Chromatogram obtained for **2**. Eluent, hexane–ethanol (80:20, v/v). (c) Separation of the optical isomers of **3**. Eluent, hexane–ethanol (85:15, v/v). Other conditions given in the experimental section.

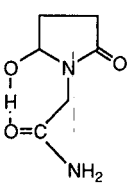

Fig. 2. Proposed hydrogen bonding that can occur in **2**, preventing the resolution of the optical isomers of this molecule.

The hydroxyl and carbonyl groups in **1** are too far apart for this type of intramolecular hydrogen bonding to occur. Moreover, the hydrogen bonding in **2** is expected to be favoured under non-polar conditions of chromatography. "Tying in" the hydroxyl group in intramolecular bonding hinders it and the amide carbonyl group from hydrogen bonding to the chiral support, thus allowing **2** to elute faster than oxiracetam (**1**).

The lack of separation of the optical isomers of **2** may also be an indication of the importance of the hydroxyl substituent (attached to the chiral centre) in the three-point interaction essential for chiral discrimination of the enantiomers of **1** by the Chiralcel OC column. We have carried out preliminary molecular modelling studies (results not shown) that confirm the occurrence of three hydrogen bonding interactions of **1** with the chiral stationary phase, stereoselective for interactions involving the hydroxyl substituent. It is only in the *R* configuration that chiral recognition is possible. We have also modelled a number of other non-stereoselective interactions between **1** and chiral stationary phase; such interactions contribute to the extent **1** is retained on the column.

To gain further insight into the mechanism of retention of oxiracetam (**1**) on the chiral support we studied the chromatographic behaviour of **3** which has two methylene groups separating the primary amide group from the lactam. As expected, **3** has a shorter retention time than **1** (Fig. 1c) because the "extra" methylene group in **3** makes it more hydrophobic than **1**. The substituted constant π is a good measure of hydrophobicity[4] and the π values for $-CH_2CONH_2$ and $CH_2CH_3CONH_2$ are -1.68 and -1.21, respectively. The separation factor for **3** is also smaller than for **1** (Table I) indicating smaller energy differences involved in the equilibrium processes of each of the optical isomers of **3** between the mobile phase and the chiral stationary phase. These smaller differences may arise due to weaker (longer) hydrogen bond interactions of this molecule with the chiral support, leading to a low separation factor for the optical isomers of **3**.

The excellent resolution of the optical isomers of oxiracetam (**1**) make the chromatographic method outlined most suitable for studies designed to probe the enantiomeric distribution of the antipodes of **1** in biological media.

REFERENCES

1 S. Benfi, L. Dorigotti, M. P. Abbracchio, W. Bolduini, E. Coen, C. Ragusa and F. Cottabeni, *Pharm. Res. Commun.*, 16 (1984) 69.
2 G. Spignoli and G. Pepeu, *Eur. J. Pharm.*, 126 (1986) 253.
3 C. H. Lochmüller and R. W. Souter, *J. Chromatogr.*, 113 (1975) 302.
4 C. Hansch and A. Leo, *Substituent Constants for Correlation Analysis in Chemistry and Biology*, Wiley, New York, 1979.

Journal of Chromatography, 508 (1990) 212–216
Elsevier Science Publishers B.V. Amsterdam — Printed in The Netherlands

CHROM. 22 320

Note

Enantiomeric separation of racemic pterocarpans by high-performance liquid chromatography on (+)-poly(triphenylmethyl methacrylate)-coated silica gel

SANDOR ANTUS*
Research Group for Alkaloid Chemistry, Hungarian Academy of Sciences, P.O. Box 91, H-1521 Budapest (Hungary)
RUDOLF BAUER
Institut für Pharmazeutische Biologie der Universität München, Karlstrasse 29, D-8000 München 2 (F.R.G.)
AGNES GOTTSEGEN
Research Group for Alkaloid Chemistry, Hungarian Academy of Sciences, P.O. Box 91, H-1521 Budapest (Hungary)
and
HILDEBERT WAGNER
Institut für Pharmazeutische Biologie der Universität München, Karlstrasse 29, D-8000 München 2 (F.R.G.)
(Received January 19th, 1990)

In recent years, the use of high-performance liquid chromatography (HPLC) for the separation of enantiomers increased rapidly as a number of chiral stationary phases became commercially available[1–4] and some of them have been proposed for the separation of enantiomeric flavonoids. Okamoto *et al.*[5] successfully separated a racemic mixture of the unsubstituted flavanone on cellulose triphenylcarbamate supported on silica gel (Chiralcel OC; Daicel, Japan). Krause and Galensa[6] used microcrystalline cellulose triacetate as a chiral stationary phase for the separation of racemic polyhydroxy flavanones. The optical resolution of chalcone epoxides and flavanols has also been achieved by using a helical poly(triphenylmethyl methacrylate)-coated silica gel [Chiralpack OT (+); Daicel][7]. This chiral stationary phase has also shown an extraordinary selectivity for many enantiomers of rotenoids possessing a rigid non-planar structure[8].

As the naturally occurring pterocarpans, a group of compounds with phytoalexin properties, also possess a rigid non-planar structure due to *cis* B/C ring fusion, it was considered of interest to study the separation of corresponding enantiomeric mixtures on helical (+)-poly(triphenylmethyl methacrylate)-modified silica gel. In this paper we report the enantiomeric separation of synthetic and naturally occurring racemic pterocarpans (Fig. 1) and the influence of their substitution patterns on chromatographic resolution.

0021-9673/90/$03.50

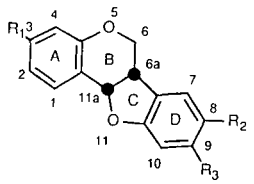

	R_1	R_2	R_3
1	H	H	H
2	OH	H	H
3	OH	H	OEt
4	OMe	H	OH
5	OH	$-OCH_2O-$	
6	OH	H	OMe
7	OMe	H	OMe
8	OnPr	H	OMe
9	OCH_2CO_2Et	H	OMe
10	$O(CH_2)_{10}CO_2Et$	H	OMe
11	OCH_2CH_2OH	H	OMe
12	$O(CH_2)_{10}CH_2OH$	H	OMe
13	OAc	H	OMe
14	$OCOCH_2CH_3$	H	OMe
15	$OCO(CH_2)_9CH_3$	H	OMe
16	OCH_2OMe	H	OMe
17	OCH_2OEt	H	OMe
18	THP	H	OMe

Fig. 1. Pterocarpans studied. Et = C_2H_5; Me = CH_3.

EXPERIMENTAL

Materials

The racemates of pterocarpan (**1**), 3-hydroxypterocarpan (**2**), 3-hydroxy-9-ethoxypterocarpan (**3**), 3-methoxy-9-hydroxypterocarpan (**4**), maackiain (**5**) and medicarpin (**6**) were synthesized by the thallium(III) nitrate method[9] starting from 2′-hydroxychalcones. Homopterocarpin (**7**) and other medicarpin derivatives (**8–18**) were prepared from **6**[10].

HPLC

The HPLC separation was carried out with a Hewlett-Packard HP 1090A instrument using an HP 1040A photodiode-array detection system and an HP 3392A integrator. Chiralpak OT (+), 250 mm × 4.6 mm (Daicel), was used as the stationary phase. The mobile phase was methanol (HPLC grade) at a regular flow-rate of 0.5 ml/min.

Photometric detection was performed at 280 nm. The injection volume was 10 μl (*ca.* 10 μg). Polarimetric detection was performed with an ACS ChiraMonitor

(Applied Chromatography Systems, Cheshire, U.K.) with a 20-μl flow cell of path length 20 mm using a 2-mW collimated near-IR laser diode (830 nm) as light source[11]. The injection volume was 50 μl (*ca.* 50 μg).

RESULTS AND DISCUSSION

Chromatographic data for the enantiomeric pterocarpan derivatives **1–18** on poly(triphenylmethyl methacrylate) using methanol as the mobile phase at 0.5 ml/min are given in Table I and Fig. 2. In this separation system most of the racemates were baseline resolved. In every instance the dextrorotatory enantiomers of 6a*S*, 11a*S* configuration[12,13] were eluted first. It is interesting that most of the known natural pterocarpans have large negative $[\alpha]_D$ values owing to the 6a*R*, 11a*R* absolute configuration, but homopterocarpin (**7**)[14], medicarpin (**6**)[14,15] and maackiain (**5**)[16,17] exist in nature in both antipodal forms and the last two also as racemates[14,17].

A very high resolution (R_s = 4.00) and separation factor (α = 2.43) were observed for the unsubstituted pterocarpan (**1**). This clearly showed that a strong π–π interaction between the aromatic parts of the substrate and the pendant trityl groups of the polymeric chain is the most important factor in the chiral recognition mechanism.

Owing to a possible hydrogen-bonding mechanism, this non-polar interaction can strongly be disturbed by the hydroxy substituent of the A-ring (**2**, R_s = 1.00) or by the primary alcoholic function of the side-chain connected at C-3 of the pterocarpan skeleton (**11**, **12**, R_s = 1.52 and 1.85, respectively). In the presence of an alkoxy group

TABLE I

CHROMATOGRAPHIC DATA FOR RACEMIC PTEROCARPANS

t_R = Retention time (min); R_s = resolution factor = 2 × (distance between the peaks of the enantiomers)/sum of band widths of the two peaks; k' = capacity factor = (retained volume of enantiomer − void volume of column)/void volume of column; α = separation factor = $k'(-)/k'(+)$.

Compound	$t_R(-)$	$k'(-)$	$t_R(+)$	$k'(+)$	α	R_s
1	23.36	5.31	11.77	2.18	2.44	4.00
2	11.14	2.01	9.21	1.49	1.35	1.00
3	13.85	2.74	9.47	1.56	1.76	1.91
4	12.50	2.38	9.25	1.50	1.59	2.00
5	11.31	2.06	9.32	1.52	1.35	2.20
6	12.17	2.29	8.97	1.42	1.61	2.10
7	19.19	4.19	13.54	2.66	1.57	2.40
8	22.92	5.19	14.66	2.96	1.75	3.03
9	22.48	5.08	14.08	2.81	1.81	2.80
10	42.35	10.45	24.55	5.64	1.85	2.04
11	12.92	2.49	9.84	1.66	1.50	1.52
12	20.95	4.66	13.70	2.70	1.73	1.85
13	13.78	2.72	11.41	2.08	1.31	1.00
14	15.32	3.14	11.16	2.02	1.56	1.75
15	23.40	5.32	14.39	2.89	1.84	1.83
16	20.41	4.52	12.98	2.51	1.80	2.92
17	19.67	4.32	13.04	2.52	1.71	2.12
18[a]	15.74/18.73	3.18/4.06	9.31/10.77	1.52/1.91	2.10/2.13	2.20/1.38

[a] Retention times with a flow-rate of 1.0 ml/min.

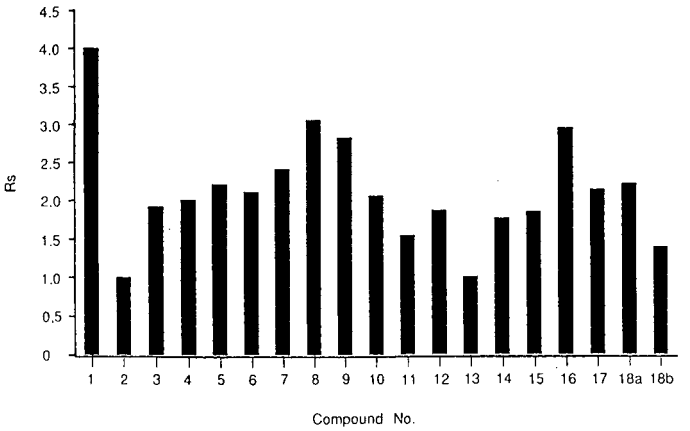

Fig. 2. Chromatographic resolution (R_s) of racemic pterocarpan derivatives on (+)-poly(triphenylmethyl methacrylate)-coated silica gel. Mobile phase: methanol at a flow-rate of 0.5 ml/min.

on the A- or D-ring, this effect decreases considerably. Therefore, an adequate resolution of the eantiomers was achieved for **3**–**6**. For maackiain (**5**) a resolution factor of 1.8 and very small capacity factors (0.166 and 0.3) have been reported by Zief[18].

On reducing the polar character of medicarpin (**6**) by etherification of the hydroxy group, the enantiomeric separation (R_s for **6** < **7** < **8** ≈ **16**) improved

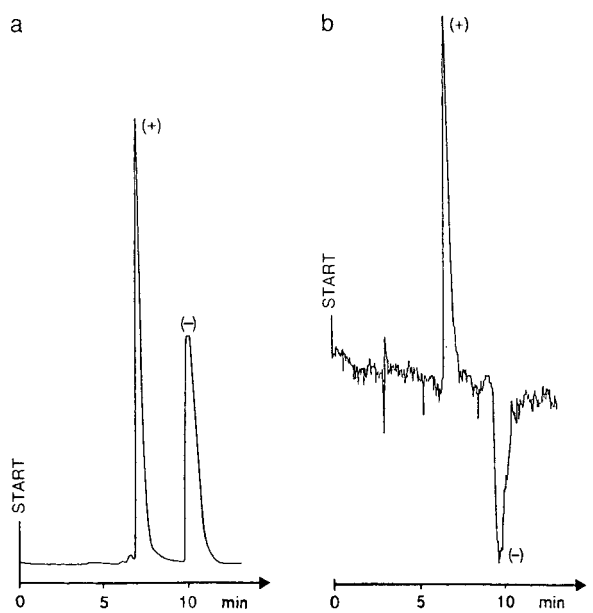

Fig. 3. HPLC separation of 46 μg 3-O-*n*-propylmedicarpin (**8**) on (+)-poly(triphenylmethyl methacrylate)-coated silica gel. Mobile phase: methanol at a flow-rate of 1.0 ml/min. Dual detection: (a) photometric detection at 280 nm (attenuation 256 × 0.01); (b) ACS ChiraMonitor (attenuation 4).

significantly (Fig. 3). The optimum length of the alkyl or alkoxy substituent seems to be *ca.* 2.5 Å, shown by the fact that elongation of the side-chain of **16** with one CH_2 group has resulted in a decreasing resolution factor (**16**, **17**, R_s = 2.92 and 2.12, respectively). The same effect was observed with ethoxycarbonylmethyl derivatives (**9**, **10**). In agreement with the findings of Takahashi *et al.*[7], replacement of the hydroxy or methoxy group on the aromatic ring by an acetoxy group also lowered the R_s values (**13**, R_s = 1.00). This unfavourable effect could be partly compensated for by the alkyl moiety of the ester group (R_s of **13** < **14** < **15**).

CONCLUSION

Poly(triphenylmethyl methacrylate) is a useful chiral stationary phase for resolving racemic hydroxypterocarpan derivatives. The efficiency of the separation is increased by derivatization of the hydroxy group with methoxymethyl or *n*-propyl functions. This technique can be applied to the optical resolution of synthetic or natural racemates of pterocarpans to obtain the corresponding optical isomers for studies of structure–activity relationships. Further investigations are in progress to study the chiral recognition mechanism with respect to the substitution pattern of pterocarpans.

ACKNOWLEDGEMENTS

We are grateful to Zinsser Analytic (Frankfurt/M., F.R.G.) for the opportunity of testing the ACS ChiraMonitor, and to Mr. Krause, Institut für Lebensmittelchemie der Technische Universität Braunschweig (Braunschweig, F.R.G.), for his valuable advice on enantiomer separations.

REFERENCES

1 R. Däppen, H. Arm and V. R. Meyer, *J. Chromatogr.*, 373 (1986) 1.
2 G. Blaschke, *J. Liq. Chromatogr.*, 9 (1986) 341.
3 V. A. Davankov, *Adv. Chromatogr.*, 22 (1983) 71.
4 D. W. Armstrong, *J. Liq. Chromatogr.*, 7 (1984) 353.
5 Y. Okamoto, M. Kawashima and K. Hatada, *J. Chromatogr.*, 363 (1986) 173.
6 M. Krause and R. Galensa, *J. Chromatogr.*, 441 (1988) 417.
7 H. Takahashi, S. Li, Y. Harigaya and M. Onda, *Heterocycles*, 26 (1987) 3239.
8 S. L. Abidi, *J. Chromatogr.*, 404 (1987) 133.
9 L. Farkas, A. Gottsegen, M. Nogradi and S. Antus, *J. Chem. Soc., Perkin Trans. 1*, (1974) 305.
10 S. Antus, R. Bauer, A. Gottsegen, P. Kolonits, O. Seligmann and H. Wagner, in preparation.
11 D. K. Lloyd, D. M. Goodall and H. Scrivener, *Anal. Chem.*, 61 (1989) 1238.
12 S. Ito, Y. Fujise and M. Mori, *Chem. Commun.*, (1965) 595.
13 H. Suginome and T. Iwadare, *Experientia*, 18 (1962) 163.
14 W. D. Ollis, in T. J. Mabry, R. E. Alston and V. C. Runeckles (Editors), *Recent Advances in Phytochemistry*, Vol. 1, Appleton–Century–Crofts, New York, 1968, pp. 329–378.
15 W. Cocker, T. B. H. McMurray and P. A. Staniland, *J. Chem. Soc.*, (1965) 1034.
16 W. Cocker, T. Dahl, C. Dempsey and T. B. H. McMurray, *J. Chem. Soc.*, (1962) 4906.
17 R. Braz F°., O. R. Gottlieb, S. L. V. Pinho, Q. J. F. Monte and A. I. D. Rocha, *Phytochemistry*, 12 (1973) 1184.
18 M. Zief, *J. Chromatogr. Sci.*, 40 (1988) 331.

Journal of Chromatography, 508 (1990) 217–219
Elsevier Science Publishers B.V., Amsterdam — Printed in The Netherlands

CHROM. 22 317

Note

Optical resolution of abscisic acid metabolites using an ovomucoid-conjugated high-performance liquid chromatographic column

MASAHIKO OKAMOTO* and HIROSHI NAKAZAWA

Biochemistry and Toxicology Laboratory, Sumitomo Chemical Co., Ltd., 1-98, 3-chome, Kasugade-naka, Konohana-ku, Osaka 554 (Japan)

(First received November 24th, 1989; revised manuscript received January 26th, 1990)

Abscisic acid (ABA, **1**) plays important roles in many aspects of plant growth and development[1]. Studies on the metabolism of ABA involve particularly difficult analytical problems. As with all studies of metabolism using racemic substrates, establishing the optical purity of the products is very important. Especially for trace components such as plant hormones and their metabolites, this can only be done with considerable difficulty.

Recently we achieved the direct optical resolution of racemic ABA by high-performance liquid chromatography (HPLC) on an ovomucoid-conjugated column, ULTRON ES-OVM[2]. Very little is known about the optical resolution of the metabolites of ABA. We report here the direct optical resolution of the metabolites of ABA, phaseic acid (PA, **2**) and the 1′,4′-diols of abscisic acid (1′,4′-*cis*- and -*trans*-diol-ABA, **3** and **4**).

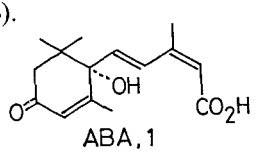

ABA, 1

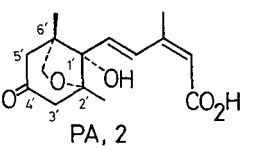

PA, 2

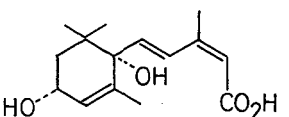

1′,4′-cis-Diol ABA, 3

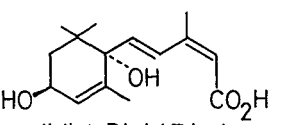

1′,4′-t-Diol ABA, 4

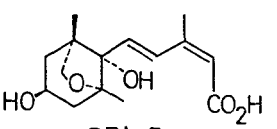

DPA, 5

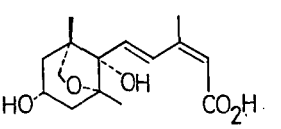

epi-DPA, 6

0021-9673/90/$03.50

EXPERIMENTAL

Apparatus

A Shimadzu LC-5A instrument equipped with an SPD-2A variable-wavelength UV Monitor was used. A stainless-steel column (150 × 4.6 mm I.D.) was packed with ovomucoid-conjugated aminopropylsilica gel (5 μm), now available as ULTRON ES-OVM (Shinwakako, Kyoto, Japan).

Chemicals

(1′*S*, 2′*R*, 6′*R*)-PA (natural form) and (1′*R*, 2′*S*, 6′*S*)-PA (unnatural form) were kindly supplied by Dr. T. Kitahara. Racemic ABA was bought from Wako (Osaka, Japan). (+)-(*S*)-ABA was provided by Dr. N. Hirai. The 1′,4′-diols of ABA were synthesized as described previously[3]. Dihydrophaseic and *epi*-dihydrophaseic acid (DPA, **5**, and *epi*-DPA, **6**) were prepared by the method of Hirai and Koshimizu[4]. All other chemicals were of analytical-reagent grade.

RESULTS AND DISCUSSION

Our previous studies[2] indicated that the resolution of ABA on the ovomucoid-conjugated column could be regulated by varying the pH and hydrophobicity of the mobile phase. This result led to the conclusion that ABA was best resolved in the use of 2% 2-propanol in 20 m*M* potassium phosphate buffer (pH 3.50) as the mobile phase. Under these conditions, we attempted to separate the enantiomers of ABA metabolites (**2**–**6**). The chromatographic results are summarized in Table I and typical chromatograms are shown in Figs. 1 and 2. In these separations, the retention of natural isomers was always longer than that of unnatural isomers, showing that the affinity between the ovomucoid and natural isomers may be more stable. The chiral ovomucoid-conjugated column (ULTRON ES-OVM) showed beter enantioselectivity for the 1′,4′-diols of ABA (**3** and **4**) than that for ABA. It is suggested that the 4′-hydroxyl group of the diols contributes more significantly than the 4′-keto group of ABA to the interaction with ovomucoid.

An excellent separation factor (α = 1.97) was obtained in the enantiomeric

TABLE I

DIRECT ENANTIOMERIC SEPARATION OF ABA AND ITS DERIVATIVES BY HPLC WITH ULTRON ES-OVM

A 2% 2-propanol–20 m*M* potassium phosphate buffer (pH 3.50) was used as the mobile phase at 1.0 ml/min at ambient temperature with UV detection (254 nm, 0.04 a.u.f.s.). ABA was best resolved under these conditions.

Compound	k'_1	k'_2	α
ABA	10.00	12.20	1.22
PA	3.53	6.94	1.97
1′,4′-*cis*-Diol-ABA	10.90	14.99	1.38
1′,4′-*trans*-Diol-ABA	4.40	6.14	1.40
DPA	1.74	–	1.00
epi-DPA	2.45	–	1.00

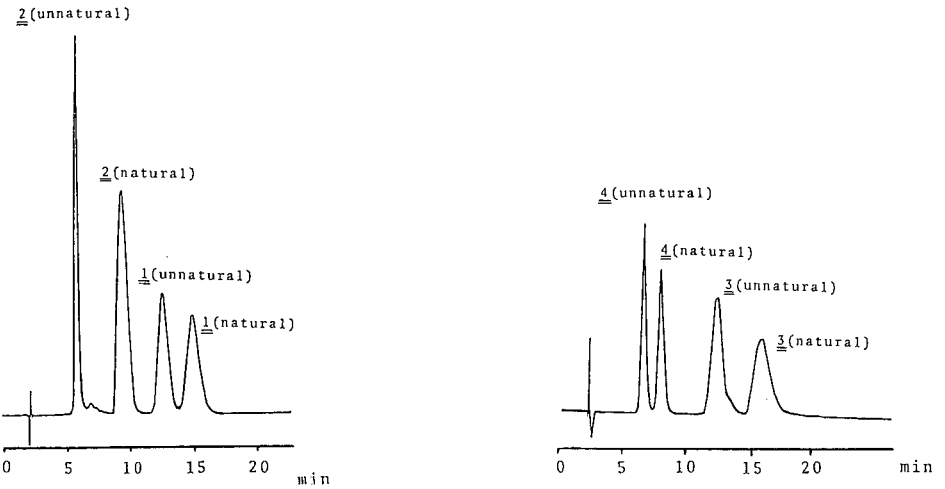

Fig. 1. Separation of the enantiomers of ABA (**1**) and PA (**2**). Chromatographic conditions as in Table I.

Fig. 2. Separation of the enantiomers of 1′,4′-*cis*- and *trans*-diol-ABA (**3** and **4**).

separation of PA. This enantioselectivity may be attributed to the fact that tetrahydrofuran bridge containing ether oxygen is available for hydrogen bonding interactions with the chiral stationary phase. This column has no enantioselectivity for DPA (**5**) and *epi*-DPA (**6**) which are very polar metabolites of ABA. The lack of enantioselectivity may be ascribed to their smaller hydrophobicity, because ABA, 1′,4′-diols of ABA and PA were separated to a considerable extent. Previously we showed[2] that hydrophobic interactions may play important roles in the retention of ABA, but that they are not essential for the resolution. This experiment shows that the ovomucoid column has advantages for the resolution of compounds with suitable hydrophobicity.

This is the first report on the optical resolution of ABA-related compounds. PA is the major catabolite of ABA which is subsequently reduced to DPA and *epi*-DPA[1]. 1′,4′-*cis*-Diol-ABA is assumed to be a natural catabolite[5]. 1′,4′-*trans*-Diol-ABA can act as a precursor of ABA rather than being a catabolite[3,6–8].

Therefore, we believe that the results of this study will be useful when examining the enantioselectivity of the enzymes which catalyse the metabolism of ABA.

ACKNOWLEDGEMENTS

We thank Dr. T. Kitahara and Professor K. Mori of the University of Tokyo for their gifts of natural and unnatural PA. We are also grateful to Dr. N. Hirai and Professor K. Koshimizu of Kyoto University for providing natural ABA standard.

REFERENCES

1 J. A. D. Zeevaart and R. A. Creelman, *Annu. Rev. Plant Mol. Biol.*, 39 (1988) 439.
2 M. Okamoto and H. Nakazawa, *J. Chromatogr.*, 504 (1990) 445.
3 N. Hirai, M. Okamoto and K. Koshimizu, *Phytochemistry*, 25 (1986) 1865.
4 N. Hirai and K. Koshimizu, *Agric. Biol. Chem.*, 47 (1983) 365.
5 W. Dathe and G. Sembdner, *Phytochemistry*, 21 (1982) 1798.
6 M. Okamoto, N. Hirai and K. Koshimizu, *Phytochemistry*, 26 (1987) 1269.
7 M. Okamoto, N. Hirai and K. Koshimizu, *Phytochemistry*, 27 (1988) 2099.
8 M. Okamoto, N. Hirai and K. Koshimizu, *Phytochemistry*, 27 (1988) 3465.

Journal of Chromatography, 508 (1990) 220–224
Elsevier Science Publishers B.V., Amsterdam — Printed in The Netherlands

CHROM. 22 312

Note

Liquid chromatographic evaluation of chiral derivatizing reagents for the resolution of amine and alcohol enantiomers

YE ZHOU* and ZENG-PEI SUN
National Institute for the Control of Pharmaceutical and Biological Products, Beijing 100050 (China)
(First received September 12th, 1989; revised manuscript received January 15th, 1990)

Chiral isocyanates are usually considered to be one of the best derivatizing reagents for the indirect separation of drug enantiomers. Only two compounds of this kind, *viz.*, *S*(−)- or *R*(+)-naphthylethyl isocyanate (NEIC) and *S*(−)- or *R*(+)-phenylethyl isocyanate (PEIC), have been reported so far. Both of them give good resolutions of optical amines[1,2], but only NEIC has been reported to resolve two enantiomeric alcohols[3,4] on heating at 80°C for 36 h during derivatization. Further, these isocyanates were prepared from their corresponding optical amines by the action of phosgene or trichlorosilane, which are toxic and not practical in an ordinary analytical laboratory.

Therefore, we first synthesized N-[(2-naphthalene)sulphonyl]prolyl isocyanate (NSPI) from L-proline. This paper describes its synthesis and liquid chromatographic evaluation for the optical separation of amines and alcohols, and the structural identification of their diastereomeric derivatives.

Moreover, an azide is usually applied as an intermediate in the synthesis of isocyanates, to conjugate with the amino group of an amino acid to form peptides in organic chemistry, having the advantage of minimum racemization[5]. We therefore need N-[(2-naphthalene)sulphonyl]prolyl azide (NSP-N_3) to resolve amine enantiomers, which has not been reported previously. This procedure retains the configurations of the chiral centres during derivatization, which is very important for the indirect separation of enantiomers.

EXPERIMENTAL

Chemicals and reagents

L-Proline (Sigma, St. Louis, MO, U.S.A.) and 2-naphthalenesulphonyl chloride (Fluka, Buchs, Switzerland) were used. Ethyl chloroformate, triethylamine, light petroleum (b.p. 60–90°C), isopropanol, toluene and other chemicals of analytical-reagent grade were purchased in China.

Racemic mexiletine hydrochloride, amphetamine and 1-phenylpropanol were obtained as drug materials. The free base of mexiletine was obtained from its hydrochloride.

0021-9673/90/$03.50

Apparatus

The high-performance liquid chromatographic (HPLC) system consisted of a Waters Model 6000A pump, a Rheodyne 7105 injector and a Shimadzu SPD-1 UV detector monitoring at 254 nm, coupled with a Hitachi 056 recorder or a Shimadzu Chromatopac C-R3A.

The stationary phase was silica gel (7-9 μm) (Tianjing, China) packed in a 30 cm × 4.0 mm I.D. column by the slurry packing method. The mobile phase was a mixture of light petroleum and isopropanol in suitable proportions.

Preparation of chiral derivatizing reagents

S(−)-N-1-(2-Naphthalenesulphonyl)-2-proline (NSP) was prepared from L-proline and 2-naphthalenesulphonyl chloride as described previously[6] and had m.p. 130–133°C.

N-[(2-Naphthalene)sulphonyl]prolyl azide (NSP-N_3) was synthesized from NSP, ethyl chloroformate and sodium azide[7]. In the IR spectrum (KBr), peaks at 2160 and 1720 cm^{-1} denoted the azide group.

N-[(2-Naphthalene)sulphonyl]prolyl isocyanate (NSPI) was prepared by heating NSP-N_3 at 80°C for 10 min, according to Pirkle et al.[8]. In the IR spectrum (KBr), the peak at 2280 cm^{-1} denoted the isocyanate group; mass spectrum (electron impact), *m/z* 302 ($M^{+}\cdot$).

To test the optical purities of the NSPI and NSP-N_3 reagents, L-(−)-1-phenylethylamine (optical purity 99%; Merck-Schuchardt) was made to react with the two reagents. No obvious chromatographic peaks of enantiomeric impurities were observed.

Synthesis of urea and carbamate with NSPI

Isocyanate is sensitive to moisture, whereas azide is comparatively stable. Therefore, we kept NSP-N_3 in a refrigerator and converted it into NSPI just before derivatization.

A solution of NSP-N_3 (0.01 mmol) in 1 ml of toluene was heated at 80°C for 10 min in a 5-ml reaction vial equipped with a reflux condenser and a calcium chloride drying tube. Racemic amine drug (0.01 mmol) was added to the above solution. The reaction mixture was kept at room temperature for 10 min, then chromatographed.

The racemic alcohol drug was reacted as above but instead of standing at room temperature the reaction solution was heated at 80°C for 1 h.

Synthesis of amide diastereomers with NSP-N_3

To a solution of NSP-N_3 (0.01 mmol) in 1 ml of toluene, an equivalent amount of racemic amine drug was added. The mixture was kept at room temperature for 10 min and then directly chromatographed.

Identification of the derivatives by mass spectrometry

Each of the above reaction solutions was mixed with chloroform and then washed with 0.1% NaOH, 0.1% HCl and water. The organic layer was dried over anhydrous sodium sulphate, then evaporated to dryness and the mass spectrum was obtained with electronic impact ionization.

TABLE I

SEPARATION AND MASS SPECTRUM IDENTIFICATION OF NSPI AND NSP-N_3 DERIVATIVES OF AMINE AND ALCOHOL ENANTIOMERS

k'_1 and k'_2 = capacity factors of the first- and second-eluted enantiomers, respectively; $M^{+\cdot}$ = molecular weight obtained by mass spectrum (electron impact).

Compound and structure	*NSPI*					*NSP-N_3*				
	k'_1	k'_2	α	R_s	$M^{+\cdot}$	k'_1	k'_2	α	R_s	$M^{+\cdot}$
Mexiletine	5.70	9.11	1.6	3.50	481	20.3	23.2	1.14	2.70	466
Amphetamine	10.7	13.8	1.29	2.31		2.47	3.35	1.36	3.2	422
1-Phenylpropanol	11.0	12.7	1.16	2.4	438					

Comparison between NSP-N_3 and NSPI for enantiomeric separation of amines

A solution of NSP-N_3 in toluene was heated at 60°C for 10 min so that only part of NSP-N_3 was converted into NSPI. An equivalent amount of racemic mexiletine was added. The reaction mixture was kept at room temperature for 10 min, then two pairs of diastereomers of NSP-N_3–mexiletine and NSPI–mexiletine were obtained and chromatographed (Fig. 5).

RESULTS AND DISCUSSION

The mass spectra showed that the isocyanate formed ureas with amines and carbamates with alcohols whereas the azide formed amides with amines.

The results in Table I demonstrated that the procedure, for the indirect separation of amine and alcohol isomers using NSPI has several advantages, such as simple and rapid operation, good resolution, the derivatives are chromatographed directly without clean-up, and with high UV absorbance and strong fluorescence. In

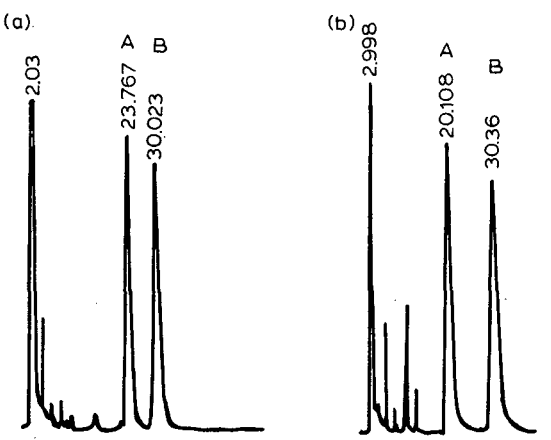

Fig. 1. Separation of NSPI derivatives of (a) racemic amphetamine (peaks A and B) at a flow-rate of 1.0 ml/min, and (b) racemic mexiletine (peaks A and B) at a flow-rate of 1.5 ml/min. Column, silica, 30 × 0.40 cm I.D.; mobile phase, light petroleum–isopropanol (100:3); detection, UV (254 nm). Numbers at peaks indicate retention times in min.

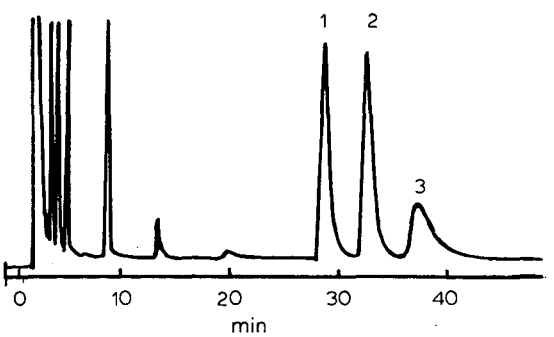

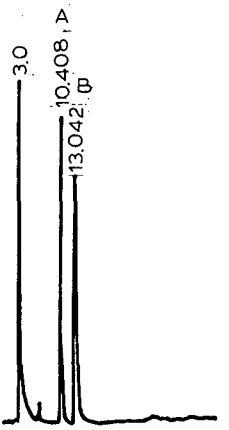

Fig. 2. Separation of the NSPI derivative of (±)-phenylpropanol (peaks 1 and 2). Peak 3 represents the compound formed by heating NSPI at 80°C for 1 h without completely removing the water used for synthesizing NSP-N_3. Mobile phase, light petroleum–isopropanol (100:1); flow-rate, 1.0 ml/min. Column and detection as in Fig. 1.

Fig. 3. Separation of the NSP-N_3 derivative of (±)-amphetamine (peaks A and B). Mobile phase, light petroleum–isopropanol (100:3); flow-rate, 1.0 ml/min. Column and detection as in Fig. 1.

particular, for the optical resolution of alcohols, NSPI can greatly shorten the derivatization time, while NEIC had been reported to resolve racemic 3-O-hexadecylglycerol after derivatization at 80°C for 36 h[3]. One of the reasons may be that the central carbon atom in the isocyanate group of NSPI is more positive and results in greater reactivity than that of NEIC because the nitrogen atom in the proline of NSPI can attract electrons whereas the naphthalene group of NEIC can repel electrons. On the

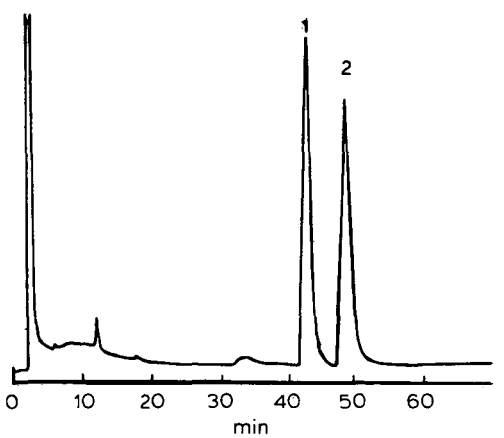

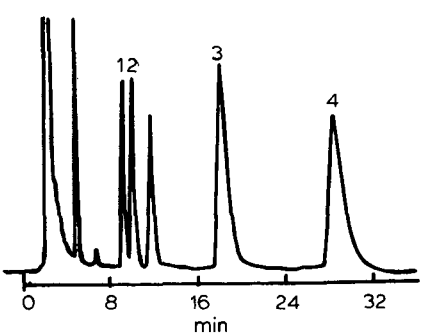

Fig. 4. Separation of the NSP-N_3 derivative of (±)-mexiletine (peaks 1 and 2). Mobile phase, light petroleum–isopropanol (100:1); flow-rate, 1.0 ml/min. Column and detection as in Fig. 1.

Fig. 5. Separation of the (±)-mexiletine derivatives formed with NSP-N_3 (peaks 1 and 2) and NSPI (peaks 3 and 4). Mobile phase, light petroleum–isopropanol (100:3); flow-rate, 1.5 ml/min. Column and detection as in Fig. 1.

other hand, the larger groups connected with the chiral carbon atom of 3-O-hexadecylglycerol may reduce the reactivity of the hydroxyl group with the isocyanate of NEIC.

It is concluded that the indirect separation of amine and alcohol enantiomers with NSPI reagent is a versatile and promising technique.

NSP-N_3 is superior to NSPI owing to shorter retention time and better resolution, as shown in Fig. 5 for the resolution of racemic mexiletine, for instance. The same result can be obtained from amphetamine by comparing Figs. 1a and 3. Amines forms amides with NSP-N_3 and ureas with NSPI. There are only two atoms between the two chiral centres in the amide derivatives, but three atoms in the urea derivatives. According to the principle that in the diastereomeric derivative molecule the distance between the asymmetric carbon atoms of the reagent and the compound to be resolved should be minimized and if possible kept to less than three atoms[9,10] diastereomeric amides should show better separations. In addition, this procedure is more convenient and rapid to operate without heating. Consequently, NSP-N_3 reagent may become a useful chiral resolving agent for amine enantiomers.

REFERENCES

1 G. Pflugmann, H. Spahn and E. Mutschler, *J. Chromatogr.*, 421 (1987) 161.
2 A. Darmon and J. P. Thenot, *J. Chromatogr.*, 374 (1986) 321.
3 P. Michelson, E. Aronsson, G. Odham and B. Åkesson, *J. Chromatogr.*, 350 (1985) 417.
4 W. H. Pirkle and M. S. Hoekstra, *J. Org. Chem.*, 39 (1974) 3904.
5 M. Bergman and L. Zervas, *Biochem. Z.*, 203 (1928) 280.
6 S. Reiji, K. Toshio, I. Kazuhiro, F. Yuzo, N. Hiroyuki and T. Nobuchika, *J. Chromatogr.*, 357 (1986) 119.
7 J. Weinstock, *J. Org. Chem.*, 26 (1961) 3511.
8 W. H. Pirkle, G. Mahler and M. H. Hyun, *J. Liq. Chromatogr.*, 9 (1986) 443.
9 B. Feibush and L. Spialter, *J. Chem. Soc., Perkin Trans. 2*, (1971) 106.
10 B. L. Karger, S. Herliczek and R. L. Stern, *Chem. Commun.*, (1969) 625.

Journal of Chromatography, 508 (1990) 225–228
Elsevier Science Publishers B.V., Amsterdam — Printed in The Netherlands

CHROM. 22 269

Note

Simultaneous determination of biogenic amines by reversed-phase high-performance liquid chromatography

SATORU SUZUKI*, KENTARO KOBAYASHI, JUNKO NODA, TETSUYA SUZUKI and KOZO TAKAMA

Department of Food Science and Technology, Faculty of Fisheries, Hokkaido University, Hakodate, Hokkaido 041 (Japan)

(First received July 31st, 1989; revised manuscript received December 6th, 1989)

Biogenic amines including polyamines are known to be present in many biological materials. Prokaryotic cells produce biogenic amines[1] which are also found in foodstuffs contaminated by putrefactive organisms[2]. Among the biogenic amines, histamine is well known as a causative agent of allergy-like food poisoning[3], in which cadaverine or putrescine acts as a stimulator of the allergy-like symptom[4]. On the other hand, some of polyamines are useful for the quality assessment of foodstuffs, especially fresh marine food[2,5–7]. As has been well recognized, the extent of allergy-like symptoms caused by amines is dose dependent[3], and amines that participate in marine food quality are also closely related to the metabolism of some common amino acids, those amines which are related to allergy-like food poisoning or quality of food being derived from common or closely related amino acids. Whether particular foodstuffs benefit from polyamines or may cause allergy-like food poisoning seems to be delicately balanced.

In view of the above, there is a need for a rapid and economical method for determining histamine and other polyamines simultaneously. For sea food, the detection of agmatine is also important, because it is an index of freshness for the assessment of squid[6]. The greatest but most difficult requirement is to determine histamine and other polyamines including agmatine simultaneously.

Several methods have been proposed for the determination of histamine and other polyamines. Seiler and Knödgen[8] reported the reversed-phase high-performance liquid chromatography (RP-HPLC) of polyamines using gradient elution. Subsequently, several improved methods were developed[9–13]. However, to separate histamine, agmatine and polyamines, generally more than 40 min is required for one analysis. Also, the gradient programmes are sometimes complicated and the separation of each component is not necessarily satisfactory.

Gamoh and Fujita[14] reported the rapid and simultaneous determination of biogenic polyamines by RP-HPLC using an ion-pair method. Although their method seems to be very useful for clinical analysis, they did not give information on the separation of histamine and agmatine.

0021-9673/90/$03.50

We also have attempted to develop a highly sensitive, economic, simple, rapid and reproducible method for the simultaneous determination of histamine and major biogenic polyamines. We found that using sodium hexanesulphonate in place of octanesulphonate achieved a sufficient separation of histamine and other major biogenic polyamines within 35 min.

The present improved method is based on the post-column HPLC method of Gamoh and Fujita[14], *i.e.*, hexanesulphonate was used for ion pairing and the *o*-phthalaldehyde (OPA) method was used for post-column derivatization. By modifying their method, we established improved conditions for the determination biogenic amines such as histamine agmatine and other polyamines. This method should be useful not only in food science but also in clinical medicine.

EXPERIMENTAL

Chemicals

Standard amines were obtained from Sigma (St. Louis, MO, U.S.A.) and sodium hexanesulphonate from Tokyo Kasei Kogyo (Tokyo, Japan); all other reagents were of guaranteed-reagent grade from Wako (Osaka, Japan). All reagents and buffers were filtered through a 0.2-μm membrane filter (Millipore, Bedford, MA, U.S.A.) before use. Standard amines (hydrochloride form) were dissolved in distilled water.

Apparatus

Hitachi Model L-6200 high-performance liquid chromatograph equipped with a loop injector (Rheodyne, Cotati, CA, U.S.A.) and a fluorescence detector (Hitachi 650-10M) was used. Elution peaks were detected fluorimetrically using the excitation wavelength at 345 nm and emission wavelength at 455 nm. The separation of the amine mixture was carried out by reversed-phase chromatography on a Shim-Pak CLC-ODS column (15 cm × 6.0 mm I.D.) (Shimadzu, Kyoto, Japan) kept at 50°C.

The post-column labelling reaction of amines with *o*-phthalaldehyde (OPA) reagent was effected at 20 ± 5°C through a PTFE coil (70 cm × 0.25 mm I.D.) by mixing the eluates with OPA reagent. The OPA reagent was purified with a Hitachi Model L-6000 pump. A Hitachi Model D-2500 data processor was used.

Solvents and gradient system

The elution system consisted of the gradient system shown in Table I, which was prepared from two buffer systems: (A) 0.1 *M* sodium perchlorate (pH 4.0) containing 0.01 *M* sodium hexanesulphonate and (B) a mixture of buffer A and methanol (1:3, v/v) maintained at pH 3.0. The flow-rate of the elution buffer was 1.1 ml/min and that of the OPA reagent was 0.5 ml/min.

OPA reagent

The buffer for OPA reagent consisted of 24.7 g of boric acid, 10 g of sodium hydroxide and 1 g of Brij-35 in 1 l of distilled water. A 5-ml volume of OPA solution (250 mg in 5 ml of ethanol) and 1 ml of 2-mercaptoethanol were mixed with 494 ml of the buffer solution for OPA reagent prepared as mentioned above. The OPA reagent was prepared immediately before use.

Preparation of sample

Herring muscle that had been dried in a flow of air for 3 days at 20°C was used as the material for amine analysis. A 5-g amount of the dry herring muscle was homogenized with 20 ml of 10% trichloroacetic acid (TCA) in a mortar. After centrifugation at 550 *g* for 20 min, the precipitate was used for re-extraction of amines by the same procedure as above. The supernatants were pooled and diluted to 50 ml. The TCA extract thus prepared was then filtered through a 0.22-μm membrane filter (Millipore) and 5 μl of the sample solution were injected directly into the HPLC system.

RESULTS AND DISCUSSION

A good separation of the major biogenic amines was obtained using the gradient elution programme shown in Table I. Fig. 1 shows a representative elution profile of authentic amines. The calibration graphs for putrescine, cadaverine, histamine, agmatine and spermidine were linear in the range 5–100 pmol for the each amine, but for spermine good linearity was obtained in the range 20–100 pmol (data not shown). Acetylpolyamines, 1,3-diaminopropane and 1,8-diaminooctane were also separated from the amines tested here.

Under the given analytical conditions, the data were highly reproducible and sensitive enough for microscale analysis. The combination of hexanesulphonate for ion pairing and sodium perchlorate as the separation buffer in the elution solvent gave a satisfactory separation of polyamines in a relatively short elution time compared with previously reported systems[7,12].

As mentioned the main task was to accomplish the simultaneous micro-determination of major biogenic amines on a HPLC column. The system developed here permits the simultaneous micro-determination of major food-borne polyamines. Fig. 2 shows an example of the practical application of the system to the determination of biogenic amines in the dried herring. The sample solution containing TCA-extractable materials was directly injected into the HPLC system without any pretreatment except filtration. In this instance, histamine was not detected, which means that the sample was safe for consumption (Fig. 2A). We added 80 pmol of histamine to the sample solution to test whether this method can be used in practice. The exogenously added histamine was separated with other endogenous amines (Fig. 2B), and the

TABLE I

ELUTION PROGRAMME FOR POLYAMINE ANALYSIS

Time (min)	*Buffer A (%)*	*Buffer B (%)*	*Gradient mode*
0	96	4	–
7	96	4	Isocratic
10	85	15	Linear
22.5	65	35	Linear
30	65	35	Isocratic
30.5	96	4	Linear
35	96	4	Isocratic

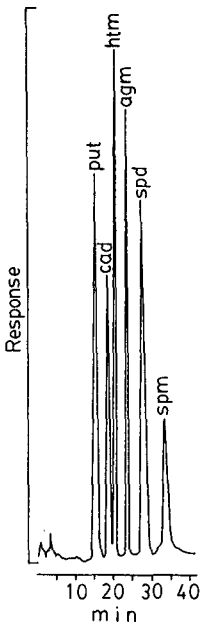

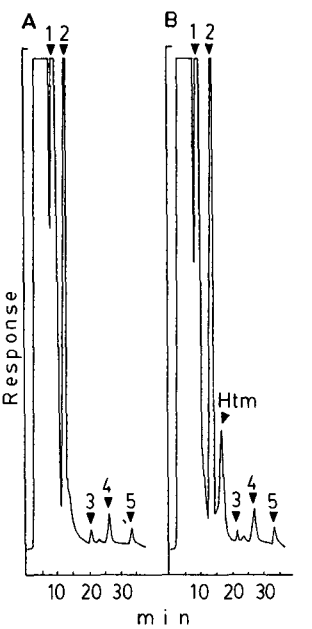

Fig. 1. Chromatogram of authentic biogenic amines. A 100-pmol amount of each amine was injected. Put = putrescine; cad = cadaverine; htm = histamine; agm = agmatine; spd = spermidine; spm = spermine.

Fig. 2. Representative chromatogram of amines extracted from dried herring: (A) dried herring extract; (B) A + histamine (80 pmol). Peaks 1 = put; 2 = cad; 3 = agm; 4 = spd; 5 = spm (abbreviations as in Fig. 1).

amounts of all the amines could be calculated reproducibly from the calibration graph.

Using this method, the time courses of the change in content of biogenic amines in dried herring and polyamine species in many foodstuffs have been determined and details will be reported elsewhere.

REFERENCES

1 C. W. Tabor and H. Tabor, *Microbiol. Rev.*, 49 (1985) 81.
2 J. L. Mietz and E. Karmas, *Assoc. Off. Anal. Chem.* 61 (1978) 139.
3 S. L. Taylor, *CRC Crit. Rev. Toxicol.*, 17 (1987) 91.
4 J. Monger, *Br. J. Pharmacol.*, 12 (1957) 140.
5 H. Yamanaka, K. Shimakura, K. Shiomi and T. Kikuchi, *Bull. Jpn. Soc. Sci. Fish.*, 52 (1986) 127.
6 H. Yamanaka, K. Shiomi and T. Kikuchi, *J. Food Sci.*, 52 (1987) 936.
7 E. Karmas and J. Mietz, *Lebensm. Wiss. Technol.*, 11 (1978) 333.
8 N. Seiler and B. Knödgen, *J. Chromatogr.*, 221 (1980) 227.
9 P. K. Bondy and Z. Canellakis, *J. Chromatogr.*, 224 (1981) 371.
10 J. Wanger, C. Danzin and P. Mamont, *J. Chromatogr.*, 227 (1982) 349.
11 J. Wanger, C. Danzin, S. Huot-Oliver, N. Claverie and M. G. Palfreyman, *J. Chromatogr.*, 290 (1984) 247.
12 N. Seiler and B. Knödgen, *J. Chromatogr.*, 339 (1985) 45.
13 C. Loser, U. Wunderlich and U. R. Folsch, *J. Chromatogr.*, 430 (1988) 249.
14 K. Gamoh and T. Fujita, *Shimadzu Rev.*, 44 (1987) 237.

Journal of Chromatography, 508 (1990) 229–231
Elsevier Science Publishers B.V., Amsterdam — Printed in The Netherlands

CHROM. 22 294

Note

Separation of spermidine derivatives by reversed-phase high-performance liquid chromatography using a UV-absorbing counter ion

BENGT FRANSSON, M. LURDES S. ALMEIDA, LEIF GREHN and ULF RAGNARSSON*
Department of Biochemistry, University of Uppsala, Biomedical Center, P.O. Box 576, S-751 23 Uppsala (Sweden)
(First received September 20th, 1989; revised manuscript received December 18th, 1989)

Polyamines are cationic substances with a wide distribution in living organisms. Although on the cellular level their functions are, at least in part, still obscure[1], they are essential for the growth, proliferation and differentiation of cells[1,2]. *In vitro* they are known to interact with DNA.

In the course of our synthetic studies on spermidines[3,4], we required the simplest method possible for establishing the purity of the final products. This paper describes a convenient isocratic chromatographic system that is particularly useful for the analysis of acetylated spermidines. It exploits a UV-absorbing counter ion and indirect detection[5]. Consequently, no derivatization is involved.

Several sensitive procedures are already available for the analysis of spermidine and its acetylated derivatives in physiological samples[6]. A well known procedure[7,8] exploits *n*-octanesulphonate as the ion-pairing agent and *o*-phthalaldehyde for post-column derivatization. UV-absorbing counter ions have been widely used for the separation and detection of amines. However, to our knowledge they have not been applied to polyamines, probably because detection based on fluorescence gives a higher sensitivity. In the present instance, however, simplicity was more important than very high sensitivity.

EXPERIMENTAL

The acetylated spermidines originated from our laboratory[4]. The ethyl derivatives were obtained by reduction with Red-Al of the corresponding acetyl compounds. All other amines were commercial samples.

The isocratic mobile phases used were phosphate buffers prepared from orthophosphoric acid and sodium dihydrogenphosphate (ionic strength 0.01 *M*, pH 2.0), with ethanol as modifier. 2-Naphthalenesulphonate was added at a concentration of 0.0004 *M*.

The liquid chromatographic system used consisted of two Constametric pumps

0021-9673/90/$03.50

(one should be sufficient), an M 1601 Gradient Master, a Spectromonitor III and a Rheodyne Model 7125 injector.

The columns (150 × 4.6 mm I.D.) were obtained from Polymer Labs. (PLRP-S, 100 Å, 5 μm) and Phase Separations (Spherisorb, ODS-2, 10 μm).

The solvent reservoirs, the injection device and the separation columns were carefully thermostated at 25.0 ± 0.1°C in a water-bath.

RESULTS AND DISCUSSION

The separation of three acetylated spermidines on the PLRP-S column is shown in Fig. 1. The three peaks appear with k' values between 2 and 4 and α values of about 1.3. The baseline is satisfactory but careful thermostating is essential. Qualitatively similar results could be obtained on the Spherisorb column but in this case the selectivity was lower ($\alpha < 1.2$). The compounds appeared in the same order. On this column less ethanol was required (2.5%).

The separation of N^1- and N^8-ethylspermidine proved much more difficult than that of the acetylated derivatives. At higher ethanol concentrations with the compounds eluting before the system peaks, no separation of these isomers was obtained on either column. Spermidine itself was, however, easily separated from these ethyl analogues and appeared earlier in the chromatograms. At lower ethanol concentrations with the compounds eluting after the system peaks, separation was only obtained on the Spherisorb column (0.9% ethanol, $k'_{SP} = 12.6$, $k' = 19.7$–21.5, $\alpha = 1.08$). In this way we could prove that both of the ethylspermidines were pure isomers.

As an additional demonstration of the usefulness and convenience of the described procedure, the separation of the underivatized homologous diamines putrescine, cadaverine and hexamethylenediamine was undertaken. On a C_{18} column the peaks appeared in order of increasing hydrophobicity, as demonstrated in Fig. 2.

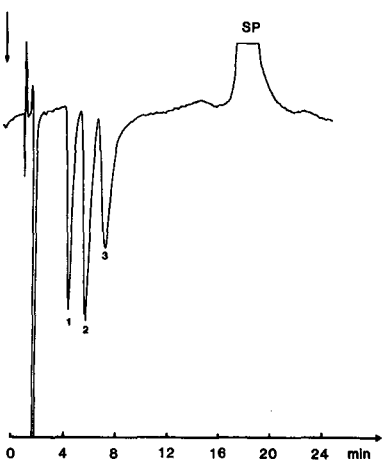

Fig. 1. Separation of three monoacetylated spermidines. Mobile phase, 0.01 *M* phosphate buffer (pH 2.0)–ethanol (94:6); counter ion, 4×10^{-4} *M* 2-naphthalenesulphonate; support, PLRP-S, 100 Å, 5 μm; flow-rate, 1.0 ml/min; detection wavelength, 254 nm at 0.1 a.u.f.s.; temperature, 25.0°C. Peaks: 1 = N^4-acetyl-, 2 = N^1-acetyl- and 3 = N^8-acetylspermidine; SP = system peak.

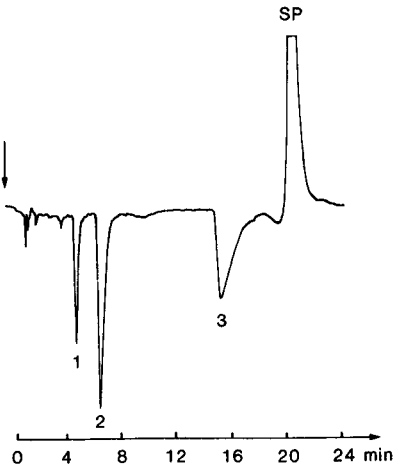

Fig. 2. Separation of (1) putrescine, (2) cadaverine and (3) hexamethylenediamine. Mobile phase, 0.01 *M* phosphate buffer (pH 2.0) alone; counter ion, 4×10^{-4} *M* 2-naphthalenesulphonate; support, Spherisorb C_{18}, ODS-2, 10 μm; flow-rate, detection wavelength and temperature as in Fig. 1. SP = system peak.

The procedure described is suitable for the detection of a variety of di- and polyamines and our aim was to keep it as simple as possible. It is primarily intended for qualitative work when extreme sensitivity is not required. With respect to the sensitivity of the system, it can be stated that 30–50 pmol of N-acetyl- or N-ethylspermidine are easily detected, which is satisfactory in a synthetic context. The detection limit, however, is lower.

ACKNOWLEDGEMENTS

This work was supported by a grant from the Swedish Natural Science Research Council and by a scholarship (to M.L.S.A.) from the Swedish Institute. M.L.S.A. also acknowledges leave of absence from the University of Porto, Portugal.

REFERENCES

1 C. W. Tabor and H. Tabor, *Annu. Rev. Biochem.*, 53 (1984) 749.
2 O. Heby, *News Physiol. Sci.*, 1 (1986) 12.
3 M. Lurdes S. Almeida, L. Grehn and U. Ragnarsson, *J. Chem. Soc., Perkin Trans. 1*, (1988) 1905.
4 M. Lurdes S. Almeida, L. Grehn and U. Ragnarsson, *Acta Chem. Scand.*, 43 (1989) 990.
5 G. Schill and J. Crommen, *Trends Anal. Chem.*, 6 (1987) 111.
6 N. Seiler, *J. Chromatogr.*, 379 (1986) 157.
7 N. Seiler and B. Knödgen, *J. Chromatogr.*, 221 (1980) 227.
8 C. Löser, U. Wunderlich and U. R. Fölsch, *J. Chromatogr.*, 430 (1988) 249.

Journal of Chromatography, 508 (1990) 232–235
Elsevier Science Publishers B.V., Amsterdam — Printed in The Netherlands

CHROM. 22 335

Note

High-performance liquid chromatographic determination of chloroplast pigments with optimized separation of lutein and zeaxanthin

RENÉ K. JUHLER and RAYMOND P. COX*
Institute of Biochemistry, Odense University, Campusvej 55, 5230 Odense M (Denmark)
(First received November 7th, 1989; revised manuscript received February 6th, 1990)

High-performance liquid chromatography (HPLC) is the ideal technique for the determination of the chlorophylls and carotenoids in plants and photosynthetic microorganisms. The pigments to be analysed have a wide range of polarities and it has not been easy to devise methods that combine rapid elution of the most strongly retained components with separation of closely related compounds, such as the structural isomers lutein and zeaxanthin. Good resolution of these two compounds can be obtained with mixtures of standards[1,2], but in methods designed for the determination of all the major photosynthetic pigments[3–6] the two peaks overlap or are very closely associated. This raises questions about the degree of resolution that would be obtained when attempting to use these methods with column materials from different manufacturers or with different batches of material of the same type. Good resolution is particularly critical in studies of the role of zeaxanthin in the xanthophyll cycle[7], when it frequently has to be measured in the presence of a large excess of lutein.

Our aim here was to develop a method with optimized separation of zeaxanthin from lutein, while still allowing the analysis of the other chlorophylls and carotenoids in a reasonable time. The novelty of the approach lies in the use of gradients of tetrahydrofuran in water rather than the commonly used gradients of ethyl acetate or other non-polar solvents in acetonitrile[3–6]. This allows us to propose a method that combines quantitative measurements of zeaxanthin content with the determination of the other chlorophylls and carotenoids in chloroplast extracts within 20 min.

EXPERIMENTAL

Extraction of pigments

Leaves of field-grown barley plants were frozen in liquid nitrogen and ground in a mortar and pestle in the presence of an equimolar mixture of solid KH_2PO_4 and Na_2HPO_4. Pigments from 2 g of leaf material were extracted with 8 ml of acetone and then re-extracted twice with 4 ml of acetone, the residue being separated by centrifugation after each extraction. Pigments were extracted from isolated spinach chloroplasts in a similar manner.

0021-9673/90/$03.50

HPLC system

An HPLC system consisting of two Kontron 420 pumps, a Kontron 432 UV–visible detector with a halogen lamp set at 450 nm, a Kontron 460 autosampler and a Kontron 450 data system was used. The column was 120 mm × 4 mm I.D. and was packed with octadecylsilica (Shandon Hypersil, 5-μm spherical particles). The column temperature was maintained at 30°C. A mixing chamber was inserted between the two pumps and the column.

Chromatographic separation

Separation of pigments was achieved in a gradient of tetrahydrofuran and water. The flow-rate was 1 ml/min. At the time of injection the solvent was tetrahydrofuran–water (51:49). After 5 min at this composition, the tetrahydrofuran content was increased linearly until the ratio at 13 min after injection was 90:10. During repetitive measurements the composition was then decreased linearly to 51:49 over the next 5 min, and then maintained at this level for 3 min (total analysis time 21 min).

Tetrahydrofuran was of HPLC grade (Rathburn). Solvents were degassed by ultrasonic treatment under vacuum and the solvent reservoirs were bubbled with helium during chromatography.

Calibration

Calibration was carried out using pigments isolated from spinach using reversed-phase thin-layer chromatography as described by Henry *et al.*[8]. Concentrations were determined using data provided by Davies[9] and Lichtenthaler[10]. Authentic samples of lutein and zeaxanthin were kindly provided by Dr. Jan Lundquist (Roche, Hvidovre, Denmark).

RESULTS AND DISCUSSION

Preliminary experiments using simple gradients of tetrahydrofuran and water showed satisfactory separation of all the pigments of interest in chloroplast extracts, except for the isomers lutein and zeaxanthin. We therefore investigated the effect of solvent composition on the separation of mixtures of the purified compounds under isocratic conditions. The results (Fig. 1) showed that optimum resolution (1.44) of the two compounds was obtained at 51% tetrahydrofuran. The resolution of neoxanthin and violaxanthin was better than that of lutein and zeaxanthin over the whole concentration range studied. The time required to elute the xanthophylls was much increased at lower concentrations of tetrahydrofuran. Elution of the slowest component, lutein, required 6.2 min with 51% tetrahydrofuran and 26 min with 45% tetrahydrofuran.

An example of the isocratic separation of mixtures of lutein and zeaxanthin using 52% tetrahydrofuran is given in Fig. 2. The optimized separation can be incorporated in a procedure to determine all the major photosynthetic pigments in higher plant chloroplasts by combining isocratic elution of the xanthophylls with a gradient of tetrahydrofuran in water to elute the less polar components. Fig. 3 shows the retention times for seven components with isocratic elution at various tetrahydrofuran concentrations for 5 min followed by a linear gradient up to 90% for the next 8 min. The slope of this gradient was chosen so as to obtain a good separation of

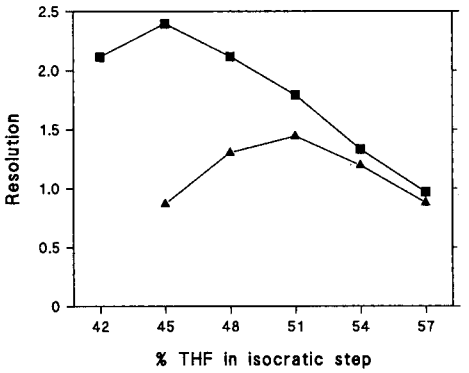

Fig. 1. Effect of concentration of tetrahydrofuran (THF) in water on the resolution of pairs of xanthophylls under isocratic conditions. ▲ = Separation of mixture of purified lutein and zeaxanthin; ■ = separation of neoxanthin and violaxanthin in spinach chloroplast extract.

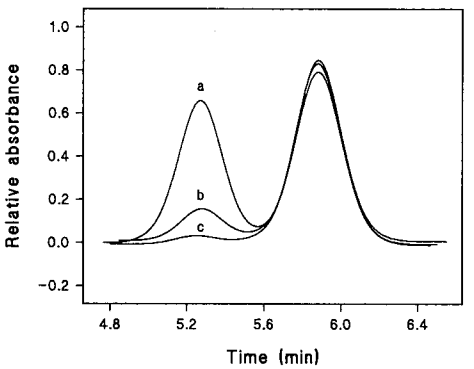

Fig. 2. Separation of lutein and zeaxanthin using isocratic elution with tetrahydrofuran–water (52:48). (a) 1:1 Mixture; (b) zeaxanthin–lutein (1:10); (c) lutein standard containing a trace of zeaxanthin. Other conditions as described in the text.

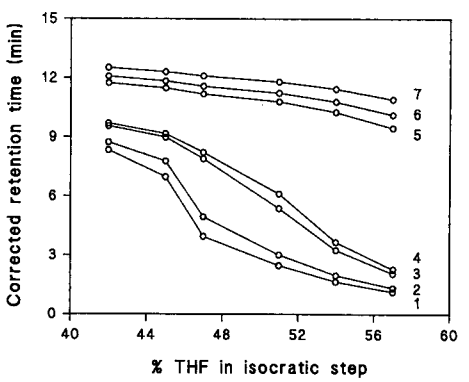

Fig. 3. Retention times for seven components in spinach chloroplast extracts with added zeaxanthin. Isocratic elution with the concentration of tetrahydrofuran (THF) shown was followed after 5 min by a linear gradient up to 90% THF after 13 min. 1 = Neoxanthin; 2 = violaxanthin; 3 = zeaxanthin; 4 = lutein; 5 = chlorophyll *b*; 6 = chlorophyll *a*; 7 = β-carotene.

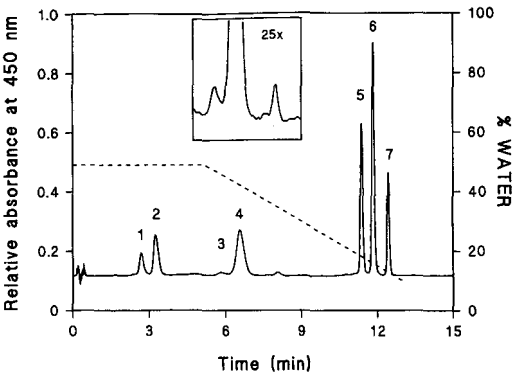

Fig. 4. Separation of the pigments of barley leaves supplemented with a trace of purified zeaxanthin (about 4% of the concentration of lutein) using the method described in the text. Peaks: 1 = neoxanthin; 2 = violaxanthin; 3 = zeaxanthin; 4 = lutein; 5 = chlorophyll *b*; 6 = chlorophyll *a*; 7 = β-carotene. The inset shows the separation of zeaxanthin and lutein on an expanded scale. The small peak after lutein is an unidentified component.

chlorophylls *a* and *b* and β-carotene whilst allowing a reasonably short analysis time. Fig. 3 shows that optimized separation of the xanthophylls is not at the expense of resolution of the less polar chlorophylls and carotenes.

Fig. 4 shows a chromatogram of the pigments from barley leaves using this approach with an isocratic step using 51% tetrahydrofuran. This demonstrates that the same protocol can be used both to measure the concentrations of the major pigments and to determine small amounts of zeaxanthin, as is necessary in studies of the xanthophyll cycle.

ACKNOWLEDGEMENTS

This research was supported by the Danish Natural Sciences Research Council. The HPLC equipment used was partially funded by a grant from the Carlsberg Foundation. We are grateful to Roche, Hvidovre, for the gift of standard carotenoids.

REFERENCES

1 H. J. C. F. Nelis and A. P. De Leenheer, *Anal. Chem.*, 55 (1983) 270.
2 M. Ruddat and O. H. Will, III, *Methods Enzymol.*, 111 (1985) 189.
3 S. W. Wright and J. D. Shearer, *J. Chromatogr.*, 294 (1984) 281.
4 D. Siefermann-Harms, *J. Chromatogr.*, 448 (1988) 411.
5 C. A. Bailey and B. H. Chen, *J. Chromatogr.*, 455 (1988) 396.
6 J. de las Rivas, A. Abadía and J. Abadía, *Plant Physiol.*, 91 (1989) 190.
7 A. Hager, in F.-C. Czygan (Editor), *Pigments in Plants*, Gustav Fischer, Stuttgart, 1980, p. 57.
8 L. E. A. Henry, J. D. Mikkelsen and B. L. Møller, *Carlsberg Res. Commun.*, 48 (1983) 131.
9 B. H. Davies, in T. W. Goodwin (Editor), *Chemistry and Biochemistry of Plant Pigments*, Vol. 2, Academic Press, London, 1976, p. 38.
10 H. K. Lichtenthaler, *Methods Enzymol.*, 148 (1987) 350.

Journal of Chromatography, 508 (1990) 236–240
Elsevier Science Publishers B.V., Amsterdam — Printed in The Netherlands

CHROM. 22 310

Note

High-performance liquid chromatographic determination of five widespread flavonoid aglycones

A. HASLER and O. STICHER*
Department of Pharmacy, Swiss Federal Institute of Technology (ETH) Zurich, CH-8092 Zürich (Switzerland)
and
B. MEIER
Zeller AG, CH-8590 Romanshorn (Switzerland)
(First received October 30th, 1989; revised manuscript received January 26th, 1990)

Flavonoids are widespread compounds of the flora and there is special interest in medicinal plants. They normally occur as glycosides but it is difficult to determine all glycosides[1] in a crude plant extract because most reference compounds are not available commercially. Isorhamnetin, kaempferol, luteolin, myricetin and/or quercetin have been recognized as the major aglycones of medicinal plants such as *Arnica* sp., *Betula* sp., *Calendula officinalis, Epilobium* sp., *Equisetum arvense, Tussilago farfara, Filipendula ulmaria, Ginkgo biloba, Juglans regia, Primula* sp., *Prunus* sp., *Sambucus nigra, Solidago virgaurea, Tilia* sp. and *Verbascum* sp.

The hydrolysis of the glycosides and their spectrophotometric detection as an aluminium chloride chelate complex is the current method for determining the amount of flavonoids in a plant extract[2,3]. This method, described in several Pharmacopoeias, is not very specific and permits only a limited statement regarding the total flavonoids in plants. A detailed description of the qualitative and quantitative composition of the aglycones is not possible. With using reversed-phase high-performance liquid chromatography (RP-HPLC) and diode-array detection[4], a simple and rapid method was developed and validated for determining the above aglycones.

The conditions of the hydrolysis were optimized and tested with rutin. For the hydrolysis of rutin hydrochloric acid and trifluoroacetic acid[5] were tested in various concentrations together with the solvents acetone and methanol. Complete hydrolysis of rutin could only be achieved within 30 min by using methanol and hydrochloric acid.

EXPERIMENTAL

Standards and solvents

Isorhamnetin, kaempferol, luteolin, myricetin and quercetin dihydrate (Rotichrom HPLC) were obtained from Roth (Basle, Switzerland) and morin (Fluka

0021-9673/90/$03.50

standard for microscopy) and rutin (purum) were purchased from Fluka (Buchs, Switzerland). All the organic solvents used were of HPLC grade (Romil Chemicals, Shepshed, U.K.). Trifluoroacetic acid (purum), hydrochloric acid and orthophosphoric acid (analytical-reagent grade) were obtained from Fluka. Pure water was delivered by a NANOpure Cartridge System (Skan, Basel-Allschwil, Switzerland). Bond Elut C_{18} (3 ml) disposable extraction columns (Analytichem International, Harbor City, CA, U.S.A.) were used for sample clean-up.

Columns

Knauer (Berlin, F.R.G.) pre-packed column cartridges (100 × 4 mm I.D.) filled with the following different C_{18} materials were examined: Hypersil ODS, 3 and 5 μm (Shandon, Runcorn, U.K.); LiChrospher RP-18, 10 μm (Merck, Darmstadt, F.R.G.); LiChrosorb RP-18, 5 μm (Merck); Nucleosil 100-C_{18}, 3 and 5 μm (Macherey, Nagel & Co., Düren, F.R.G.); Partisil ODS-3, 5 μm (Whatman, Maidstone, U.K.); and Spherisorb S 5 ODS II, 5 μm, and S 3 ODS II, 3 μm (Phase Separations, Queensferry, U.K.).

Apparatus

HPLC analyses were performed using a Hewlett-Packard instrument (79994A Analytical Workstation, 1090 LC, 1040 DAD). The mobile phase consisted of solvent A (methanol) and solvent B (0.5% orthophosphoric acid) with the following gradient (% A): 0 min, 38%; 12 min, 48.2%; 12.01 min (washing), 100%; 17 min, 100%; and 17.01 min (equilibration), 38%. The flow-rates were 1 ml/min (3 μm), 2 ml/min (5 μm) or 3 ml/min (10 μm), the column temperature 25.0°C, injection volume 10 μl and detection was effected at 370 nm (flavonols) or 349 nm (luteolin).

Sample preparation

A 4-g amount of pulverized plant or plant extract material was refluxed with 70 ml of methanol and 10 ml of 25% hydrochloric acid for 30 min. After cooling, the solution was filtered through a G3 glass filter covered with an LS 14 paper filter. The supernatant was washed with 100 ml of methanol. The solution was evaporated under vacuum to about 80 ml and then diluted to 100 ml with methanol in a volumetric flask. A 5-ml volume of this solution was filtered through Bond Elut C_{18} which was equilibrated with methanol. The cartridge was washed with 4 ml of methanol and the solution was diluted to 10 ml with methanol in a volumetric flask. A 10-μl volume of this solution was injected into the HPLC system.

RESULTS AND DISCUSSION

The method was applied to *Ginkgo* and *Betula* analysis. The identification of the peaks after hydrolysis (*Betula*, myricetin and quercetin; *Ginkgo*, quercetin, kaempferol and isorhamnetin) was made with an automated library search system from Hewlett-Packard (Operating software, Rev. 5.03, 1988). This application includes the peak purity (comparison of the spectra upslope, apex, downslope and correlation between the peak at different wavelengths) and compares the spectra of the peaks in the chromatogram with the spectra of the reference compounds stored in the library. This comparison also considers the retention time (time window ±6%) of the peaks in

the chromatogram and in the library. Myricetin and quercetin in *Betula* and quercetin and kaempferol in *Ginkgo* were identified with a peak purity match index of >998 and a library match index of >994 (maximum 1000).

The linearity of the determination of all flavonoid aglycones and of the internal standard (morin) was verified by regression analysis (seven-point measurement, $r^2 \geqslant 0.994$). The determination was carried out with six samples (Table I). Each sample was injected three times by HPLC or measured by UV–VIS sopectrometry.

It is well known and was confirmed by our experimental work that the flavonoids require very well elaborated chromatographic procedures[7]. Different mobile and stationary phases were evaluated. The examination of the mobile phases was restricted to solvents currently used in RP-HPLC such as acetonitrile, 1,4-dioxane, ethanol, methanol, 2-propanol and tetrahydrofuran. A good separation of the five aglycones in less than 12 min was obtained with a methanol–water gradient. In addition, the influence of the various solvents on the UV spectra was studied, but no significant differences were observed.

The well known tailing problem with flavonoids, which depends on the mobile and especially on the stationary phase, disturbs the automatic integration. Therefore, different C_{18} materials were tested. Further, the influence of the addition of 0.5% of orthophosphoric acid to the solvent was examined. This modifier markedly reduced the tailing. With the requirements of high peak symmetry ($1 \leqslant T_f < 1.2$, at 5% peak height)[8], t_R (last peak) < 12 min, and $R_s > 1.5$, a successful and reproducible separation could be obtained only with Hypersil ODS, 5 μm (Table II and Figs. 1–3). The differences between the tested materials were very significant (Table III).

Comparing the chromatographic parameters of the different stationary phases, it can be concluded that reversed-phase materials have to be evaluated for the analysis of flavonoids.

Morin, a flavonol derivative that is commercially available and found so far only in four Moraceae sp. and one Anacardiaceae sp.[9], is proposed as an internal standard. However, quantitative analyses were established with external standards.

TABLE I

DETERMINATION OF THE FLAVONOLS IN *BETULA* AND *GINKGO*

Component	*Betulae folium, Dixa Lot No. 237*		*Ginkgo extractum, Flachsmann Lot No. 85375: HPLC*
	HPLC	*UV/VIS*[a]	
Myricetin (%)	0.34		–
Quercetin (%)	0.61		0.39
Kaempferol (%)	–		0.51
Isorhamnetin (%)	–		0.10
Calculated as total amount of:			
Aglycones (%)	0.95		1.00
Hyperoside (%)	1.47	1.57	–
Rutin (%)	–	–	2.12

[a] Determination according to ref. 6.

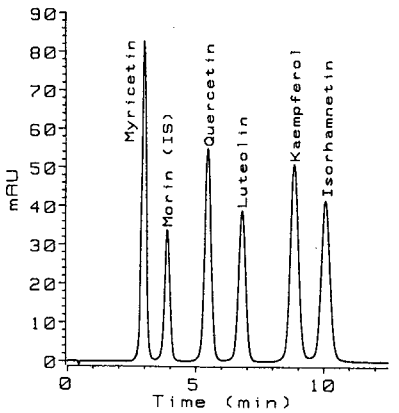

Fig. 1. Chromatogram of the five aglycones separated on Hypersil ODS, 5 μm. Amounts (μg per 10 μl) of the different aglycones injected: myricetin, 0.889; morin, 0.903; quercetin, 0.865; luteolin, 0.856; kaempferol, 0.999; isohamnetin, 0.863.

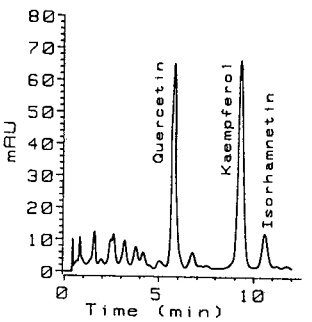

Fig. 2. Chromatogram of *Ginkgo* extractum after hydrolysis.

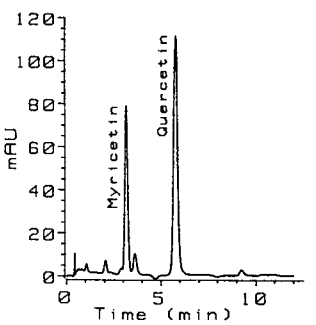

Fig. 3. Chromatogram of *Betulae folium* after hydrolysis.

TABLE II

CHARACTERIZATION OF THE CHROMATOGRAPHIC PARAMETERS OBTAINED WITH HYPERSIL ODS, 5 μm

T_f = Tailing factor according to ref. 8; t_R = retention time.

t_R (min)						T_f
Myricetin	*Morin*	*Quercetin*	*Luteolin*	*Kaempferol*	*Isorhamnetin*	
2.984	3.868	5.464	6.803	8.832	10.056	1.06

TABLE III

CHARACTERIZATION OF THE TESTED COLUMNS

R_s (5/6) = resolution factor between kaempferol and isorhamnetin; T_f = tailing factor according to ref. 8; t_R = retention time.

Stationary phase	t_R (min)[a]						R_s (5/6)	T_f
	1	*2*	*3*	*4*	*5*	*6*		
Hypersil, 3 μm	6.137	7.89	10.244	12.062	14.955	16.273	2.341	2.14
Hypersil, 5 μm	2.984	3.868	5.464	6.803	8.832	10.056	1.966	1.06
LiChrosorb, 5 μm	4.329	5.346	7.527	9.056	11.558	12.668	1.449	1.43
LiChrosorb, 10 μm	3.741	4.856	6.843	8.243	10.843	12.036	0.976	2.86
Nucleosil, 3 μm	8.639	10.762	13.785	15.925	19.276	20.608	2.79	1.82
Nucleosil, 5 μm	6.848	8.524	11.163	13.252	16.048	17.392	2.526	1.56
Partisil, 5 μm	5.278	6.87	8.876	10.843	13.328	14.445	0.698	5.83
Spherisorb, 3 μm	7.83	9.729	12.733	14.665	18.096	19.524	1.142	3.47
Spherisorb, 5 μm	3.41	4.529	6.257	7.613	10.188	11.42	1.135	5.14

[a] 1 = Myricetin; 2 = morin; 3 = quercetin; 4 = luteolin; 5 = kaempferol; 6 = isorhamnetin.

ACKNOWLEDGEMENT

Financial support from Zeller (Romanshorn, Switzerland) is gratefully acknowledged.

REFERENCES

1 K. Dallenbach-Tölke, Sz. Nyiredy, B. Meier and O. Sticher, *Planta Med.*, 53 (1987) 189.
2 H. Glasl and U. Becker, *Dtsch. Apoth.-Ztg.*, 124 (1984) 2147.
3 T. J. Mabry, K. R. Markham and M. B. Thomas, *The Systematic Identification of Flavonoids*, Springer, Heidelberg, New York, 1970, pp. 51–61.
4 B. Meier and O. Sticher, *Pharm. Ind.*, 48 (1986) 87.
5 M. Morrison, *Phytochemistry*, 27 (1988) 1097.
6 *Pharmacopoea Helvetica*, Editio Septima, Eidgenössische Drucksachen- und Materialzentrale, Bern, 1987.
7 D. J. Daigle and E. J. Conkerton, *J. Liq. Chromatogr.*, 11 (1988) 309.
8 M. T. Gilbert, *High Performance Liquid Chromatography*, Wright, Bristol, 1987, p. 11.
9 W. Karrer, *Konstitution und Vorkommen der Organischen Pflanzenstoffe*, Ergänzungsband 2, Birkhäuser, Basle, Boston, Stuttgart, 1981, p. 349.

Journal of Chromatography, 508 (1990) 241–246
Elsevier Science Publishers B.V., Amsterdam — Printed in The Netherlands

CHROM. 22 315

Note

Separation and determination of lanatosides in *Digitalis lanata* leaves by high-performance liquid chromatography

YOUICHI FUJII*, YUKARI IKEDA, ICHIRO OKAMOTO and MITSURU YAMAZAKI
School of Pharmacy, Hokuriku University, 3 Ho, Kanagawa-machi, Kanazawa 920-11 (Japan)
(First received July 14th, 1989; revised manuscript received December 18th, 1989)

Digitalis lanata leaf is known to contain lanatosides and their secondary glycosides. These compounds are pharmaceutically important drugs for the treatment of congestive heart failure. For the determination of lanatosides in *Digitalis lanata*, thin-layer chromatography (TLC) was applied, utilizing measurement of the spot areas[1], spectrophotometric determination (*in situ*) on a thin layer[2] or spectrophotometric measurement of solutions obtained after spot elution[3,4]. However, high-performance liquid chromatography (HPLC) appears to be the most effective method for the analysis of digitalis glycosides. The determination of digoxin in *Digitalis lanata* by HPLC has been proposed by Cobb[5] and Brugidou *et al.*[6]. Also, the separation of a mixture of pure lanatosides was accomplished employing a normal-phase silica column[7,8] and a reversed-phase column[9]. Orosz *et al.*[10] have determined lanatoside C in *Digitalis lanata* using an ODS column, but no data on lanatoside A and B were given.

Previously, we reported the separation and determination of digitalis glycosides in *Digitalis purpurea* by reversed-phase micro-HPLC[11,12]. This paper describes a method for the simultaneous determination of lanatosides in *Digitalis lanata* leaves, which involves clean-up with Sep-Pak cartridges and subsequent separation by normal-phase partition HPLC.

EXPERIMENTAL

Instruments

The liquid chromatograph consisted of a Model KHP-010 pump (Kyowa Seimitsu, Tokyo, Japan), a Model KHP-UI-130 injector (Kyowa Seimitsu), a Model UVILOG-5 III A variable-wavelength detector (Oyo-bunko Kiki, Tokyo, Japan) and a Chromatopac C-R3A data processor (Shimadzu, Kyoto, Japan). The stainless-steel column (250 × 4.6 mm I.D.) was packed with TSK-gel Amide-80 (Tosoh, Tokyo, Japan). This was a column containing 5-μm porous silica particles derivatized with carbamoyl groups. The detector was set at 220 nm. The separations were performed under ambient conditions.

0021-9673/90/$03.50

Materials

Lanatoside A, B and C were purchased from E. Merck (Darmstadt, F.R.G.), desacetyllanatoside C from the National Institute of Hygienic Sciences (Tokyo, Japan) and Sep-Pak cartridges from Waters Assoc. (Milford, MA, U.S.A.). Desacetyllanatoside A and B were prepared from lanatoside A and B, respectively, according to the procedure of Pekić and Miljković[13] and recrystallized repeatedly from dichloromethane–ethanol. The structures of these cardiac steroids are given in Fig. 1. 14α,15α-Epoxy-"β"-anhydrodesacetyllanatoside A, used as the internal standard, was synthesized in four steps from desacetyllanatoside A by the method adapted from Sawlewicz *et al.*[14]. All of these materials were checked for homogeneity by TLC, and solvents were purified by redistillation prior to use.

Preparation of the leaf powder

Leaves of *Digitalis lanata* EHRH. plant in the second year were collected in the medicinal botanical garden of Hokuriku University (Kanazawa, Japan) on July 29, 1987. The freshly harvested leaves were quickly washed with water, freeze-dried in a Neocool Model DC-55A apparatus (Yamato Scientific, Tokyo, Japan) and then dried using phosphorus pentoxide under reduced pressure at room temperature. The dried leaves were pulverized and sifted through a sieve of mesh width 500 μm. The leaf powder obtained was further dried under reduced pressure for 5 days.

Extraction and clean-up procedures

Approximately 50 mg of leaf powder were accurately weighed and extracted with 25 ml of ethanol–chloroform (2:1) containing an internal standard (125.9 μg) in an ultrasonic cleaning bath for 1 h. The extract was filtered and evaporated to dryness at 40°C using a rotary evaporator. The residue was dissolved in 2 ml of ethyl acetate–ethanol (100:1) and applied to the Sep-Pak silica cartridge. Then 18 ml of ethyl acetate–ethanol (100:1) and 10 ml of ethyl acetate–ethanol (5:1) were successively passed through the cartridge. The latter fraction (10 ml) was collected and evaporated at 40°C using a rotary evaporator. The residue obtained was dissolved in 1 ml of methanol–water (2:3) and loaded on the Sep-Pak C_{18} cartridge. After washing with 14 ml of methanol–water (2:3), cardiac glycosides were eluted with 15 ml of methanol–

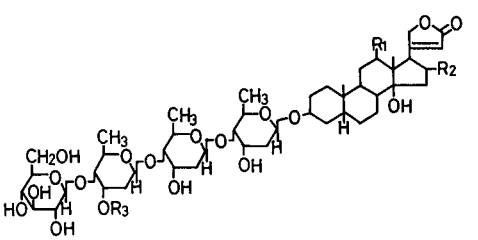

Lanatoside A : $R_1=R_2=H$, $R_3=COCH_3$ — Desacetyllanatoside A : $R_1=R_2=R_3=H$

Lanatoside B : $R_1=H$, $R_2=OH$, $R_3=COCH_3$ — Desacetyllanatoside B : $R_1=R_3=H$, $R_2=OH$

Lanatoside C : $R_1=OH$, $R_2=H$, $R_3=COCH_3$ — Desacetyllanatoside C : $R_1=OH$, $R_2=R_3=H$

Fig. 1. Structures of lanatosides and desacetyllanatosides.

water (2:1). The eluate was evaporated at 40°C *in vacuo* and the resulting material was dissolved in 0.1 ml of acetonitrile–water (96:4) and analysed by HPLC.

HPLC of lanatosides

A 10-μl volume of the purified sample solution (0.1 ml) was injected into the liquid chromatograph and acetonitrile–water (96:4) was employed as the mobile phase at a flow-rate of 0.8 ml/min. The mobile phase used for the separation of desacetyllanatosides was acetonitrile–water (9:1). The effluent was monitored by UV absorption at 220 nm. Calibration graphs were constructed using the average peak areas from three chromatograms.

TLC procedure

Normal- and reversed-phase TLC were performed on 5 × 10 cm high-performance silica gel 60 F_{254} plates (E. Merck) and 5 × 10 cm $KC_{18}F$ plates (Whatman, Clifton, NJ, U.S.A.), respectively. After development and air drying, the plates were checked by fluorescence quenching of the layers under UV radiation at *ca.* 254 nm, and then sprayed with concentrated sulphuric acid and heated in an oven at 120°C for 10 min.

RESULTS AND DISCUSSION

An initial study was focused on the selection of an internal standard and the chromatographic separation of cardiac glycosides. Many compounds were investigated and 14α,15α-epoxy-"β"-anhydrodesacetyllanatoside A was found to be the most suitable. HPLC was performed on a carbamoyl-bonded silica column using acetonitrile–water as eluent. A detection wavelength of 220 nm was employed, account being taken of the α,β-unsaturated lactone ring attached at the C-17 position of the steroid nucleus. The separation of lanatoside A, B and C and the internal standard was achieved when acetonitrile–water (96:4) was used as the eluent, as illustrated in Fig. 2. The retention times of desacetyllanatoside A, B and C were 80, 129 and 135 min, respectively. Also, Fig. 3 shows the chromatogram of lanatosides, desacetyllanatosides

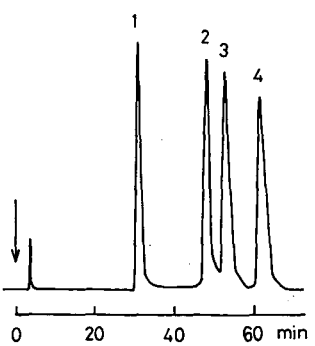

Fig. 2. Separation of a mixture of lanatosides and the internal standard. Peaks: 1 = lanatoside A (0.40 μg); 2 = lanatoside B (0.43 μg); 3 = lanatoside C (0.59 μg); 4 = 14α,15α-epoxy-"β"-anhydrodesacetyllanatoside A (0.84 μg). Conditions: TSK-gel Amide 80 column (250 × 4.6 mm I.D.); mobile phase, acetonitrile–water (96:4); flow-rate, 0.8 ml/min; UV detection at 220 nm; sample volume, 10 μl.

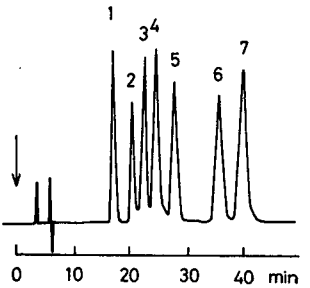

Fig. 3. Separation of a mixture of lanatosides, desacetyllanatosides and the internal standard. Peaks: 1 = lanatoside A (0.15 μg); 2 = lanatoside B (0.15 μg); 3 = lanatoside C (0.20 μg); 4 = 14α,15α-epoxy-"β"-anhydrodesacetyllanatoside A (0.22 μg); 5 = desacetyllanatoside A (0.27 μg); 6 = desacetyllanatoside B (0.45 μg); 7 = desacetyllanatoside C (0.55 μg). Conditions: mobile phase, acetonitrile–water (9:1); flow-rate, 0.5 ml/min; other conditions as in Fig. 2.

and the internal standard. These compounds were separated into seven peaks using acetonitrile–water (9:1) as the eluent. The separations are of sufficient quality and reproducibility to permit quantitative work.

The determination of lanatosides in *Digitalis lanata* leaves was carried out by an internal standard method. The leaves were dried and then extracted with ethanol–chloroform (2:1) by ultrasonication. In order to remove the many other plant materials in the extract, it is necessary to introduce a purification step prior to HPLC. Sep-Pak cartridges packed with silica gel and ODS-bonded gel were used to clean up the extract. For the complete HPLC separation of lanatosides in the purified extract, acetonitrile–water (96:4) was employed as the mobile phase. When acetonitrile–water (9:1) was used, the presence of co-extracted constituents of the leaves interfered with the peak of lanatoside C. Fig. 4 depicts a typical chromatogram of the extract after addition of the internal standard. From the chromatogram of the extract in the absence of the internal standard, the co-existing substances present in the leaves were ascertained not to disturb the internal standard peak. The eluate corresponding to each peak was collected and analysed by TLC. Both normal-phase TLC (lanatoside A, R_F 0.46; lanatoside C, R_F 0.39) using chloroform–methanol–water (80:20:2.5) as developing solvent and reversed-phase TLC (lanatoside A, R_F 0.40; lanatoside C, R_F 0.68) using acetonitrile–0.5 *M* sodium chloride (10:13) indicated single components in each zone with retention times corresponding to lanatoside A and C.

Linear calibration graphs were obtained by plotting the peak-area ratios (y) of lanatosides to an internal standard against the amount of lanatosides (x μg); the regression equations and correlation coefficients (r) were $y = 0.0108\,x - 0.0004$ ($r = 0.997$) for lanatoside A and $y = 0.0101\,x + 0.150$ ($r = 0.998$) for lanatoside C. The plot was from 10 to 70 μg for lanatoside A and over the required range from 40 to 180 μg for lanatoside C. The intra-assay relative standard deviations ($n = 9$) were 0.9–2.5% for lanatoside A (10–70 μg) and 1.0–1.7% for lanatoside C (44–177 μg), and the inter-assay relative standard deviations ($n = 9$) were 2.1–3.0% for lanatoside A and 1.7–2.8% for lanatoside C.

The assay results obtained from ten dry leaf powder samples (mean of three determinations per sample) are collected in Table I. The data indicate that the leaves contained 66.9 ± 4.4 μg (mean ± S.D.) for lanatoside A and 216.3 ± 7.1 μg for

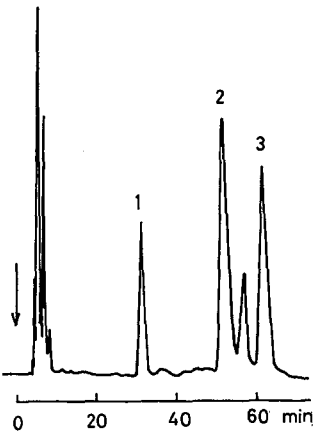

Fig. 4. Chromatogram of the extract of *Digitalis lanata* leaves with the internal standard. Peaks: 1 = lanatoside A; 2 = lanatoside C; 3 = 14α,15α-epoxy-"β"-anhydrodesacetyllanatoside A. Conditions as in Fig. 2.

lanatoside C per 100 mg of the dry leaf powder. The amount of lanatoside C was three times higher than that of lanatoside A. The quantitative usefulness of this technique was confirmed by the relative standard deviations of 6.6% and 3.3% for lanatoside A and C, respectively.

The recovery was examined by adding pure lanatoside A and C equivalent to half of the amounts contained in the leaves and applying the described procedure. Both of the compounds were recovered satisfactorily (>95%). The limits of quantitative measurements of lanatosides and desacetyllanatosides with the present method were 2–4 μg per 50 mg of dry leaf powder, considering the interfering peaks of impurities originating from the leaves. The amounts of lanatoside B and desacetyllanatosides in the leaves examined were below the limits of determination.

Previously, the separation of lanatoside and desacetyllanatoside standards[7,8], the qualitative analysis of cardiac glycosides in *Digitalis lanata*[9] and the determination of digoxin in the leaves[5,6] were reported. However, these studies were not concerned with the quantification of lanatosides in *Digitalis lanata*. For the simultaneous determination of lanatoside A, B and C in the leaves, the elimination of interfering

TABLE I

CONTENTS OF LANATOSIDE A AND LANATOSIDE C IN *DIGITALIS LANATA* LEAVES DETERMINED BY THE PROPOSED METHOD

Glycoside	*Found (μg)*[a]	*Mean ± S.D. (μg)*	*Relative standard deviation (%)*
Lanatoside A	63.4, 72.0, 68.1, 72.1, 66.0, 67.9, 66.2, 72.0, 60.0, 61.1	66.9 ± 4.4	6.6
Lanatoside C	223.4, 209.1, 223.9, 224.8, 209.1, 212.6, 219.4, 222.7, 209.2, 209.1	216.3 ± 7.1	3.3

[a] Amount of lanatoside A or C per 100 mg of a dry leaf powder sample.

peaks by the pretreatment step before the HPLC analysis is of great importance. The described clean-up procedure with the Sep-Pak cartridges was much more efficient and convenient for the determination of cardiac glycosides in *Digitalis* leaves than the previous method[11] involving a solvent-partition sequence and preparative TLC. In fact, the secondary glycosides such as digitoxin and digoxin were eluted with ethyl acetate–ethanol (100:1) and the primary glycosides (lanatosides) were eluted subsequently with ethyl acetate–ethanol (5:1) on a Sep-Pak silica cartridge.

Recently, the TSK-gel Amide-80 column material made of silica gel modified with carbamoyl groups has been developed, which permits the separation of monosaccharides, oligosaccharides and sugar alcohols. On this normal-phase partition column, a reversed-phase type solvent system composed of acetonitrile–water can be used, which has good ultraviolet transparency at a wavelength (220 nm) nearer the λ_{max} of the butenolide ring. Therefore, the use of this column is preferable to the quantification of digitalis glycosides.

In conclusion, the HPLC method described here has been demonstrated to be accurate, precise and selective for the determination of lanatosides in *Digitalis lanata* leaves. This method can be useful for estimation of the quality of the leaves.

ACKNOWLEDGEMENT

The authors thank the staff of the medicinal botanical garden of Hokuriku University for providing the leaves of *Digitalis lanata*.

REFERENCES

1 M. A. Elkiey, Z. F. Ahmed, E. M. Abdelkader and S. M. Abdelwahab, *J. Pharm. Sci. U.A.R.*, 5 (1964) 139.
2 E. Bancher, Th. Prey and F. Wurst, *Planta Med.*, 29 (1976) 393.
3 S. M. Khafagy and A. N. Girgis, *Planta Med.*, 25 (1974) 350.
4 P. Horváth, *Acta Pharm. Hung.*, 52 (1982) 133.
5 P. H. Cobb, *Analyst (London)*, 101 (1976) 768.
6 C. Brugidou, M. Jacques, L. Cosson, F. X. Jarreau and T. Ogerau, *Planta Med.*, 54 (1988) 262.
7 W. Lindner and R. W. Frei, *J. Chromatogr.*, 117 (1976) 81.
8 P. A. Linley and A. G. M. Mohamed, *J. High Resolut. Chromatogr. Chromatogr. Commun.*, 4 (1981) 239.
9 M. Wichtl, M. Mangkudidjojo and W. Wichtl-Bleier, *J. Chromatogr.*, 234 (1982) 503.
10 F. Orosz, M. Nuridsány and J. Ovádi, *Anal. Biochem.*, 156 (1986) 171.
11 Y. Fujii, H. Fujii and M. Yamazaki, *J. Chromatogr.*, 258 (1983) 147.
12 Y. Fujii, Y. Ikeda and M. Yamazaki, *J. High Resolut. Chromatogr. Chromatogr. Commun.*, 10 (1987) 137.
13 B. Pekić and D. Miljković, *Planta Med.*, 27 (1975) 178.
14 L. Sawlewicz, H. H. A. Linde and K. Meyer, *Helv. Chim. Acta*, 51 (1968) 1353.

Journal of Chromatography, 508 (1990) 247–251
Elsevier Science Publishers B.V., Amsterdam — Printed in The Netherlands

CHROM. 22 397

Note

High-performance liquid chromatographic analysis of phenylpyrroles produced by *Pseudomonas cepacia*

NOREEN E. MAHONEY* and JAMES N. ROITMAN

U.S. Department of Agriculture, Agricultural Research Service, Western Regional Center, 800 Buchanan Street, Albany, CA 94710 (U.S.A.)

(First received October 31st, 1989; revised manuscript received February 9th, 1990)

Pyrrolnitrin (III, Fig. 1), 3-chloro-4-(2-nitro-3-chlorophenyl)pyrrole, is a potent antifungal compound first isolated from *Pseudomonas pyrrocinia*[1]. It was subsequently found that a number of Pseudomonads form pyrrolnitrin as a product of tryptophan metabolism[2]. Other less active phenylpyrroles were also produced by this metabolic pathway; these include aminopyrrolnitrin (II)[3], 2-chloropyrrolnitrin (V)[3], isopyrrolnitrin [2,3-dichloro-4-(2-nitrophenyl)pyrrole][4], and oxypyrrolnitrin [3-chloro-4-(2-nitro-3-chloro-6-hydroxyphenyl)pyrrole][5]. Gas chromatographic[6] and thin-layer chromatographic (TLC)[2] techniques have been used to analyze for these phenylpyrroles from Pseudomonads.

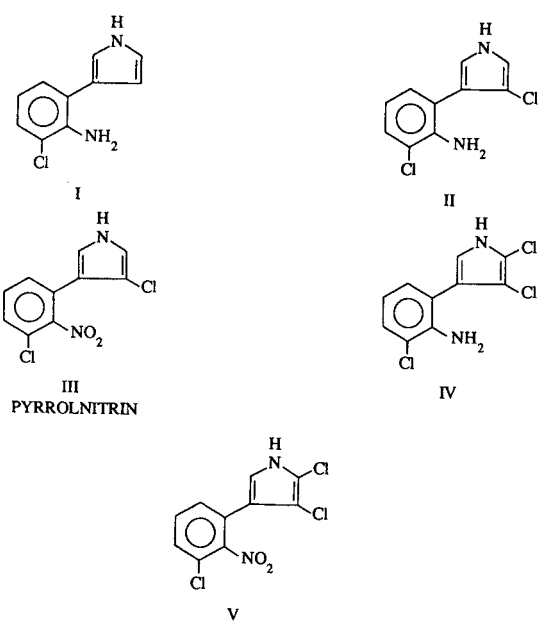

Fig. 1. Structures of phenylpyrroles.

0021-9673/90/$03.50

A strain of *Pseudomonas cepacia*, isolated from apple leaves, inhibited the growth of *Botrytis cinerea* and *Penicillium expansum* on apples and pears, and was found to produce pyrrolnitrin[7]. We have isolated other phenylpyrroles from *P. cepacia*, including compounds II and V. In addition, we found 3-(2-amino-3-chlorophenyl)pyrrole (I), previously isolated from a Pseudomonad grown in the presence of 7-chlorotryptophan[8], and 2,3-dichloro-4-(2-amino-3-chlorophenyl)pyrrole (IV)[9], not reported previously. A high-performance liquid chromatographic (HPLC) method was developed for the separation and quantitative analysis of these five phenylpyrroles in *P. cepacia* fermentations.

EXPERIMENTAL[a]

The medium used in the fermentation of *P. cepacia* consisted of the following: 8 g/l Difco Nutrient Broth, 5 g/l Difco Yeast Extract, and 10 g/l glucose.

Chromatography was performed on an IBM 9533 liquid chromatograph with a Rheodyne 7125 injector, a Waters 450 variable-wavelength detector, and a Hewlett-Packard 3390A reporting integrator. All solvents used were of HPLC grade and were obtained from various manufacturers.

An IBM (Wallingford, CT, U.S.A.) 5-μm C_{18} column (250 mm × 4.6 mm I.D.) and a 50 mm × 4.6 mm I.D. guard column were used for HPLC; analyses were conducted isocratically with an ultrasonically degassed solution composed of acetonitrile–methanol–water (1:1:1.1) at a flow-rate of 1.0 ml/min, and peaks were detected by UV monitoring at 254 nm.

Whatman (Hillsboro, OR, U.S.A.) $KC_{18}F$ plates were used for TLC and were developed in acetonitrile–methanol–water (1:1:1). Phenylpyrrole spots were visualized with diazotized sulfanilic acid (DSA) spray.

Isolation and preparation of standards

Compounds II, III, IV, and V were isolated from *P. cepacia* as previously described[9]. Compound I was isolated using the same procedure with the following changes: *P. cepacia* was grown in the fermentation broth described above. The reversed-phase HPLC fraction containing II was rechromatographed on a Rainin Dynamax (Emeryville, CA, U.S.A.) 8-μm silica column (250 mm × 21.4 mm I.D.) with a 50 mm × 21.4 mm I.D. guard column and an eluent of hexane–chloroform (3:1) at a flow-rate of 20 ml/min and detection at 254 mm. The separation of I (retention time 5.6 min) from II (retention time 6.3 min) was thus achieved. After recrystallization from chloroform–hexane (1:5), compound I was identified from its NMR and mass spectra.

Analysis of standards

Accurately weighed 10-mg samples of each of the five phenylpyrroles were dissolved in 10 ml of methanol. Aliquots of this stock solution were taken such that seven standard solutions were prepared containing 5, 25, 50, 100, 250, 500, and 1000

[a] Reference to a company and/or product named by the Department is only for purposes of information and does not imply approval or recommendation of the product to the exclusion of others which may also be suitable.

μg/ml of each phenylpyrrole. HPLC analyses of 20 μl were made in triplicate from each standard solution. A standard curve correlating the amount of phenylpyrrole in a 20-μl injection to its area was prepared for each phenylpyrrole.

Analysis of fermentation broth

A Fernbach flask (2800 ml) containing 500 ml of sterile fermentation broth was inoculated with *P. cepacia* and agitated on a rotary shaker at 200 rpm at 33°C. Duplicate 10-ml aliquots were removed at 12, 24, 48, and 168 h. Aliquots were centrifuged at 8000 *g*, the broth was discarded, and the cells were extracted by ultrasonification with 10 ml acetone. The suspension was recentrifuged at 5500 *g*, the supernatant evaporated under vacuum, and the residue dissolved in 200 μl methanol. Duplicate 20-μl injections were analyzed by HPLC. The amount of each phenylpyrrole per 20 μl was calculated from its standard curve using a linear regression program. This value is equivalent to the mg/l phenylpyrrole in fermentation broth.

Analysis of a second 10-ml acetone extract of the cells revealed that 98% of the phenylpyrroles are contained in the first extract. To determine if phenylpyrroles are transferred by *P. cepacia* into the broth, an aliquot taken at 48 h was centrifuged and the supernatant freeze-dried. The solids were extracted with chloroform, the solution was filtered, and the solvent removed under reduced pressure. The residue was taken up in methanol for HPLC analysis. Results indicate that the broth contains only 1% of the phenylpyrroles produced by the cells during fermentation.

RESULTS AND DISCUSSION

A chromatogram of the phenylpyrrole standards (Fig. 2) shows baseline separation well suited for quantitative analysis; the capacity factors are listed in Table

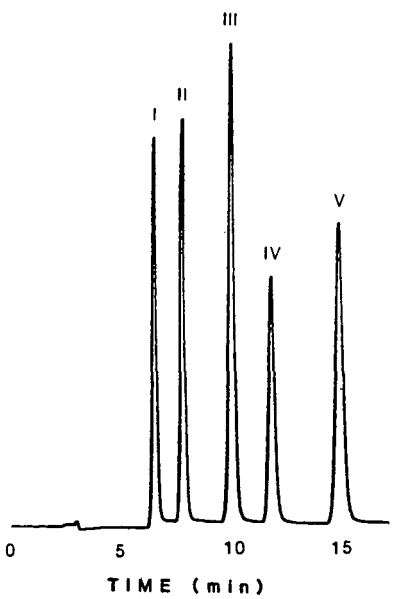

Fig. 2. Chromatogram of standard phenylpyrroles (20 μg each). For chromatographic conditions see text.

TABLE I

HPLC AND TLC CHARACTERISTICS OF *P. CEPACIA* PHENYLPYRROLES

Phenylpyrrole	*HPLC capacity factor (k')*	*TLC R_F value*	*Color reaction with DSA*
I	1.16	0.40	Maroon
II	1.64	0.38	Maroon
III	2.42	0.31	Maroon
IV	3.02	0.28	Orange
V	4.11	0.22	Orange

TABLE II

CONCENTRATIONS OF PHENYLPYRROLES IN *P. CEPACIA* FERMENTATION BROTH AT VARIOUS ELAPSED FERMENTATION TIMES

Phenylpyrrole	*Concentration (mg/l)*			
	12 h	*24 h*	*48 h*	*168 h*
I	0.8	0.2	0.1	0.1
II	0.1	10.4	5.8	4.7
III	0.2	6.8	13.1	13.3
IV	–[a]	2.3	4.1	2.8
V	–[a]	0.4	1.5	1.5

[a] Not detected.

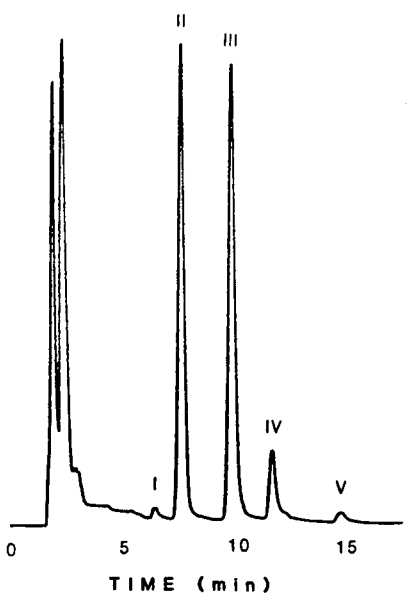

Fig. 3. Chromatogram of phenylpyrroles from *P. cepacia*. I = 0.2 μg; II = 10.4 μg; III = 6.8 μg; IV = 2.3 μg; V = 0.4 μg. For chromatographic conditions see text.

I. For the external standardization, each phenylpyrrole gave a linear response curve in the range tested (0.1–20 μg injected) as shown by correlation coefficients of 0.9994–0.9999.

The concentrations of the five phenylpyrroles at various time intervals during a 168-h fermentation of *P. cepacia* are given in Table II. A chromatogram of a sample taken at 24 h is shown in Fig. 3; note the absence of any interfering peaks. The presence of each phenylpyrrole was verified by reversed-phase TLC as described above; R_F values and the color reactions are given in Table I.

The proposed biochemical pathway for the formation of these phenylpyrroles is corroborated by their changes in concentration during fermentation. Tryptophan is believed to undergo chlorination, rearrangement, and decarboxylation to form compound I[10], which is further chlorinated to II[8], followed by oxidation to III[3]. It is likely that compound IV is similarly formed by chlorination of I or II followed by oxidation to V. The results in Table II show that compound I is present in the highest concentration early in the fermentation. As the fermentation continues compounds II and IV accumulate, followed by a decline in their concentrations and an accompanying rise in the concentrations of III and V, respectively.

With an uncomplicated sample preparation scheme and an HPLC analysis time of only 18 min, this quantitative procedure proves to be an excellent method for monitoring phenylpyrrole production in *P. cepacia* during fermentation.

REFERENCES

1 K. Arima, H. Imanaka, M. Kousaka, A. Fukuda and G. Tamura, *Agric. Biol. Chem.*, 28 (1964) 575.
2 D. H. Lively, M. Gorman, M. E. Haney and J. A. Mabe, *Antimicrob. Agents Chemother.*, 1966 (1967) 462.
3 R. Hamill, R. Elander, J. Mabe and M. Gorman, *Antimicrob. Agents Chemother.*, 1967 (1968) 388.
4 M. Hashimoto and K. Hattori, *Bull. Chem. Soc. Jpn.*, 39 (1966) 410.
5 M. Hashimoto and K. Hattori, *Chem. Pharm. Bull.*, 14 (1966) 1314.
6 R. L. Hamill, H. R. Sullivan and M. Gorman, *Appl. Microbiol.*, 18 (1969) 310.
7 W. J. Janisiewicz and J. Roitman, *Phytopathology*, 78 (1988) 1697.
8 K. van Pée, O. Salcher and F. Lingens, *Angew. Chem. Int. Ed. Engl.*, 19 (1980) 828.
9 J. N. Roitman, N. E. Mahoney, W. J. Janisiewicz and M. Benson, *J. Agric. Food Chem.*, 38 (1990) 538.
10 W. Weisner, K. van Pée and F. Lingens, *J. Biol. Chem.*, 27 (1988) 13 725.

Journal of Chromatography, 508 (1990) 252–258
Elsevier Science Publishers B.V., Amsterdam — Printed in The Netherlands

CHROM. 22 279

Note

Determination of preservatives in cosmetic products by reversed-phase high-performance liquid chromatography. IV

L. GAGLIARDI, G. CAVAZZUTTI and L. TURCHETTO
Istituto Superiore di Sanità, Rome (Italy)
F. MANNA
Università "La Sapienza", Rome (Italy)
and
D. TONELLI*
Istituto di Scienze Chimiche, Università di Bologna, Via San Donato 15, 40127 Bologna (Italy)
(First received September 20th. 1989; revised manuscript received December 27th, 1989)

In the last few years we have been interested in the analytical routine control of cosmetics with the aim of verifying their adherence to the legislation of the European Economic Community (EEC). Single preservatives, but more often combinations of preservatives, are always used in commercial samples in order to prevent degradation and contamination of the complex formulation present in the product. In this regard, the original EEC Council Directive 76/768 has been amended many times, and at present there are about 60 preservatives that are definitively or provisionally permitted for use at specified maximum concentrations.

In previous papers[1–4] we reported some high-performance liquid chromatographic (HPLC) methods suitable for the rapid identification and quantification of groups of related preservatives. In one of them[3], describing the separation of phenolic and/or halogenated preservatives, we were unable to separate triclosan from triclocarban under the chromatographic conditions used and the problem was solved by carrying out a further extraction from the cosmetic sample in order to separate the neutral (such as triclocarban) from the acidic (such as triclosan) compounds. We have now developed a reversed-phase HPLC method that allows the complete separation of 22 preservatives, including triclosan and triclocarban, with optimization of the mobile phase composition. The preservatives considered are reported in Table I together with their maximum admissible concentrations according to EEC Council Directive 76/768 (Annex VI) and subsequent adjournments. All of them are listed in the current Directive except hexachlorophene, which has recently been deleted, and dichloro-*m*-xylenol, tetrabromocresol and halocarban, which are no longer included.

EXPERIMENTAL

Chemicals

All the preservatives were kindly supplied by the Keuringsdienst van Waren

0021-9673/90/$03.50

TABLE I

PRESERVATIVE MATERIALS

Compound No.	*EEC name*	*Common name*	*Maximum authorized concentration (%)*
1	2-Phenoxyethanol		1.0
2	*p*-Hydroxybenzoic acid, methyl ester (acid)	Methylparaben	0.4
3	1-Phenoxy-2-propanol		1.0
4	Glycerol *p*-chlorophenyl ether	Chlorphenesin	0.5
5	*p*-Hydroxybenzoic acid, ethyl ester (acid)	Ethylparaben	0.4
6	2,4-Dichlorobenzyl alcohol		0.15
7	*p*-Chloro-*m*-cresol		0.2
8	4-Chloro-3,5-dimethylphenol	*p*-Chloro-*m*-xylenol	0.5
9	4-Isopropyl-3-methylphenol		0.1
10	*p*-Hydroxybenzoic acid, *n*-butyl ester (acid)	Butylparaben	0.4
11	*o*-Phenylphenol (phenol)		0.2
12	*p*-Hydroxybenzoic acid, benzyl ester (acid)	Benzylparaben	0.1
13	Sorbic acid, isopropyl ester (acid)		0.6
14	2,4-Dichloro-3,5-dimethylphenol (I.S.)	Dichloro-*m*-xylenol	–
15	5,5′-Dichloro-2,2′-dihydroxydiphenyl-methane	Dichlorophene	0.2
16	2-Benzyl-4-chlorophenol	Chlorophene	0.2
17	2,4,4′-Trichloro-2′-hydroxydiphenyl ether	Triclosan	0.3
18	3,4,4′-Trichlorocarbanilide	Triclocarban	0.2
19	Tetrabromo-*o*-cresol		–
20	4,4′-Dichloro-3-trifluoromethyl-carbanilide	Halocarban	–
21	3,3′-Dibromo-5,5′-dichloro-2,2′dihydroxy-diphenylmethane	Bromochlorophene	0.1
22	2,2′-Dihydroxy-3,3′,5,5′,6,6′-hexachloro-diphenylmethane	Hexachlorophene	–

(Enschede, The Netherlands), and were used as received. All chemicals were of analytical-reagent grade. Water was deionized and doubly distilled in glass. Methanol was of special HPLC grade (Carlo Erba, Milan, Italy). All solvents and solutions for HPLC analysis were filtered through a Millipore filter, pore size 0.45 μm, and vacuum degassed by sonication before use.

Apparatus

A Model 5000 liquid chromatograph (Varian, Zug, Switzerland) equipped with a Valco AH 60 injection valve, a Varian Polychrom 9060 photodiode-array detector and a Varian 4290 integrator was used. The analytical column was 5-μm ODS Ultrasphere (250 × 4.6 mm I.D.) (Beckman).

Chromatographic conditions

The mobile phase was methanol–water containing 1% (v/v) acetic acid with the following linear gradient of methanol concentration: 0 min, 20%; 15 min, 30%; 25 min, 40%; 35 min, 60%; 40 min, 70%; 50 min, 80%; 60 min, 85%; and 65 min, 90%. The column temperature was 25°C, injection volume 10 μl, flow-rate 2.3 ml/min, detection wavelength 280 nm and chart speed 0.25 cm/min.

Calibration graphs

Stock solutions were prepared by dissolving weighed amounts of the preservatives in 100 ml of a solution of acetic acid (1%, v/v) in tetrahydrofuran (THF) containing 1 mg/ml of dichloro-*m*-xylenol as the internal standard (I.S.). These solutions, and the set of solutions produced by serial dilutions, were processed using the HPLC conditions described above. The ratios of the peak areas relative to that of the I.S. were plotted against the amounts of preservative injected.

Assay of preservatives in cosmetic samples

A test portion of *ca.* 1 g of sample was accurately weighed into a glass centrifuge tube with a screw-cap. After addition of 10 ml of the solution containing the I.S., the tube was closed and immersed for 15 min in an ultrasonic bath thermostated at 60°C to melt any lipid phase and to facilitate the extraction of the preservative into the organic phase. After cooling and centrifugation, the supernatant was diluted to volume (25 ml) with THF containing 1% acetic acid. Aliquots of 10 μl of the solution were submitted to HPLC analysis.

RESULTS AND DISCUSSION

Fig. 1 shows a typical chromatogram of a standard solution of the preservatives examined and the I.S., obtained by setting the detector at 280 nm. As can be seen, good

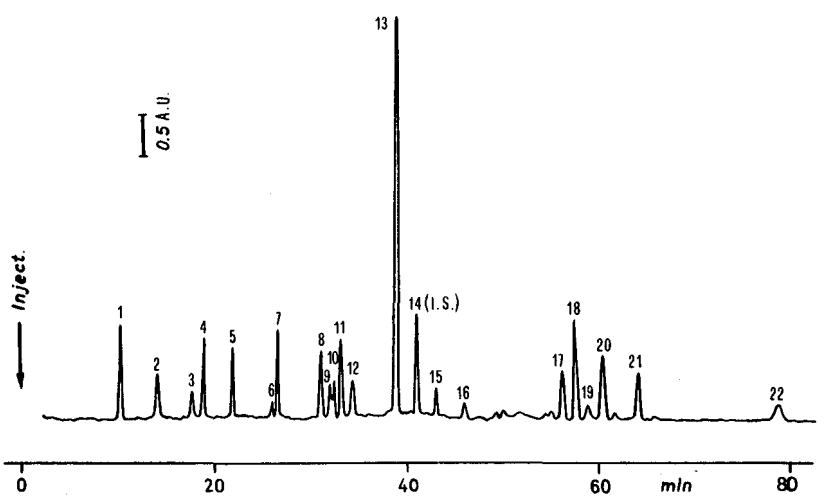

Fig. 1. Typical chromatogram of a solution containing 0.5 mg/ml of each preservative, recorded at 280 nm. Numbers on the peaks are compounds as listed in Table I.

resolution was obtained for all compounds except for slight overlapping of peaks 9 and 10. Table II reports the retention times, which were reproducible under the experimental conditions used, the detection limits (ng injected), calculated as the response three times the noise level, and the response factors relative to the I.S., calculated from the weight ratio. The photodiode-array detector allowed the purity parameter (Varian) format values[5] (λ_w), which were calculated over the wavelength range 234–311 nm, to be obtained. These values, which are shown in Table II, are useful in confirming peak identifications and in determining peak purities. When checking the compliance of a cosmetic product with the EEC legislation, a knowledge of this parameter is very helpful, particularly if the compound under investigation seems to be present at a concentration exceeding the maximum admissible level.

Calibration graphs were constructed from five consecutive injections and were linear for all the compounds considered over the range of concentrations used, *i.e.*, from 0.1 to 30 μg or from 0.02 to 6 μg injected, depending on the kind of preservative. The coefficients of linear regression ranged from 0.9979 to 0.9998 and the reproducibility was very good. In fact, if the calibration graphs were obtained on the same day, the average relative standard deviation (R.S.D.) was less than 2.0%. If the standard solutions were injected for 15 consecutive days, the variability of the assay was slightly greater, the average R.S.D. being about 3.0%.

TABLE II

RETENTION TIMES, RESPONSE FACTORS, DETECTION LIMITS AND PURITY FORMAT VALUES OF THE COMPOUNDS TESTED

Each value is the mean of five determinations.

Compound No.	*Retention time (min)*	*Relative response at 280 nm*	*Detection limit (ng injected) at 280 nm*	λ_w *(234–311)*
1	10.70	0.22	15	266.35
2	13.96	2.03	5	255.28
3	18.39	0.19	20	266.67
4	19.50	0.75	15	243.99
5	22.16	2.00	5	255.39
6	26.47	0.26	50	250.53
7	26.93	1.21	15	252.67
8	31.49	1.00	20	248.03
9	32.53	1.26	20	249.07
10	32.87	1.80	15	255.11
11	33.72	3.03	10	269.46
12	34.67	1.40	20	251.74
13	39.46	3.08	5	258.99
14 (I.S.)	41.35	1.00	20	253.79
15	42.54	1.52	20	256.71
16	43.62	1.12	30	254.08
17	57.20	1.43	15	246.45
18	58.45	3.80	5	262.66
19	59.57	0.37	60	248.43
20	61.31	3.60	5	263.64
21	65.35	0.87	20	261.39
22	79.90	0.91	40	250.28

TABLE III

RECOVERIES OF PRESERVATIVES IN COMMERCIAL PRODUCTS

Each value is the mean of five determinations.

Compound No.	*Amount added (%, w/w)*	*Day cream*			*Night cream*			*Shampoo*			*Body lotion*		
		Recovery (%)	*R.S.D. (intra-) (%)*	*R.S.D. (inter-) (%)*	*Recovery (%)*	*R.S.D. (intra-) (%)*	*R.S.D. (inter-) (%)*	*Recovery (%)*	*R.S.D. (intra-) (%)*	*R.S.D. (inter-) (%)*	*Recovery (%)*	*R.S.D. (intra-) (%)*	*R.S.D. (inter-) (%)*
1	1.00	101	1.9	2.6	100	1.7	2.9	100	1.5	1.8	96	1.9	2.1
2	0.40	96	2.1	3.2	94	1.6	2.4	98	1.8	2.9	99	1.7	2.5
3	1.00	100	1.6	1.8	96	1.5	1.9	99	1.7	2.3	96	1.1	1.4
4	0.50	98	1.4	1.9	100	1.0	1.4	98	0.9	1.0	96	1.6	2.2
5	0.40	97	2.1	2.7	94	1.5	2.0	96	2.0	2.6	96	2.1	2.8
6	0.15	97	1.5	2.2	95	1.9	2.9	93	1.2	1.7	100	1.1	1.4
7	0.20	95	1.8	2.3	96	2.0	2.8	95	2.3	3.1	94	1.5	2.1
8	0.50	94	1.8	2.7	95	1.6	2.4	96	1.2	1.9	98	1.8	2.7
9	0.10	98	2.0	2.9	93	1.9	2.5	100	1.0	1.5	97	1.5	2.0
10	0.40	100	1.6	2.2	98	2.0	3.0	98	1.6	2.7	94	1.0	1.3
11	0.20	101	1.5	2.3	99	1.1	1.7	96	1.5	2.1	98	1.2	1.8
12	0.10	92	1.9	2.7	97	2.2	3.0	94	1.8	2.9	93	1.4	2.6
13	0.60	100	1.4	2.0	99	1.9	2.6	98	0.9	1.5	96	2.1	3.0
15	0.20	93	1.7	2.6	98	1.3	2.1	97	1.1	1.9	98	2.0	3.0
16	0.20	94	1.9	2.8	96	1.8	2.9	95	2.2	3.0	99	1.0	1.7
17	0.30	96	1.1	1.8	93	2.1	3.2	93	1.8	2.7	94	1.9	2.2
18	0.20	97	1.7	2.6	94	2.0	3.0	94	1.8	2.6	93	1.9	3.0
19	0.30	98	1.5	2.2	96	2.2	3.1	93	1.6	2.9	96	2.0	2.9
20	0.30	99	1.9	2.8	95	1.5	2.1	98	1.5	2.6	100	1.7	2.2
21	0.10	96	1.0	1.9	92	2.1	3.2	97	1.8	2.5	95	1.5	2.2
22	0.10	95	1.9	2.8	94	1.6	2.2	100	1.7	2.5	98	1.8	2.8

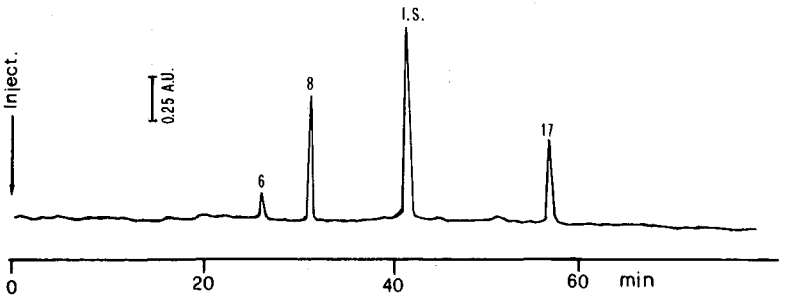

Fig. 2. Chromatogram obtained for a commercial day cream containing preservatives 6, 8 and 17.

The applicability of the proposed method for the determination of compounds 1–22 in cosmetic products was demonstrated by studying their recoveries from four different samples prepared in-house and spiked with the maximum amounts of the preservatives permitted by the EEC legislation. The recoveries obtained are shown in Table III, together with the R.S.D.s obtained either when the assays were performed on the same day (intra-assay R.S.D.) or over a period of 15 days (inter-assay R.S.D.). As the variability was almost the same, it can be inferred that the reproducibility of the method was very good even over a period of several days.

The HPLC procedure was applied to a variety of cosmetic products purchased from local outlets, and containing unknown preservatives. Fig. 2 shows a chromatogram obtained for a sample of day cream. Peak identities were confirmed by determining the purity parameters, which were in good agreement with the values calculated for the standard compounds and reported in Table II. The results of the analyses are given in Table IV. No cosmetic sample contained hexachlorophene and the levels of the preservative identified were in compliance with the EEC Directive.

To our knowledge, in the literature only the paper by Matissek[6] describes the separation and determination of a number of phenolic preservatives in cosmetic

TABLE IV

DETERMINATION OF PRESERVATIVES IN COMMERCIAL COSMETIC PRODUCTS

Each value is the mean of three determinations.

Cosmetic product	*Preservatives found and their percentages (in parentheses)*
Day cream	6(0.16) + 17(0.30) + 8(0.50)
Night cream	5(0.08) + 8(0.30) + 6(0.10) + one not identified
Shampoo	2(0.10) + 5(0.10) + 10(0.10) + 11(0.10)
Body lotion	1(0.30) + 9(0.10) + 13(0.42)
Deodorant	5(0.10) + 1(0.40) + 15(0.15)
Day cream	5(0.20) + 8(0.20) + 15(0.10) + one not identified
Hand cream	8(0.35) + 9(0.05) + 3(0.25)
Body emulsion	7(0.20) + 9(0.10) + 11(0.20)
Shampoo	2(0.20) + 1(0.40) + one not identified
Shampoo	2(0.10) + 5(0.05) + 10(0.05) + 1(0.40)
Night cream	18(0.21) + 15(0.20) + 21(0.10)

products as large as that considered here, using chromatographic techniques. Whereas gas chromatography allowed a good separation of twelve preservatives, the resolution obtained by HPLC on LiChrosorb RP-8 with isocratic elution was poor, as all the esters of *p*-hydroxybenzoic acid coelute and so do *o*-phenylphenol and *p*-chloro-*m*-xylenol.

In contrast, the chromatographic separation obtained here using an ODS column and gradient elution is very good. This fact, together with the simple extraction procedure and the good accuracy and precision, make the proposed method suitable both for rapid screening and for the quantitative determination of the 22 preservatives considered in cosmetic products.

REFERENCES

1 L. Gagliardi, A. Amato, G. Cavazzutti, V. Zagarese, E. Gattavecchia and D. Tonelli, *J. Chromatogr.*, 294 (1984) 442.
2 L. Gagliardi, A. Amato, A. Basili, G. Cavazzutti, E. Gattavecchia and D. Tonelli, *J. Chromatogr.*, 315 (1984) 465.
3 L. Gagliardi, A. Amato, G. Cavazzutti, E. Gattavecchia and D. Tonelli, *J. Chromatogr.*, 325 (1985) 353.
4 L. Gagliardi, A. Amato, A. Basili, G. Cavazzutti, E. Federici, F. Chimenti, M. G. Casanova, E. Gattavecchia and D. Tonelli, *J. Chromatogr.*, 348 (1985) 321.
5 T. Alfredson, T. Sheehan, T. Lenert, S. Aamodt and L. Correia, *J. Chromatogr.*, 385 (1987) 213.
6 R. Matissek, *Z. Lebensm.-Unters.-Forsch.*, 176 (1983) 95.

Journal of Chromatography, 508 (1990) 259–264
Elsevier Science Publishers B.V., Amsterdam — Printed in The Netherlands

CHROM. 22 420

Note

Direct determination of corrosion inhibitor in aviation fuel by a column-switching technique using gel-permeation chromatography

G. E. HAYES

Directorate of Quality Assurance/Technical Support, Materials Centre, Royal Arsenal East, London SE18 6TD (U.K.)

(First received November 21st, 1989; revised manuscript received February 22nd, 1990)

Hitec E580 is added to aviation fuel as an antiwear agent and corrosion inhibitor. The normal concentration range is 10–20 ppm and the level may be determined by measuring the concentration of the major active ingredient, namely dimer acid (technical-grade dilinoleic acid).

The method of Hillman *et al.*[1] involves multiple extractions of the dimer acid from a large volume of fuel and measurement is achieved by gel-permeation chromatography (GPC) with refractive index detection. A modified version of this method has been used to determine the concentration of a range of similar corrosion inhibitors in jet fuel and to examine the depletion of the active ingredient on contact with sea water and metal surfaces[2,3]. A method using reversed-phase ion-exclusion chromatography with UV detection has also been described[4].

Hillman *et al.*'s method[1] cannot be applied to the small amounts of fuel, 10 ml or less, which may be all that is available as part of an accident investigation. Also, the manual extraction steps are time-consuming and cannot be readily automated. This paper describes an improved method of measuring Hitec E580 in aviation fuel which overcomes these problems. The method uses an on-line precolumn, containing a polar packing, to extract the dimer acid from the fuel. Operation of a switching valve allows the precolumn to be flushed with tetrahydrofuran (THF), thus transferring the dimer acid to a GPC column. Refractive index detection is used. The two methods give results which are in acceptable agreement.

EXPERIMENTAL

Apparatus

The apparatus consisted of two Waters 510 reciprocating pumps, one directly connected to a Waters automated switching valve and the other connected to the valve via a Rheodyne 7120 sample injector fitted with a 2-ml loop. The switching valve was fitted with a Waters Guard-Pak precolumn module containing a cyano insert. Separations were carried out on a 50-Å and a 100-Å PL-Gel column (250 mm × 4.6

0021-9673/90/$03.50

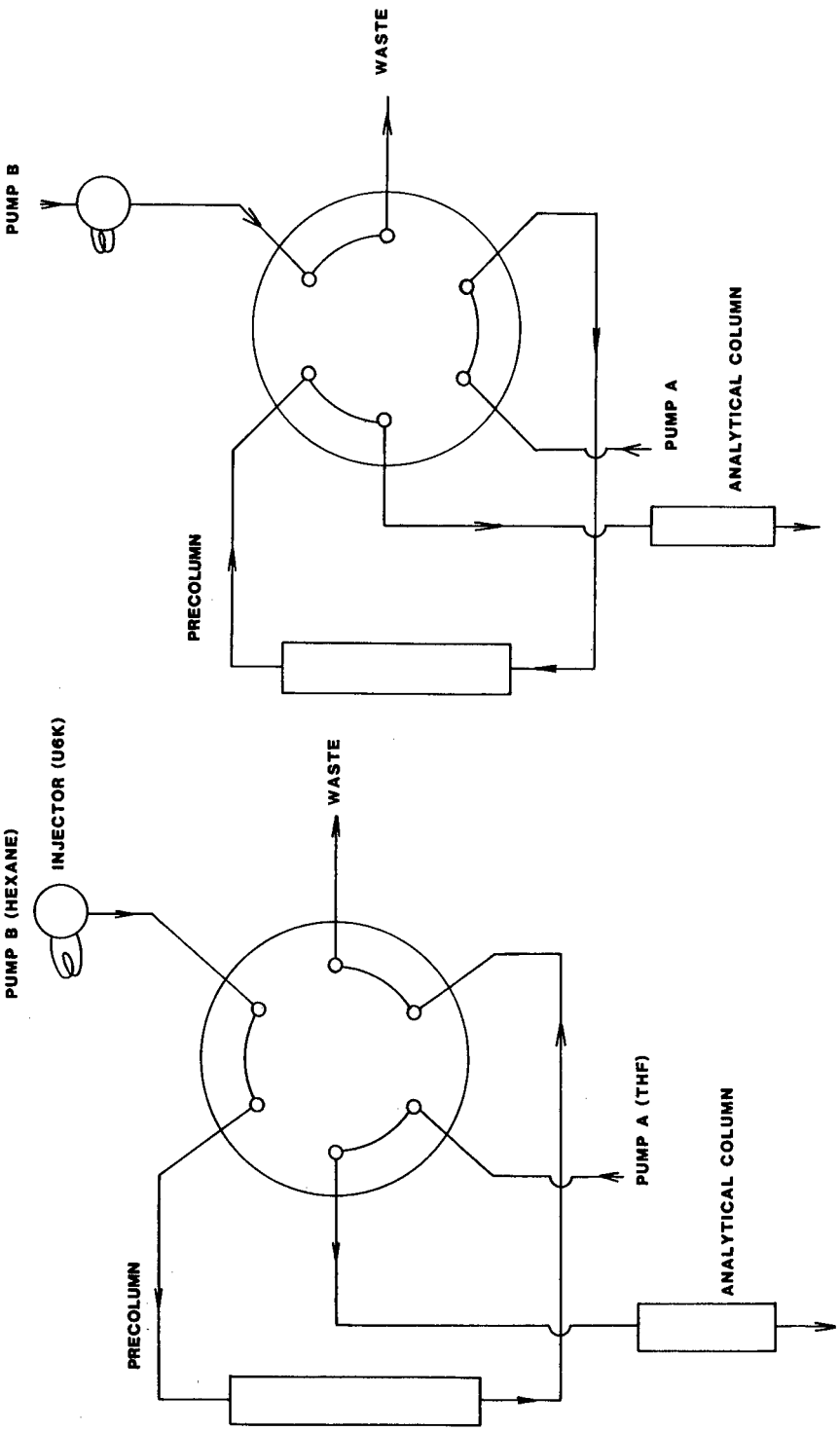

Fig. 1. (A) Rheodyne valve in configuration 1 (load precolumn). (B) Rheodyne valve in configuration 2 (flush precolumn).

mm I.D.), containing 5-μm packing, connected in series. The detector was a Waters 410 differential refractometer. System control and data collection were achieved with a Waters 840 data station (see Fig. 1A and B). Unstabilised THF and hexane, both HPLC grade, were obtained from Rathburn (Walkerburn, U.K.).

Procedure

The first stage in the analysis was a combined preconcentration/sample clean-up step; this was required due to the low level of additive present in a large excess of potentially interfering compounds. It was achieved by injecting 2 ml of fuel onto an in-line precolumn containing a disposable cartridge filled with a polar bonded phase packing. The dimer acid was retained on the precolumn and the remainder of the fuel was removed by pumping hexane through the cartridge.

The precolumn module was connected across an automatic switching valve which, when operated, changed the solvent flowing through the cartridge from hexane to THF. This flushed the dimer acid onto the analytical columns and then into the refractive index detector. A sample chromatogram is shown in Fig. 2. The peak eluting just before the main dimer acid peak is believed to be due to trimer acid. The sum of the peak areas was used for quantitation.

Standards were prepared by dilution of a stock solution of Hitec E580 dissolved in an additive-free reference fuel.

RESULTS AND DISCUSSION

The refractive index detector was shown to have a linear response over the required concentration range (Fig. 3). The correlation coefficient was 0.9994.

In order to evaluate the method a number of aviation turbine fuel (AVTUR) samples were analysed. The level of Hitec E580 in these samples has also been determined by the standard extraction method[1]. The results obtained from the two procedures are shown in Table I.

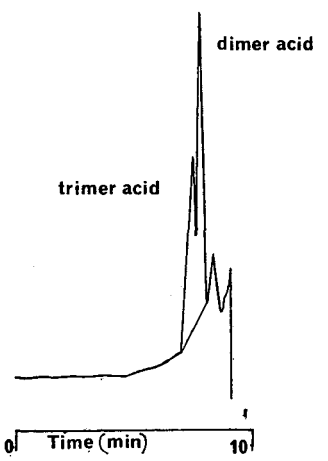

Fig. 2. Chromatogram of Hitec E580 (20 ppm).

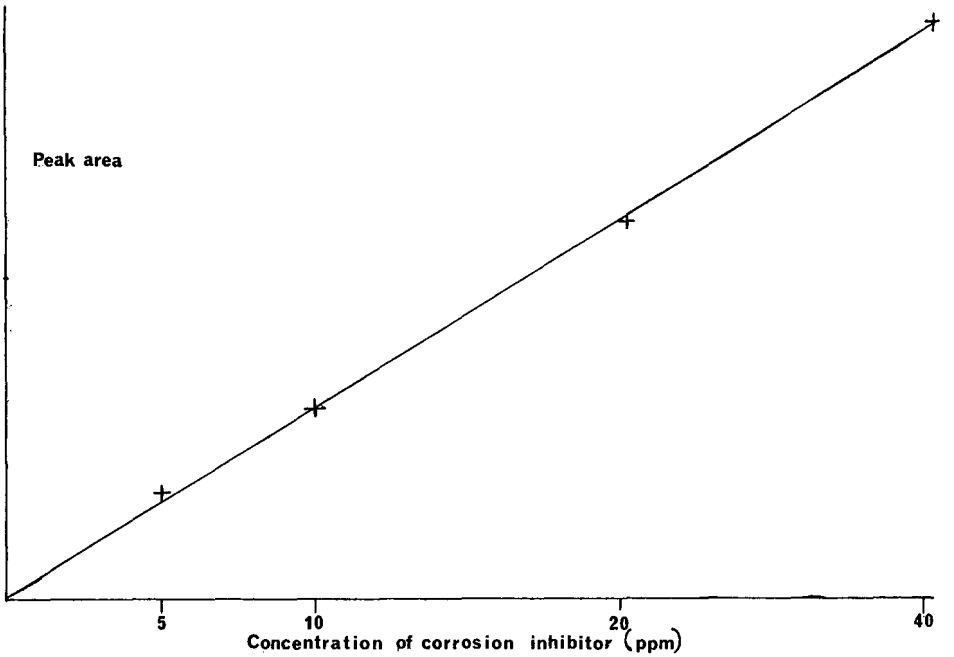

Fig. 3. Calibration curve for determination of Hitec E580 in aviation fuel.

The mean relative standard deviation for the proposed method is 4.1%, which is close to the value of 4.4% reported for the method of Hillman *et al.*[1]. The levels of Hitec E580 found by the two methods are in acceptable agreement.

Sample 5 was markedly different from the other samples in having a deep yellow colour due to ageing. It could not be analysed by the column-switching method due to the presence of a large interfering peak. Old samples can also sometimes cause problems with the extraction method, since the dimer acid peak is only apparent as a shoulder on the side of a large peak arising from co-extracted material.

Both methods were also used to determine the levels of Hitec E580 in AVCAT, the high-flash-point fuel used on ship-based aircraft. Table II shows the results obtained, which are again seen to be in acceptable agreement.

TABLE I

DETERMINATION OF HITEC E580 IN AVTUR SAMPLES

Sample No.	*Concentration of Hitec E580 (ppm)*			
	Extraction method	*Column-switching method*	*Mean*	*Relative standard deviation (%)*
1	11	11.0, 11.5, 11.0, 10.4, 11.0	11.0	3.6
2	12	12.0, 12.5, 12.5	12.3	2.3
3	9	11.0, 10.5, 10.4	10.6	3.0
4	10	11.0, 12.5, 11.0	11.5	7.5
5	11	Interference found	–	–

TABLE II

DETERMINATION OF HITEC E580 IN AVCAT SAMPLES

Sample No.	*Concentration of Hitec E580 (ppm)*		
	Column-switching method	*Mean*	*Extraction method*
1	25, 24	24.5	20
2	39, 40	39.5	40
3	17, 17	17.0	14
4	15, 15	15.0	15
5	15, 14	14.5	14
6	6, 6	6.0	8
7	6, 6	6.0	5

CONCLUSIONS

A method has been developed for the quantitative determination of dimer acid, and hence Hitec E580, in aviation fuel. The accuracy and precision are close to that of the standard extraction method, and it has the following advantages.

(i) Only 2 ml of fuel are required, compared to 800 ml in the extraction method. This makes the new method suitable for use with the limited amounts of fuel which may be available in an accident investigation.

(ii) The elimination of the manual extraction steps means that the new method is faster and more convenient to operate.

(iii) The method can be fully automated.

The equipment used in this investigation included a detector with a very high signal-to-noise ratio. The estimated limit of detection was 1 ppm Hitec E580 (which corresponds to a dimer acid concentration of around 0.4 ppm). If a less sensitive detector is used then a larger sample volume is required, in order to maintain the same limit of detection. The upper limit of sample volume is provided by the breakthrough volume of the precolumn insert.

Several other commercially available corrosion inhibitors/lubricity additives are based on dimer acid, and the column-switching method is expected to be suitable for their determination. However, one additive is known to contain other dibasic acids in addition to dimer acid, and the method has not been extended to the examination of this type of sample.

ACKNOWLEDGEMENTS

I would like to record the contribution of Mr. John Hawke, late of the Naval Aircraft Materials Laboratory, who initiated this project. Also Mr. Leigh Clare, DQA/TS, who carried out the analyses by the extraction method is acknowledged.

REFERENCES

1 D. E. Hillman, J. I. Paul and D. G. Cobbold, in D. R. Hodges (Editor), *Recent Developments in the Petroleum Industry*, Applied Science Publishers, 1977, pp. 47–58.
2 D. R. Hardy, B. H. Black and M. A. Wechter, *J. Chromatogr.*, 366 (1986) 351–361.
3 B. H. Black, M. A. Wechter and D. R. Hardy, *J. Chromatogr.*, 437 (1988) 203–210.
4 T. B. Biddle and W. H. Edwards, *AFWAL-TR-88-236*, Air Force Wright Aeronautical Laboratories, Wright Patterson AFB, OH, July 1988.

Journal of Chromatography, 508 (1990) 265–270
Elsevier Science Publishers B.V., Amsterdam — Printed in The Netherlands

CHROM. 22 383

Note

Determination of borate at trace levels in environmental samples by ion-exclusion chromatography

H. C. MEHRA, K. DAVIS HUYSMANS and W. T. FRANKENBERGER, Jr.*
Department of Soil and Environmental Sciences, University of California, Riverside, CA 92521 (U.S.A.)
(First received July 18th, 1989; revised manuscript received February 2nd, 1990)

Boron can be toxic to higher plants when present in soil solution at levels (0.5–5.0 $\mu g\ ml^{-1}$) not much greater than trace amounts needed for normal growth[1]. Minerals containing boron are found in naturally occurring igneous, metamorphic and sedimentary rocks. Chemical weathering of these minerals releases soluble boron that is readily available for plant uptake. Boron is probably the most troublesome microelement in managing saline and alkaline soils[2]. While boron is essential for plant growth at low concentrations, most crops are extremely sensitive to this element. Boron toxicities are more prevalent than are boron deficiencies among crops grown on saline soils[1].

Boron in drinking water in many regions of the world has been reported to be 100 $\mu g\ l^{-1}$ or less[1]. The recommended maximum concentration for boron in irrigation water is 750 $\mu g\ l^{-1}$ (ref. 3).

Ion-exclusion chromatography has wide applications for the separation of ionic species[4–6]. It is an accepted technique for organic acid analysis and is increasingly being used for weakly ionized inorganic solutes. In this paper, we have applied ion-exlusion chromatography for the trace determination of borate in soils, sediments and water samples using D-sorbitol in the mobile phase. This method also has applications in the determination of bicarbonate. Two ion-exclusion columns were evaluated for their efficiencies in separation of borate. This ion-exclusion chromatography technique enables separation, detection and quantification of borate from various matrices obtained from several environmental problem sites. Results obtained by ion-exclusion chromatography were compared with a standard spectrophotometric method for determination of borate.

EXPERIMENTAL

Chromatographic instrumentation

The high-performance liquid chromatographic (HPLC) assembly consisted of a Beckman Model 332 liquid chromatograph equipped with a Model 110A pump and a Model 210 sample injector. Conductometric detection was carried out with a Wescan (San Jose, CA, U.S.A.) Model 213 detector. The ion-exclusion chromatography

0021-9673/90/$03.50

system was composed of the following: a Wescan ion-exclusion column (No. 269-006) (300 mm × 7.8 mm I.D.), particle size 10 μm, connected to a Wescan ion guard anion-exclusion column (No. 269-007); Interaction (Mountain View, CA, U.S.A.) ORH-801 anion-exclusion column (No. 25310) (300 mm × 6.5 mm I.D.), particle size 8 μm, and an Elden (Elden Labs., Menlo Park, CA, U.S.A.) Model III thermostatic column heater. A Hewlett-Packard (Avondale, CA, U.S.A.) Model 3390A printer–plotter integrator with variable input voltage was used to monitor the signal output with a chart speed of 0.5 cm min^{-1}. Sample injection loops of 100, 200, 500 and 1000 μl were employed to establish detection limits.

Reagents

The mobile phase consisting of D-sorbitol (Sigma, St. Louis, MO, U.S.A.) was prepared as 0.025–0.4 *M* solutions. The flow-rate was 2 ml min^{-1} for the Wescan column and 1.0 ml min^{-1} for the Interaction column. The column inlet pressure was approximately 1200 p.s.i. (Wescan) or 1500 p.s.i. (Interaction). The detector output was 10 mV. The eluent was passed through an LC-SCX tube (5-8997M) (Supelco, Bellefonte, PA, U.S.A.) to remove ionic impurities, filtered through a 0.22-μm GS membrane filter (Millipore, Bedford, MA, U.S.A.) and degassed under vacuum prior to conditioning the column.

Solutions were made by dissolving sodium borate ($Na_2B_4O_7 \cdot 10H_2O$) (Mallinckrodt, Paris, KY, U.S.A.) and sodium bicarbonate ($NaHCO_3$) (Mallinckrodt) in HPLC-grade water. HPLC-grade water was obtained by filtering deionized water through an HN organic removal resin (Barnstead, Boston, MA, U.S.A.), then HN Ultrapure DI exchange column (Barnstead) and finally a 0.22-μm Millipore GS filter.

Field samples and preparation

Sediment samples were collected from an evaporation pond facility at the Sumner Peck Ranch and from the San Luis Drain near Fresno, CA, U.S.A., containing agricultural drainage water that had percolated through boron-rich soils.

Saline surface soil samples (Traver and Twisselman) were collected from Kern County, CA, U.S.A. and San Bernardino, CA, U.S.A. The soil samples were allowed to air-dry, passed through a 2-mm-mesh screen and homogenized.

Water samples from local lakes (Riverside, CA, U.S.A.) were also analyzed for borate. No sample preparation was needed for the water samples except diluting with deionized water and then passing through a 0.22-μm Millipore GS filter before analysis.

Air-dry soil or sediment (10 g) was boiled under reflux with 30 ml of water for 10 min. The samples were then subjected to shaking for 2 h and filtered through Whatman No. 3 filter paper. Organic impurities were removed by passing the extract through a Supelcosil LC-Si tube (5-8974M) (Supelco). The extract was then passed through a 0.22-μm Millipore GS membrane filter before the ion-exclusion chromatographic analysis.

To check the reproducibility of the ion-exclusion chromatography method, a minimum of ten injections of combined standards containing borate and a bicarbonate mixture were used. The detection limits for borate and bicarbonate with various sample sizes were calculated as the three-fold signal-to-noise ratio of the baseline ($S/N = 3$).

Spectrophotometry

Determination of the borate content in soils, sediments and water samples was also carried out by the method of John *et al.*[7]. This method involves the spectrophotometric determination of a borate azomethine–H (Pierce, Rockford, IL, U.S.A.) complex stable at pH 5.1 and measuring the absorbance at 420 nm.

RESULTS AND DISCUSSION

Ion-exclusion chromatography was chosen because of the high pK_a value of borate (9.2). With ion-exclusion chromatography, retention is due primarily to an exclusion–partition mechanism on a polymeric cation-exchange resin although non-polar interactions may also affect retention. The basis for separation of borate by ion-exclusion chromatography involves the use of a polyalcohol in the mobile phase which forms a polyborate complex[6,8–10].

$$B(OH)_3 + 2LH_2 \rightleftarrows H^+ + L_2B^- + 3H_2O$$

The formation of such a complex is dependent upon the concentration, pH and nature of the polyol[8]. A mannitol–boric acid complex has been previously studied with 0.1 *M* mannitol – 0.001 *M* hydrochloric acid in the mobile phase for borate determination by ion-exclusion chromatography with suppresed ion chromatography (IC)[6]. The suppressed IC system was inherently non-linear and had unavoidable deposition of halides on the suppressor column.

In this study, D-sorbitol in the mobile phase forms a stable and detectable complex with borate. The retenion time of this complex was only 3.5 min compared to approximately 12 min reported in the suppressed IC system[6].

Optimization parameters for ion-exclusion chromatography

Studies were carried out to determine the optimum concentration of D-sorbitol for separation and detection of borate. An increasing concentration of D-sorbitol up to 0.4 *M* did not cause an increase in background conductance. Higher sensitivity of borate detection was observed in the range 0.2–0.3 *M versus* <0.2 *M* D-sorbitol (Fig. 1). The response of borate was not affected by a change in the pH (5–10) of the

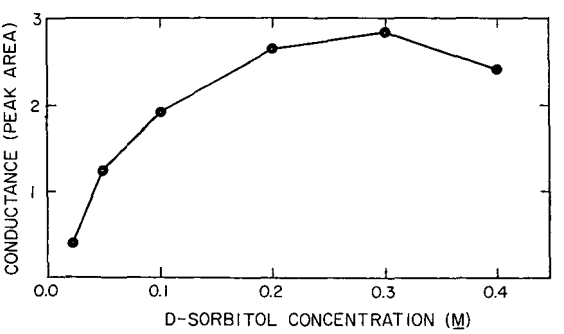

Fig. 1. Dependence of signal response of borate on the concentration of D-sorbitol in the mobile phase (other chromatographic conditions as in Table I).

mobile phase, while bicarbonate decreased with increasing pH (5–7) of 0.3 *M* D-sorbitol. There was no effect on retention times of borate and bicarbonate (100–1000 mg l^{-1}) with variations in sample pH (5–10) and injection volume (100–1000 μl). The optimum concentration of D-sorbitol for borate determination was 0.3 *M* (pH 5.3). Broader peaks were observed at concentrations lower than 0.2 *M*. At higher D-sorbitol concentrations (>0.4 *M*), the solubility of D-sorbitol was limited.

Comparison of D-sorbitol (0.3 *M*) with D-mannitol (0.3 *M*) showed that retention times were considerably less with D-sorbitol when used in the mobile phase with the Wescan column. Borate and bicarbonate eluted at 3.45 and 5.60 min, respectively, with D-sorbitol, and 4.04 and 6.22 min, respectively, with D-mannitol. D-Sorbitol was preferred over mannitol because of its higher solubility in water, its lower cost and lower detection limits. The effect of column temperature was studied with maximum sensitivity observed in the temperature range 25–30°C. Higher temperatures resulted in decreased sensitivity, possibly due to the decomposition of the borate–sorbitol complex.

Comparison of columns

Two columns were evaluated for borate determination. Both columns were composed of functionalized polystyrene–divinylbenzene with ionic groups. The difference in their behavior could be due to their degree of cross-linkages. Each was compared in terms of retention time, number of theoretical plates (*N*) and height equivalent to a theoretical plate (HETP). The retention time for borate was 3.45 min with the Wescan column compared to 5.06 min with the Interaction column. The *N* and HETP for borate were 2055 (0.15 mm) and 1592 (0.19 mm) with the Wescan and Interaction columns, respectively. It was on the basis of these comparative parameters that the Wescan column was selected for further studies in the separation of borate.

Precision, linearity of response and detection limits

The precision of this ion-exclusion chromatography method for the analysis of borate as determined by repeated injections made of standards is given in Table I. The results show that the relative standard deviations (R.S.D.) of borate ranged from 0.68 to 1.42% with a 500-μl loop. A calibration plot was obtained by plotting peak area against the borate concentration. The plot was linear within the range 0.10–

TABLE I

PRECISION OF THE ION-EXCLUSION CHOMATOGRAPHY METHOD IN THE DETERMINATION OF BORATE AND BICARBONATE (n = 10)

Column, Wescan (300 mm × 7.8 mm I.D.); mobile phase, 0.3 *M* D-sorbitol; detection, conductometric; temperature, 25°C. Values in parentheses are R.S.D. values (%).

Sample volume (μl)	*Concentration (mg l^{-1})*	
	Borate	*Bicarbonate*
100	7.4 (1.04)	28.0 (2.26)
200	4.2 (0.72)	14.5 (2.90)
500	1.1 (0.48)	6.4 (1.42)
1000	0.6 (0.68)	7.0 (1.52)

9.60 mg l^{-1}. The minimum detection limit for borate was 0.05 ng obtained by injecting 500 μl of a 0.1 μg ml^{-1} sample. For bicarbonate, the calibration curve was linear from 1 to 100 mg l^{-1} with the limit of detection being 1.25 ng.

Interferences

One of the major concerns in the analysis of environmental samples is the accurate determination of the ion of interest in the presence of other inherent ions. The response due to such ions when present in large amounts could easily mask the signal of the target analyte, particularly with conductometric detection. With ion exclusion, strong mineral acid anions such as Cl^-, NO_3^- and SO_4^{2-} eluted rapidly giving an early single peak before the borate complex was detected. Further tests with weak anions (AsO_3^{3-}, F^-, $H_2PO_4^-$, HCO_3^-, SO_3^{2-}, TeO_4^{2-}, TeO_3^{2-} and SiO_3^{2-}) under the conditions described (500-μl sample) cause no interferences in the determination of borate.

Comparison of methods

A close relationship was observed by the proposed ion-exclusion chromatography method and the colorimetric azomethine-H procedure in determination of borate in soil, sediment and lake water samples (Table II). The relationship can be expressed as follows: $y_{\text{azomethine}} = 1.06x_{\text{ion exclusion}} - 0.43, r^2 = 0.997 (P < 0.001)$. The unity in slope indicates excellent agreement between the two methods.

Determination of borate by ion-exclusion chromatography

A typical chromatogram of a hot water soil extract is shown in Fig. 2. The solutes (borate and bicarbonate) were separated into well defined peaks with a total time of analysis of 7 min. Calculation with external standards indicated that this soil extract contained 3.4 mg borate per kg soil.

TABLE II

COMPARISON OF ION-EXCLUSION CHROMATOGRAPHY AND AZOMETHINE-H METHODS FOR BORATE DETERMINATION IN ENVIRONMENTAL SAMPLES (n = 3)

Values in parentheses are R.S.D. values (%).

Sample type	*Borate concentration*	
	Ion-exclusion chromatography	*Azomethine-H*
Evaporation pond sediments (mg kg^{-1})		
Peck	6.7 (0.81)	6.5 (0.92)
San Luis Drain	14.4 (1.02)	15.3 (1.42)
Saline soils from Kern County, CA, U.S.A. (mg kg^{-1})		
Traver silt loam	0.8 (0.56)	0.8 (2.44)
Traver II loam	7.5 (1.14)	7.3 (1.55)
Twisselman clay loam	3.4 (0.84)	3.2 (0.78)
Lake water (mg l^{-1})		
Sample I	2.1 (0.55)	2.0 (1.31)
Sample II	3.2 (0.76)	3.3 (1.12)

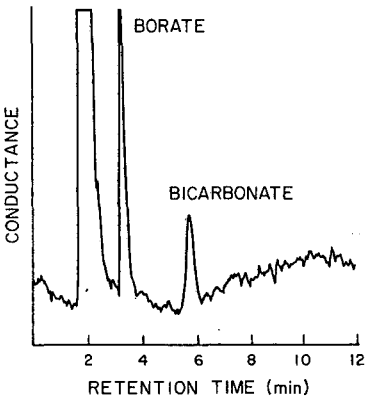

Fig. 2. Chromatogram of a soil extract (chromatographic conditions as in Table I).

ACKNOWLEDGEMENTS

The authors are grateful to Wescan Instruments, Inc. and Interaction Chemicals for the gifts of the analytical columns used in this study.

REFERENCES

1 D. C. Adriano, *Trace Elements in the Terrestrial Environment*, Springer, New York, 1986.
2 A. Kobota-Pendias and H. Pendias, *Trace Elements in Soils and Plants*, CRC Press, Boca Raton, FL, 1986.
3 J. M. Montgommery Engineers, *Water Treatment, Principles and Design*, Wiley, New York, 1985.
4 R. E. Smith, *Ion Chromatography Applications*, CRC Press, Boca Raton, FL, 1988.
5 D. T. Gjerde and H. Mehra, in P. Jandik and R. M. Cassidy (Editors), *Advances in Ion Chromatography*, Vol. 1, Century International, Boston, MA, 1989, pp. 139–175.
6 J. P. Wilshire and W. A. Brown, *Anal. Chem.*, 54 (1982) 1647.
7 M. K. John, H. H. Chuah and J. H. Neufeld, *Anal. Lett.*, 8 (1975) 559.
8 R. E. Braman, in I. M. Kolthoff and P. J. Elving (Editors), *Treatise on Analytical Chemistry*, Vol. 10, Part II, Wiley, New York, 1978, pp. 3–101.
9 T. Okada and T. Kuwamoto, *Anal. Chem.*, 58 (1986) 1375.
10 J. Boeseken, *Adv. Carbohydr. Chem.*, 4 (1949) 189.

Journal of Chromatography, 508 (1990) 271–274
Elsevier Science Publishers B.V., Amsterdam — Printed in The Netherlands

CHROM. 22 381

Note

Sulfite–disulfite equilibrium on an ion chromatography column

BRIAN J. JOHNSON
Chemistry Department, University of Nevada, Las Vegas 4505 S. Maryland Parkway, Las Vegas, NV 89154 (U.S.A.)
(Received November 24th, 1989)

Sulfite compounds (including SO_3^{2-}, HSO_3^-, $S_2O_5^{2-}$ and SO_2) are widely used in industrial processes as antioxidants and preservatives. Their use in food products has come under closer scrutiny lately due to adverse physiological reactions in some individuals. Ion chromatography has been successfully used for determination of aqueous S^{IV} compounds in industrial mixtures[1,2] and offers considerable advantages in time, sensitivity and selectivity over older methods[3–5].

In the course of investigating new eluents for the resolution of sulfite from sulfate using a commercial column, unexpected behavior was observed for the sulfite peak when certain eluents were used, namely, distortion of peak shape and shortened retention time with increased concentration. This behavior is described in terms of a sulfite–disulfite equilibrium occurring on the column. Conditions for a baseline resolution of sulfite and sulfate are also presented.

EXPERIMENTAL

All chromatograms were obtained on a Qic Analyzer ion chromatograph (Dionex, Sunnyvale, CA, U.S.A.) equipped with a 50-μl sample loop, an AG4 guard column, an AS4A ion separator column, a membrane-based background suppressor and a conductivity detector cell. The AS4A is a strong anion-exchange column, consisting of tetralkylammonium moieties bound to a polystyrene resin. The flow-rate was 2.0 ml/min, and eluents of various concentration were made from reagent-grade NaOH (Fisher), $NaHCO_3$ (MCB) and/or primary standard grade Na_2CO_3 (Thorn Smith), dissolved in 18-M-Ω water (Milli-Q system, Millipore, Bedford, MA, U.S.A.). Chromatograms were obtained on a strip-chart recorder, with retention times and peak heights measured manually.

A stock sulfite standard was made by dissolving *ca.* 0.6 g of reagent grade sodium bisulfite (Baker) in dilute aqueous formaldehyde [*ca.* 0.030 mol from 37% (w/w) aqueous formaldehyde; Mallinckrodt] and making up to 500 ml with high-purity water. The solution was standardized by oxidizing 5-ml aliquots in alkaline hydrogen peroxide (30%; MCB) and heating over a hot plate until excess peroxide was destroyed. These solutions were cooled, made up to volume and analyzed for sulfate by

0021-9673/90/$03.50

TABLE I

CHARACTERISTICS OF SELECTED ELUENTS

Eluent No.	*Chemical composition*	*pH*	*Ionic strength*
1	$8.5 \cdot 10^{-3}$ *M* HCO_3^- $6.3 \cdot 10^{-4}$ *M* CO_3^{2-}	9.19	$1.0 \cdot 10^{-2}$
2	$8.5 \cdot 10^{-3}$ *M* HCO_3^- $8.5 \cdot 10^{-4}$ *M* CO_3^{2-}	9.30	$1.1 \cdot 10^{-2}$
3	$1.7 \cdot 10^{-3}$ *M* HCO_3^- $1.8 \cdot 10^{-3}$ *M* CO_3^{2-}	10.26	$7.1 \cdot 10^{-3}$
4	$2.6 \cdot 10^{-4}$ *M* HCO_3^- $2.2 \cdot 10^{-3}$ *M* CO_3^{2-}	10.70	$7.0 \cdot 10^{-3}$
5	$8.5 \cdot 10^{-5}$ *M* HCO_3^- $2.2 \cdot 10^{-3}$ *M* CO_3^{2-}	10.75	$6.8 \cdot 10^{-3}$
6	$2.2 \cdot 10^{-3}$ *M* CO_3^{2-} $7.7 \cdot 10^{-4}$ *M* OH^-	11.05	$7.5 \cdot 10^{-3}$

ion chromatography. A small sulfate contribution attending the unoxidized standard was subtracted from this value.

RESULTS

The composition data for six different eluents used in the study are given in Table I. At these pH levels, the form of aqueous S^{IV} will be sulfite (*i.e.*, 99% or greater). Capacity factors for five different anions are plotted for each of these eluents in Fig. 1. Note that in eluents 1 and 2 sulfite elutes after sulfate, while in the other eluents the order is reversed. Furthermore, the retention time for the sulfite peak in the first two eluents is concentration-dependent. The percent decreases in retention from eluent 1–6

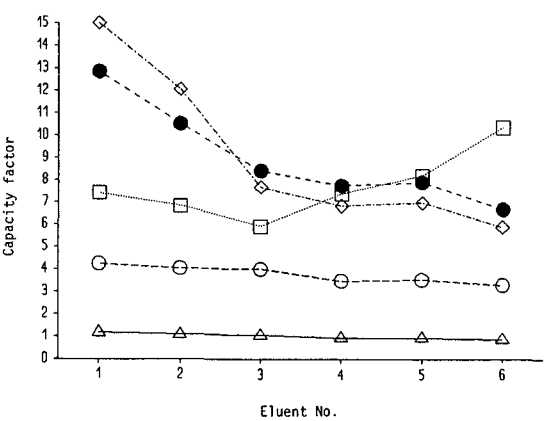

Fig. 1. Capacity factors for five anions using six different eluents. △ = Chloride; ○ = nitrate; □ = phosphate; ● = sulfate; ◇ = S^{IV}.

are 23% for Cl^-, 21% for NO_3^- and 47% for SO_4^{2-}, *i.e.*, in approximate ratio to their charge.

In Fig. 2, chromatograms are shown for different concentrations of sulfite using eluent 1. Note that not only does the retention time shorten with increasing concentration, but the peak broadens abnormally and develops an asymmetric front tail. Similar behavior is observed with eluent 2, but to a lesser degree. Agreement of absolute retention times between different batches of eluent is variable, largely because of the sensitivity to small changes in the carbonate concentration.

These findings are consistent with the following series of reactions:

$$2\,SO_3^{2-}(\text{ads}) + H_2O \overset{K_1}{\rightleftharpoons} S_2O_5^{2-}(\text{ads}) + 2\,OH^- \tag{1}$$

$$2\,OH^- + 2\,HCO_3^- \overset{1/K_b}{\rightleftharpoons} 2\,CO_3^{2-} + 2\,H_2O \tag{2}$$

$$2\,SO_3^{2-}(\text{ads}) + 2\,HCO_3^- \rightleftharpoons S_2O_5^{2-}(\text{ads}) + 2\,CO_3^{2-} + H_2O \tag{3}$$

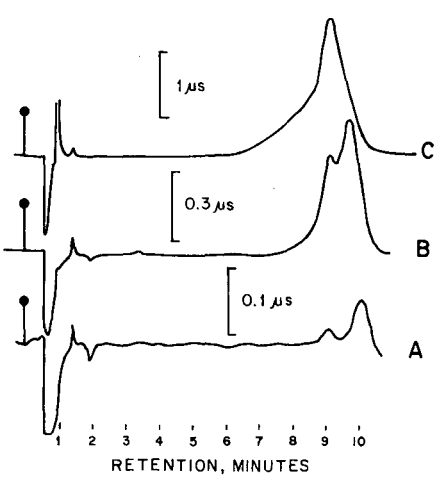

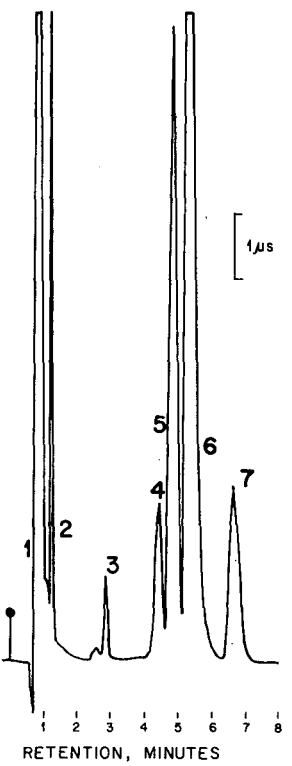

Fig. 2. Chromatograms of sulfate and "sulfite" as a function of sulfite concentration: (A) 1.2 ppm; (B) 11.6; (C) 46.4 ppm. Sulfate concentration is about 5% of sulfite values.

Fig. 3. Chromatogram of white table wine (25:1 dilution with 0.6 mg formaldehyde). Peaks: 1 = organic acids; 2 = chloride; 3 = nitrate; 4 = sulfite; 5 = sulfate; 6 = tartrate; 7 = phosphate.

Disulfite or pyrosulfite, $S_2O_5^{2-}$, forms in concentrated aqueous solutions of bisulfite ($K = 7 \cdot 10^{-2}$) (ref. 6), but not in solutions of sulfite. However, a reaction sequence such as described by reactions 1–3 could readily be facilitated by the conditions present in this experiment and is consistent with observations.

The hydrophobic yet positively charged stationary phase will support relatively high sulfite concentrations with the exclusion of water at the surface, favoring formation of disulfite. Disulfite, on the basis of mass-to-charge ratio, should elute earlier than sulfite, accounting for the concentration dependence of retention. The concentration and pH dependence of retention are also readily explained by the reaction sequence, whereas an alternative mechanism such as oxidation is inconsistent with observations. Formation of carbonate (as indicated in reaction 2) would increase its local concentration, inducing competition with sulfite and disulfite for surface absorption sites. Further reduction of elution time would result, and since this phenomenon is also dependent on the concentration of sulfite, the front-tailing is rationalized.

No concentration dependence of sulfite retention occurs for eluents 3–6, and of these, eluent 6 seems to offer the optimal situation with regard to sensitivity, rapidity and resolution of other common anions (see Fig. 1). A typical least-squares calibration curve using standards of 0.4, 1.7, 7.0, 29.0 and 116 μg/ml (as HSO_3^-) gave the equation $y = 0.345x - 0.060$ ($r > 0.999$). Based on extrapolation from the lowest standard, a conservative detection limit of 0.8 ng of bisulfite is obtained. This sensitivity corresponds to 16 parts per 10^9 using a 50-μl sample loop; correspondingly lower limits are possible with larger sample loops.

A chromatogram illustrating the separation of sulfite from sulfate in a white table wine is shown in Fig. 3. Even though the sulfate peak is much larger (corresponding to ≈ 200 μg/ml), the sulfite is sufficiently well resolved to permit an accurate analysis; simultaneous determination of tartrate and phosphate is also possible. At lower levels of sulfate and sulfite, the peaks are resolved at the baseline.

REFERENCES

1 D. M. Sullivan and R. L. Smith, *Food Technol.*, 39 (1985) 45.
2 D. B. Easty, M. L. Borchardt and A. A. Webb, *Pap. Puu*, 67 (1985) 501.
3 H. D. Axelrod, J. E. Bonelli and J. P. Lodge, *Anal. Chem.*, 42 (1970) 512.
4 E. Jungreis and Z. Anavi, *Anal. Chim. Acta*, 45 (1969) 190.
5 H. G. C. King and G. Pruden, *Analyst (London)*, 94 (1969) 43.
6 R. M. Golding, *J. Chem. Soc.*, 741 (1960) 3711.

Journal of Chromatography, 508 (1990) 275–277
Elsevier Science Publishers B.V., Amsterdam — Printed in The Netherlands

CHROM. 22 337

Letter to the Editor

Identification of fatty acids longer than C_{32} in a sulphate-reducing bacterium by reversed-phase high-performance liquid chromatography and gas chromatography–mass spectrometry

Sir,

The development of improved analytical techniques has made it possible to obtain more detailed information about sources of very long-chain fatty acids (VLCFAs). The presence of VLCFAs in the microbial, plant and animal kingdom has recently been reviewed[1]. In prokaryotes, with the exception of mycobacteria[2–5], VLCFAs hardly occur. *Lactobacillus*[6], in which VLCFAs up to C_{30}, either saturated or monoenoic, could be identified, is one of the few exceptions. In a recent paper[7] we described the possible selective enrichment of a fatty acid (FA) mixture by VLCFAs using a combination of reversed-phase high-performance liquid chromatography (RP-HPLC) and gas chromatography–mass spectrometry (GC–MS). In previous work on VLCFAs in sulphate-reducing bacteria[8], FAs up to C_{34} were demonstrated by means of a special chromatographic technique. In this work we tried to enrich FAs from the bacterium *Desulfotomaculum* sp. by a combination of RP-HPLC and GC–MS techniques.

EXPERIMENTAL

Fatty acid methyl esters (FAMEs) were obtained from the sulphate-reducing bacterium *Desulfotomaculum* sp. strain 43 as described[8]. Portions of 50 mg of FAMEs were injected four times repeatedly and 172 μg of VLCFAs (C_{33} and higher) were obtained.

RP-HPLC

A semi-preparative separation of FAMEs was carried out by using a G-1 gradient LC system (Shimadzu, Kyoto, Japan) with two LC-6A pumps (4 ml/min), an SIL-1A sample injector and a C-R3A data processor. An SPLC-18 semi-preparative column (25 cm × 10 mm I.D.) (Supelco, Gland, Switzerland) was employed. The column was first eluted with methanol for 60 min, then with diethyl ether for 15 min and finally with methanol for 15 min. The fraction collected up to 27 min was discarded and that obtained within the interval 27–90 min was used for further analysis.

0021-9673/90/$03.50

GC–MS

The FAMEs (fraction 27–90 min) were analysed on a Finnigan MAT (San Jose, CA, U.S.A.) 1020 B instrument with an SPB-1 column (15 m × 0.25 mm I.D.) with a 0.25-μm film thickness (Supelco). The injection temperature was 100°C. The column temperature was programmed from 100°C (maintained for 1 min) at 20°C/min to 230°C and at 3°C/min to 320°C. The carrier gas was helium at a flow-rate of 70 cm/s.

RESULTS AND DISCUSSION

Fig. 1 shows that by semi-preparative RP-HPLC it was possible to separate all FAMEs longer than 33 carbon atoms. Although high FAME homologues were involved, by means of GC on a non-polar capillary column it was possible to separate straight-chain FAMEs. We were not able to obtain evidence that the abrupt decrease in the concentration of higher homologues resulted from incomplete enrichment of because they were not adequately recovered from the column. Nevertheless, we think that their concentration in the original sample was very low and, therefore, they could not be enriched to a greater extent.

From the mass spectra it was possible to identify peaks up to 40:0, *i.e.*, up to FAMEs of tetracontanoic acid. The complete mass spectrum of peaks 33–36 was obtained, indicating that in the spectra 33:0–36:0 FAME molecular ions (M^+) and corresponding splits in the region M^+ are always present. This situation is illustrated in Fig. 2. It can be seen that M^+ reaches almost 90% of the base peak (*i.e.*, the ion of *m/z* 74), isotope peak $(M + 1)^+$, *i.e.*, the ion of *m/z* 551 amounts to two fifths of its abundance. The ions of *m/z* 521 (M − 29), 519 (M − 31) and 507 (M − 43) confirmed the structure of methyl ester of hexatriacontanoic acid. As described earlier[7], ions of general formula $(CH_2)_nCOOCH_3$, where $n = 2, 6, 10, \ldots$, are also present and *m/z* assumes values of 87, 143, 199, ... In longer homologues (C_{37} and higher) a sharp decrease in their content in the mixture occurs and, unfortunately, the corresponding ions are not present in the M^+ region. We think that this phenomenon can be explained by a large decrease in the ion current of these homologues, resulting in a loss of the

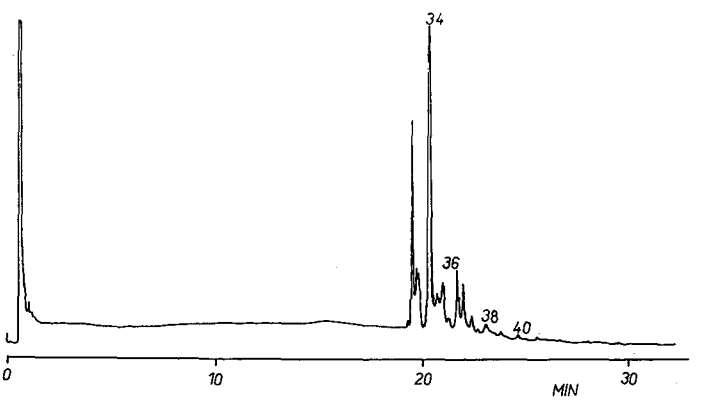

Fig. 1. GC–MS of total ion current of VLCFAs longer than 32. The peaks above 18.5 min are methyl esters; only even-carbon fatty acids are indicated, the numbers on the peaks representing the number of carbon atoms.

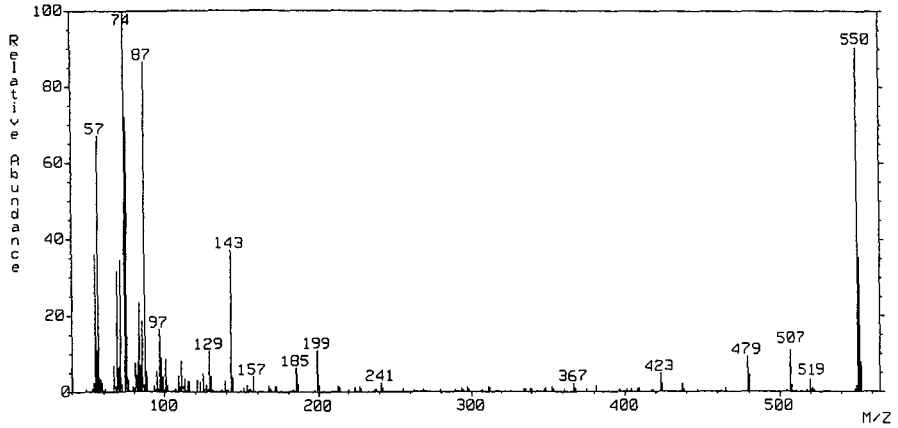

Fig. 2. Mass spectrum of 36:0 FAME.

diagnostic ions in the M^+ region. The structure of these higher homologues can be deduced either from values of the equivalent chain length (ECL) or from the mass spectra.

The mass spectra contained ions of up to *ca.* *m/z* 200, and an ion of *m/z* 74, *i.e.*, typical of saturated methyl esters (formed by McLafferty rearrangement), was also present. Compared with prokaryotes, only mycobacteria can compete in the length of VLCFAs with this sulphate-reducing bacterium. It is concluded that the so far highest FAMEs, *i.e.*, VLCFAs of up to 40:0, could be demonstrated.

The combination of RP-HPLC and high-temperature capillary GC–MS thus extends the analytical possibilities of both methods and contributes to the acquisition of new information on biological materials.

Institute of Microbiology,
Vídeňská 1083, 142 20 Prague
(Czechoslovakia)

TOMÁŠ ŘEZANKA*

Institute of Microbiology,
Prosp. 60-letia Oktiabrya 7/2,
117811 Moscow (U.S.S.R.)

MIKHAIL Yu. SOKOLOV

1 T. Řezanka, *Prog. Lipid Res.*, 28 (1989) 147.
2 N. Quereshi, K. Takayama and H. K. Schnoes, *J. Biol. Chem.*, 225 (1980) 182.
3 N. Sathyamoorthy, N. Quereshi and K. Takayama, *Can. J. Microbiol.*, 31 (1985) 214.
4 K. Takayama, N. Quereshi and H. K. Schnoes, *Lipids*, 13 (1978) 575.
5 K. Takayama, H. K. Schnoes, E. L. Amstrong and R. W. Boyle, *J. Lipid Res.*, 16 (1975) 308.
6 K. Uchida, *Biochim. Biophys. Acta*, 348 (1974) 86.
7 T. Řezanka, T. Koza, R. Kysilka, I. Víden and M. Wurst, *J. Chromatogr.*, 472 (1989) 290.
8 T. Řezanka, M. Yu. Sokolov and I. Víden, *FEMS Microbiol. Ecol.*, 73 (1990) in press.

(First received November 28th, 1989; revised manuscript received February 5th, 1990)

PUBLICATION SCHEDULE FOR 1990

Journal of Chromatography and Journal of Chromatography, Biomedical Applications

MONTH	J	F	M	A	M	J	
Journal of Chromatography	498/1 498/2 499	500 502/1	502/2 503/1 503/2 504/1	504/2 505/1	505/2 506 507 508/1	508/2 509/1 509/2 510	The publication schedule for further issues will be published later
Cumulative Indexes, Vols. 451–500		501					
Bibliography Section		524/1		524/2		524/3	
Biomedical Applications	525/1	525/2	526/1	526/2 527/1	527/2	528/1 528/2	

INFORMATION FOR AUTHORS

(Detailed *Instructions to Authors* were published in Vol. 478, pp. 453–456. A free reprint can be obtained by application to the publisher, Elsevier Science Publishers B.V., P.O. Box 330, 1000 AH Amsterdam, The Netherlands.)

Types of Contributions. The following types of papers are published in the *Journal of Chromatography* and the section on *Biomedical Applications:* Regular research papers (Full-length papers), Notes, Review articles and Letters to the Editor. Notes are usually descriptions of short investigations and reflect the same quality of research as Full-length papers, but should preferably not exceed six printed pages. Letters to the Editor can comment on (parts of) previously published articles, or they can report minor technical improvements of previously published procedures; they should preferably not exceed two printed pages. For review articles, see inside front cover under Submission of Papers.

Submission. Every paper must be accompanied by a letter from the senior author, stating that he is submitting the paper for publication in the *Journal of Chromatography*. Please do not send a letter signed by the director of the institute or the professor unless he is one of the authors.

Manuscripts. Manuscripts should be typed in double spacing on consecutively numbered pages of uniform size. The manuscript should be preceded by a sheet of manuscript paper carrying the title of the paper and the name and full postal address of the person to whom the proofs are to be sent. Authors of papers in French or German are requested to supply an English translation of the title of the paper. As a rule, papers should be divided into sections, headed by a caption (*e.g.*, Summary, Introduction, Experimental, Results, Discussion, etc.). All illustrations, photographs, tables, etc., should be on separate sheets.

Introduction. Every paper must have a concise introduction mentioning what has been done before on the topic described, and stating clearly what is new in the paper now submitted.

Summary. Full-length papers and Review articles should have a summary of 50–100 words which clearly and briefly indicates what is new, different and significant. In the case of French or German articles an additional summary in English, headed by an English translation of the title, should also be provided. (Notes and Letters to the Editor are published without a summary.)

Illustrations. The figures should be submitted in a form suitable for reproduction, drawn in Indian ink on drawing or tracing paper. Each illustration should have a legend, all the *legends* being typed (with double spacing) together on a *separate sheet*. If structures are given in the text, the original drawings should be supplied. Coloured illustrations are reproduced at the author's expense, the cost being determined by the number of pages and by the number of colours needed. The written permission of the author and publisher must be obtained for the use of any figure already published. Its source must be indicated in the legend.

References. References should be numbered in the order in which they are cited in the text, and listed in numerical sequence on a separate sheet at the end of the article. Please check a recent issue for the layout of the reference list. Abbreviations for the titles of journals should follow the system used by *Chemical Abstracts*. Articles not yet published should be given as "in press" (journal should be specified), "submitted for publication" (journal should be specified), "in preparation" or "personal communication".

Dispatch. Before sending the manuscript to the Editor please check that the envelope contains three copies of the paper complete with references, legends and figures. One of the sets of figures must be the originals suitable for direct reproduction. Please also ensure that permission to publish has been obtained from your institute.

Proofs. One set of proofs will be sent to the author to be carefully checked for printer's errors. Corrections must be restricted to instances in which the proof is at variance with the manuscript. "Extra corrections" will be inserted at the author's expense.

Reprints. Fifty reprints of Full-length papers, Notes and Letters to the Editor will be supplied free of charge. Additional reprints can be ordered by the authors. An order form containing price quotations will be sent to the authors together with the proofs of their article.

Advertisements. Advertisement rates are available from the publisher on request. The Editors of the journal accept no responsibility for the contents of the advertisements.

(Coal Science Technology, 15)

Advanced Methodologies in Coal Characterization

edited by **H. Charcosset,** *assisted by* **B. Nickel-Pepin-Donat,** *CNRS, Institut de Recherches sur la Catalyse, Villeurbanne, France*

The history of basic research in coal science in France is treated in this book, followed by a presentation of a minibank of 5 French coals of different rank. The main part of the book deals with a description of improved methods of coal characterization and their applications to the coals of the minibank. The results are divided into three sections: 1) Raw coals, 2) Products of extraction, oxidation and pyrolysis and 3) Macerals. An overall discussion of the whole assembly of new methods and information follows the series of research papers.

This volume will be of value to those involved in the field of coal characterization for conversion processes, both in the short term and in the future. Since these methodologies are not restricted to coal characterization but extend to carbonaceous materials in general, e.g. oil shales, petroleum residues and heavy petroleums, this book will be of interest to a wide ranging readership.

1990 xii + 442 pages
Price: US$ 182.00 / Dfl. 355.00
ISBN 0-444-88695-8

ELSEVIER SCIENCE PUBLISHERS

P.O. Box 211, 1000 AE Amsterdam, The Netherlands
P.O. Box 882, Madison Square Station, New York, NY 10159, USA